

THE CALCULATION OF HIGH ENERGY ELECTRON-  
CAPTURE CROSS-SECTIONS USING THE  
CONTINUUM DISTORTED WAVE (CDW) AND  
CONTINUUM INTERMEDIATE STATES (CIS) METHODS

by

George William Shirtcliffe

A thesis submitted to the  
UNIVERSITY OF LEICESTER  
for the degree of  
DOCTOR OF PHILOSOPHY  
in the Faculty of Science  
1982

UMI Number: U632525

All rights reserved

INFORMATION TO ALL USERS

The quality of this reproduction is dependent upon the quality of the copy submitted.

In the unlikely event that the author did not send a complete manuscript and there are missing pages, these will be noted. Also, if material had to be removed, a note will indicate the deletion.



UMI U632525

Published by ProQuest LLC 2015. Copyright in the Dissertation held by the Author.  
Microform Edition © ProQuest LLC.

All rights reserved. This work is protected against  
unauthorized copying under Title 17, United States Code.



ProQuest LLC  
789 East Eisenhower Parkway  
P.O. Box 1346  
Ann Arbor, MI 48106-1346



THESIS  
661201  
97 3 2 3

To

my Father and Mother, Ronald and Georgina Shirtcliffe,  
without whose contribution this thesis would not have  
been possible.

## ACKNOWLEDGEMENTS

I wish to thank Professor J.L. Beeby for the opportunity to work in the Department of Physics, Leicester University.

A special thanks goes to Mrs. M.E. Garner (typing) for her co-operation and patience during the typing of this thesis. For the preparation of this thesis, I am also indebted to Mrs. R. Littler, Mr. J. Kerruish and Mr. J. Driver (graphics), and Mrs. R. Bubb (copying).

I would like also to express my appreciation for the assistance provided by the personnel of the Computer Laboratory and members, past and present, of the Quantum Molecular Physics group, Leicester University.

Above all, thanks must go to Dr. K.E. Banyard for his wise counsel on every aspect of this work. His patience and advice, as both a friend and a supervisor, made this research very enjoyable.

## CONTENTS

	Page
Acknowledgements	i
General Introduction	1
References - General Introduction	16

### PART ONE

The calculation of electron-capture cross-sections for fast protons and alpha-particles in  $\text{Li}^+$  using the Continuum Distorted Wave (CDW) method, plus an analysis of the effects of electron correlation and of the trends in capture cross-sections for two-electron targets.

#### CHAPTER

1.1	Introduction	18
1.2	The CDW transition amplitude	23
1.3	Evaluation of the CDW cross-section	33
1.4	Electron-capture from $\text{Li}^+$ by fast protons and alpha-particles	42
1.5	An analysis of trends in capture cross-sections for two-electron targets	45
1.6	Conclusion	52
	Tables and Figures to Part 1	55
	References - Part 1	68

### PART TWO

Application of the Continuum Distorted Wave (CDW) method to electron-capture from a many-electron target and the calculation of capture cross-sections for the three-electron target atom Li, and its ions, by fast protons.

#### CHAPTER

2.1	Introduction	70
2.2	The application of the CDW method to electron-capture from a many-electron atom by fast protons	73
2.3	Electron-capture from Li, $\text{Li}^+$ and $\text{Li}^{2+}$ by fast protons	76
2.4	Conclusion	82
	Tables and Figures to Part 2	84
	References - Part 2	91

PART THREE

The Continuum Intermediate States (CIS) method and its application to electron-capture from hydrogen by a simple structured projectile in the form of (a) fast H atoms, and (b) fast Li ions.

## CHAPTER

3.1	Introduction	93
3.2	Derivation of the Continuum Intermediate States (CIS) transition amplitude for electron-capture by a simple structured projectile	98
3.3	Evaluation of the transition amplitude	106
3.4	An examination of electron-capture in H-H collisions	114
3.5	Electron-capture from H atoms by fast Li ions	120
3.6	Conclusion	135
	Tables and Figures to Part 3	139
	References - Part 3	164

APPENDIX A

	The formal quantal derivation of the CDW transition amplitude	166
A1	Formal theory for rearrangement collisions	167
A2	Application to proton-hydrogen charge transfer	170
	Figure A1	178
	References - Appendix A	179

# GENERAL INTRODUCTION

## General Introduction

In the quantum mechanical treatment of ion-atom collisions much work has been done in calculating cross-sections for electron-capture reactions involving multi-charged ions in collision with simple atoms. Such reactions are of considerable interest, not only theoretically but also in many areas of experimental research. An example of current research, in which electron-capture processes may play an important role, can be found in connection with the practical aspects of controlled thermo-nuclear fusion development (see for example Barnett<sup>1</sup>).

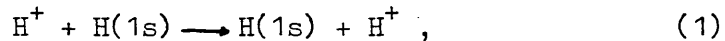
Information such as electron-capture cross-sections is required in connection with the methods of producing the plasma in the thermonuclear fusion devices by the neutral injection of fast beams (150-200 keV) of hydrogen atoms in highly excited states, and also in the study of plasma instabilities that occur due to collisions between the neutral hydrogen atoms and the small percentage of highly stripped impurity atoms. Consequently, as stated by Barnett<sup>1</sup>, atomic physical processes, such as electron-capture by fast singly or multi-charged ions, are expected to play an increasingly important role in the plasma physicist's and engineer's quest for thermonuclear power.

Also electron-capture from one- and two-electron atoms by fast projectiles is of importance in the study of post collisional phenomena such as projectile x-ray emission. These emissions may prove to be of considerable interest in the field of astrophysics which, if detectable, may be used in the study of cosmic ray intensities and the properties of interstellar gases, as discussed by Belkic and McCarroll<sup>2</sup>.

Consequently the capture of electrons by fast projectiles from atoms has received a great deal of attention over the years and has

been the subject of many theoretical investigations. Although at high energies it is the ionisation process which dominates the electron loss process, there has been in recent years considerable interest in high energy electron-capture following the suggestion of Bassel and Gerjouy<sup>3</sup> that 1st order methods may be inadequate in the treatment of electron-capture at high energy, which is of practical significance if the methods of calculating electron-capture cross-sections are to predict accurately the high-energy dependence of such cross-sections.

The simplest electron-capture reaction is the resonant charge transfer process



which has been the subject of many theoretical calculations in the region of high proton impact energies (see for example McCarroll and Salin<sup>4</sup> and the work of Dettmann and Leibfried<sup>5</sup>), and has since, due to the exact nature of the atomic wavefunctions, served as a testing ground for new theories and methods. If the incident proton is denoted by (1) and the hydrogen nucleus by (2) and the bound electron (3), the exact matrix element from which the cross-section may be found is

$$T_{if} = \langle \Psi_f | V_{12} + V_{23} | \Psi_i^+ \rangle , \quad (2)$$

where  $V_{ij}$  are the interaction potentials between the particles  $i$  and  $j$  of the system, while  $\Psi_i^+$  is the complete wavefunction of the total hamiltonian  $H$  with eigenvalue  $E$  and can be shown to satisfy the integral equation

$$\Psi_i^+ = (1 + G^+ V_i) \Psi_i , \quad (3)$$

where  $G^+$  is the Greens function  $(E - H + i\epsilon)^{-1}$  and  $V_i$  is the initial perturbing potential which in this case is

$$V_i = V_{12} + V_{13} ; \quad (4)$$

$\Psi_i$  and  $\Psi_f$  are the unperturbed wavefunctions for the initial and final state respectively.

Physical arguments suggest that for high impact energies, in particular for proton velocities much in excess of the orbital velocity of the captured electron (a proton energy of 25 keV for protons incident on hydrogen),  $T_{if}$  would be accurately represented by the Born approximation, obtained by replacing  $\Psi_i^+$  in equation (3) by the initial unperturbed wave function  $\Psi_i$  such that

$$T_{if} = \langle \Psi_f | V_{12} + V_{23} | \Psi_i \rangle . \quad (5)$$

The question has often been raised as to whether the inter-nuclear potential should be retained or omitted, and the calculations of cross-sections for charge-exchange, involving the Born approximation, generally falls into two categories - those following the argument of Oppenheimer<sup>6</sup> and Brinkman and Kramers<sup>7</sup> that the coulomb repulsion between the nuclei,  $V_{12}$ , may be neglected, such that

$$T_{if} = \langle \Psi_f | V_{23} | \Psi_i \rangle , \quad (6)$$

and those in which it is retained (equation (5)) and which are generally referred to as the 'Born approximation'.

However, Belkic, Gayet and Salin<sup>8</sup>, in a recent review of electron-capture in high energy ion-atom collisions have brought attention to the fact that at high impact energies the electron-capture cross-sections should not be influenced by the internuclear potential, and show conclusively that if the internuclear coulomb potential is accounted for exactly to first order in  $m/\mu$  (where  $m$  is the electron mass and  $\mu$  the reduced mass) then the total cross-section for the forward charge-exchange is entirely independent of this potential. This effectively means that if we wish to calculate the cross-section in the limit  $m/\mu \rightarrow 0$  we may use the impact parameter method to

formulate the scattering problem (see also McCarroll and Salin<sup>9,10</sup>).

In the impact parameter treatment the nuclei are assumed to behave like classical particles and quantum perturbation theory is applied to determine the chance of a transition from one electronic state to another. During the encounter we assume that the relative velocity vector of the nuclei remains constant and this then enables the internuclear potential to be removed from the perturbing potential in a systematic manner to give simply a phase factor in the transition amplitude  $a_{if}(b)$ , which later disappears on forming  $|a_{if}(b)|^2$ . We note that in the Brinkman and Kramers approximation the internuclear potential is therefore accounted for exactly in that it is removed from the calculation. The fact that the Born approximation is in better agreement with experiment than the Brinkman and Kramers approximation is considered to be fortuitous (see for example the discussion by Bransden and Cheshire<sup>11</sup>).

Before discussing the theoretical methods which go beyond the first Born approximation it is important to understand what the first Born approximation represents in terms of quantum perturbation theory. The matrix element in the first Born approximation (equation (5)) can be shown, by expanding the integral equation for  $\Psi_i^+$  (equation (3)) to be the first term in a series expansion called the 'Born series'. Obviously the convergence of this 'Born series' is of utmost importance. The argument for the use of the first Born approximation for rearrangement collisions is that at high impact energies,  $E$ , distortions will be small and the series will converge, one hopes rapidly, to the first term as  $E \rightarrow \infty$ , and that as a result  $T_{if}$  represents the leading term in an asymptotically converging series. Consequently the convergence of the Born series and of the physical matrix element for rearrangement collisions has received a considerable amount of attention<sup>12,13,14</sup>. Of particular interest however is the work of Drisko<sup>15,11</sup> who has suggested

that for electron-capture the Born series does not converge to its first term in the high energy limit and therefore in order to obtain accurate cross-sections at high impact energies one must use at least a second order method.

The work of Drisko showed that in the second Born approximation the capture cross-section for reaction (1) behaves at high energies as  $(0.2946 + 5\pi v^{-12})Q_{BK}$  (where  $Q_{BK}$  is the Brinkman Kramers cross-section and behaves at high energies as  $v^{-12}$ , where  $v$  is the impact velocity). Drisko also estimated that the third order Born approximation would again have a different high energy dependence, namely  $(0.319 + 5\pi v^{-12})Q_{BK}$ , although essentially both the second and third order approximations predict a behaviour of  $E^{-11/2}$  for large impact energy  $E$ , which is in full agreement with the prediction given by Thomas<sup>16</sup> using classical trajectory theory.

Among the calculations going beyond first order methods, which are valid at high impact energies, is the impulse approximation (see Bransden and Cheshire<sup>11</sup>, Cheshire<sup>17</sup>). In this method the unperturbed wavefunction in the matrix element, equation (5), is replaced by one employing outgoing wave boundary conditions, and although the internuclear potential is included in the matrix element its importance and contribution to the cross-section is very much reduced. Although the total cross-sections derived from the impulse and Born approximations are similar, virtually the whole of the impulse approximation cross-section is derived from the Brinkman-Kramers term. Furthermore, at high energies,  $E > 1$  MeV, the impulse approximation behaves like  $E^{-11/2}$ , which is in full agreement with Drisko's prediction for a second order Born approximation mentioned earlier. Thus, physically the impulse approximation is an improvement over the first Born approximation and the similarity in cross-sections between

the two methods adds further evidence to the suggestion that the success of the 'Born approximation' for total cross-sections must be to some extent accidental.

The most recent and successful second order method developed for calculating electron-capture cross-sections, at high impact energies, is the Continuum Distorted Wave (CDW) method introduced by Cheshire<sup>18</sup>. Unlike the impulse approximation the CDW method incorporates wavefunctions which have the correct asymptotic form, and indeed this was one of the factors that motivated Cheshire in its derivation. The correct initial and final boundary conditions of the problem are ensured in the CDW method and this is achieved by taking full account of the continuum intermediate states in the charge-exchange process, in both the entrance and exit channels. This is an important feature of the CDW method since when the incident velocity is high the dominant inelastic transitions will be ionization and excitation, and, since all intermediate channels are open, it is not surprising that the charge-exchange cross-section will be influenced by the inclusion of the continuum intermediate states. Also the internuclear interaction  $V(R)$  is removed from the perturbing potentials in the CDW transition amplitude in a consistent manner. This is done in such a way that  $V(R)$  is exactly accounted for within the total wavefunction (to first order in  $m/\mu$ ) so as to give zero contribution to the final cross-section.

Originally the CDW method was introduced by Cheshire<sup>18</sup> within the scheme of the well known impact parameter method, but the main features with respect to scattering theory, are shown in the formal quantal treatment by Gayet<sup>19</sup> (see also the review by Belkic et al<sup>8</sup>). Essentially the problem that arises when trying to obtain a second order approximation to  $T_{if}$  in equation (2), as pointed out by Greider and Dodd<sup>20</sup>, is that terms arise in the expansion of  $T_{if}$  which bring

about the divergence of the operator Born series. However, Dodd and Greider<sup>21</sup> have suggested a means by which the divergence can be overcome. The basic feature of their method is the introduction of an arbitrary perturbing potential, say  $v_x$ , into the distorting potential, which could then be chosen hopefully 'to achieve a satisfactory compromise between realism and tractability'. Exploiting the work of Dodd and Greider<sup>21</sup>, Gayet<sup>19</sup> makes a suitable choice for  $v_x$  and arrives at a transition amplitude equal to that of Cheshire's<sup>18</sup> multiplied by an arbitrary phase factor. We note also that the high energy behaviour of the method is in full agreement with that of the second Born approximation.

In the work presented here the derivation of transition amplitudes is achieved using the somewhat more transparent and elementary approach based on the impact parameter formalism, as used by Cheshire<sup>18</sup>. However, for the purpose of completeness an outline of the so-called wave formalism of the CDW method, as presented by Gayet<sup>19</sup>, is given in Appendix A of this thesis.

Since its introduction by Cheshire<sup>18</sup> the CDW method has been investigated thoroughly by workers such as Salin<sup>22</sup>, Belkic and Janev<sup>23</sup>, Belkic and Gayet<sup>24</sup>, and Belkic and McCarroll<sup>2</sup>, for the purpose of comparing the calculated cross-sections with experimental data. For impact velocities greater than the Bohr orbit velocity of the target electron the theoretical cross-sections were found to be in good agreement with experiment. Therefore, the CDW approximation has proved to be an adequate second - order method for calculating charge exchange cross-sections at large impact energies, and is thus an improvement over that of the Born calculations. This is particularly so in the case of electron-capture by highly charged ions which was examined within the CDW framework by Belkic and McCarroll<sup>2</sup>.

For electron-capture from targets having more than one electron the question arises as to the sensitivity of the method in question with respect to the target electronic wavefunction. The CDW method was examined with this respect for the He target by Belkic and Gayet<sup>24</sup>, who found it to be more sensitive than the corresponding first Born calculations. An improvement in the electronic wavefunction usually involves an inclusion of electron correlation and its effect on the CDW cross-sections for electron-capture from the He and H<sup>-</sup> was the subject of an investigation by the workers Banyard and Szuster<sup>25</sup> and Moore<sup>26</sup>.

In Part 1 of this thesis the work of Banyard, Szuster and Moore is extended to include electron-capture from Li<sup>+</sup> by fast protons and alpha-particles. The sensitivity of the cross-sections with respect to changes in the Li<sup>+</sup> wavefunction is examined and a study is made of the trends in cross-sections obtained when the target nuclear charge is systematically increased. By analysing the CDW expression for the cross-section, it is noted that the cross-section obtained is sensitive to the description of the electrons in the two-electron target and, in particular, the shape of the electronic wavefunction close to the origin for electron-capture at high projectile velocities.

In Part 2 the CDW method is applied to electron-capture by fast protons from a three-electron target, and cross-sections are calculated for protons on Li. When performing a calculation involving a many-electron atom approximations are invariably made to remove the difficulties which arise due to the presence of the inter-electron potential terms. In this section a modification is suggested to the so-called 'perfect screening' approach used by others for two-electron targets<sup>23</sup>. The resulting cross-sections are compared with experiment and agreement is found to be more satisfactory than that obtained from previous theoretical calculations. The modification of the 'perfect screening'

method is applied also to the  $\text{Li}^+$  ion and to complete the ionization series, cross-sections are calculated for the one-electron target  $\text{Li}^{2+}$ .

As demonstrated in Parts 1 and 2, electron-capture from small atomic targets by fast structureless projectiles, such as protons or alpha-particles, can be described quite successfully by modifying the CDW method of Cheshire<sup>18</sup>. However, also of interest is the problem of charge-exchange involving structured projectiles (e.g. atoms or ions with one or two electrons). This presents a more difficult problem due to the interaction between the target active electron and the passive electrons residing on the projectile.

Despite the success of the CDW method in predicting electron-capture cross-sections for fast structureless projectiles, Belkic<sup>27</sup>, in referring to the work of Shakeshaft<sup>28</sup>, has stated that the agreement between the CDW method and the second Born approximation in the limit of high impact projectile velocity is accidental since it results from the incorrect asymptotic behaviour of the CDW transition amplitude at large impact parameters. As a consequence Belkic<sup>27</sup> has proposed another second order method called the Continuum Intermediate States (CIS) approximation. The CIS method is not only satisfactory in providing an accurate total capture cross-section for fast protons ( $E > 25$  keV) incident on H, but also, in contrast to the CDW method, it predicts a transition amplitude for large impact parameters, and large incident velocities, which is 'essentially in agreement' with the second Born approximation and the classical treatment of Thomas<sup>16</sup>.

The CIS method differs from that of the CDW approach in that it takes account of distortion effects by inclusion of the continuum intermediate states in only one of the collision channels. For example, in the prior form, the prior interaction is treated as a perturbing potential while the post interaction is treated fully as a coulomb distorted

wave. Although this feature of the method leads to the boundary condition of the problem being preserved in only one channel, we show in Part 3 that as a consequence of this the CIS method is rendered in a form which is particularly suitable for adaptation to the more general case of ion-atom collisions.

For the reasons stated above the CIS method will be especially applicable to electron-capture into excited states for incident heavy ions at high impact energies, for which large impact parameters will be important. This subject has in recent years attracted renewed interest<sup>29,2</sup>, not only from a theoretical point of view but also in connection with the practical aspects of thermonuclear fusion<sup>1</sup> and astrophysics<sup>2</sup>, as stated earlier.

Therefore, in Part 3, the subject of electron-capture with respect to the more general case of ion-atom collisions is discussed, and a procedure is presented, based on an adaptation of the CIS method, for determining cross-sections for charge exchange between simple structured systems. A critical test of the scheme proposed is provided by application to H-H collisions in which  $H^-$  is formed in the exit channel. Finally, total cross-sections for electron-capture by  $Li^+$ ,  $Li^{2+}$  and  $Li^{3+}$  incident on H atoms are calculated and compared with experiment.

Since in the present work calculations are performed involving electron correlated wavefunctions we now present a brief summary of the correlation problem.

In order to obtain the exact wavefunction for an atomic or molecular system it is necessary to find an exact solution to the relevant Schrödinger equation. For the hydrogen atom and hydrogen molecular ion, each with a single electron, the Schrodinger wave equation may be solved exactly. However, for a large atom or molecule

the problem is made more complicated by the presence of potential energy terms which arise from the mutual repulsion between any two electrons. In practice the exact solution to the Schrodinger equation for a many-electron system is unobtainable and therefore varying degrees of approximation to the exact wavefunction must be made.

The electronic structure of many atoms and molecules has been studied, with some success, by means of the independent particle approximation. The simplifying assumption of the model is that the inter-electronic potential field experienced by an electron, located at some point in space, will depend only on the average position of all the other electrons. The Schrodinger equation describing an N-electron system is then reduced to N single-particle wave equations coupled together only through an average coulomb field. The total wavefunction  $\Psi$  is then written as a simple product of one-particle wavefunctions, and when evaluated numerically it is called the Hartree wavefunction<sup>30</sup>. Unfortunately, when the total wavefunction  $\Psi$  is determined according to this prescription it does not take into account the indistinguishability of the electrons, nor does it obey the Pauli exclusion principle. These difficulties are overcome by writing  $\Psi$  as a single Slater determinant<sup>31</sup> of one-electron wavefunctions, known as the atomic spin orbitals. Any spin orbital may be written as the product of a spatial orbital and a spin function. If  $\Psi$  is determined numerically in this way, it is called a Hartree Fock (HF) function<sup>32</sup>. Interchanging the coordinates of any two electrons merely interchanges the corresponding rows in the Slater determinant and, by the theory of determinants, causes  $\Psi$  to change sign - this antisymmetry is the wave mechanical fulfilment of the Pauli exclusion principle.

Within the HF approximation the probability of finding two electrons with parallel spins at the same point in space is zero<sup>33,34</sup>.

Such a point may be termed the centre of a "Fermi hole"<sup>35</sup> and is a consequence of the antisymmetry of the wavefunction. Although the HF method allows electrons with the same spin properties to avoid one another, no allowance is made for any spatial correlation between electrons with opposite spins. The effect of correlation between all electrons can only be examined by means of wavefunctions which are more flexible than the HF determinant. When described by wavefunctions beyond the HF level each electron lies in a "coulomb hole"<sup>36</sup>: a region of space which is largely devoid of other electrons due to coulombic repulsions.

A wavefunction that incorporates the description of the so-called 'coulomb hole' and has an eigenenergy beyond  $\epsilon_{\text{HF}}$  is termed an electron correlated wavefunction. The energy change  $\delta\epsilon$  arising from the allowance for electron correlation is clearly not measurable by experiment but is usually defined as<sup>37</sup>  $\delta\epsilon = \epsilon_{\text{EXACT}} - \epsilon_{\text{HF}}$ , where  $\epsilon_{\text{EXACT}}$  is the true non-relativistic energy and is generally deduced from experimental observation.

The correlation energy of an atom or molecule is usually of the order of magnitude of 1% of the total energy. Although this is relatively small it can be comparable to spectral transition energies, binding energies and dissociation energies in molecules. For example, the  $^1\text{S}$  description of  $\text{H}^-$  is particularly sensitive to electron correlation since without correlation the existence of the ground-state is not even predicted. Electron correlation also plays an important role in the determination of the correct dissociation products of the  $\text{H}_2$  molecule. When the ground state of  $\text{H}_2$  is described by using the HF scheme there is equal probability of dissociation into  $\text{H}^-$  and  $\text{H}^+$  as there is for the observed dissociation into two H atoms. This is a consequence of the HF method allowing electrons of opposite spins to

accumulate on the same atom. Hence, at large internuclear distances, a total energy is obtained which is higher than that for the true dissociation products.

Although the recent development of high-speed computers has made the electron correlation problem more tractable, it was first discussed as early as 1929 by Hylleraas<sup>38</sup> who proposed three methods of constructing correlated wavefunctions. The procedure used in this work is of the configuration-interaction (CI) type. In this approach the wavefunction is expanded as a linear combination of Slater determinants, each of which is composed from a basis set of orbitals; the problem being to determine the configuration coefficients. The term configuration refers to a combination of Slater determinants which has the required angular and spin dependence of the state under study. This mixing together of various electronic states of the system under study, subject to certain angular momentum requirements, can be shown to introduce spatial correlation between the electrons. Clearly provided that the set of basis orbitals can be made complete and provided that all possible configurations are used, we can, in principle, calculate a CI wavefunction that will yield an exact eigenenergy for the system under consideration. In practice, of course, there is a restriction on the number of configurations that can conveniently be handled, although the more terms that can be accommodated, the better the calculated energy. The main drawback of the CI calculation is that, at the outset, it is not certain which configurations will be most effective in lowering the energy. In addition it is found that the energy convergence is notoriously slow. These difficulties can be overcome by expressing the wavefunction in terms of the so-called natural spin-orbitals<sup>39,40</sup> (NSO's). Löwdin has defined these (orthonormal) spin-orbitals  $\Omega(\underline{x}_i)$  as being those which produce a diagonal representation of the first order density

matrix  $e(\underline{x}'_1, \underline{x}_1)$ :

$$\begin{aligned}
 e(\underline{x}'_1, \underline{x}_1) &= N \int \Psi(\underline{x}_1, \underline{x}_2, \dots, \underline{x}_N) \Psi^*(\underline{x}_1, \underline{x}_2, \dots, \underline{x}_N) dx_2 dx_3 \dots dx_N \\
 &= \sum_i c_i \Omega_i(\underline{x}'_1) \Omega_i^*(\underline{x}_1) \quad (7)
 \end{aligned}$$

where  $\underline{x}_i$  refers to the collective space and spin coordinates of electron  $i$ . The coefficient  $c_i$  is known as the occupation number of the  $i^{\text{th}}$  natural orbital (NO), and clearly satisfy  $\sum_i c_i = N$ . Using a theorem due to Schmidt<sup>41</sup> it can be shown that any spin-orbital whose population is negligible may be omitted from a CI expansion. In other words the convergence of a CI wavefunction can be vastly improved by including only those natural spin orbitals having the highest occupation number. This result may appear to be of little value, since in order to determine the natural orbitals it is first necessary to calculate the density, which in turn requires a knowledge of the exact wavefunction. Nevertheless, by diagonalising the density matrix at any stage in a CI calculation and then selecting the configurations involving the most heavily populated NSO's, one may dramatically shorten the expansion.

However, for the purpose of calculating such quantities as the electron-capture cross-sections it is the use of the natural orbitals as a means to further our understanding of electron correlation that is of primary importance here. This end is achieved by expanding the existing CI wavefunction in terms of natural orbitals which are then grouped into natural configurations. Such a representation is generally known as the natural expansion of the wavefunction, and exhibits features which are of particular relevance to our present work. Firstly, the terms appearing in the natural expansion are found to be well-ordered by virtue of their energetically decreasing importance. Secondly, the correlation within the wavefunction is conveniently

partitioned both in terms of its radial and angular components and also according to the size of its correlation contributions. It is thus in a convenient form for our electron correlation study.

In Parts 1 and 3 the natural expansion representation of the CI wavefunction is used to demonstrate how the radial and angular correlation, included within the CI wavefunction, influences the calculated electron-capture cross-sections. In particular, in Part 3 attention is drawn to the opposing effects of radial and angular correlation.

## References - General Introduction

1. C.F. Barnett, Proc. 9th Int. Conf. on Physics of Electronic and Atomic Collisions. (Invited Paper of the above Conference) 846 (1976)
2. Dž Belkić and R. McCarroll, J. Phys. B. 10, 1933 (1977)
3. R.H. Bassel and E. Gerjuoy, Phys. Rev. 109, 355 (1958)
4. R. McCarroll and A. Salin, Proc. Roy. Soc. A300, 202 (1967)
5. K. Dettmann and G. Leibfried, Z. Phys. 218, 1 (1969)
6. J.R. Oppenheimer, Phys. Rev. 51, 349 (1928)
7. H.C. Brinkman and H.A. Kramers, Proc. Acad. Sci., Amsterdam 33, 973 (1930)
8. Dž Belkić, R. Gayet and A. Salin, Physics Reports (Review Section of Physics Letters). 56, 281 (1979)
9. R. McCarroll and A. Salin, Compt. Rend. Acad. Sci. 263, 329 (1966)
10. R. McCarroll and A. Salin, J. Phys. B. 1, 163 (1968)
11. B.H. Bransden and I.M. Cheshire, Proc. Phys. Soc. 81, 820 (1963)
12. R. Aaron, R.D. Amado and B.W. Lee, Phys. Rev. 121, 319 (1961)
13. K. Dettmann and G. Leibfried, Phys. Rev. 148, 1271 (1966)
14. K. Dettmann and G. Leibfried, Z. Physik 218, 1 (1968)
15. R.M. Drisko, Thesis, Carnegie Institute of Technology (1955)
16. L.H. Thomas, Proc. Roy. Soc. A114, 561 (1927)
17. I.M. Cheshire, Proc. Phys. Soc. 82, 113 (1963)
18. I.M. Cheshire, Proc. Phys. Soc. 84, 89 (1964)
19. R. Gayet, J. Phys. B. 5, 483 (1972)
20. K.R. Greider and L.R. Dodd, Phys. Rev. 146, 671 (1966)
21. L.R. Dodd and K.R. Greider, Phys. Rev. 146, 675 (1966)
22. A. Salin, J. Phys. B. 3, 937 (1970)
23. Dž Belkić and R.K. Janev, J. Phys. B. 6, 1020 (1973)
24. Dž Belkić and R. Gayet, J. Phys. B. 10, 1923 (1977)
25. K.E. Banyard and B.J. Szuster, Phys. Rev. A. 16, 129 (1977)

26. J.C. Moore and K.E. Banyard, J. Phys. B. 9, 1613 (1978)
27. Dž Belkić, J. Phys. B. 10, 3491 (1977)
28. R. Shakeshaft, J. Phys. B. 7, 1734 (1974)
29. M.D. Brown, L.D. Ellsworth, J.A. Guffey, T. Chiao, E.W. Pettus,  
L.M. Winters and J.R. Macdonald, Phys. Rev. A. 10, 1255 (1974)
30. D.R. Hartree, Proc. Camb. Phil. Soc. 24, 89, 111 (1928)
31. J.C. Slater, Phys. Rev. 34, 1293 (1929)
32. V. Fock, Z-Physik 61, 12 (1930),  
V. Fock, Z-Physik 62, 755 (1930), and  
D.R. Hartree, 'The Calculation of Atomic Structures', Wiley: New  
York (1957)
33. E.P. Wigner and F. Seitz, Phys. Rev. 43, 804 (1933)
34. E.P. Wigner and F. Seitz, Phys. Rev. 46, 509 (1934)
35. See, for some calculations on the size and shape of the Fermi hole,  
V.W. Maslen, Proc. Phys. Soc. A69, 734 (1956) and G. Sperber,  
Int. J. Quart. Chem. 5, 189 (1971)
36. C.A. Coulson and A.H. Neilson, Proc. Phys. Soc. 78, 831 (1961)
37. P.-O. Lowdin, Adv. Chem. Phys. 2, 207 (1959)
38. E.A. Hylleraas, Z. Physik 65, 209 (1930)
39. P.-O. Lowdin, Phys. Rev. 97, 1474(1955)
40. E.R. Davidson, Rev. Mod. Phys. 44, 451 (1972)
41. E. Schmidt, Math. Ann. 63, 433 (1907)

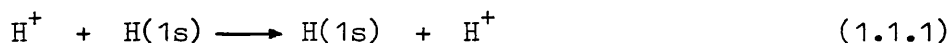
## PART ONE

The calculation of electron-capture cross-sections for fast protons and alpha-particles in  $\text{Li}^+$  using the Continuum Distorted Wave (CDW) method, plus an analysis of the effects of electron correlation and of the trends in capture cross-sections for two-electron targets.

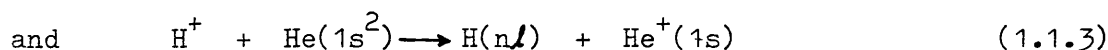
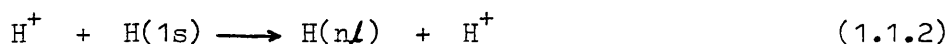
## CHAPTER 1.1

### Introduction

The continuum distorted wave (CDW) approximation was introduced by Cheshire<sup>1</sup> who used it to calculate cross-sections for the resonant charge transfer process

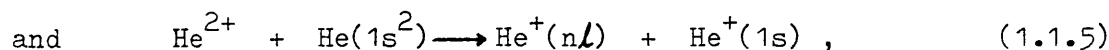
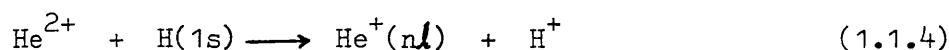


and compared his results with those of the Bates<sup>2</sup>, Born<sup>3</sup> and impulse<sup>4</sup> approximations. Although no comparison with experiment was made, Cheshire showed that the CDW method, when formulated with wavefunctions having the correct boundary conditions, has a correct high energy behaviour which is in full agreement with the second Born<sup>5</sup> approximation but, at low energies, the cross-sections were found to increase too rapidly with decreasing energy. The CDW approximation was extended to more complex collisions by Salin<sup>6</sup>, who calculated individual capture cross-sections,  $\sigma(nl)$ , for the reactions



for  $nl = 1s, 2s, 2p$  and  $3s$  in the impact energy range  $400 \text{ keV} \leq E \leq 3 \text{ MeV}$ .

Using the Oppenheimer  $n^{-3}$  rule<sup>7</sup> to estimate individual cross-sections for  $n > 2$ , Salin evaluated the total cross-sections  $Q = \sum_{nl} \sigma(nl)$  and found them to be in good agreement with experiment throughout the whole energy range. Belkic and Janev<sup>8</sup> generalised the method to electron-capture from any two-electron system by a fast nucleus and applied it to the reactions



for  $nl = 1s, 2s, 2p, 3s$  and  $3p$ ; the energy of the alpha-particles ranged from 25 keV to 3 MeV. The total cross-sections  $Q$  were obtained using the

---

<sup>7</sup> see also reference 25, p.395.

same  $n^{-3}$  sum rule<sup>6</sup> employed by Salin and, for reaction (1.1.5), the results were found to be in satisfactory agreement with experiment when  $E > 600$  keV. Belkic and Janev comment that it can be expected, from the work of Gayet<sup>9</sup>, that the CDW approximation for charge exchange processes should be reliable down to 30-50 keV. However, such a comparison of  $Q$  with experiment will be restricted in this energy region by the reliability of the Oppenheimer  $n^{-3}$  rule<sup>7</sup>. As a consequence, Belkic and Gayet<sup>10,11</sup> have calculated the CDW individual cross-sections  $\sigma(nl)$  for reactions (1.1.2-5), when  $nl = 1s, 2s, 2p, 3s, 3p, 3d$  and  $4s$ , for the purpose of comparing them with experimental data. The total cross-sections  $Q$  were evaluated using a more appropriate  $n^{-3}$  sum rule<sup>10</sup> which was expected to be valid at low impact energies - down to about 50 keV for the  $H^+ - H$  collisions. For reactions (1.1.2) and (1.1.3), they reported that the total cross-sections were in excellent agreement with experiment for  $E > 40$  keV and  $E > 80$  keV, respectively. A satisfactory agreement with experiment for alpha-particles was observed down to 100 keV for reaction (1.1.4) and down to 500 keV for reaction (1.1.5).

For electron-capture into atomic hydrogen states with non-zero values of the angular quantum number  $l$ , Belkic and Gayet<sup>10</sup> reported that no firm conclusion could be drawn on the accuracy of the CDW method until more extensive measurements have been performed. However, for the formation of atomic hydrogen in the  $1s, 2s, 3s$  and  $4s$  states, the CDW method works well for the H and He targets down to proton impact energies of roughly 50 keV and 80 keV, respectively.

In the earlier work of Salin<sup>6</sup> the CDW cross-sections were found to be sensitive to the nature of the He wavefunction. Using the simple one-parameter variational wavefunction of Hylleraas<sup>12</sup> and the open-shell wavefunction of Eckart<sup>13</sup>, discrepancies between the two sets of results

were quite significant. The difference was about 10% for  $E < 1$  MeV and within 20% for  $E > 1$  MeV. In view of this large percentage change, Banyard and Szuster<sup>14</sup> studied reaction (1.1.3), for  $25 \text{ keV} \leq E \leq 3 \text{ MeV}$ , and examined the sensitivity of the CDW individual and total cross-sections with respect to improvements in the He wavefunction up to and beyond the Hartree-Fock description. In going from the Hartree-Fock (HF) wavefunction of Clementi<sup>15</sup> to the correlated wavefunction of Weiss<sup>16</sup>, changes in  $Q$  were relatively small - of the order of 4% - although for capture into the individual hydrogen states the percentage changes were slightly larger. However, improvement in the target wavefunction from a simple one-parameter wavefunction up to the HF level produced, at  $E > 1000$  keV, much larger changes in  $Q$ : the relative changes were about 25-30%. A study of the cross-section dependence for reaction (1.1.5) revealed similar trends.<sup>17</sup> Banyard and Szuster concluded that it is essential to describe the target by at least an HF wavefunction if meaningful comparisons are to be made with experiment. An atomic system for which it is essential to go beyond the HF description is the hydrogen negative ion - since without an allowance for electron-correlation  $\text{H}^-$  is essentially unstable. Moore and Banyard<sup>18,19</sup> studied  $\text{H}^-$  as a target for electron capture by protons and alpha-particles over an energy range  $100 \text{ keV} \leq E \leq 10 \text{ MeV}$  and  $500 \text{ keV} \leq E \leq 10 \text{ MeV}$ , respectively, with emphasis on the change in cross-sections due to variations in the  $\text{H}^-$  wavefunction. Using the correlated function of Weiss<sup>1</sup> and the HF function of Curl and Coulson<sup>20</sup> they found that correlation reduced  $Q$  by at least 16% over both energy ranges. As for He, they also observed that percentage changes for capture into the individual hydrogen states,  $n\ell = 1s, 2s, \text{ and } 2p$ , were larger, roughly 26-30% for both protons and alpha-particles.

The factors that influence the cross-section for an electron-capture process include not only the nature of the bound state atomic wavefunctions but also such features as the distorting or perturbing potentials (acting either in the inward or outward channels), the changes in the electronic binding energies, and the relative velocity of the incident projectile. These may be coupled together in a complicated manner and their individual effects upon the cross-sections is often lost in the mathematical analysis and the final numerical calculations involved. However, the analysis and study of these factors may not only be pleasing from an aesthetic point of view but could prove useful in understanding both the relative magnitudes of capture cross-sections for different targets or projectiles and the changes which occur when improving the target wavefunctions. Such knowledge can be helpful when attempting to modify the method itself.

In the chapters that follow we evaluate the CDW electron-capture cross-sections for fast protons and alpha-particles incident on the  $\text{Li}^+$  ion. This not only extends the work already done on two-electron systems but, in particular, it will allow us to examine the trends in  $Q$  obtained when systematically increasing the target nuclear charge. Thus we analyse the CDW expression for the general capture cross-section  $\sigma(nl, n'l')$  for the three systems  $\text{H}^-$ ,  $\text{He}$  and  $\text{Li}^+$  at progressively increasing projectile velocity. The quantum numbers  $nl$  and  $n'l'$  represent the bound states of the 'active' (or captured) and 'passive' electrons, respectively. For protons and alpha-particles incident on  $\text{Li}^+$  the capture cross-sections are calculated in the energy ranges 100-3000 keV and 100-10000 keV. The cross-sections  $\sigma(nl)$  for each reaction are calculated for the capture states  $nl = 1s, 2s$  and  $2p$  and the total cross-section,  $Q = \sum_{nl} \sigma(nl)$ , is determined by using the  $n^{-3}$  rule. We also examine the sensitivity of the cross-sections with respect to changes in the  $\text{Li}^+$  wavefunction in order

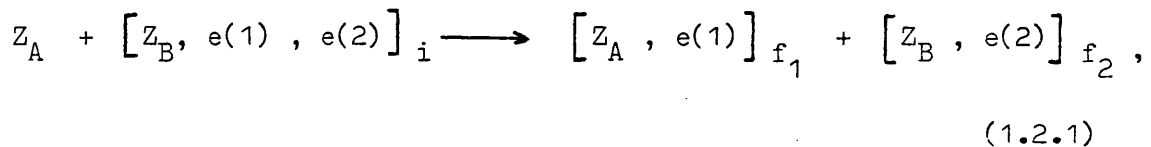
to study the variation of the effect of electron-correlation as the nuclear charge of the two-electron target is increased. Finally, the total cross-sections are compared with recent experimental data.

In order to facilitate the analysis of the cross-sections mentioned above, and to aid the resulting discussion, it is clearly appropriate that we first present a derivation of the CDW transition amplitude. Thus, in Chapters 2 and 3 we derive the CDW method for the general case of electron-capture from a two-electron atom by a structureless projectile, and then discuss the evaluation of the transition amplitude and resulting cross-section. The method is developed within the somewhat more transparent scheme of the impact-parameter approach used by Cheshire but the full quantal treatment of the CDW approximation, due to Gayet<sup>9</sup>, is presented in Appendix A.

## CHAPTER 1.2

### The CDW transition amplitude

Consider an encounter in which a nucleus A, of charge  $Z_A$ , is incident on an atom or ion consisting of two electrons (1) and (2) bound to a nucleus B, charge  $Z_B$ . Let  $\underline{x}_1$  and  $\underline{x}_2$  be the position vectors of electron (1) and (2) with respect to the nucleus of B and  $\underline{s}_1$ ,  $\underline{s}_2$  be the corresponding vectors relative to the nucleus A. The reaction we are considering is therefore of the type (see Figure 1.1):



where  $i$  and  $f$  denote the initial and final states respectively. We shall calculate the cross-section for capture of electron 1 (the so-called 'active' electron) and, since the electrons are indistinguishable and therefore the capture of either electron is equally probable, the final cross-section is simply twice that for the capture of electron 1.

We shall adopt the approach of Cheshire<sup>1</sup> and formulate the problem using the Impact Parameter (IP) method<sup>\*</sup>. In the IP approximation it is assumed that A moves with a constant velocity  $\underline{v}$  with respect to the fixed nucleus B. Thus if  $\underline{R}$  is the position vector of A relative to B then

$$\underline{R} = \underline{b} + \underline{v}t \quad (1.2.2)$$

where  $t$  is the time, chosen such that at  $t = 0$  the nuclei A and B have a minimum separation  $\underline{b}$  - this being the impact parameter for the collision. Let O be an arbitrary origin along AB, and let  $\underline{r}_1$  and  $\underline{r}_2$  be the position vectors of electrons (1) and (2) with respect to the origin O. Bates<sup>21</sup> and McCarroll have shown that the results of the theory are independent of the choice of origin O; therefore for convenience we shall always take

---

\* see reference 25, p.108.

O to be the mid-point of the line AB. The complete Schrodinger equation describing the motion of the electrons during collision is

$$\left[ \frac{1}{2} \nabla_{\underline{r}_1}^2 + \frac{1}{2} \nabla_{\underline{r}_2}^2 + \frac{Z_B}{x_1} + \frac{Z_B}{x_2} + \frac{Z_A}{s_1} + \frac{Z_A}{s_2} - \frac{1}{x_{12}} - \frac{Z_A Z_B}{R} \right] \Psi(\underline{r}_1, \underline{r}_2, t) = -i \frac{\partial \Psi(\underline{r}_1, \underline{r}_2, t)}{\partial t} \quad (1.2.3)$$

where  $x_{12}$  is the distance between electrons (1) and (2).

In the frame of reference with an origin at point O the active electron (1) has, in addition to its orbital motion about the target B, a velocity  $-\frac{1}{2}\underline{v}$  by virtue of being bound to B. Similarly, an electron bound to the nucleus A would have a velocity  $\frac{1}{2}\underline{v}$ . If a collision produces only the excitation of the target atom, the active electron continues to move with the nucleus B and its translational motion remains unchanged since  $\underline{v}$  is assumed constant. However, in the case of a rearrangement collision, the electron, which was originally moving with B, is captured by A and must therefore acquire the linear velocity of A. The consequent change in momentum of the electron might be expected to have an increasingly important effect on the electron capture cross-section as the projectile energy is increased. It was therefore suggested by Bates and McCarroll<sup>21</sup> that a set of wavefunctions which take into account the energy and momentum associated with the translational motion of the active electron should be used as the basis for the expansion of the electronic wavefunction  $\Psi(\underline{r}_1, \underline{r}_2, t)$ .

The complete electronic wavefunction  $\Psi(\underline{r}_1, \underline{r}_2, t)$  will satisfy the following boundary conditions:

$$\Psi_i(\underline{r}_1, \underline{r}_2, t) \xrightarrow[t \rightarrow -\infty]{} \Phi_i(\underline{r}_1, \underline{r}_2, t) \quad \text{and} \quad \Psi_f \xrightarrow[t \rightarrow +\infty]{} \Phi_f(\underline{r}_1, \underline{r}_2, t) \quad (1.2.4)$$

where

$$\Phi_i(\underline{r}_1, \underline{r}_2, t) = \Omega_i(\underline{r}_1, \underline{r}_2, t) \exp\left(-\frac{i Z_A(Z_B - 2)}{v} \ln(vR - v^2 t)\right) \quad (1.2.5)$$

and

$$\Phi_f(\underline{r}_1, \underline{r}_2, t) = \Omega_f(\underline{r}_1, \underline{r}_2, t) \exp\left(-\frac{i(Z_A - 1)(Z_B - 1)}{v} \ln(vR + v^2 t)\right). \quad (1.2.6)$$

It follows that the functions  $\Phi_{i,f}(\underline{r}_1, \underline{r}_2, t)$  are the solutions to the equations

$$\left(\frac{1}{2} \nabla_{\underline{r}_1}^2 + \frac{1}{2} \nabla_{\underline{r}_2}^2 + \frac{Z_B}{x_1} + \frac{Z_B}{x_2} - \frac{1}{x_{12}} - \frac{Z_A(Z_B - 2)}{R} + \frac{i\partial}{\partial t}\right) \Phi_i(\underline{r}_1, \underline{r}_2, t) = 0 \quad (1.2.7)$$

$$\left(\frac{1}{2} \nabla_{\underline{r}_1}^2 + \frac{1}{2} \nabla_{\underline{r}_2}^2 + \frac{Z_A}{s_1} + \frac{Z_B}{x_1} - \frac{(Z_A - 1)(Z_B - 1)}{R} + \frac{i\partial}{\partial t}\right) \Phi_f(\underline{r}_1, \underline{r}_2, t) = 0. \quad (1.2.8)$$

Following the suggestion of Bates<sup>2</sup> we may write

$$\Omega_i(\underline{r}_1, \underline{r}_2, t) = \phi_i(\underline{x}_1, \underline{x}_2) \exp\left\{-i\left[\frac{1}{2} \underline{v} \cdot \underline{r}_1 + \frac{1}{2} \underline{v} \cdot \underline{r}_2 + \frac{1}{4} v^2 t + \epsilon_i t\right]\right\} \quad (1.2.9)$$

and

$$\Omega_f(\underline{r}_1, \underline{r}_2, t) = \psi_{f_1}(\underline{s}_1) \chi_{f_2}(\underline{x}_2) \exp\left\{-i\left[-\frac{1}{2} \underline{v} \cdot \underline{r}_1 + \frac{1}{2} \underline{v} \cdot \underline{r}_2 + \frac{1}{4} v^2 t + (\epsilon_{f_1} + \epsilon_{f_2}) t\right]\right\}, \quad (1.2.10)$$

where  $\phi_i(\underline{x}_1, \underline{x}_2)$ ,  $\psi_{f_1}(\underline{s}_1)$ ,  $\chi_{f_2}(\underline{x}_2)$  are the bound state electronic wavefunctions in the initial and final states with corresponding eigen-energies  $\epsilon_i$ ,  $\epsilon_{f_1}$ ,  $\epsilon_{f_2}$  such that

$$\left(\frac{1}{2} \nabla_{\underline{r}_1}^2 + \frac{1}{2} \nabla_{\underline{r}_2}^2 + \frac{Z_B}{x_1} + \frac{Z_B}{x_2} - \frac{1}{x_{12}} + \epsilon_i\right) \phi_i(\underline{x}_1, \underline{x}_2) = 0, \quad (1.2.11)$$

$$\left( \frac{1}{2} \nabla_{\underline{r}_1}^2 + \frac{Z_A}{s_1} + \epsilon_{f_1} \right) \psi_{f_1}(\underline{s}_1) = 0, \quad (1.2.12)$$

and

$$\left( \frac{1}{2} \nabla_{\underline{r}_2}^2 + \frac{Z_B}{x_2} + \epsilon_{f_2} \right) \chi_{f_2}(\underline{x}_2) = 0. \quad (1.2.13)$$

We now introduce the distorted waves  $\chi_i$  and  $\chi_f$  defined as the solutions of the equations

$$\left[ \frac{1}{2} \nabla_{\underline{r}_1}^2 + \frac{1}{2} \nabla_{\underline{r}_2}^2 + \frac{Z_B}{x_1} + \frac{Z_B}{x_2} - \frac{1}{x_{12}} - \frac{Z_A(Z_B-2)}{R} + \frac{i\partial}{\delta t} + U_i \right] \chi_i(\underline{r}_1, \underline{r}_2, t) = 0 \quad (1.2.14)$$

and

$$\left[ \frac{1}{2} \nabla_{\underline{r}_1}^2 + \frac{1}{2} \nabla_{\underline{r}_2}^2 + \frac{Z_A}{s_1} + \frac{Z_B}{x_2} - \frac{(Z_A-1)(Z_B-1)}{R} + \frac{i\partial}{\delta t} + U_f \right] \chi_f(\underline{r}_1, \underline{r}_2, t) = 0 \quad (1.2.15)$$

with the boundary conditions

$$\chi_i \xrightarrow[t \rightarrow -\infty]{} \phi_i \quad \text{and} \quad \chi_f \xrightarrow[t \rightarrow +\infty]{} \phi_f. \quad (1.2.16)$$

Clearly the distorting potentials  $U_i$  and  $U_f$  must be chosen such that they will vanish in the limit of large internuclear separation.

If  $\Psi_i$  and  $\Psi_f$  are the solutions of equation (1.2.3) with boundary conditions (1.2.4) then the 'prior' transition amplitude  $a_{if}$  is obtained by projecting the initial state on to the complete wavefunction  $\Psi_f$ .

Therefore

$$\begin{aligned} a_{if} &= \lim_{t \rightarrow -\infty} \int \underline{dr}_1 \int \underline{dr}_2 \Psi_f^* \phi_i \\ &= \lim_{t \rightarrow -\infty} \int \underline{dr}_1 \int \underline{dr}_2 \Psi_f^* \chi_i. \end{aligned} \quad (1.2.17)$$

Now consider the term

$$\frac{d}{dt} \int d\underline{r}_1 d\underline{r}_2 \Psi_f^* \chi_i = \int d\underline{r}_1 d\underline{r}_2 \left[ \frac{\partial \Psi_f^*}{\partial t} \chi_i + \Psi_f^* \frac{\partial \chi_i}{\partial t} \right] .$$

Using equation (1.2.14), the right-hand side of the above equation becomes

$$\begin{aligned} \frac{d}{dt} \int d\underline{r}_1 d\underline{r}_2 \Psi_f^* \chi_i &= \frac{1}{i} \int d\underline{r}_1 d\underline{r}_2 \left[ \frac{i \partial \Psi_f^*}{\partial t} \chi_i + \Psi_f^* \left( -\frac{1}{2} \nabla_{\underline{r}_1}^2 - \frac{1}{2} \nabla_{\underline{r}_2}^2 \right. \right. \\ &\quad \left. \left. - \frac{Z_B}{x_1} - \frac{Z_B}{x_2} + \frac{1}{x_{12}} + \frac{Z_A(Z_B-2)}{R} - U_i \right) \chi_i \right] . \end{aligned} \quad (1.2.18)$$

By noting the relation that

$$\int \psi_a^* Q \psi_b d\underline{r} = \int Q^* \psi_a^* \psi_b d\underline{r} , \quad (1.2.19)$$

when  $Q$  is an Hermitian operator, and by making use of equation (1.2.3)

we find that (1.2.18) becomes

$$\frac{d}{dt} \int d\underline{r}_1 d\underline{r}_2 \Psi_f^* \chi_i = \frac{1}{i} \int d\underline{r}_1 d\underline{r}_2 \Psi_f^* \left( \frac{Z_A}{s_1} + \frac{Z_A}{s_2} - \frac{2Z_A}{R} - U_i \right) \chi_i . \quad (1.2.20)$$

Let us consider the integral

$$P_{if} = - \frac{1}{i} \lim_{t \rightarrow -\infty} \int_t^{\infty} dt \int d\underline{r}_1 d\underline{r}_2 \Psi_f^* \left( \frac{Z_A}{s_1} + \frac{Z_A}{s_2} - \frac{2Z_A}{R} - U_i \right) \chi_i \quad (1.2.21)$$

which by equation (1.2.20), is

$$P_{if} = - \lim_{t \rightarrow -\infty} \int_t^{\infty} dt \left[ \int d\underline{r}_1 d\underline{r}_2 \Psi_f^* \chi_i \right] . \quad (1.2.22)$$

Now provided

$$\lim_{t \rightarrow +\infty} \int d\underline{r}_1 d\underline{r}_2 \Psi_f^* \chi_i = 0 , \quad (1.2.23)$$

we can integrate equation (1.2.22) to obtain

$$P_{if} = \lim_{t \rightarrow -\infty} \int d\underline{r}_1 d\underline{r}_2 \Psi_f^* \chi_i = a_{if} . \quad (1.2.24)$$

Therefore we have shown that, provided condition (1.2.23) holds,

$$a_{if} = i \int_{-\infty}^{+\infty} dt \int d\underline{r}_1 d\underline{r}_2 \Psi_f^* \left( \frac{Z_A}{s_1} + \frac{Z_A}{s_2} - \frac{2Z_A}{R} - U_i \right) \chi_i . \quad (1.2.25)$$

Alternatively we could consider the time reversed reaction to obtain the 'post' transition amplitude  $b_{if}$  in the form

$$b_{if} = i \int_{-\infty}^{+\infty} dt \int d\underline{r}_1 d\underline{r}_2 \left[ \left( \frac{Z_B}{x_1} + \frac{Z_A}{s_2} - \frac{1}{x_{12}} - \frac{Z_B}{R} - \frac{Z_A}{R} + \frac{1}{R} - U_f^* \right) \chi_f^* \right] \Psi_i , \quad (1.2.26)$$

which is true provided that

$$\lim_{t \rightarrow +\infty} \int \chi_f^* \Psi_i d\underline{r}_1 d\underline{r}_2 = 0 . \quad (1.2.27)$$

The cross-section  $\sigma_{if}$  is obtained by integrating over all possible impact parameters

$$\sigma_{if} = 2 \int_0^{+\infty} b |a_{if}|^2 db (\pi a_0^2) = 2 \int_0^{+\infty} b |b_{if}|^2 db (\pi a_0^2) . \quad (1.2.28)$$

### The Distorted Wave Functions

We represent the solutions  $\Psi_i$  and  $\Psi_f$  in the form

$$\Psi_i(\underline{r}_1, \underline{r}_2, t) = \Omega_i(\underline{r}_1, \underline{r}_2, t) \mathcal{L}_i(\underline{s}_1, \underline{s}_2, t) \quad (1.2.29)$$

and

$$\Psi_f(\underline{r}_1, \underline{r}_2, t) = \Omega_f(\underline{r}_1, \underline{r}_2, t) \mathcal{L}_f(\underline{x}_1, \underline{s}_2, t) . \quad (1.2.30)$$

Clearly, in the limit,  $\mathcal{L}_i$  and  $\mathcal{L}_f$  must tend towards the correct phase factors given in equations (1.2.5) and (1.2.6) in order that the solutions for  $\Psi_i$  and  $\Psi_f$  will have the correct asymptotic behaviour. Substituting for  $\Psi_i$  and  $\Psi_f$  into equation (1.2.3), we see that  $\mathcal{L}_i$  and  $\mathcal{L}_f$  are solutions of

$$\left[ \frac{1}{2} \nabla_{\underline{r}_1}^2 + \frac{1}{2} \nabla_{\underline{r}_2}^2 + \frac{Z_A}{s_1} + \frac{Z_A}{s_2} - \frac{Z_A Z_B}{R} - \frac{i}{2} \underline{v} \cdot \nabla_{\underline{r}_1} - \frac{i}{2} \underline{v} \cdot \nabla_{\underline{r}_2} + i \frac{\partial}{\partial t} \right] \mathcal{L}_i(\underline{s}_1, \underline{s}_2, t) = - \sum_{j=1}^2 \left[ \nabla_{\underline{r}_j} \log_e \phi_i(\underline{x}_1, \underline{x}_2) \right] \cdot \left[ \nabla_{\underline{r}_j} \mathcal{L}_i(\underline{s}_1, \underline{s}_2, t) \right] , \quad (1.2.31)$$

$$\left[ \frac{1}{2} \nabla_{\underline{r}_1}^2 + \frac{1}{2} \nabla_{\underline{r}_2}^2 + \frac{Z_B}{x_1} + \frac{Z_A}{s_2} - \frac{1}{x_{12}} - \frac{Z_A Z_B}{R} + \frac{i}{2} \underline{v} \cdot \nabla_{\underline{r}_1} - \frac{i}{2} \underline{v} \cdot \nabla_{\underline{r}_2} + \frac{i\partial}{\partial t} \right] \times$$

$$\mathcal{L}_f(\underline{x}_1, \underline{s}_2, t) = - \sum_{j=1}^2 \left[ \nabla_{\underline{r}_j} \log_e \left\{ \psi_{f_1}(\underline{s}_1) \chi_{f_2}(\underline{x}_2) \right\} \right] \cdot \left[ \nabla_{\underline{r}_j} \mathcal{L}_f(\underline{x}_1, \underline{s}_2, t) \right]$$

(1.2.32)

Equations (1.2.31) and (1.2.32) are exact. The exact solution to  $\mathcal{L}_i$  and  $\mathcal{L}_f$  cannot be obtained without solving the complete scattering problem. First-order approximations to  $\mathcal{L}_i$  and  $\mathcal{L}_f$ , denoted by  $\mathcal{L}'_i$  and  $\mathcal{L}'_f$ , are obtained by neglecting the right-hand sides of equations (1.2.31) and (1.2.32). In solving such equations for  $\mathcal{L}'_i$  and  $\mathcal{L}'_f$  attention should be paid to the fact that the dominant contribution to the single electron-capture amplitude in reaction (1.2.1) comes from the region of small values of  $|\underline{x}_2|$ . This implies that in the equations for  $\mathcal{L}'_i$  and  $\mathcal{L}'_f$  we can replace  $1/s_2$  by  $1/R$  and  $1/x_{12}$  by  $1/x_1$  to a good approximation. We will refer to this as the 'perfect-screening' approximation, since we are effectively saying that the 'passive' electron perfectly screens the target nucleus such that the 'active' electron experiences a charge of  $Z_B - 1$ . In this way the coordinate  $s_2$  of the 'passive' electron disappears from these equations reducing our two-electron problem to a one-electron problem. The functions  $\mathcal{L}'_i$  and  $\mathcal{L}'_f$  then become solutions of

$$\left( \frac{1}{2} \nabla_{\underline{r}_1}^2 + \frac{Z_A}{s_1} - \frac{Z_A(Z_B - 1)}{R} - \frac{i}{2} \underline{v} \cdot \nabla_{\underline{r}_1} + \frac{i\partial}{\partial t} \right) \mathcal{L}'_i(\underline{s}_1, t) = 0$$

(1.2.33)

and

$$\left( \frac{1}{2} \nabla_{\underline{r}_1}^2 + \frac{(Z_B - 1)}{x_1} - \frac{Z_A(Z_B - 1)}{R} + \frac{i}{2} \underline{v} \cdot \nabla_{\underline{r}_1} + \frac{i\partial}{\partial t} \right) \mathcal{L}'_f(\underline{x}_1, t) = 0,$$

(1.2.34)

with the boundary conditions

$$\lim_{t \rightarrow -\infty} \mathcal{L}'_i = \exp \left\{ \frac{iZ_A(Z_B - 2)}{v} \ln(vR - v^2 t) \right\}$$

(1.2.35)

and

$$\lim_{t \rightarrow +\infty} \mathcal{L}'_f = \exp \left\{ -i \frac{(Z_A - 1)(Z_B - 1)}{v} \ln(vR + v^2 t) \right\} . \quad (1.2.36)$$

Solving\* for  $\mathcal{L}'_i$  and  $\mathcal{L}'_f$  we obtain

$$\mathcal{L}'_i(\underline{s}_1, t) = N_A(v) {}_1F_1 \left[ i\nu_1; 1; i(vs_1 + \underline{v} \cdot \underline{s}_1) \right] \exp \left\{ \frac{iZ_A(Z_B - 1)}{v} \ln(vR - v^2 t) \right\} \quad (1.2.37)$$

and

$$\mathcal{L}'_f(\underline{x}_1, t) = N_B^*(v) {}_1F_1 \left[ -i\nu_2; 1; -i(vx_1 + \underline{v} \cdot \underline{x}_1) \right] \exp \left\{ \frac{-iZ_A(Z_B - 1)}{v} \ln(vR + v^2 t) \right\} , \quad (1.2.38)$$

where

$$N_A(v) = e^{\pi \nu_1 / 2} \Gamma(1 - i\nu_1) \quad (1.2.39a)$$

$$\nu_1 = Z_A / v \quad (1.2.39b)$$

$$N_B^*(v) = e^{\pi \nu_2 / 2} \Gamma(1 + i\nu_2) \quad (1.2.40a)$$

$$\nu_2 = (Z_B - 1) / v . \quad (1.2.40b)$$

The confluent hypergeometric functions  ${}_1F_1$  are the coulomb wavefunctions that describe the distortion of the active electron by a coulomb potential, and have the following asymptotic forms

$$N_A(v) {}_1F_1 \left[ i\nu_1; 1; i(vs + \underline{v} \cdot \underline{s}) \right] \underset{s \rightarrow \infty}{\sim} \exp \left\{ -\frac{iZ_A}{v} \ln(vs + \underline{v} \cdot \underline{s}) \right\} , \quad (1.2.41)$$

and

$$N_B^*(v) {}_1F_1 \left[ -i\nu_2; 1; -i(vx + \underline{v} \cdot \underline{x}) \right] \underset{x \rightarrow \infty}{\sim} \exp \left\{ +\frac{i(Z_B - 1)}{v} \ln(vx + \underline{v} \cdot \underline{x}) \right\} . \quad (1.2.42)$$

It follows that the boundary conditions (1.2.35) and (1.2.36) are obeyed

since we have

$$\lim_{t \rightarrow -\infty} \ln \left\{ \frac{vR - v^2 t}{vs + \underline{v} \cdot \underline{s}} \right\} = 0 \quad (1.2.43a)$$

\* see reference 25, P. 239

and

$$\lim_{t \rightarrow +\infty} \ln \left\{ \frac{vR + v^2 t}{vx + v \cdot \underline{x}} \right\} = 0 \quad (1.2.43b)$$

We now look for solutions of the distorted wave equations (1.2.14) and (1.2.15) in the form

$$\chi_i(\underline{r}_1, \underline{r}_2, t) = \Omega_i(\underline{r}_1, \underline{r}_2, t) \mathcal{L}'_i(\underline{s}_1, t) \quad (1.2.44)$$

and

$$\chi_f(\underline{r}_1, \underline{r}_2, t) = \Omega_f(\underline{r}_1, \underline{r}_2, t) \mathcal{L}'_f(\underline{x}_1, t) \quad (1.2.45)$$

by making the appropriate choice for the distorting potentials  $U_i$  and  $U_f$ .

In the CDW method these turn out to be

$$U_i = \frac{Z_A}{s_1} + \frac{Z_A}{s_2} - \frac{2Z_A}{R} + A_i \quad (1.2.46)$$

and

$$U_f = \frac{Z_B}{x_1} + \frac{Z_A}{s_2} - \frac{1}{x_{12}} - \frac{Z_B}{R} - \frac{Z_A}{R} + \frac{1}{R} + A_f, \quad (1.2.47)$$

where  $A_i$  and  $A_f$  are perturbing potentials that vanish at large internuclear separations and are chosen so as to obtain the desired solutions for  $\chi_i$  and  $\chi_f$ . Substituting (1.2.44) and (1.2.45) into equations (1.2.14) and (1.2.15) we find that  $\mathcal{L}'_i$  and  $\mathcal{L}'_f$  are given by equations (1.2.33) and (1.2.34) provided we define the potential operators  $A_{i,f}$  such that

$$A_i \chi_i = -\Omega_i \left[ \nabla_{\underline{r}_1} \log_e \phi_i(\underline{x}_1, \underline{x}_2) \right] \cdot \left[ \nabla_{\underline{r}_1} \mathcal{L}'_i(\underline{s}_1, t) \right] \quad (1.2.48)$$

and

$$A_f \chi_f = -\Omega_f \left[ \nabla_{\underline{r}_1} \log_e \left\{ \psi_{f_1}(\underline{s}_1) \chi_{f_2}(\underline{x}_2) \right\} \right] \cdot \left[ \nabla_{\underline{r}_1} \mathcal{L}'_f(\underline{x}_1, t) \right]. \quad (1.2.49)$$

Substituting for  $U_i$  and  $U_f$  in equations (1.2.25) and 1.2.26), we obtain

$$a_{if} = -i \int_{-\infty}^{+\infty} dt \int d\underline{r}_1 d\underline{r}_2 A_i \chi_i \Psi_f^* \quad (1.2.51)$$

and

$$b_{if} = -i \int_{-\infty}^{+\infty} dt \int d\underline{r}_1 d\underline{r}_2 A_f^* \chi_f^* \Psi_i. \quad (1.2.52)$$

The continuum distorted wave approximation consists of the replacement of  $\Psi_i, \Psi_f$  in equations (1.2.26) and (1.2.25) by  $\chi_i, \chi_f$  respectively.

It is easily seen that in this approximation the distorted wavefunctions

$\chi_i$  and  $\chi_f$  have the correct asymptotic conditions: from equations (1.2.44)

and (1.2.45) we have that  $\chi_i = \Omega_i \mathcal{L}'_i$  and  $\chi_f = \Omega_f \mathcal{L}'_f$  ;

therefore, by virtue of equations (1.2.35) and (1.2.36),

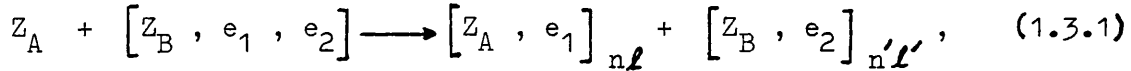
$$\chi_i \xrightarrow[t \rightarrow -\infty]{} \Phi_i \xrightarrow[t \rightarrow -\infty]{} \Psi_i \quad \text{and} \quad \chi_f \xrightarrow[t \rightarrow +\infty]{} \Phi_f \xrightarrow[t \rightarrow +\infty]{} \Psi_f, \quad \text{which}$$

are the required conditions.

CHAPTER 1.3

Evaluation of the CDW cross-section

Let us now examine, in detail, the evaluation of the CDW cross-section  $\sigma_{if} = \sigma[nl, n'l']$  for the general reaction



where the target atom will be considered to be in its ground state - hence  $i = 1s^2$ , and  $n\ell = 1s, 2s,$  and  $2p$ . The nature of the steps involved will depend upon the type of wavefunction employed to describe the ground-state target atom. In the present work we describe the two-electron target atom by the natural expansion<sup>22</sup> of the 35-term configuration-interaction (CI) wavefunction of Weiss<sup>16</sup>, which is of the general form

$$\Psi_x(1, 2) = N_x \sum_{i=1}^x \frac{c_i}{(2\ell_i+1)^{\frac{1}{2}}} \sum_{m=-\ell_i}^{\ell_i} \Omega_m^i(1) \Omega_m^i(2) \quad (1.3.2)$$

The Weiss function is given by  $x = 15$  although varying approximations to

$\Psi_x(1,2)$  can be obtained by suitable truncation of the expansion in (1.3.2). The normalised natural orbitals  $\Omega_m^i$  are linear combinations of the fifteen normalised STO's,  $\mathcal{C}_{n_j, \ell_j, m}$ , used by Weiss in the construction of his CI wavefunction:

$$\Omega_m^i = \sum_{j=1}^{15} b_j^i \mathcal{C}_{n_j, \ell_j, m} \quad (1.3.3)$$

For ease of discussion and to assist in writing down the equations we

re-write  $\Psi_x(1,2)$  as

$$\Psi_x(\underline{x}_1, \underline{x}_2) = D_{\alpha\beta\gamma} \mathcal{C}_{\alpha\beta}(\underline{x}_1) \mathcal{C}_{\alpha\gamma}(\underline{x}_2), \quad (1.3.4)$$

where

$$D_{\alpha\beta\gamma} = N_x \sum_{\alpha=1}^x \frac{c_\alpha}{(2\ell_\alpha+1)^{\frac{1}{2}}} \sum_{m=-\ell_\alpha}^{+\ell_\alpha} \sum_{\beta=1}^{15} \sum_{\gamma=1}^{15} b_\beta^\alpha b_\gamma^\alpha, \quad (1.3.5)$$

$$\psi_{\alpha\beta}(\underline{x}_1) = R_{\alpha\beta}(\underline{x}_1) Y_{l\alpha}^m(\theta_{x_1}, \phi_{x_1}), \quad (1.3.6)$$

$$\psi_{\alpha\gamma}(\underline{x}_2) = R_{\alpha\gamma}(\underline{x}_2) Y_{l\alpha}^{-m}(\theta_{x_2}, \phi_{x_2}), \quad (1.3.7)$$

and

$$R_{\alpha\beta}(\underline{r}) = N(\eta_\beta, \xi_\beta) r^{\eta_\beta - 1} e^{-\xi_\beta r}. \quad (1.3.8)$$

The functions  $\psi_{\alpha\beta}(\underline{x}_1)$  and  $\psi_{\alpha\gamma}(\underline{x}_2)$  represent the basis orbitals describing the 'active' and 'passive' electrons, respectively, within the natural expansion and  $N_x$  and  $N(\eta_\beta, \xi_\beta)$  are the appropriate normalisation constants. The following analysis is general for any two-electron wavefunction which is separable into the form (1.3.4) and thus the steps involved can easily be reduced or adapted to the case of an HF or split-shell ( $1s1s'$ ) wavefunction<sup>23</sup>, i.e.

$$\Psi_{\text{HF}}(1,2) = N \phi(\underline{x}_1) \phi(\underline{x}_2) \quad (1.3.9)$$

$$\Psi_{1s1s'}(1,2) = \frac{N}{\sqrt{2}} \left[ \phi_\alpha(\underline{x}_1) \phi_\beta(\underline{x}_2) + \phi_\beta(\underline{x}_1) \phi_\alpha(\underline{x}_2) \right]. \quad (1.3.10)$$

The transition amplitude we wish to evaluate is given by equation (1.2.51)

$$a(nl, n'l') = -i \int_{-\infty}^{+\infty} dt \int d\underline{r}_1 d\underline{r}_2 A_i \chi_i \Psi_f^*, \quad (1.3.11)$$

where

$$A_i \chi_i = -\Phi_i \left[ \nabla_{\underline{r}_1} \log_e \Psi_x(\underline{x}_1, \underline{x}_2) \right] \cdot \left[ \nabla_{\underline{r}_1} \mathcal{L}'_i(\underline{s}_1, t) \right]. \quad (1.3.12)$$

The integral representation for the coulomb function<sup>24</sup> is given by

$${}_1F_1(i\nu; 1; iq) = \frac{1}{2\pi i} \oint \frac{d\omega}{\omega} \left(1 + \frac{1}{\omega}\right)^{-i\nu} e^{-i\omega q}, \quad (1.3.13)$$

where the contour encloses the points 0 and -1. Substituting for  $\mathcal{L}'_i$  from equation (1.2.37) and making use of the representation (1.3.13), equation (1.3.12) then becomes

$$A_i \chi_i = -\oint_i \nabla_{\underline{r}_1} \log_e \Psi_x(\underline{x}_1, \underline{x}_2) \cdot \nabla_{\underline{r}_1} \left\{ \frac{N_A(v)}{2\pi i} \oint \frac{d\omega}{\omega} \left(1 + \frac{1}{\omega}\right)^{-i\nu_i} x \right. \\ \left. e^{-i\omega(vs_1 + \underline{v} \cdot \underline{s}_1)} \exp \left[ \frac{iZ}{v} \mathcal{L}_n(vR - v^2t) \right] \right\}, \quad (1.3.14)$$

where  $Z = Z_A(Z_B - 1)$ . Therefore,

$$a(nl, n'l') = -i \int_{-\infty}^{+\infty} dt \int d\underline{r}_1 \int d\underline{r}_2 \left\{ \frac{v}{2\pi} N_A(v) \exp \left[ \frac{iZ}{v} \mathcal{L}_n(vR - v^2t) \right] \Omega_i x \right. \\ \left. \left[ \frac{\underline{s}_1 \cdot \underline{x}_1}{s_1 x_1} + \frac{\underline{v} \cdot \underline{x}_1}{v x_1} \right] \frac{\partial}{\partial x_1} \left[ \log_e \Psi_x(\underline{x}_1, \underline{x}_2) \right] \oint d\omega \left(1 + \frac{1}{\omega}\right)^{-i\nu_i} x \right. \\ \left. e^{-i\omega(vs_1 + \underline{v} \cdot \underline{s}_1)} \right\} \Psi_f^*. \quad (1.3.15)$$

Replacing  $\Psi_f^*$  by  $\chi_f^* = \Omega_f^* \mathcal{L}_f^*$ , and substituting for  $\Omega_f^*$  and  $\Omega_i$ , we obtain

$$a(nl, n'l') = -\frac{vN_A(v)N_B(v)}{4\pi^2} (bv)^{2iZ/v} \int_{-\infty}^{+\infty} dt e^{-i\Delta\epsilon t} \oint d\omega \oint \frac{d\xi}{\xi} x \\ \left(1 + \frac{1}{\omega}\right)^{-i\nu_1} \left(1 + \frac{1}{\xi}\right)^{-i\nu_2} \int d\underline{r}_1 \int d\underline{r}_2 \Psi_{nl}^*(\underline{s}_1) \chi_{n'l'}^*(\underline{x}_2) \frac{\partial}{\partial x_1} \Psi_x(\underline{x}_1, \underline{x}_2) x \\ e^{-i \underline{v} \cdot \underline{r}_1} e^{-i\omega(vs_1 + \underline{v} \cdot \underline{s}_1)} e^{-i\xi(vx_1 + \underline{v} \cdot \underline{x}_1)} \left[ \frac{\underline{s}_1 \cdot \underline{x}_1}{s_1 x_1} + \frac{\underline{v} \cdot \underline{x}_1}{v x_1} \right], \quad (1.3.16)$$

where  $\Psi_x(\underline{x}_1, \underline{x}_2)$ ,  $\psi_{nl}(\underline{s}_1)$ ,  $\chi_{n'l'}(\underline{x}_2)$  are the target atom, the final capture state and residual target atom electronic wavefunctions with the corresponding eigenenergies  $\epsilon_B(1s^2)$ ,  $\epsilon_A(nl)$  and  $\epsilon_B(n'l')$  and where the energy decrement  $\Delta\epsilon = \epsilon_B(1s^2) - \epsilon_A(nl) - \epsilon_B(n'l')$ . Equation (1.3.16) may be re-written in the form

$$a(nl, n'l') = -\frac{vN_A(v)N_B(v)}{4\pi^2} (bv)^{2iZ/v} D_{\alpha\beta\gamma} \int_{-\infty}^{+\infty} dt e^{-i\Delta\epsilon t} \oint d\omega \oint \frac{d\xi}{\xi} x \\ \left(1 + \frac{1}{\omega}\right)^{-i\nu_1} \left(1 + \frac{1}{\xi}\right)^{-i\nu_2} I_{\alpha\beta} R_{\alpha\beta}, \quad (1.3.17)$$

where  $I_{\alpha\beta} = \int d\underline{r}_2 \chi_{1s}^*(\underline{x}_2) \mathcal{U}_{\alpha\beta}(\underline{x}_2)$  (1.3.18)

and

$$R_{\alpha\beta} = \int d\underline{r}_1 \psi_{nl}^*(\underline{s}_1) \frac{\partial}{\partial x_1} \mathcal{U}_{\alpha\beta}(\underline{x}_1) e^{-i\underline{v} \cdot \underline{r}_1} e^{-i\omega(v s_1 + \underline{v} \cdot \underline{s}_1)} \times$$

$$e^{-i\xi(\underline{v} x_1 + \underline{v} \cdot \underline{x}_1)} \left[ \frac{\underline{v} \cdot \underline{x}_1}{v x_1} + \frac{\underline{s}_1 \cdot \underline{x}_1}{s_1 x_1} \right]. \quad (1.3.19)$$

Using the Fourier transform method of evaluating two-centre integrals\*,

it is easily shown that

$$a(nl, n'l') = - \frac{v N_A(v) N_B(v)}{4\pi^2 (2\pi)^6} (bv)^{2iZ/v} D_{\alpha\beta\gamma} \int_{-\infty}^{+\infty} dt e^{-i\Delta E t} \oint d\omega \oint \frac{d\xi}{\xi} \times$$

$$\left(1 + \frac{1}{\omega}\right)^{-i\gamma_1} \left(1 + \frac{1}{\xi}\right)^{-i\gamma_2} I_{\alpha\beta} \int d\underline{r}_1 e^{-i\underline{v} \cdot \underline{r}_1} \int d\underline{k} \int d\underline{K} F_{nl}^*(\underline{k}) G_{\alpha\beta}(\underline{K}) \times$$

$$e^{i\underline{k} \cdot \underline{s}_1} e^{-i\underline{K} \cdot \underline{x}_1}, \quad (1.3.20)$$

where

$$F_{nl}^*(\underline{k}) G_{\alpha\beta}(\underline{K}) = \int d\underline{s}_1 \int d\underline{x}_1 \psi_{nl}^*(\underline{s}_1) e^{-i\omega(v s_1 + \underline{v} \cdot \underline{s}_1)} \times$$

$$e^{-i\underline{k} \cdot \underline{s}_1} \frac{\partial}{\partial x_1} \mathcal{U}_{\alpha\beta}(\underline{x}_1) e^{-i\xi(\underline{v} x_1 + \underline{v} \cdot \underline{x}_1)} e^{i\underline{K} \cdot \underline{x}_1} \left[ \frac{\underline{v} \cdot \underline{x}_1}{v x_1} + \frac{\underline{s}_1 \cdot \underline{x}_1}{s_1 x_1} \right]. \quad (1.3.21)$$

After noting that

$$\frac{\underline{s} \cdot \underline{x}}{s x} = \cos \theta_x \cos \theta_s + \sin \theta_x \sin \theta_s \cos(\phi_s - \phi_x)$$

$F^*(\underline{k}) G(\underline{K})$  then becomes

$$F^*(\underline{k}) G(\underline{K}) = \sum_{m=1}^4 f_m^*(\underline{k}) g_m(\underline{K}), \quad (1.3.22)$$

\* see reference 25, p.213.

where

$$f_1^*(\underline{k}) = \int \psi_{nl}(\underline{s}_1) e^{i\omega q} e^{i\underline{k} \cdot \underline{s}_1} d\underline{s}_1 \quad (1.3.23)$$

$$f_2^*(\underline{k}) = \int \psi_{nl}(\underline{s}_1) e^{i\omega q} \cos \theta_{s_1} e^{i\underline{k} \cdot \underline{s}_1} d\underline{s}_1 \quad (1.3.24)$$

$$f_3^*(\underline{k}) = \int \psi_{nl}(\underline{s}_1) e^{i\omega q} \sin \theta_{s_1} \cos \phi_{s_1} e^{i\underline{k} \cdot \underline{s}_1} d\underline{s}_1 \quad (1.3.25)$$

$$f_4^*(\underline{k}) = \int \psi_{nl}(\underline{s}_1) e^{i\omega q} \sin \theta_{s_1} \sin \phi_{s_1} e^{i\underline{k} \cdot \underline{s}_1} d\underline{s}_1 \quad (1.3.26)$$

with

$$q = v s_1 + \underline{v} \cdot \underline{s}_1, \quad (1.3.27)$$

and

$$g_1(\underline{K}) = g_2(\underline{K}) = \int \frac{\partial}{\partial x_1} \mathcal{Q}_{\alpha\beta}(\underline{x}_1) e^{-i\underline{\xi} \cdot \underline{P}} \cos \theta_{x_1} e^{i\underline{K} \cdot \underline{x}_1} d\underline{x}_1 \quad (1.3.28)$$

$$g_3(\underline{K}) = \int \frac{\partial}{\partial x_1} \mathcal{Q}_{\alpha\beta}(\underline{x}_1) e^{-i\underline{\xi} \cdot \underline{P}} \sin \theta_{x_1} \cos \phi_{x_1} e^{i\underline{K} \cdot \underline{x}_1} d\underline{x}_1 \quad (1.3.29)$$

$$g_4(\underline{K}) = \int \frac{\partial}{\partial x_1} \mathcal{Q}_{\alpha\beta}(\underline{x}_1) e^{-i\underline{\xi} \cdot \underline{P}} \sin \theta_{x_1} \sin \phi_{x_1} e^{i\underline{K} \cdot \underline{x}_1} d\underline{x}_1 \quad (1.3.30)$$

with  $\underline{P} = v \underline{x}_1 + \underline{v} \cdot \underline{x}_1$ .

The  $f$  and  $g$  integrals were then evaluated by making use of the expansions

$$e^{-i\underline{k} \cdot \underline{s}} = \left(\frac{2\pi}{ks}\right)^{\frac{1}{2}} \sum_{\ell=0}^{\infty} \frac{(2\ell+1)}{2} i^{\ell} J_{\ell+\frac{1}{2}}(ks) P_{\ell}(\cos \theta_{ks}) \quad (1.3.31)$$

and

$$P_{\ell}(\cos \theta_{ks}) = \frac{4\pi}{(2\ell+1)} \sum_{m=-\ell}^{\ell} Y_{\ell,m}^*(\theta_s, \phi_s) Y_{\ell,m}(\theta_k, \phi_k). \quad (1.3.32)$$

Returning now to equation (1.3.20) we have, for the coordinate system describing the collision process (see Figure 1.1), the relationships  $\underline{x}_1 = r_1 + \frac{1}{2}\underline{R}$  and  $\underline{s}_1 = \underline{r}_1 - \frac{1}{2}\underline{R}$ . Substituting for  $\underline{x}_1$  and  $\underline{s}_1$  using the Dirac relationships

$$(2\pi)^{-3} \int e^{i(\underline{k}-\underline{k}_0) \cdot \underline{r}} d\underline{r} = \delta(\underline{k} - \underline{k}_0) \quad (1.3.33a)$$

and

$$\int f(\underline{k}) \delta(\underline{k} - \underline{k}_0) d\underline{k} = f(\underline{k}_0) \quad (1.3.33b)$$

we can then integrate over the variables  $\underline{r}_1$  and  $\underline{k}$  in equation (1.3.20).

The substitution  $u = vt$  and use of (1.3.33a) enables us to evaluate the integral over time  $t$ . Taking cartesian coordinates for  $\underline{K}$  and  $\underline{y}$  with  $\underline{y}$  defining the  $z$ -direction we may then integrate over  $K_z$  by making further use of equations (1.3.33a-33b). The result is

$$a(nl, n'l') = - \frac{N_Z(v) N_B(v)}{4\pi^2 (2\pi)^2} (bv)^{2iZ/v} D_{\alpha\beta\gamma} \oint d\omega \oint \frac{d\xi}{\xi} \left(1 + \frac{1}{\omega}\right)^{-i\gamma_1} \times \\ \left(1 + \frac{1}{\xi}\right)^{-i\gamma_2} I_{\alpha\gamma} \int_{-\infty}^{+\infty} dK_x e^{-ibK_x} \int_{-\infty}^{+\infty} dK_y F_{nl}^*(K_x, K_y, \frac{v}{2} - \frac{\Delta E}{v}) G_{\alpha\beta}(K_x, K_y, \frac{v}{2} - \frac{\Delta E}{v}). \quad (1.3.34)$$

By making the substitution  $K_y = \eta \cos \theta$  and  $K_x = \eta \sin \theta$  and then integrating over  $\theta$ ,  $\omega$  and  $\xi$  the expression for  $a(nl, n'l')$  may be

$$\text{reduced further to yield} \\ a(nl, n'l') = -(bv)^{2iZ/v} \int_0^\infty \eta^{q+1} J_q(b\eta) W_{nl, n'l'}(\eta) d\eta, \quad (1.3.35)$$

where  $q = 0$  for  $nl = 1s, 2s, 2p_z$  and  $q = 1$  for  $nl = 2p_x$ ;

$J_q(b\eta)$  is a Bessel function of order  $q$  and  $W_{nl, n'l'}(\eta)$  is given by

$$W_{nl, n'l'}(\eta) = N_x \sum_{\alpha=1}^x \frac{c_\alpha}{(2l_\alpha+1)^{\frac{1}{2}}} \sum_{m=-l_\alpha}^{+l_\alpha} \sum_{\beta=1}^{15} \sum_{\gamma=1}^{15} b_\beta^\alpha b_\gamma^\alpha I_{\alpha\gamma}(\mathcal{Q}_{\alpha\beta}(x_2) | \chi_{nl}(x_2)) \\ f_1(\eta, v, \mathcal{Q}_{\alpha\beta}(x_1), \Delta E) \cdot g_1(\eta, v, \mathcal{Q}_{\alpha\beta}(x_1), \psi_{nl}(s_1), v_1, v_2, \Delta E). \quad (1.3.36)$$

We note here that in the evaluation of the integrals in (1.3.34) the polar axis  $\underline{z}$  is defined along the direction of the velocity  $\underline{y}$  of the incident projectile and the impact parameter  $\underline{b}$  is chosen to lie along the  $x$ -axis. As a consequence of this choice the cross-section for capture into the  $2p$  state of projectile A is given by

$$\sigma(2p, n'l') = \sigma(2p_z, n'l') + \sigma(2p_x, n'l') \quad (1.3.37)$$

since, in the present mathematical framework,  $\sigma(2p_y, n'l')$  is identically zero.

Before proceeding with the evaluation of  $\sigma(nl, n'l')$  it is of interest to examine the quantity  $I_{\alpha\gamma}$  defined in equation (1.3.18).  $I_{\alpha\gamma}$  is the overlap integral between the initial and final-state orbitals of the 'passive' (or uncaptured) electron. This is easily demonstrated since by using the Fourier transform technique we have that

$$I_{\alpha\gamma} = \int d\underline{r}_2 \chi_{n'l'}^*(\underline{x}_2) \mathcal{Q}_{\alpha\gamma}(\underline{x}_2) = h_{\alpha\gamma}^* (\underline{L} = 0) ,$$

where, generally,

$$h_{\alpha\gamma}(\underline{L}) = \int \chi_{n'l'}(\underline{x}_2) \mathcal{Q}_{\alpha\gamma}(\underline{x}_2) e^{i\underline{L} \cdot \underline{x}_2} d\underline{x}_2 ,$$

which means

$$I_{\alpha\gamma} = \int \chi_{n'l'}(\underline{x}_2) \mathcal{Q}_{\alpha\gamma}(\underline{x}_2) d\underline{x}_2 \quad (1.3.38)$$

The wavefunction  $\chi_{n'l'}(\underline{x}_2)$  is the description of the residual target atom and, in our case,  $\mathcal{Q}_{\alpha\gamma}(\underline{x}_2)$  are the basis orbitals used in describing the 'passive' electron within the natural expansion representation of the target wavefunction. From a correlation point of view, the behaviour of  $I_{\alpha\gamma}$  has a significant effect on the transition amplitude. The wavefunction  $\chi_{n'l'}(\underline{x}_2)$  is given by

$$\chi_{n'l'}(\underline{x}_2) = R_{n'l'}(\underline{x}_2) Y_{l'}^{m'}(\theta_{x_2}, \phi_{x_2}) \quad (1.3.39)$$

Therefore

$$I_{\alpha\gamma} = \int R_{n'l'}(\underline{x}_2) R_{\alpha\gamma}(\underline{x}_2) Y_{l'}^{m'}(\theta_{x_2}, \phi_{x_2}) Y_{l\alpha}^{-m}(\theta_{x_2}, \phi_{x_2}) d\underline{x}_2 , \quad (1.3.40)$$

where we have made use of equation (1.3.7). Consider the integral over the azimuthal angle  $\phi_{x_2}$ ; the integral will be of the form

$$\int_0^{2\pi} e^{i(m' - m)\phi_{x_2}} d\phi_{x_2} = \begin{cases} 2\pi & \text{if } m = m' \\ 0 & \text{if } m \neq m' \end{cases} \quad (1.3.41)$$

and therefore  $m$  is restricted to the value of  $m'$ . This means that equation (1.3.40) can be written as

$$I_{\alpha\gamma} = \int_0^{\infty} R_{n'l'}(x_2) R_{\alpha\gamma}(x_2) x_2^2 dx_2 \int_0^{\pi} \int_0^{2\pi} Y_{l'}^m(\theta_{x_2}, \phi_{x_2}) Y_{l\alpha}^{-m}(\theta_{x_2}, \phi_{x_2}) \sin\theta_{x_2} d\theta_{x_2} d\phi_{x_2} \quad (1.3.42)$$

However, we know that

$$\int_0^{\pi} \int_0^{2\pi} Y_{l'}^m(\theta_{x_2}, \phi_{x_2}) Y_{l\alpha}^{-m}(\theta, \phi) \sin\theta d\theta d\phi = \begin{cases} 1 & \text{if } l\alpha = l' \\ 0 & \text{if } l\alpha \neq l' \end{cases} \quad (1.3.43)$$

Thus, the contributions to  $\sigma(nl, n'l')$  from all natural configurations using basis functions with  $l\alpha \neq l'$  will be zero. If we consider the most likely case, when  $n'l' = 1s$ , then only radial correlation terms within the target wavefunction will contribute to the cross-section  $\sigma[nl, 1s]$ . It is also evident that if we were considering, for example, a process in which the residual target atom is left in a 2p state then only configurations involving  $l\alpha = 1$  will contribute to the cross-section. Consequently, within the present approximation, a zero cross-section would be predicted for such a process unless angular correlation is included in the description of the target atom ground state. The orthogonality condition (1.3.43) in  $I_{\alpha\gamma}$  has arisen because, in equations (1.2.33-34), we have eliminated the 'passive' electron from the distorted wavefunction  $\chi_i'$  and  $\chi_f'$ . If this had not been done, an operator of the type  $e^{i\omega'(v\mathbf{s}_2 + \mathbf{v} \cdot \mathbf{s}_2)}$  would have been introduced into  $I_{\alpha\gamma}$  - destroying the orthogonality condition and therefore retaining contributions from all angular-type correlation terms.

In order to evaluate  $\sigma[nl, n'l']$  it is not necessary to perform the integration in (1.3.35) since, by substituting equation (1.3.35) into (1.2.28) and noting that

$$\sqrt{\eta\eta'} \int_0^{\infty} J_t(b\eta) J_t(b\eta') b db = \delta(\eta - \eta'), \quad (1.3.44)$$

where the order  $t$  is arbitrary, we obtain for the capture cross-section

$$\sigma [nl, n'l'] = 4 \int_0^{\infty} \eta^{2q+1} |W_{nl, n'l'}(\eta)|^2 d\eta. \quad (1.3.45)$$

In the above equation  $q = 0$  for  $nl = 1s, 2s, 2p_z$  and  $q = 1$  for  $nl = 2p_x$ .

Let us now restrict the description of the target atom ground-state wavefunction to that of an HF wavefunction (see equation (1.3.9)). The form for  $W_{nl, n'l'}(\eta)$  is easily obtained by considering only the first term in the expansion (1.3.2), setting  $c_j = 1$  and removing the summation over  $m$  since  $l_j = 0$  for a  $1^1S$  state. The cross-section can now be written

$$\sigma (nl, n'l') = 4 \left\{ I \left( \sum_{\beta} b_{\beta} \varphi_{\beta}(\underline{x}_2) \mid \chi_{n'l'}(\underline{x}_2) \right) \right\}^2 \cdot \int_0^{\infty} \left| \sum_{\beta} b_{\beta} f_1(\eta, \nu, \varphi_{\beta}(\underline{x}_1), \Delta E) \cdot g_1(\eta, \nu, \varphi_{\beta}(\underline{x}_1), \Psi_{nl}(\underline{s}_1), \nu_1, \nu_2, \Delta E) \right|^2 d\eta, \quad (1.3.46)$$

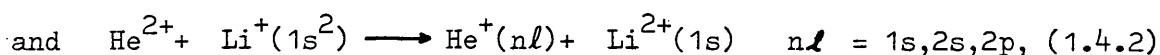
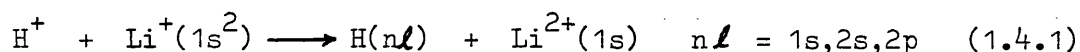
where the functional form of  $f_1$  contains the initial orbital description of electron 1 whilst  $g_1$  involves the orbital description of the active electron in both its initial,  $\varphi_{\beta}(\underline{x}_1)$ , and final capture state,

$\Psi_{nl}(\underline{s}_1)$ . We note that in  $g_1$  the initial and final capture-state are linked together in an intricate manner due to the distortion in the outward channel via  $\nu_2$ ; this feature will prove to be of importance when we analyse our results in Chapters 1.4 and 1.5.

## CHAPTER 1.4

### Electron-capture from $\text{Li}^+$ by fast protons and alpha-particles

In this chapter we present and discuss our results for the capture cross-sections  $\sigma(nl)$  obtained within the continuum distorted wave (CDW) approximation for the reactions



for the impact energy range  $100 \text{ keV} \ll E \ll 3000 \text{ keV}$  and  $100 \text{ keV} \ll E \ll 10 \text{ MeV}$ , respectively. The ground-state  $\text{Li}^+$  atom was described by the 35 term configuration interaction (CI) wavefunction of Weiss<sup>16</sup> expressed in its natural expansion form, and in order to assess the influence of electron correlation calculations were also performed using the  $\text{Li}^+$  HF wavefunction of Clementi and Roetti<sup>26</sup>. The cross-sections correspond to the 'prior' form of the CDW transition amplitude  $a_{if}$ , see equations (1.3.11 - 16), and the results for the above reactions are presented in Tables 1.1 and 1.2, respectively. The total cross-section  $Q$  is calculated using the Oppenheimer<sup>7</sup>  $n^{-3}$  rule by means of the formula

$$Q = \sum_{n,\ell} \sigma(n\ell) \approx \sigma(1s) + 1.616(\sigma(2s) + \sigma(2p)). \quad (1.4.3)$$

We note that the cross-section  $\sigma(2p)$  is given by  $\sigma(2p) = \sigma(2p_z) + \sigma(2p_x)$ , since, as a consequence of our coordinate system, we have that

$\sigma(2p_y) = 0$ . Although we have not tabulated the cross-sections  $\sigma(2p_z)$  and  $\sigma(2p_x)$ , we found that throughout the energy ranges  $\sigma(2p_z) > \sigma(2p_x)$ .

Of particular interest to us are the percentage changes,  $\Delta$  (HF  $\rightarrow$  CI), in cross-sections due to improving the  $\text{Li}^+$  wavefunction from the HF to the CI description. These are reported for both  $\text{H}^+$  and  $\text{He}^{2+}$  projectiles

at selected impact energies in Tables 1.3 and 1.4, respectively. Comparing the values of  $\Delta(\text{HF} \rightarrow \text{CI})$  for the three capture states  $n\ell = 1s, 2s$  and  $2p$  we see the same trend that was observed by Banyard and Szuster<sup>14</sup> in their studies on He: that is, for proton projectiles, a strong similarity in the values of  $\Delta(\text{HF} \rightarrow \text{CI})$  for  $\nabla(1s)$  and  $\nabla(2s)$  while both are slightly different from the values for  $\nabla(2p)$ , particularly for large  $E$ . Since the percentage changes for  $\text{Li}^+$  are small this is best seen when

$\Delta(\text{HF} \rightarrow \text{CI})$  is plotted against the proton impact energy, see Figure 1.2.

As the impact energy increases the major contribution to the electron-capture cross-section comes from smaller and smaller impact parameters. This means that the 'active' electron is captured from regions of high momentum within the target atom and consequently is captured into corresponding regions in the final capture state i.e. regions close to the origin. Thus the reason for the trends in  $\Delta(\text{HF} \rightarrow \text{CI})$  is now apparent since the  $2p$  orbital in  $\text{H}(n\ell)$  is quite distinct in shape from the  $1s$  and  $2s$  orbitals and will thus have different high momentum characteristics. In contrast, the  $1s$  and  $2s$  orbitals are very similar in shape at the origin<sup>†</sup>. Throughout the energy range the ordering in cross-sections with respect to the capture state is  $\nabla(1s) > \nabla(2s) > \nabla(2p)$  and  $\nabla(1s)$  is found to represent  $\sim 80\%$  of the total cross-section in the case of proton projectiles and  $\sim 75-80\%$  for alpha-particle projectiles.

In Figure 1.3 we compare our total cross-sections for reaction (1.4.1) with the recent experimental data of Sewell et al<sup>27</sup> and with the earlier experimental curve due to Bodgonav et al<sup>28</sup>. Also shown is the theoretical curve due to Obyedkov and Pavlov<sup>29</sup> obtained using the Brinkman-Kramers method<sup>30</sup>. Unfortunately, experimental data could not be found for  $E > 221$  keV for which the CDW method should become more accurate. The experimental points of Sewell et al<sup>27</sup> appear to reach a

---

<sup>†</sup> see reference 31, page 142

turning point at approximately  $E = 40$  keV, at which the CDW cross-sections become too large. However, for  $E > 200$  keV, the CDW curve appears to be tending towards the experimental curve and we have an agreement within the experimental error bars at  $E = 221$  keV. Our theoretical CDW results strongly suggest that the data of Bogdanov et al is much too low. Their data was obtained from experiments concerned with the formation of a high-temperature plasma in which fast protons are formed within a lithium arc by the dissociation of  $H_2^+$  ions. Bogdanov clearly states that in such a method the study of charge-exchange is complicated by a number of interfering factors, such as charge-exchange with residual gases and the presence in the proton beams of  $H_2^+$  ions with energies equal to half of those of the protons. Thus the experimental data of Sewell et al<sup>27</sup>, obtained using pure proton beams in a standard beam crossing technique, is the more reliable of the two sets of data.

The theoretical curve due to Obyedkov and Pavlov<sup>29</sup> obtained using the Brinkman-Kramers method<sup>30</sup> clearly predicts a different high-energy result from that of the CDW method. However, the success of the CDW method in predicting the correct high energy behaviour of electron-capture cross-sections from one and two-electron atoms<sup>6,10,11</sup> suggests that the curve of Obyedkov and Pavlov may be inaccurate at high impact energies.

## CHAPTER 1.5

### An analysis of trends in capture cross-sections for two-electron targets

In order to compare the three systems  $H^-$ , He and  $Li^+$  as targets for electron-capture we report in Table 1.5 the total cross-sections for both proton and alpha-particle projectiles at selected E; in each case the target electrons are described by the 35-term CI wavefunction of Weiss<sup>16</sup>. To assess and compare the influence of electron correlation within the three systems we also quote, for each E, the percentage change

$\Delta(HF \rightarrow CI)$  in Q when going from the HF to the CI description of the target electrons. The HF wavefunctions for He and  $Li^+$  were those of Clementi and Roetti<sup>26</sup> and for  $H^-$  the fitted function of Curl and Coulson<sup>20</sup> was used. The  $\Delta(HF \rightarrow CI)$  values are seen to reflect a rapid decrease in the importance of electron correlation as we progress from  $H^-$  to  $Li^+$ . For a given target it was also noted that, at a common projectile velocity, the proton and alpha-particle reactions possessed similar

$\Delta(HF \rightarrow CI)$  values - the magnitudes being almost identical at high velocities.

Since the electrons are very weakly bound in the  $H^-$  atom one might expect  $H^-$  to have the largest electron-capture cross-section - this would certainly be true for small impact energies. However, Table 1.5 shows that, for  $E > 100$  keV, the ordering in Q for each projectile is  $Li^+ > He > H^-$ , and that as E becomes larger the differences between the cross-sections for the three systems increases; for example, for protons at 200 keV,  $Q(Li^+) \approx 9 \times Q(H^-)$  whilst at 3000 keV, we have  $Q(Li^+) \approx 150 \times Q(H^-)$ .

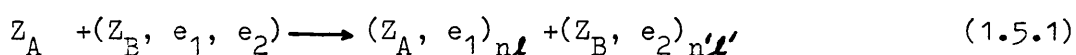
In attempting to account for the above ordering in Q there are three main points of interest.

(i) The essential feature of the CDW method is that it takes into account the Coulomb distortions acting on the 'active' electron in both the entrance and exit channels. It does this by taking full account of the continuum intermediate states in the charge-exchange process via the Coulomb wavefunctions of the 'active' electron with respect to the incident projectile in the inward channel, and the residual target in the outward channel (see equation 1.2.37,38). Since, in the present formulation of the CDW method with respect to two-electron targets, the outward distortion is a function of the net charge on the residual target (see equation 1.2.38-40b) and thus opposes electron capture, its effect for the three systems considered should be to produce an ordering of  $Q$  which is the reverse of that observed.

(ii) Although the energy decrement  $\Delta\epsilon$  (defined as the difference in energy between the initial and final atomic states and determined here from the theoretical values) is different for each of the three systems it appears in the expression for the cross-section in the terms  $\frac{v}{2} + \frac{\Delta\epsilon}{v}$  and, as a result, the cross-sections are found to become insensitive to  $\Delta\epsilon$  in the limit of high projectile velocities.

(iii) An obvious difference in the systems will be the description of the 'active' electron in the parent atom. Thus it follows from (i) and (ii) that the observed trends in  $Q$  must be dominated by the differences in the target wavefunctions.

We now proceed, by analysis of the individual CDW cross-sections  $\sigma[n\ell, n'\ell']$ , to account for the trends in  $Q$  for the more general reaction



when the target electrons are described by an HF wavefunction

$$\Phi(1,2) = \sum_{\beta} b_{\beta} \psi_{\beta}(1) \sum_{\gamma} b_{\gamma} \psi_{\gamma}(2), \text{ where each member of the basis}$$

set  $\{\varphi\}$  is normalized and the coefficients  $b_p$  and  $b_r$  are the usual variation constants. It follows from equation (1.3.46) that the CDW cross-section  $\sigma[nl, n'l']$  for a relative impact velocity  $v$  corresponding to an energy  $E$ , when the capture-state wavefunction is  $\psi_{nl}(1)$ , can be expressed as

$$\sigma[nl, n'l'] = N \left\{ I \left( \sum_p b_p \varphi_p(2) \mid n'l' \right) \right\}^2 \int_0^\infty \left| \sum_p b_p f_1(\eta, v, \varphi_p(1), \Delta E) \right. \\ \left. , g_1(\eta, v, \varphi_p(1), \psi_{nl}(1), \nu_1, \nu_2, \Delta E) \right|^2 d\eta, \quad (1.5.2)$$

where  $N$  is a constant and  $I \left( \sum_p b_p \varphi_p(2) \mid n'l' \right)$  is the overlap integral between the initial and final states which describe the 'passive' electron  $e_2$ . The integration over  $\eta$  is a result of performing a Fourier transform of the transition amplitude from position space to a two-dimensional vector space  $\underline{\eta}$  (see Appendix A), and the functions  $\nu_1$  and  $\nu_2$  arise from the Coulomb distortions acting in the entrance and exit channels, respectively, and are defined as  $\nu_1 = Z_A/v$  and  $\nu_2 = (Z_B - 1)/v$ . We note that  $f_1$  and  $g_1$  are both functions of  $\varphi_p(1)$  and hence the strong dependence of the ordering in the cross-sections on  $\Phi(1,2)$  is still not apparent. However, since the occurrence of the distortion in the exit channel inhibits capture, we can - without prejudice - proceed with our analysis by setting  $\nu_2 = 0$  for the general reaction (1.5.1). As a consequence of this the  $\varphi_p(1)$  dependence in  $g_1$  is now removed and the expression for  $\sigma[nl, n'l']$  when  $\nu_2 = 0$  becomes

$$\sigma[nl, n'l']_{\nu_2=0} = N I^2 \int_0^\infty \left( F_1(\eta, v, \sum_p b_p \varphi_p(1), \Delta E) \right)^2 \\ \cdot \left| G_1(\eta, v, \psi_{nl}, \nu_1, \Delta E) \right|^2 d\eta. \quad (1.5.3)$$

Except for the presence of the energy decrement  $\Delta E$ , the functional form of  $G_1$  is independent of the target parameters. At high projectile

velocities,  $G_1$  is found to be insensitive to  $\Delta\epsilon$  and thus, for a particular capture state ( $n\ell$ ), the function  $G_1$  becomes identical for our three examples of a two-electron target ( $Z_B, e_1, e_2$ ). When the basis set  $\{\psi\}$  is represented, for example by Slater-type orbitals (STO's), the function  $F_1$  takes the form

$$F_1 = \sum_{\beta} b_{\beta} (-1)^{n_{\beta}} N(n_{\beta}, \xi_{\beta}) \frac{\partial^{(n_{\beta}-1)}}{\partial \xi_{\beta}^{(n_{\beta}-1)}} \left[ \frac{\xi_{\beta}}{(\xi^2 + \eta^2 + (\frac{v}{2} + \frac{\Delta\epsilon}{v})^2)^2} \right], \quad (1.5.4)$$

where  $n_{\beta}, \xi_{\beta}$ , and  $N(n_{\beta}, \xi_{\beta})$  are the principal quantum number, orbital exponent and normalisation constant, respectively, of the basis function  $\psi_{\beta}$ . Analysis of  $F_1^2$  shows that it represents the probability density of finding the 'active' electron,  $e_1$  with a z-component of momentum equal to

$$\left| \frac{v}{2} + \frac{\Delta\epsilon}{v} \right| \text{ or, conversely, of finding } e_1 \text{ with a total momentum}$$

$p \gg \left| \frac{v}{2} + \frac{\Delta\epsilon}{v} \right|$  and, therefore,  $F_1^2$  can be interpreted as a two-dimensional momentum density. We note that the z-component of momentum is not unique and its definition is simply a consequence of choosing our coordinate system such that  $\underline{\eta} \cdot \underline{v} = 0$ , with  $\underline{v} = (0, 0, v_z)$ .

Let us now particularise equation 1.5.3 by choosing  $Z_A$  to be a proton and by setting  $n\ell = n'\ell' = 1s$  for the targets  $H^-$  and  $Li^+$ . In Figure 1.4, for each system, we plot  $F_1^2$  and  $G_1^2$  as a function of  $\eta$  for  $\sigma[1s, 1s]_{\nu_2=0}$  at  $E = 500, 1000$  and  $2000$  keV. We note here that for the case of  $H^-$  the residual target is the neutral H atom and therefore the captured electron experiences no Coulomb distortion in the exit channel. Thus we only need to set  $\nu_2 = 0$  for the He and  $Li^+$  systems since this is already the case for  $H^-$  for which  $\sigma[1s, 1s] = \sigma[1s, 1s]_{\nu_2=0}$ . For subsequent discussion and ease of comparison, Table 1.6 contains

$\sigma[1s, 1s]$  and  $\sigma[1s, 1s]_{\nu_2=0}$  at a few selected E; R - defined later -

is a ratio of the cross-sections for different targets when  $v_2=0$ . Throughout Fig. 1.4 and Table 1.6 each target was described by the HF wavefunction. As anticipated, Fig. 1.4 shows that the  $G_1^2$  functions for each target are very similar - particularly at large E values. Therefore, the ordering of the cross-sections in Table 1.6 is a direct consequence of the differences in the electron densities in momentum space as represented by  $F_1^2$ . When the projectile velocity is increased, the 'active' electron is captured from regions of increasingly higher momentum within the target atom; thus the cross-sections reflect the characteristics of the target wavefunctions near the origin. Indeed, in the limit  $v \rightarrow \infty$ , the function  $F_1$  may be expressed as

$$F_1 \xrightarrow{(v \rightarrow \infty)} \sum_{\beta} b_{\beta} \frac{\partial \psi_{\beta}^{(1)}}{\partial x_1} \Big|_{x_1=0} \frac{1}{(\eta^2 + v^2/4)^2} \quad (1.5.5)$$

and hence

$$\sigma [nl, n'l'] \Big|_{v_2=0} \xrightarrow{(v \rightarrow \infty)} N I^2 \left[ \sum_{\beta} b_{\beta} \frac{\partial \psi_{\beta}^{(1)}}{\partial x_1} \right]_{x_1=0}^2 \int_0^{\infty} |G_2(\eta, v, \psi_{nl}, v_1)|^2 d\eta, \quad (1.5.6)$$

where  $\underline{x}_1$  is the position vector of the 'active' electron with respect to the target nucleus. The  $\eta$  and  $v$  dependence in equation (1.5.6) occurs only in the new function  $G_2$  and, in the limit, we note that this function is also independent of  $\Delta E$ . Therefore, if we examine the ratio  $R [nl, n'l']$  of the cross-sections for two targets 'a' and 'b', when the distortion in the exit channel is removed, we obtain

$$R [nl, n'l'] = \frac{\sigma_a [nl, n'l']}{\sigma_b [nl, n'l']} \Big|_{v_2=0} \xrightarrow{v \rightarrow \infty} \frac{I_a^2 S_a^2}{I_b^2 S_b^2}, \quad (1.5.7)$$

where  $S$  is the slope or gradient of the HF wavefunction for the 'active' electron at the origin ( $x_1 = 0$ ) and, as before,  $I$  is the 'passive' overlap

integral. In Table 1.6 we present the ratios  $R[1s,1s]$  for (i)  $a \equiv \text{He}$  and  $b \equiv \text{H}^-$ , and (ii)  $a \equiv \text{Li}^+$  and  $b \equiv \text{He}$ . As  $E$  increases, these ratios are seen to approach the values of 52.8 for (i) and 8.86 for (ii) as predicted by equation (1.5.7), which again illustrates how the ordering of the cross-sections is dictated by the relative behaviour of the target wavefunctions. In passing, we note that when  $\text{H}^-$ ,  $\text{He}$  and  $\text{Li}^+$  are described by HF wavefunctions, the 'passive' overlap integral for  $n'l' = 1s$  is 0.922, 0.984 and 0.993, respectively; thus the limiting ratios in this instance are governed essentially by the relative values of  $S$ .

If  $\Phi(1,2)$  is a correlated wavefunction, it is of interest to examine the form of the function, say  $\mathfrak{F}^2$ , which replaces  $I_{F_1}^2$  in equation (1.5.3). For an examination of electron correlation the most convenient form of a CI wavefunction is its natural expansion which was discussed in Chapter 1.3.

Thus, by setting  $\nu_2 = 0$  in equation (1.3.36) we find that for the Weiss<sup>16</sup> function the functional form of  $\mathfrak{F}^2$  can be written

$$\mathfrak{F}^2 = \left\{ \sum_{\alpha=1}^{\infty} \frac{c_{\alpha}}{(2l_{\alpha} + 1)^{\frac{1}{2}}} \sum_{m=-l_{\alpha}}^{+l_{\alpha}} I_{\alpha} \left( \sum_{\gamma=1}^{15} b_{\gamma} \varphi_{\alpha\gamma}(\underline{x}_2) \mid \chi_{n'l'}(\underline{x}_2) \right) \cdot E_{\alpha}(\eta, \nu, \sum_{\beta=1}^{15} \varphi_{\alpha\beta}(\underline{x}_1), \Delta\epsilon) \right\}^2, \quad (1.5.8)$$

where the basis set  $\{\varphi\}$  used to describe the electrons consist of normalised S.T.O's. The natural orbitals are represented by the summation over  $\beta$  and  $\gamma$  and the summation over all the natural configurations  $\alpha$  represents the total CI wavefunction. When  $\alpha > 1$ , each natural configuration in the summation corresponds to the addition of a correlation term composed of  $\varphi$ 's with either radial or angular symmetry; when  $\alpha = 1$  only, we recover the  $I_{F_1}^2$  term in equation (1.5.3). Thus, by using the

natural expansion and by setting  $\nu_2 = 0$ , the nature of the influence of the correlation terms on the CDW cross-section becomes transparent and we see that the relative importance of each natural orbital is determined solely by its occupation coefficient  $c_\alpha$ , and the passive overlap integral  $I_\alpha$ . As a consequence, when improving the target wavefunction up to a CI description, any change in the cross-section at large  $v$  will be independent of the projectile charge  $Z_A$  (since at large  $v$ ,  $\nu_2 \rightarrow 0$ ) but may be strongly influenced by the final state of the passive electron. For example, in the case of electron-capture from  $H^-$  by protons, Moore and Banyard<sup>18</sup> reported a percentage change  $\Delta(HF \rightarrow CI) \sim 247\%$  for  $\sigma(1s, 2s)$  as compared to  $-27\%$  for  $\sigma(1s, 1s)$ .

As discussed in Chapter 1.3, equations (1.3.38-43), when the residual target atom is left in its ground state, or an excited state of radial symmetry i.e.  $l' = 0$ , then the passive overlap  $I_\alpha$  is found to be zero for those natural orbitals which have angular symmetry as opposed to radial symmetry. As a consequence only radial correlation terms in the target wavefunction  $\Phi(1,2)$  contribute to the cross-section in the present CDW calculations. In Figure 1.5 we show, for  $\sigma(1s, 1s)_{\nu_2=0}$ , plots of the first three radial terms of  $\mathcal{F}^2$ , i.e.  $c_\alpha I_\alpha F_\alpha$ , as a function of  $\eta$  at  $E = 1000$  keV. For He and  $Li^+$  the first three radial terms correspond to  $\alpha = 1, 3$  and 6 while for  $H^-$  they are  $\alpha = 1, 2$  and 6. The curves indicate clearly not only the dominance of the  $\alpha = 1$  term, but also that as we go from  $H^-$  to  $Li^+$  the higher natural orbitals become rapidly less important; note that at  $\eta = 0$  for  $H^-$ ,

$$c_{2\beta\gamma} I_{2\gamma} F_{2\beta} \approx \frac{1}{7} \times c_{1\beta\gamma} I_{1\gamma} F_{1\beta} \text{ while for } Li^+,$$

$$c_{3\beta\gamma} I_{3\gamma} F_{3\beta} \approx \frac{1}{300} \times c_{1\beta\gamma} I_{1\gamma} F_{1\beta} .$$

## CHAPTER 1.6

### Conclusion

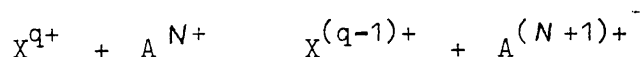
In view of the success of the CDW method in calculating the electron-capture cross-sections for the He target it is not too surprising that a reasonable agreement with experiment would be obtained for electron-capture from  $\text{Li}^+$  by fast protons. By comparing with available experimental data we were able to give credibility to the data of Sewell et al<sup>27</sup>. Although the total cross-sections were below the experimental points the agreement is satisfactory considering the fact that the CDW method is an appropriate approximation for large impact energies. Also, in order to evaluate  $Q$ , we have used the  $n^{-3}$  sum rule based on individual capture cross-sections for  $n \leq 2$ . At low impact energies this may lead to an under-estimation of the total cross-section since, at these energies, electron capture at large impact parameters and thus capture into highly excited states becomes important and may result in a breakdown of the  $n^{-3}$  rule for  $n \leq 3$ . The use of a more accurate  $n^{-3}$  sum rule may give us a better agreement with the data of Sewell et al<sup>27</sup> although this would mean calculating cross-sections for capture into the various  $n = 3$  quantum states. Also by comparing with the theoretical work of Obyedkov and Pavlov<sup>29</sup> we have also demonstrated the inadequacy of using a first-order method such as the Brinkman-Kramers approximation<sup>30</sup> to predict electron-capture cross-sections at large impact energies.

In attempting to rationalize the trends in the CDW cross-sections for the three targets  $\text{H}^-$ , He and  $\text{Li}^+$  we have analysed the individual capture cross-sections  $\sigma [nl, n'l']$ , which became tractable by setting  $\nu_2 = 0$ . As a result, not only were we able to explain the ordering in

Q observed for the three systems, but we also gained insight into the way factors such as relative impact velocity, energy decrement, electron correlation and the target wavefunction combine to influence the CDW cross-section. We have demonstrated that, as the projectile velocity increases, the 'active' electron is captured from regions of increasingly higher momentum within the target atom, and that in this region it is the characteristics of the wavefunction for small electron-nuclear separations which govern the trends in total cross-section when comparing different targets. Thus the accuracy of the wavefunction near the origin is of importance if a meaningful comparison with experiment is to be made at large impact energies.

Whenever any method is applied to cases involving more than one electron difficulties arise due to the electron-electron repulsive potential terms which render equations insolvable. Inevitably, the many-electron problem is usually reduced to a one-electron problem by making some suitable approximation to the potential terms involving  $1/x_{ij}$  (where  $x_{ij}$  is the separation between any two electrons  $i$  and  $j$ ). In this work we have used the formulism of the CDW method as originally devised by Cheshire<sup>1</sup> and, in applying the method to a two-electron problem, we have followed the suggestion of Belkic and Janev<sup>8</sup> which is to replace  $1/x_{12}$  by  $1/x_1$  and  $1/s_1$  by  $1/R$  (see equations 1.2.31-34). We call this the 'perfect screening' approximation and this results in the removal of the coordinates of the 'passive' electron from the problem. This simplification, which ultimately meant that only pure radial correlation terms would contribute to the cross-section, means that we have effectively removed electron correlation from within the method itself but still allow it to be included in the target wavefunction. In the case of a two-electron target the perfect screening approximation seems very reasonable and is appropriate to the physics of

the capture process, i.e. that maximum contribution to the capture cross-section will occur when the 'active' electron experiences perfect shielding of the target nucleus by the 'passive' electron. However, in the case of electron-capture from the 'K' shell of a many-electron atom having more than two electrons the application of the perfect screening approximation to the outer-shell electrons becomes questionable due to the low probability of finding the outer, say 2s or 2p, electrons lying within the 'K' shell. This suggests that, for electron-capture from a many electron target, approximations concerning the 'passive' electrons would have to be made that are more suitable to the physics of the particular capture process involved. As already pointed out, at large impact energies we expect the electron to be captured from regions close to the target nucleus. Thus, electron-capture from the 'K' shell will dominate the total capture cross-section at large energies, although for small impact energies and for capture into excited states the capture from the outer shells will give a non-negligible contribution. Therefore it will be interesting to apply the CDW method to charge transfer reactions of the type



where  $X^{q+}$  is a structured projectile and  $A N^+$  is a many-electron atom or ion, for which Li,  $Be^+$  or Be would provide an ideal simple first example.

E keV	$\sigma(1s)$	$\sigma(2s)$	$\sigma(2p)$	$Q^a$
100	$1.074^{-1}{}^b$	$1.098^{-2}$	$8.816^{-3}$	$1.3935^{-1}$
200	$2.934^{-2}$	$3.632^{-3}$	$1.005^{-3}$	$3.683^{-2}$
300	$9.593^{-3}$	$1.250^{-3}$	$2.502^{-4}$	$1.202^{-2}$
400	$3.766^{-3}$	$4.992^{-4}$	$8.580^{-5}$	$4.711^{-3}$
500	$1.695^{-3}$	$2.260^{-4}$	$3.540^{-5}$	$2.118^{-3}$
600	$8.461^{-4}$	$1.129^{-4}$	$1.657^{-5}$	$1.055^{-3}$
700	$4.573^{-4}$	$6.094^{-5}$	$8.517^{-6}$	$5.695^{-4}$
800	$2.633^{-4}$	$3.503^{-5}$	$4.706^{-6}$	$3.275^{-4}$
900	$1.596^{-4}$	$2.119^{-5}$	$2.756^{-6}$	$1.983^{-4}$
1000	$1.010^{-4}$	$1.338^{-5}$	$1.692^{-6}$	$1.254^{-4}$
1500	$1.601^{-5}$	$2.100^{-6}$	$2.423^{-7}$	$1.979^{-5}$
2000	$4.049^{-6}$	$5.277^{-7}$	$5.781^{-8}$	$4.995^{-6}$
2500	$1.349^{-6}$	$1.750^{-7}$	$1.857^{-8}$	$1.662^{-6}$
3000	$5.389^{-7}$	$6.967^{-8}$	$7.255^{-9}$	$6.633^{-7}$

Table 1.1 Individual  $\sigma(nl)$  and total capture cross-sections  $Q$ , at selected impact energy  $E$ . for the reaction  $H^+ + Li^+(1s^2) \rightarrow H(nl) + Li^{2+}(1s)$  in units of  $\pi a_0^2$  where  $a_0$  is the atomic unit of length. The target electrons are described by the 35-term configuration interaction (CI) wavefunction of Weiss<sup>16</sup>.

(a) The total capture cross-section  $Q$  was obtained from the "Oppenheimer  $n^{-3}$  rule":

$$Q \approx \sigma(1s) + 1.616(\sigma(2s) + \sigma(2p)).$$

(b) The superscript denotes the power of ten by which each entry should be multiplied.

E keV	$\sigma(1s)$	$\sigma(2s)$	$\sigma(2p)$	$Q^a$
100	$3.835^{+1b}$	$6.522^{-1}$	4.667	$4.695^{+1}$
300	5.118	$3.552^{-1}$	$3.777^{-1}$	6.302
500	1.617	$1.876^{-1}$	$1.013^{-1}$	2.084
800	$4.817^{-1}$	$7.056^{-2}$	$2.966^{-2}$	$6.437^{-1}$
1000	$2.553^{-1}$	$3.965^{-2}$	$1.556^{-2}$	$3.446^{-1}$
2000	$2.691^{-2}$	$4.374^{-3}$	$1.397^{-3}$	$3.624^{-2}$
3000	$5.884^{-3}$	$9.309^{-4}$	$2.546^{-4}$	$7.800^{-3}$
5000	$7.063^{-4}$	$1.061^{-4}$	$2.313^{-5}$	$9.152^{-4}$
8000	$8.397^{-5}$	$1.205^{-5}$	$2.109^{-6}$	$1.069^{-4}$
10000	$2.900^{-5}$	$4.083^{-6}$	$6.462^{-7}$	$3.664^{-5}$

Table 1.2 Individual  $\sigma(nl)$  and total capture cross-sections  $Q$ , at selected impact energy  $E$ , for the reaction  $\text{He}^{2+} + \text{Li}^+(1s^2) \rightarrow \text{He}^+(nl) + \text{Li}^{2+}(1s)$  in units of  $\pi a_0^2$  where  $a_0$  is the atomic unit of length. The target electrons are described by the 35-term configuration interaction (CI) wavefunction of Weiss<sup>16</sup>.

(a) The total capture cross-section  $Q$  was obtained from the "Oppenheimer  $n^{-3}$  rule":

$$Q \approx \sigma(1s) + 1.616(\sigma(2s) + \sigma(2p)).$$

(b) The superscript denotes the power of ten by which each entry should be multiplied.

E keV	$\sigma(1s)$	$\sigma(2s)$	$\sigma(2p)$	$Q^a$
	$\Delta(\text{HF} \rightarrow \text{CI})^b$	$\Delta(\text{HF} \rightarrow \text{CI})$	$\Delta(\text{HF} \rightarrow \text{CI})$	$\Delta(\text{HF} \rightarrow \text{CI})$
100	-4.98%	-3.47%	-1.37%	-4.44%
400	-1.33%	-1.15%	-1.67%	-1.32%
600	-1.32%	-1.18%	-1.70%	-1.33%
800	-1.39%	-1.26%	-1.41%	-1.37%
1000	-1.44%	-1.33%	-1.09%	-1.42%
2000	-1.62%	-1.52%	+0.22%	-1.57%
3000	-1.73%	-1.64%	+1.25%	-1.66%

Table 1.3 The percentage change  $\Delta(\text{HF} \rightarrow \text{CI})$  in individual and total capture cross-sections, at selected impact energy E, for the reaction  $\text{H}^+ + \text{Li}^+(1s^2) \rightarrow \text{H}(nl) + \text{Li}^{2+}(1s)$  when going from the Hartree-Fock (HF) to the CI description for the target electrons.

(a) The total capture cross-section Q is given by

$$Q \cong \sigma(1s) + 1.616(\sigma(2s) + \sigma(2p)), \text{ and}$$

$$\Delta(\text{HF} \rightarrow \text{CI}) \text{ is defined as } \left[ \frac{Q_{\text{CI}} - Q_{\text{HF}}}{Q_{\text{HF}}} \right] \times 100\%.$$

(b) For the individual cross-sections  $\Delta(\text{HF} \rightarrow \text{CI})$  is

$$\text{defined as } \left[ \frac{(\sigma(nl)_{\text{CI}} - \sigma(nl)_{\text{HF}})}{\sigma(nl)_{\text{HF}}} \right] \times 100\%.$$

E keV	$\sigma(1s)$	$\sigma(2s)$	$\sigma(2p)$	$Q^a$
	$\Delta(HF \rightarrow CI)^b$	$\Delta(HF \rightarrow CI)$	$\Delta(HF \rightarrow CI)$	$\Delta(HF \rightarrow CI)$
100	-6.55%	-5.29%	-6.64%	-6.54%
500	-1.71%	-2.52%	-0.74%	-1.75%
1000	-1.31%	-1.36%	-1.56%	-1.34%
3000	-1.44%	-1.29%	-1.41%	-1.41%
5000	-1.53%	-1.42%	-1.62%	-1.52%
10000	-1.71%	-1.63%	-1.69%	-1.69%

Table 1.4 The percentage change  $\Delta(HF \rightarrow CI)$  in individual and total capture cross-sections, at selected impact energy E, for the reaction  $He^{2+} + Li^+(1s^2) \rightarrow He(nl) + Li^{2+}(1s)$  when going from the Hartree-Fock (HF) to the CI description for the target electrons.

(a) The total capture cross-section Q is given by

$$Q \cong \sigma(1s) + 1.616(\sigma(2s) + \sigma(2p)), \text{ and}$$

$$\Delta(HF \rightarrow CI) \text{ is defined as } \left[ \frac{Q_{CI} - Q_{HF}}{Q_{HF}} \right] \times 100\%.$$

(b) For the individual cross-sections  $\Delta(HF \rightarrow CI)$  is

$$\text{defined as } \left[ \frac{(\sigma(nl)_{CI} - \sigma(nl)_{HF})}{\sigma(nl)_{HF}} \right] \times 100\%.$$

TABLE 1.5

E(keV)	Protons			Alpha Particles		
	H <sup>-</sup> $\Delta$ (HF+Cl)	He <sup>(a)</sup> $\Delta$ (HF+Cl)	Li <sup>+(b)</sup> $\Delta$ (HF+Cl)	H <sup>-</sup> $\Delta$ (HF+Cl)	He <sup>(a)</sup> $\Delta$ (HF+Cl)	Li <sup>+(b)</sup> $\Delta$ (HF+Cl)
100	6.681 <sup>-2(c)</sup> -19.8%	3.482 <sup>-1</sup> -4.0%	1.394 <sup>-1</sup> -4.5%	1.630 <sup>+1</sup> -16.4%	5.196 <sup>+1</sup> -4.7%	4.695 <sup>+1</sup> -5.8%
200	3.922 <sup>-3</sup> -17.1%	3.477 <sup>-2</sup> -3.8%	3.683 <sup>-2</sup> -2.2%	1.700 <sup>-1</sup> -16.9%	1.512 <sup>0</sup> -3.8%	2.084 <sup>0</sup> -1.9%
500	5.585 <sup>-5</sup> -15.9%	8.456 <sup>-4</sup> -4.2%	2.118 <sup>-3</sup> -1.3%	1.268 <sup>-2</sup> -16.6%	1.661 <sup>-1</sup> -4.1%	3.446 <sup>-1</sup> -1.4%
800	5.200 <sup>-6</sup> -15.9%	9.912 <sup>-5</sup> -4.3%	3.275 <sup>-4</sup> -1.4%	6.619 <sup>-4</sup> -16.4%	1.203 <sup>-2</sup> -4.1%	3.624 <sup>-2</sup> -1.3%
1000	1.622 <sup>-6</sup> -16.0%	3.418 <sup>-5</sup> -4.3%	1.254 <sup>-4</sup> -1.4%	2.460 <sup>-5</sup> -16.0%	5.947 <sup>-4</sup> -4.4%	2.396 <sup>-3</sup> -1.5%
2000	3.864 <sup>-8</sup> -16.2%	1.064 <sup>-6</sup> -4.4%	4.995 <sup>-6</sup> -1.6%	3.138 <sup>-6</sup> 16.1%	8.794 <sup>-5</sup> -4.5%	4.052 <sup>-4</sup> -1.6%
3000	4.083 <sup>-9</sup> -16.3%	1.270 <sup>-7</sup> -4.4%	6.633 <sup>-7</sup> -1.7%	2.104 <sup>-7</sup> -16.3%	6.932 <sup>-6</sup> -4.5%	3.664 <sup>-5</sup> -1.7%

Table 1.5

Total electron-capture cross-sections  $Q$ , in units of  $\pi a_0^2$  for targets  $H^-$ , He and  $Li^+$  for both proton and alpha-particle projectiles. Each system is described by the 35-term configuration-interaction (CI) function of Weiss<sup>16</sup> and, in square brackets, we give the percentage change

$\Delta(HF \rightarrow CI)$  in going from the Hartree-Fock (HF) to the CI description for the target electrons;  $\Delta(HF \rightarrow CI)$  is defined as  $\left[ (Q_{CI} - Q_{HF}) / Q_{HF} \right] \times 100\%$ .

- (a) The results for He supercede those reported by Banyard and Szuster<sup>14</sup> which contained a small computing error.
- (b) Total capture cross-section  $Q$  was obtained from the "Oppenheimer  $n^{-3}$  rule",  $Q \doteq \sigma(1s) + 1.616(\sigma(2s) + \sigma(2p))$ .
- (c) The superscript denotes the power of ten by which each entry should be multiplied.

TABLE 1.6

E(keV)	H <sup>-</sup>	He	Li <sup>+</sup>	He ( $\nu_2=0$ )	R <sub>(i)</sub>	Li <sup>+</sup> ( $\nu_2=0$ )	R <sub>(ii)</sub>
500	4.760 <sup>-5(a)</sup>	6.880 <sup>-4</sup>	1.718 <sup>-3</sup>	8.239 <sup>-4</sup>	17.3	1.986 <sup>-3</sup>	2.4
1000	1.427 <sup>-6</sup>	2.833 <sup>-5</sup>	1.025 <sup>-4</sup>	3.621 <sup>-5</sup>	25.4	1.382 <sup>-4</sup>	3.8
3000	3.665 <sup>-9</sup>	1.068 <sup>-7</sup>	5.484 <sup>-7</sup>	1.420 <sup>-7</sup>	38.7	8.465 <sup>-7</sup>	6.0
5000	2.077 <sup>-10</sup>	6.766 <sup>-9</sup>	3.880 <sup>-8</sup>	9.063 <sup>-9</sup>	43.6	6.137 <sup>-8</sup>	6.8
10000	4.042 <sup>-12</sup>	1.434 <sup>-10</sup>	9.181 <sup>-10</sup>	1.944 <sup>-10</sup>	48.1	1.483 <sup>-9</sup>	7.6

Table 1.6

Cross-sections  $\sigma [1s, 1s]$  and  $\sigma [1s, 1s]_{\nu_2=0}$  in units of  $\pi a_0^2$ , at selected E for electron capture by protons from the targets  $H^-$ , He and  $Li^+$ . Since the distortion in the exit channel due to the Coulomb interaction is zero for  $H^-$  (i.e.  $\nu_2 = 0$ ), we note that  $\sigma [1s, 1s] = \sigma [1s, 1s]_{\nu_2=0}$ . We also tabulate values of  $R = (\sigma_a [1s, 1s] / \sigma_b [1s, 1s])_{\nu_2=0}$  for (i)  $a \equiv He$  and  $b \equiv H^-$ , and (ii)  $a \equiv Li^+$  and  $b \equiv He$ . In each instance, the target electrons are described by Hartree-Fock wavefunctions.

- (a) The superscript denotes the power of ten by which each entry should be multiplied.

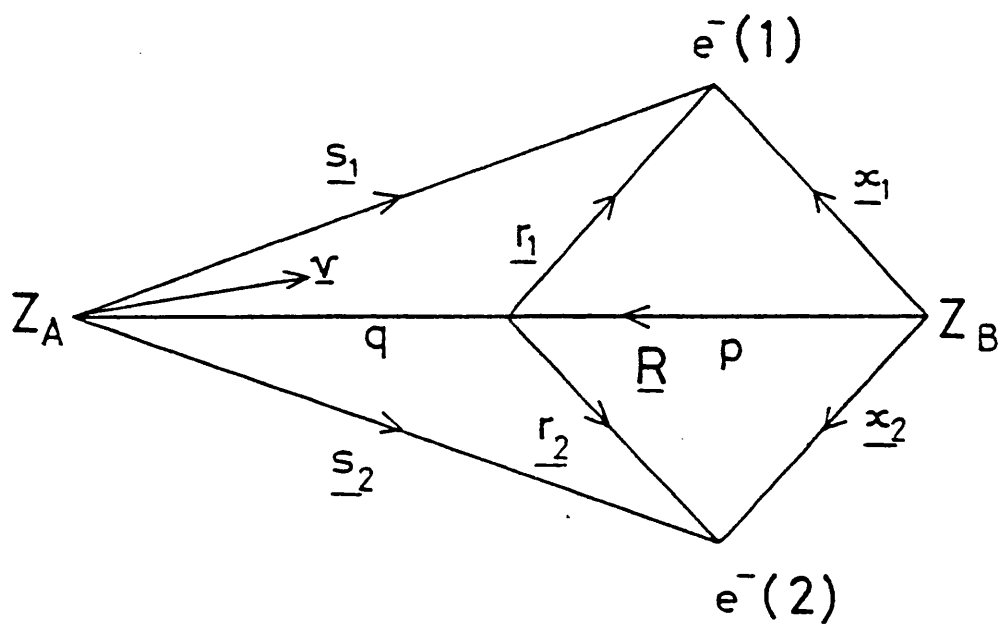


Figure 1.1 Coordinate system for reaction (1.2.1). The arbitrary origin is shown here to be at the mid-point of the internuclear line.

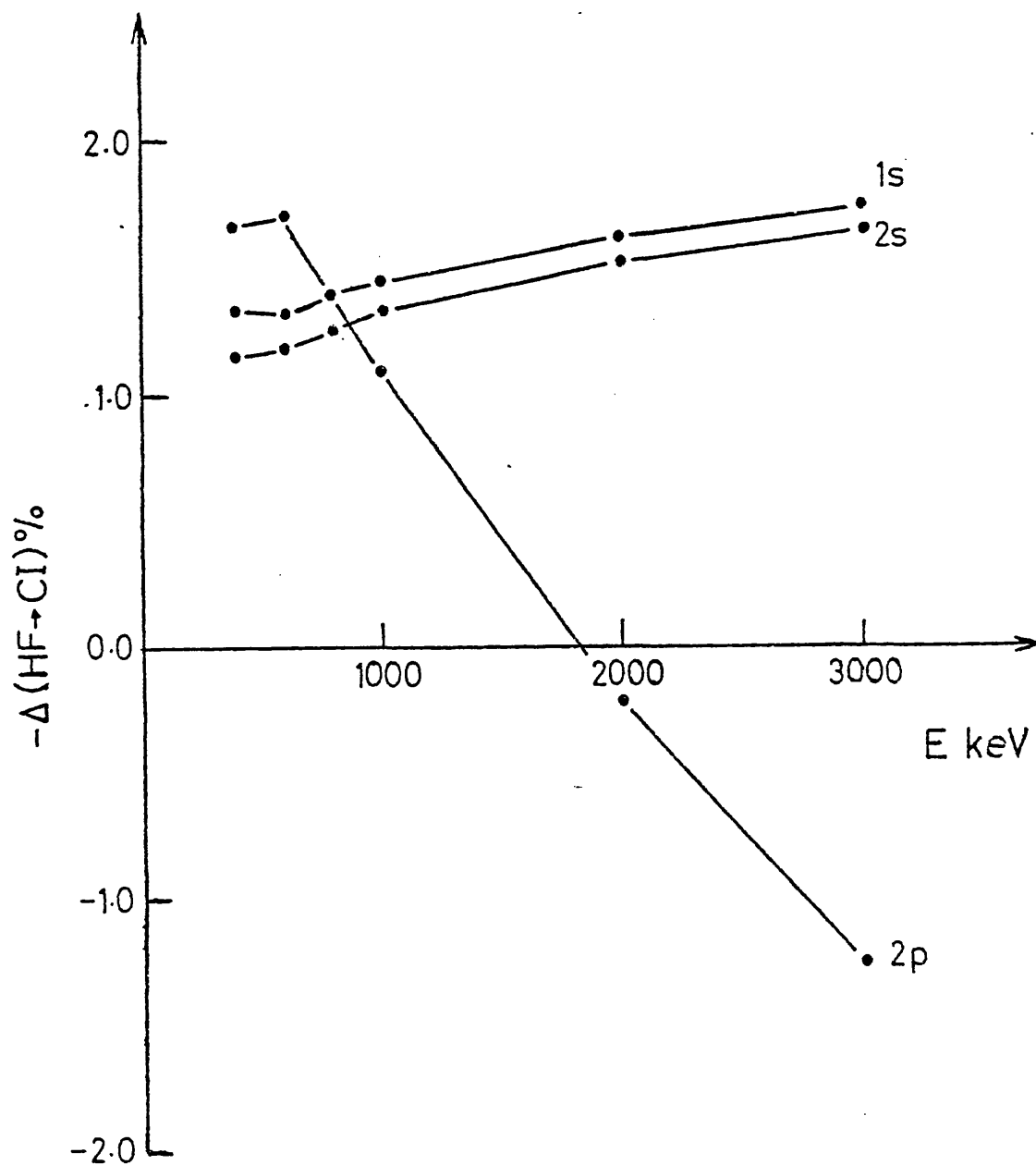


Figure 1.2 The percentage changes  $\Delta(\text{HF} \rightarrow \text{CI})$ , listed in Table 1.3, for individual cross-sections  $\sigma(nl)$ , plotted against impact energy E.

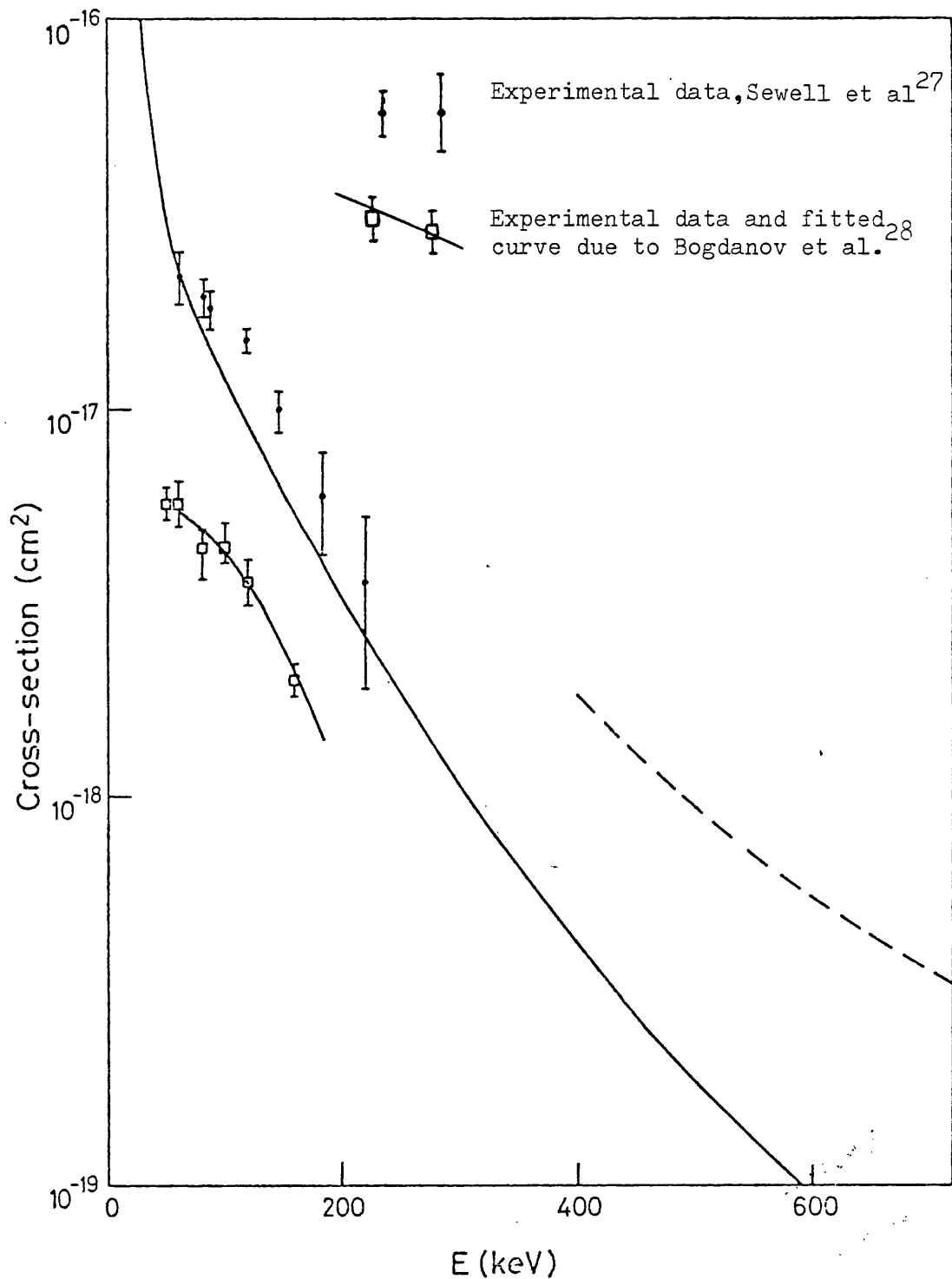


Figure 1.3 The theoretical total cross-sections  $\sigma$  for protons impinging on  $\text{Li}^+$  compared with the experimental data of Sewell et al.<sup>27</sup> and that due to Bogdanov et al.<sup>28</sup>. Present CDW results \_\_\_\_\_, theoretical curve due to Cb'yedkov and Pavlov<sup>29</sup> using the Brinkman-Kramers<sup>30</sup> method ----- .

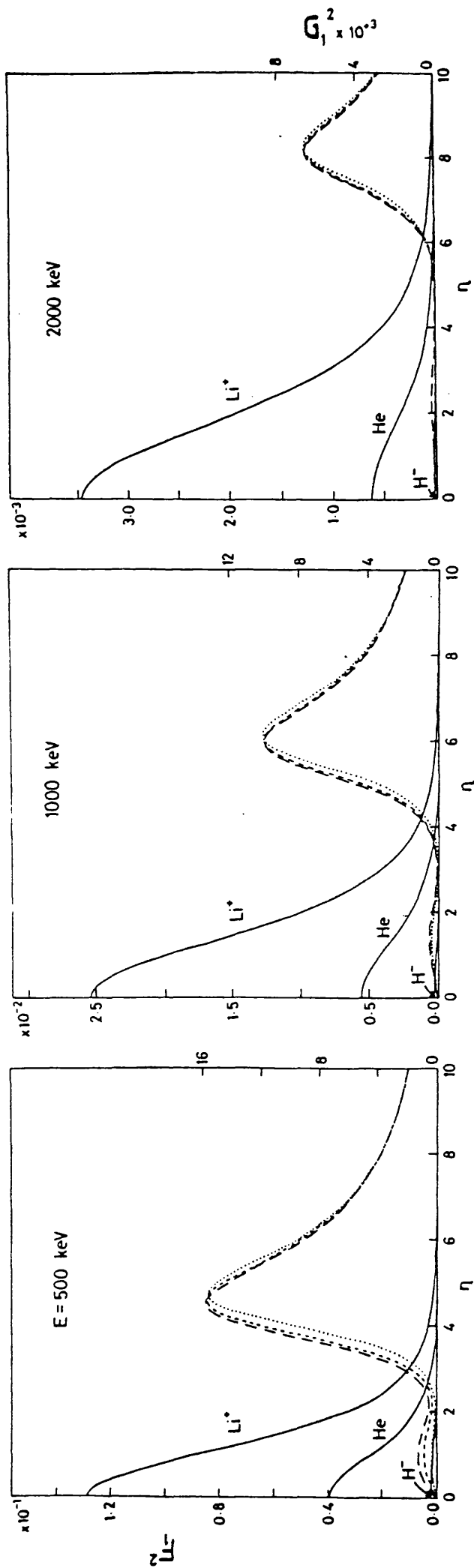


Figure 1.4 Plots, at three selected impact energies  $E$ , of  $F_1^2$  and  $G_1^2$  against  $n$  for each of the targets  $\text{H}^-$ ,  $\text{He}$  and  $\text{Li}^+$  corresponding to  $\sigma[1s, 1s]_{\nu_2=0}$  in equation (1.5.3). The projectiles are protons and the target electrons are described by the Hartree-Fock wavefunctions<sup>20,26</sup> stated in the text. The curves for  $G_1^2$  are -----  $\text{H}^-$ , -----  $\text{He}$ , and .....  $\text{Li}^+$ .

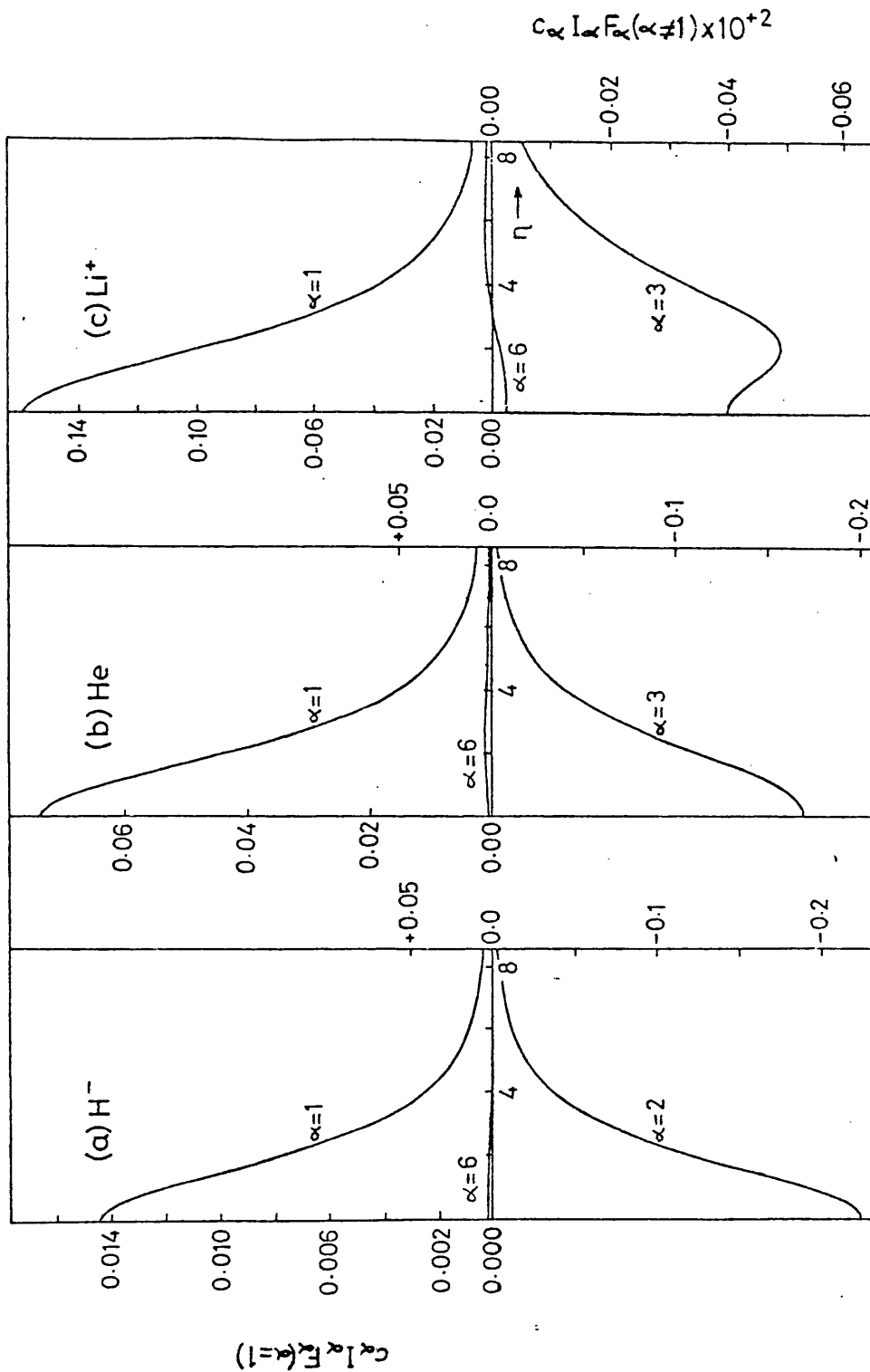


Figure 1.5 Plots of  $c_{\alpha} I_{\alpha} F_{\alpha}$  vs.  $\eta$ , defined in equation (1.5.3), where each  $\alpha$  value represents a natural configuration within the natural expansion formulation of  $\sigma[1s, 1s]_{\nu_2=0}$  for a proton impact energy of 1000 keV. (a)  $\text{H}^-$  for  $\alpha = 1, 2$  and 6, (b) He for  $\alpha = 1, 3$  and 6, and (c)  $\text{Li}^+$  for  $\alpha = 1, 3$  and 6. Each target was described by the natural expansion of the 35-term CI wavefunction of Weiss<sup>16</sup>, and the  $\alpha$  values quoted represent natural configurations constructed from orbitals of radial symmetry.

References - Part 1

1. I.M. Cheshire, Proc. Phys. Soc. 84, 89 (1964)
2. D.R. Bates, Proc. Roy. Soc. A. 247, 294 (1958)
3. R. McCarroll, Proc. Roy. Soc. A. 264, 547 (1961)
4. I.M. Cheshire, Proc. Phys. Soc. 82, 113 (1963)
5. R.M. Drisko, Thesis, Carnegie Institute of Technology (1955)
6. A. Salin, J. Phys. B. 3, 937 (1970)
7. J.R. Oppenheimer, Phys. Rev. 31, 349 (1928)
8. Dž Belkić and R.K. Janev, J. Phys. B. 6, 1020 (1973)
9. R. Gayet, J. Phys. B. 5, 483 (1972)
10. Dž Belkić and R. Gayet, J. Phys. B. 10, 1911 (1977)
11. Dž Belkić and R. Gayet, J. Phys. B. 10, 1923 (1977)
12. E. Hylleraas, Z. Physik, 54, 347 (1929)
13. C. Eckart, Phys. Rev. 36, 878 (1930)
14. K.E. Banyard and B.J. Szuster, Phys. Rev. A. 16, 129 (1977)
15. E. Clementi and C. Roetti, Atom. Data Nucl. Data Tables. 14 (New York, London: Academic Press) (1974)
16. A.W. Weiss, Phys. Rev. 122, 1826 (1961)
17. K.E. Banyard and B.J. Szuster, J. Phys. B. 10, L503 (1977)
18. J.C. Moore and K.E. Banyard, J. Phys. B. 11, 1613 (1978)
19. K.E. Banyard and J.C. Moore, J. Phys. B. 11, 3899 (1978)
20. R.F. Curl and C.A. Coulson, Proc. Phys. Soc. 85, 647 (1964)  
- J. Phys. B. 1, 325 (1968)
21. D.R. Bates and R. McCarroll, Proc. Roy. Soc. A245, 175 (1958)
22. P.O. Lowdin, Phys. Rev. 97, 1474 (1955)
23. J.N. Silverman, O. Platas and F.A. Matsen, J. Chem. Phys. 32,  
1402 (1960)
24. S. Borowitz and M.M. Klein, Phys. Rev. 103, 612 (1956)
25. M.R.C. McDowell and J.P. Coleman, 'Introduction to the Theory of  
Ion-Atom Collisions', (North-Holland, 1970).

26. E. Clementi and C. Roetti, 'Atomic Data and Nuclear Data Tables' 14 (New York, London: Academic Press, 1974)
27. E.C. Sewell, G.C. Angel, K.F. Dunn and H.B. Gilbody, J. Phys. B. 13, 2269 (1980)
28. G.F. Bogdanov, A.N. Karkhov and Yu. A. Kucheryaev, Atomnaya Énergiya (USSR). 19, 1316 (1965)
29. V.D. Ob'yedkov and V.E. Pavlov, Atomnaya Energiya (USSR). 23, 345 (1967)
30. H. Brinkman and H. Kramers, Proc. Acad. Sci. Amsterdam. 33, 973 (1930)
31. L. Pauling and E.B. Wilson, 'Introduction to Quantum Mechanics', (McGraw-Hill, 1935) P. 142.

## PART TWO

Application of the Continuum Distorted Wave (CDW) method to electron-capture from a many-electron target and the calculation of capture cross-sections for the three-electron target atom Li, and its ions, by fast protons.

## CHAPTER 2.1

### Introduction

As an aid to the experimental program into plasma heating considerable experimental work has been done to obtain a multiplicity of charge transfer cross-sections, involving many-electron atoms, that may be of importance in the development of thermonuclear fusion.<sup>1</sup> Multi-electron atoms, such as Li, may prove to be useful in the production of fast beams of neutral hydrogen atoms for injection into plasma devices, and the Li atom itself is of practical interest in the production of hot plasmas with the use of lithium arcs in devices such as "OGRA".<sup>2</sup>

As stated in the general introduction, when calculating charge transfer cross-sections which involve fast structureless projectiles the correct high energy behaviour requires the use of a second order method, and that one of the most recent satisfactory second order methods is the continuum distorted wave (CDW) method developed initially by Cheshire<sup>3</sup> for proton-hydrogen collisions. In applying any method or performing a calculation involving a many-electron atom the calculations are complicated by the presence of the inter-electron potential terms. Invariably approximations are made to remove any difficulties which arise and usually involve either an averaged potential or, as in the case of the CDW method, the introduction of some screening effect. For instance, in the generalisation of the CDW method to a two-electron target Belkic and Janev<sup>4</sup> comment that the probability of capturing the so-called 'active' electron should be greatest when the 'passive' electron is very close to the target nucleus, and as a consequence of this we saw in Part 1, Chapter 1.2, how the 'passive' electron could then be removed from the equations defining the distorted waves by invoking maximum or 'perfect' screening of the target nucleus. Thus, in the description of the outward channel, for example, the residual

target was represented by the target nucleus with its charge decreased by unity. This 'perfect screening' approximation was used in Part 1 for the  $\text{Li}^+$  target and it was also used in the first application of the CDW method to electron-capture by protons from He by Salin<sup>5</sup> and also in the later examinations of electron-capture from  $\text{H}^-$  by Janev and Salin<sup>6</sup> and by Moore and Banyard<sup>7</sup>. This approximation not only makes physical sense but it also ensures that the outward-channel distorted wave has the correct phase factor in the asymptotic limit as  $t \rightarrow +\infty$ . However, when considering multi-electron target atoms the invoking of perfect screening may not reflect the true picture, particularly when capturing from say the K shell of the atom.

The calculation of capture cross-sections from large atoms is still relatively rare and generally restricted to first order methods. For example, Mapleton<sup>8</sup> applied the first Born approximation<sup>9</sup> to oxygen and Mapleton<sup>10</sup>, Nicolaev<sup>11</sup>, and Lodge and May<sup>12</sup> have studied various target atoms, such as He, Li, Ne, N and Ar, using the Oppenheimer<sup>13</sup> Brinkman-Kramers approximation.<sup>14</sup> It is partially due to their convenience that the OBK cross-sections are widely used in estimating capture cross-sections, and it is important to note that the absolute agreement with experiment is achieved by the introduction of screening corrections and by applying appropriate scaling factors.

Therefore, in Part 2 we apply the CDW method to a many-electron system and, as a simple example, we evaluate the K- and L-shell capture cross-sections for a Li target atom in its ground-state. For such a system, a 'passive' electron will now exist in a different shell from that of the 'active' electron. Thus, a modification is suggested to the 'perfect screening' procedure used by others for two-electron targets. We also examine the effect of such a modification on the capture cross-sections

for the related ion  $\text{Li}^+$  and, finally, to complete the ionization series, cross-sections are calculated for the one-electron target  $\text{Li}^{2+}$ . In each instance the projectiles are protons within an energy range of  $200 \text{ keV} \leq E \leq 10 \text{ MeV}$  - the lower limit being a rough measure of the minimum  $E$  for which the CDW calculations, involving lithium ions, can be considered reliable.

CHAPTER 2.2

The application of the CDW method to electron-capture  
from a many-electron atom by fast protons

Before applying the CDW method directly to electron-capture from Li we first present a generalisation of the CDW transition amplitude for electron-capture from a many electron atom. As in the case of a two-electron target the many-electron problem is reduced to a one-electron problem by applying the 'perfect screening' approximation to the 'passive' electrons. However, we also present an alternative procedure to the 'perfect screening' approach which will be more appropriate for capture from the inner shells of a many-electron target atom. Both models are then applied to electron-capture from Li and  $\text{Li}^+$  by fast protons. Let us consider a high energy nucleus charge  $Z_A$ , energy  $E$  and velocity  $v$ , in collision with a stationary many electron target atom whose nuclear charge is  $Z_B$  and having  $N$  orbital electrons such that  $N \ll Z_B$ . It follows from a generalisation of equation (1.2.3) that the Schrodinger equation for such a reaction is

$$\left[ \sum_{i=1}^N \left( \frac{1}{2} \nabla_{\mathbf{r}_i}^2 + \frac{Z_B}{x_i} + \frac{Z_A}{s_i} \right) - \sum_{i=1}^N \sum_{j=1}^{i-1} \frac{1}{x_{ij}} - \frac{Z_A Z_B}{R} + \frac{i\delta}{\delta t} \right] \Psi(\mathbf{r}_1, \mathbf{r}_2 \dots \mathbf{r}_i \dots \mathbf{r}_N, t) = 0 \quad (2.2.1)$$

Following the procedure of the CDW method, presented in Chapter 1.3, it follows from equations (1.3.11-16) that for capture of electron  $j$ , say, into any state  $n\ell$  the transition amplitude  $a_{n\ell, F}^{(b)}$ , where  $b$  is the impact parameter and  $F$  signifies the final state of the remaining target electrons, can be expressed as

$$\begin{aligned}
a_{nl,F}^{(b)} = & i N_A(v) N_B(v) (bv)^{2iZ_A [Z_B - (N-1)] / v} \\
& \times \int_{-\infty}^{+\infty} dt e^{-i\Delta\epsilon t} \int d\underline{r}_1 \int d\underline{r}_2 \dots \int d\underline{r}_N e^{-i\underline{v} \cdot \underline{r}_j} \\
& \times \varphi_{nl}^* (\underline{s}_j) \chi_F^* (\underline{x}_1, \underline{x}_2, \dots, \underline{x}_{j-1}, \underline{x}_{j+1}, \dots, \underline{x}_N) {}_1F_1 [i\underline{v}_B; 1; i(\underline{v} \cdot \underline{x}_j + \underline{v} \cdot \underline{x}_j)] \\
& \times \frac{\partial}{\partial x_j} \Psi (\underline{x}_1, \underline{x}_2, \dots, \underline{x}_j, \dots, \underline{x}_N) \nabla_{\underline{r}_j} {}_1F_1 [i\underline{v}_A; 1; i(\underline{v} \cdot \underline{s}_j + \underline{v} \cdot \underline{s}_j)] .
\end{aligned} \tag{2.2.2}$$

The energy decrement  $\Delta\epsilon$  is the difference between the initial state energy of the target and the sum of the energies of the charge exchange products, i.e.  $\Delta\epsilon = \epsilon_i - \epsilon_F - \epsilon_{nl}$ . The initial and final states of the target are described by the normalized antisymmetric wavefunctions  $\Psi(\underline{x}_1, \underline{x}_2, \dots, \underline{x}_j, \dots, \underline{x}_N)$  and  $\chi_F(\underline{x}_1, \underline{x}_2, \dots, \underline{x}_{j-1}, \dots, \underline{x}_N)$ , respectively, and the capture state of the active electron is represented by  $\varphi_{nl}(\underline{s}_j)$ . Since we have  $N$  indistinguishable electrons the projectile may capture any one of the target electrons, labelled from 1 to  $N$ , with equal probability, and thus the description of the total system in its final state  $\varphi_{nl} \chi_F$  should also be normalized and antisymmetric. The net effect of such a requirement is to multiply the transition amplitude  $a_{nl,F}^{(b)}$  in equation (2.2.2) by  $N^{\frac{1}{2}}$ .  $N_A(v)$  and  $N_B(v)$  are the normalization constants associated with the confluent hypergeometric functions for the inward and outward channels, respectively, and

$$\underline{v}_A = Z_A/v \quad \text{and} \quad \underline{v}_B = [Z_B - (N-1)] / v. \tag{2.2.3}$$

The expression for  $\underline{v}_B$  is a consequence of invoking the 'perfect screening' approximation to represent the interaction between the 'active' and 'passive' electrons. Its magnitude is a function of the net charge on the residual target as seen by the captured electron at infinity, and is a consequence of making the following approximations

$$\sum_{\substack{i=1 \\ i \neq j}}^N \frac{Z_A}{s_i} = \frac{(N-1)Z_A}{R} \quad \text{and} \quad \sum_{\substack{i=1 \\ i \neq j}}^N \frac{1}{x_{ij}} = \frac{(N-1)}{X_j} .$$

(2.2.4)

Such a model has the particular advantage of ensuring that the incoming and outgoing waves have the correct asymptotic behaviour as  $t \rightarrow -\infty$  and  $+\infty$ , respectively. However, a relaxation of the asymptotic constraint allows us to adopt a simple but somewhat more realistic way of accounting for the 'passive' electrons in a many-electron system. For capture from the target quantum state  $n'$ , say, an effective charge for the residual target, as seen by the captured electron, can be obtained from the experimental ionization energy by using the hydrogen-like expression

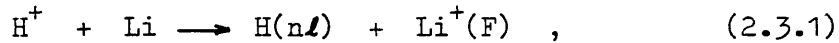
$$\begin{aligned} \text{Ionization Energy } \mathcal{E} &= Z_{\text{eff}}^2 / 2n'^2 , \\ & \text{(in atomic units)} \\ \text{hence } Z_{\text{eff}} &= \sqrt{\mathcal{E} 2 n'^2} . \end{aligned} \quad (2.2.5)$$

In this way the value of  $Z_{\text{eff}}$  reflects the charge seen by the active electron as it is ionized into the continuum prior to capture. Thus, in the expression for  $a_{n\ell, F}^{(b)}$  we redefine  $v_B$  to be  $Z_{\text{eff}}/v$ . Therefore for capture from a particular shell of a many electron atom we must define a  $Z_{\text{eff}}$  value which will incorporate the amount of screening produced by all the passive electrons. It achieves this through the ionization energy which, via the hydrogen-like expression above, will reflect the probability of finding a proportion of the charge cloud arising from the outer shell electrons, to be lying within the shell of the active electron and as a result partially screen the target atom nucleus.

CHAPTER 2.3

Electron-capture from Li, Li<sup>+</sup> and Li<sup>2+</sup> by fast protons

Electron-capture from the ground state of Li can occur from either the K- or L-shell and therefore the reactions considered here are



where F is 1<sup>1</sup>S, 2<sup>1</sup>S or 2<sup>3</sup>S and  $nl \equiv 1s, 2s$  and  $2p$ . The same  $(nl)$ -states were chosen when considering capture from the ground states of Li<sup>+</sup> and Li<sup>2+</sup>. The Hartree-Fock wavefunctions of Clementi and Roetti<sup>15</sup> were used to describe the initial states of Li and Li<sup>+</sup> and the excited-state wavefunctions for Li<sup>+</sup>, used in the calculation of the passive overlap integral for reaction (2.3.1), were taken from Cohen and McEachran.<sup>16</sup> The ionization energies, used in the calculation of the energy decrement  $\Delta\epsilon$  and the value for  $Z_{\text{eff}}$  were obtained from Moore<sup>17</sup>, Wiese et al<sup>18</sup> and Tennant<sup>19</sup>. For the Li atom target, the  $Z_{\text{eff}}$  values corresponding to F  $\equiv 1^1S, 2^1S$  and  $2^3S$ , from equation (2.2.5), are 1.260, 2.208 and 2.177, respectively, and when the target is a Li<sup>+</sup> ion then  $Z_{\text{eff}} = 2.359$ . The Li<sup>2+</sup> ion was described by using the exact energy and eigenfunction.

The total cross-section  $\sigma [nl, F]$  for electron-capture into a state  $(nl)$  may be expressed as

$$\sigma [nl, F] = 2 \int_0^{\infty} b |a_{nl, F}(b)|^2 db \text{ (in units of } \pi a_0^2 \text{) } , \quad (2.3.2)$$

where  $a_{nl, F}(b)$  is the total antisymmetrised transition amplitude given by  $a_{nl, F}(b)$  in equation (2.2.2) multiplied by  $3^{\frac{1}{2}}$  for the Li atom target and  $2^{\frac{1}{2}}$  for the Li<sup>+</sup>. The  $\sigma [nl, F]$  values for Li and Li<sup>+</sup> targets are presented in Table 2.1: the initial entry is based on the  $Z_{\text{eff}}$  approximation and the underlined entry refers to the 'perfect screening'

(ps) model. For the Li atom, the total cross-section  $Q_T$  for all capture states  $n\ell$  was obtained from

$$Q_T = Q(1^1S) + Q(2^1S) + Q(2^3S), \quad (2.3.3)$$

where each contribution  $Q(F)$  was determined by using the appropriate  $n^{-3}$  sum rule (see Chapter 1.4, equation (1.4.3)). For reaction (2.3.1) we note that the integration over spin in the antisymmetrized expression for  $a_{n\ell,F}(b)$ , when  $F \equiv 1^1S$ , produces exchange-type terms in the transition amplitude in which the label for the active electron is associated with the 1s orbital in Li as well as the expected terms arising from the initial occupation of the 2s orbital; and vice versa when  $F \equiv 2^1S$ . However, due to the near orthogonality between the 2s and 1s orbitals in the Clementi and Roetti<sup>15</sup> HF wavefunction the passive overlap integral associated with the exchange-type term is very small, and as a consequence contributions to the capture cross-sections attributable to exchange-type terms account for less than 0.3% of the magnitude of  $\sigma[n\ell, 1^1S]$  and  $\sigma[n\ell, 2^1S]$  in each instance; no such exchange-type terms arise when  $F \equiv 2^3S$ . Therefore, for ease of discussion, we will refer to  $Q(2^1S) + Q(2^3S)$  as K-shell capture, and  $Q(1^1S)$  as L-shell capture. For the evaluation of  $Q_T$  for the  $Li^+$  and  $Li^{2+}$  targets the  $n^{-3}$  sum rule was again used and the results for all three systems are listed in Table 2.2 at selected  $E$  lying between 200 keV and 10 MeV. As before, the values obtained from the ps-model are underlined. In Table 2.3 the difference between the  $Z_{eff}$  and the ps-values for each cross-section is expressed as a percentage change  $\Delta$ , with respect to the ps-value, for both Li and  $Li^+$  at selected  $E$ .

To enable graphical comparison to be made with the experimental curve of I'lin et al<sup>20</sup> for Li, values of  $Q_T$  were calculated for both models over the energy range 10-180 keV. The curves are shown in Figure 2.1 and 2.2 along with the theoretical results for electron-capture from

the individual K- and L-shells. In Figure 2.3, the  $Z_{\text{eff}}$ -values for  $Q_{\text{T}}$  over this energy range are compared with the Li calculations of Il'in et al<sup>21</sup>, Nikolaev<sup>11</sup> and Lodge and May<sup>12</sup>. Il'in et al used a Born method<sup>9</sup> in the one-electron approximation and the other workers employed the Brinkman-Kramers<sup>14</sup> approximation along with a correction factor. Nikolaev<sup>11</sup> described the Li atom in terms of hydrogen-like wavefunctions whereas the Lodge and May<sup>12</sup> curve was derived using the Hartree-Fock descriptions given by Roothaan, Sachs and Weiss<sup>22</sup>.

In Figure 2.4 the total cross-sections for the  $\text{Li}^+$  ion, for both the ps and  $Z_{\text{eff}}$ -models, are compared with the experimental data of Bogdanov et al<sup>23</sup> and with the more recent experimental data of Sewell et al<sup>24</sup>. Also shown are the theoretical results of Ob'yedkov and Pavlov<sup>25</sup>. No experimental comparison could be found for the  $\text{Li}^{2+}$  ion.

### Results and Discussion

In the analysis of the CDW approximation, presented in Part 1, we saw that the only direct reference to the 'passive' electrons in the transition amplitude occurs as an overlap integral between their initial and final quantum states. Thus, the influence of the interelectronic interactions within the present form of the CDW calculations, arises solely from the correlation effects contained in the target wavefunctions  $\Psi$  and  $\chi_{\text{F}}$ . Although electron correlation is important for a target such as  $\text{H}^-$  (see, Moore and Banyard<sup>7</sup>) the calculations in Part 1, in the present energy range, suggest that the use of a correlated wavefunction for the Li series should produce a decrease in each cross-section, with respect to the Hartree-Fock value, of less than 2%.

Comparison of the values of  $Z_{\text{eff}}$  for electron capture from the K-shells of Li and  $\text{Li}^+$  suggests that, for capture from the Li K-shell, about 20% of the shielding arises from the 2s electron: this reflects the probability of finding the L-shell electron within the K-shell. For Li, a

comparison of the results for  $Z_{\text{eff}}$  with the ps-model is also of some interest. It is found that the  $Z_{\text{eff}}$  values for K-shell capture correspond to only about 40% of the shielding in the ps-model whereas, for L-shell capture, the result for  $Z_{\text{eff}}$  indicates that the K-shell provides 87% of perfect screening. The sensitivity of each  $\sigma[n\ell, F]$  to a change in nuclear shielding can be judged by inspecting the  $Z_{\text{eff}}$ - and ps-results in Table 2.1; see also the  $\Delta$  values in Table 2.3. At low energies, Table 2.1 shows that when  $n\ell \equiv 1s$  and  $2s$  the  $Z_{\text{eff}}$ -cross-sections are larger than the ps-values whereas, for the  $2p$  capture states, the ordering is reversed - an exception being Li when  $F \equiv 2^1S$ . However, for  $E \geq 1000$  keV, the use of  $Z_{\text{eff}}$  decreases all  $\sigma[n\ell, F]$ . This latter feature is most noticeable for capture from the K-shell of the Li atom where, as Table 2.3 shows, the effect becomes larger with increasing  $E$ . At 10 MeV, for example, the  $Z_{\text{eff}}$ -calculation yields K-shell cross-sections for the  $2p$  capture state which are only about one-fifth of the magnitude of the ps-values.

For each F-state Table 2.3 reveals that, as  $E$  increases, a strong similarity occurs between the  $\Delta$  values for  $(n\ell) \equiv 1s$  and  $2s$ ; the similarity does not extend to the  $2p$  state. A corresponding trend was observed by Banyard and Szuster<sup>26</sup> in a correlation study of charge exchange in proton-helium collisions. Following their rationalization, we find that, at high projectile velocities, the major contribution to each  $\sigma[n\ell, F]$  occurs at small values of the impact parameter. Consequently, the  $\Delta$  values reflect the similarity in the characteristics of the  $1s$  and  $2s$  hydrogen orbitals at small electron-proton separations; such characteristics are, in turn, quite distinct from those of a  $2p$  hydrogen orbital.

When  $E \geq 800$  keV, the Li cross-sections are ordered as  $\sigma[n\ell, 2^3S] > \sigma[n\ell, 2^1S] > \sigma[n\ell, 1^1S]$  for each choice of  $(n\ell)$  and, as might be expected, for any given F state we have  $\sigma[1s, F] > \sigma[2s, F] > \sigma[2p, F]$ . The latter ordering also holds for  $\text{Li}^+$ . Inspection of the total cross-

sections  $Q_T$  in Table 2.2 for the ionization series shows that, for the  $Z_{\text{eff}}$  model,  $Q_T(\text{Li}^+) > Q_T(\text{Li}) > Q_T(\text{Li}^{2+})$  throughout the whole energy range. We also note that, at high energies, the  $Z_{\text{eff}}$ -results for  $Q_T$  are less than the ps-values by about 21% for Li and 6% for  $\text{Li}^+$ .

A comparison between the total cross-sections per K-shell electron for the ion targets reveals that, at low energies,  $\text{Li}^+ > \text{Li}^{2+}$  whereas, when  $E$  is large, the  $\text{Li}^{2+}$  cross-sections are significantly greater than the  $\text{Li}^+$  values. Since the transition amplitudes are evaluated in terms of momentum space, the larger momentum possessed by the unshielded active electron in  $\text{Li}^{2+}$  emphasizes that, as the projectile velocity increases, the major contribution to each cross-section arises increasingly from the high momentum region within the target.

When compared with experiment, the  $Z_{\text{eff}}$  and ps-values of  $Q_T$  for Li reveal some interesting features. Although the results of Il'in et al.<sup>20</sup> extend only as far as 180 keV, Figures 2.1 and 2.2 indicate that each CDW curve for  $Q_T$  is in general accord with experiment - the better agreement being achieved by the  $Z_{\text{eff}}$  approximation. For electron-capture from the K-shell, the ps-results are seen to reach a turning point at about 15 keV, whereas the  $Z_{\text{eff}}$  approximation produces an inflexion at about 40 keV which is similar in shape to that seen in the experimental curve at  $E \sim 60$  keV. However, Figure 2.1 shows that the increase in the L-shell capture cross-section with decreasing  $E$  masks this inflexion when evaluating the total curve.

For Li, the comparisons in Figure 2.3 between the various theoretical  $Q$  curves and experiment show that, except for the very good Nikolaev<sup>11</sup> curve, the CDW result is superior - especially in the higher energy region. It is to be noted that, unlike the CDW calculation, the Nikolaev<sup>11</sup> curve involved the use of an empirically derived velocity-dependent correcting function.

When the target is a  $\text{Li}^+$  ion, Figure 2.4 shows that both the CDW curves are a considerable improvement on the theoretical results of Ob'yedkov and Pavlov<sup>25</sup>, when compared with the experimental data of Sewell et al.<sup>24</sup>. For impact energies  $E > 50$  keV the  $Z_{\text{eff}}$  cross-sections exceed those obtained by using the ps-model, and for  $E > 100$  keV are in slightly better agreement with experiment. Overall the agreement with the experimental data of Sewell et al.<sup>24</sup> looks very good, and as in the case of the Li atom target, it would be very useful if the comparisons could be extended to much higher energies.

## CHAPTER 2.4

### Conclusion

Electron-capture cross-sections have been evaluated for fast protons in collision with the Li atom and its related ions. Such reactions are of interest in the production of hot plasmas which occur in some fusion processes. The calculations were based on the continuum-distorted wave (CDW) approximation and a simple procedure was introduced for assessing the screening of the target nucleus due to the passive electrons which, for capture from the inner shells of a many-electron target, will reflect more closely the physics of the capture process with respect to the distortion acting on the captured electron in the outward channel. The application of the CDW approximation to electron-capture from a many-electron atom becomes tractable, at present, only by reducing it to an equivalent one-electron problem. Consequently, when attempting to replace the 'perfect screening' procedure for an N-electron system by a somewhat more physical model based on the ionization energy, it was appropriate to use a hydrogen-like formula to determine  $Z_{\text{eff}}$ .

It was observed that capture into the higher quantum states ( $n\ell$ ) of hydrogen appeared to be quite sensitive to changes in the screening effects - particularly at high projectile energies  $E$  and especially for capture from the K-shell. This latter feature is of importance since for high impact energies the largest contribution to the capture cross-section for a many electron target will come progressively from the K-shell capture as the projectile velocity  $v$  increases. Although a comparison with experiment of the total cross-sections was limited to relatively low impact energies  $E$  - where both the CDW method and the  $n^{-3}$  rule tend to become less reliable - the general agreement was, nevertheless,

quite satisfactory for the Li target, particularly for impact energies  $E > 80$  keV, and for the  $\text{Li}^+$  target for  $E > 100$  keV. Comparison with experiments at larger  $E$  would obviously be most informative.

For Li we obtain for K-shell capture a kink or inflexion similar in shape to that observed in the experimental curve. This is probably fortuitous, particularly since we are at impact energies for which the CDW method cannot be considered reliable for capture from the Li target 1s shell. Note that a similar kink was obtained in the theoretical curve for capture from the  $\text{Li}^+$  ion when using the  $Z_{\text{eff}}$  model although no such kink was observed in the experimental curve. The correct cross-section curve for K-shell capture from Li is probably such to reach a maximum at  $E \sim 75$  keV and then decrease rapidly to zero as  $E$  decreases. We also note, for Li, that as the projectile velocity increases capture from the K-shell makes a greater contribution to  $Q$  than that from the L-shell, and that for  $E > 150$  keV the contribution to  $Q$  from the L-shell can be considered negligible. This emphasises once again the importance of the high momentum description of the target electrons and hence the need to use accurate wavefunctions in any 'a priori' calculation - even at high projectile velocities.

F-state E (keV)	Li atom												Li <sup>+</sup> ion		
	1 1s			2 1s			2 3S(u)			1 2s			1 2s		
	1s	2s	2p	1s	2s	2p									
200	1.868-3 1.803-3	4.606-4 3.881-4	9.147-5 1.185-4	8.166-3 5.628-3	1.048-3 7.483-4	1.467-4 1.013-4	2.167-2 1.509-2	2.789-3 2.005-3	3.983-4 2.629-3	3.550-2 2.939-3	4.474-2 3.637-3	3.550-2 2.939-3	4.474-2 3.637-3	5.893-4 1.016-3	
500	4.357-5 4.452-5	7.374-6 7.185-6	1.519-6 2.064-6	3.878-4 3.701-4	5.212-5 4.954-5	5.751-6 2.794-6	1.019-3 9.762-4	1.369-4 1.307-4	1.564-5 7.300-5	1.794-3 1.711-3	2.401-4 2.280-4	1.794-3 1.711-3	2.401-4 2.280-4	2.292-5 3.611-5	
800	5.312-6 5.520-6	7.983-7 8.084-7	1.641-7 2.233-7	5.778-5 6.191-5	7.711-6 8.228-6	7.604-7 3.473-6	1.517-4 1.626-4	2.024-5 2.162-5	2.072-6 9.088-6	2.685-4 2.668-4	3.580-5 3.548-5	2.685-4 2.668-4	3.580-5 3.548-5	3.002-6 4.773-6	
1000	1.886-6 1.972-6	2.725-7 2.794-7	5.546-8 7.543-8	2.189-5 2.444-5	2.906-6 3.231-6	2.716-7 1.226-6	5.749-5 6.414-5	7.630-6 8.479-6	7.411-7 3.209-6	1.017-4 1.025-4	1.349-5 1.357-5	1.017-4 1.025-4	1.349-5 1.357-5	1.064-6 1.710-6	
2000	6.582-8 6.960-8	8.820-9 9.255-9	1.713-9 2.316-9	8.598-7 1.042-6	1.122-7 1.354-7	9.019-9 4.074-8	2.261-6 2.731-6	2.950-7 3.549-7	2.475-8 1.068-7	3.972-6 4.118-6	5.182-7 5.367-7	3.972-6 4.118-6	5.182-7 5.367-7	3.425-8 5.761-8	
5000	5.790-10 6.158-10	7.452-11 7.904-11	1.409-11 1.896-11	8.038-9 1.018-8	1.032-9 1.301-9	7.397-11 3.461-10	2.117-8 2.670-8	2.718-9 3.412-9	2.044-10 9.078-10	3.684-8 3.881-8	4.732-9 4.979-9	3.684-8 3.881-8	4.732-9 4.979-9	2.703-10 4.836-10	
8000	4.575-11 4.875-11	5.835-12 6.204-12	1.133-12 1.523-12	6.441-10 8.243-10	8.230-11 1.048-10	5.878-12 2.801-11	1.698-9 2.162-9	2.169-10 2.749-10	1.628-11 7.350-11	2.946-9 3.114-9	3.766-10 3.975-10	2.946-9 3.114-9	3.766-10 3.975-10	2.118-11 3.884-11	
10000	1.344-11 1.433-11	1.708-12 1.818-12	3.395-13 4.563-13	1.899-10 2.440-10	2.423-11 3.096-11	1.752-12 8.411-12	5.007-10 6.401-10	6.387-10 8.122-11	4.857-12 2.207-11	8.681-10 9.184-10	1.108-10 1.171-10	8.681-10 9.184-10	1.108-10 1.171-10	6.278-12 1.163-11	

(a) The tabulated results for the F = 2 3S state include the multiplicity factor

Table 2.1

Electron-capture cross-sections  $\sigma[n\ell, F]$  for Li and Li<sup>+</sup> expressed in units of  $\pi a_0^2$  where  $a_0$  is the atomic unit of length. For each  $\sigma[n\ell, F]$ , the initial entry for a given proton energy E is derived from the  $Z_{\text{eff}}$  approximation and the 'perfect screening' (ps) value is quoted below it. The superscript denotes the power of ten by which each entry should be multiplied.

E(keV)	Li	Li <sup>+</sup>	Li <sup>2+</sup>
200	3.968-2 <u>3.367-2</u>	4.369-2 <u>3.691-2</u>	1.361-2
500	1.804-3 <u>1.860-3</u>	2.219-3 <u>2.138-3</u>	1.240-3
800	2.661-4 <u>3.003-4</u>	3.312-4 <u>3.318-4</u>	2.156-4
1000	1.005-4 <u>1.172-4</u>	1.252-4 <u>1.272-4</u>	8.506-5
2000	3.916-6 <u>4.894-6</u>	4.864-6 <u>5.078-6</u>	3.441-6
5000	3.644-8 <u>4.732-8</u>	4.493-8 <u>4.764-8</u>	2.998-8
8000	2.918-9 <u>3.827-9</u>	3.589-9 <u>3.819-9</u>	2.306-9
10000	8.604-10 <u>1.133-9</u>	1.057-9 <u>1.126-9</u>	6.686-10

Table 2.2 Total capture cross-sections  $Q_T$  for the Li, Li<sup>+</sup> and Li<sup>2+</sup> targets; the units are  $\pi a_0^2$ . The initial entry for a given E is derived from the  $Z_{\text{eff}}$ -model and the ps-value is quoted below it. For the Li atom,  $Q_T = Q(1^1S) + Q(2^1S) + Q(2^3S)$ ; see equation (2.3.3). The superscript denotes the power of ten by which each entry should be multiplied.

Target	Li atom										Li <sup>+</sup> ion		
	1 1s			2 1s			2 3s			1 2s			Q <sub>T</sub>
	1s	2s	2p	1s	2s	2p	1s	2s	2p	1s	2s	2p	
500	-2.1%	+2.6%	-26.4%	+4.8%	+5.2%	+106%	+4.4%	+4.7%	-78.6%	+4.4%	+4.8%	-36.2%	+3.8%
1000	-4.4%	-2.5%	-26.5%	-10.4%	-10.1%	-77.8%	-10.4%	-10.0%	-76.9%	-13.4%	-0.8%	-37.6%	-1.6%
2000	-5.4%	-4.7%	-26.0%	-17.5%	-17.1%	-77.9%	-17.2%	-16.9%	-76.8%	-18.1%	-3.5%	-40.5%	-4.2%
8000	-6.1%	-5.9%	-25.6%	-21.9%	-21.5%	-79.0%	-21.5%	-21.1%	-77.9%	-21.2%	-5.3%	-45.4%	-6.0%

Table 2.3 The percentage change  $\Delta$  in the capture cross-sections

$\sigma[nl,F]$  and  $Q_T$  for the Li and Li<sup>+</sup> targets, at selected E, when progressing from the ps-model to the  $Z_{\text{eff}}$ -model. The quantity  $\Delta$  is defined as

$$\left[ \frac{\{\sigma(Z_{\text{eff}}) - \sigma(\text{ps})\}}{\sigma(\text{ps})} \right] \times 100\%$$

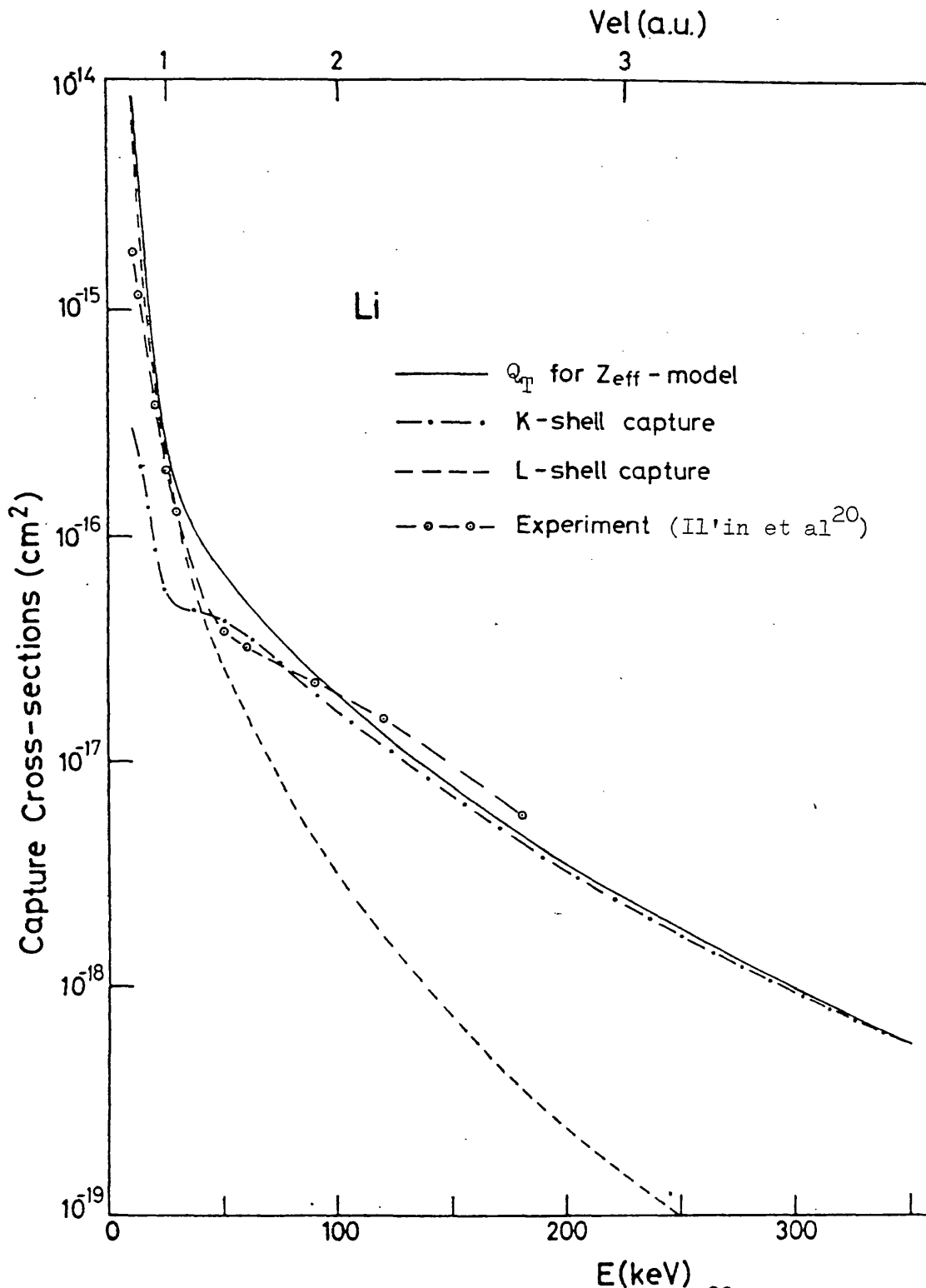


Figure 2.1 A comparison between experiment (Il'in et al<sup>20</sup>) and the total capture cross-sections  $Q_T$  for Li derived from the CDW calculations using the  $Z_{eff}$ -model. Also shown are the calculated results for the capture of a K-shell electron,  $[Q(2^1S) + Q(2^3S)]$  and the capture of the L-shell electron  $[Q(1^1S)]$ ; see equation (2.3.3).

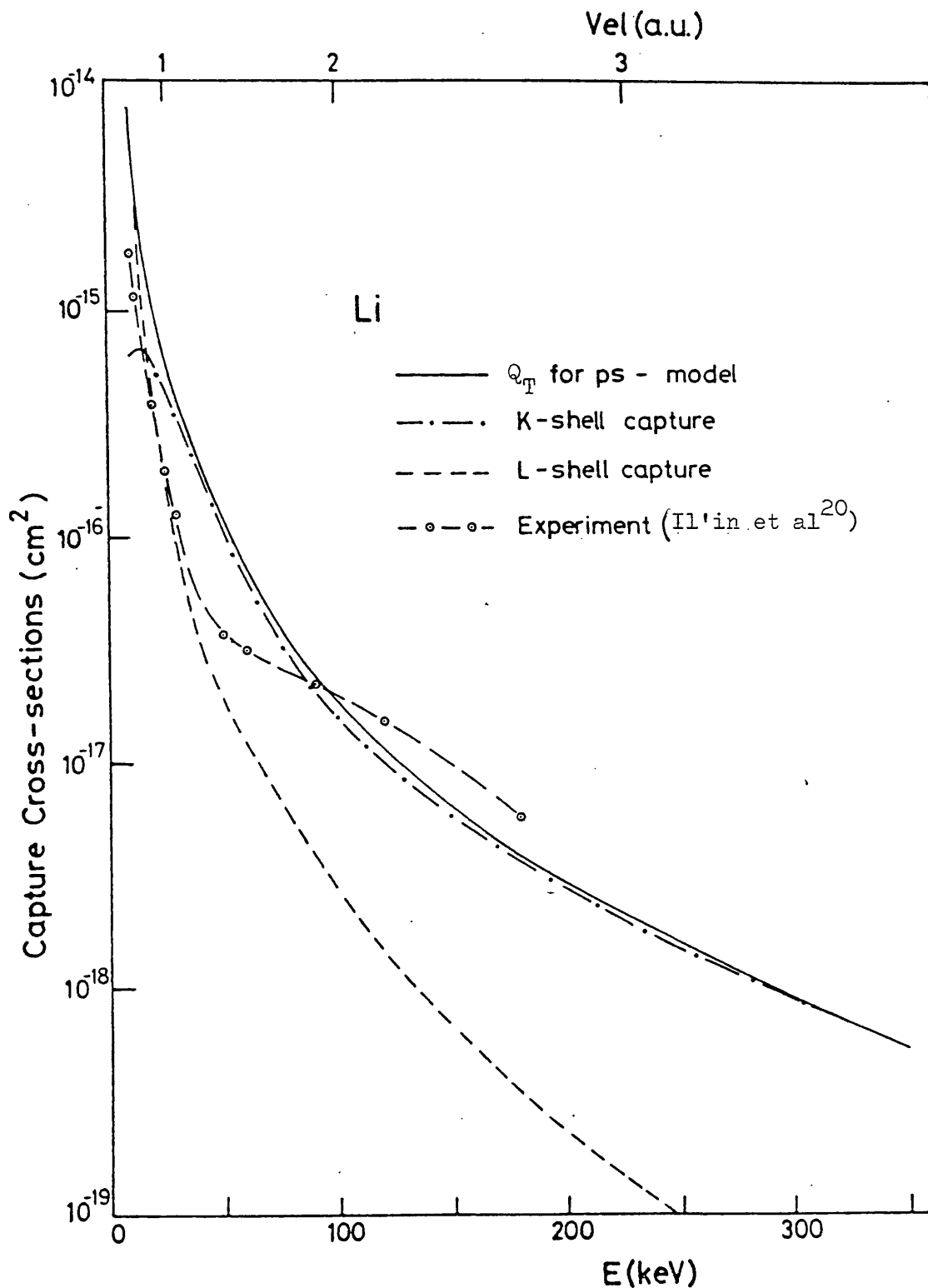


Figure 2.2 A comparison between experiment (Il'in et al<sup>20</sup>) and the the total capture cross-sections  $Q_T$  for Li derived from the CDW calculations using the ps-model. Also shown are the calculated results for the capture of a K-shell electron  $[Q(2^1s)+Q(2^3s)]$  and the capture of the L-shell electron  $[Q(1^1s)]$ ; see equation (2.3.3).



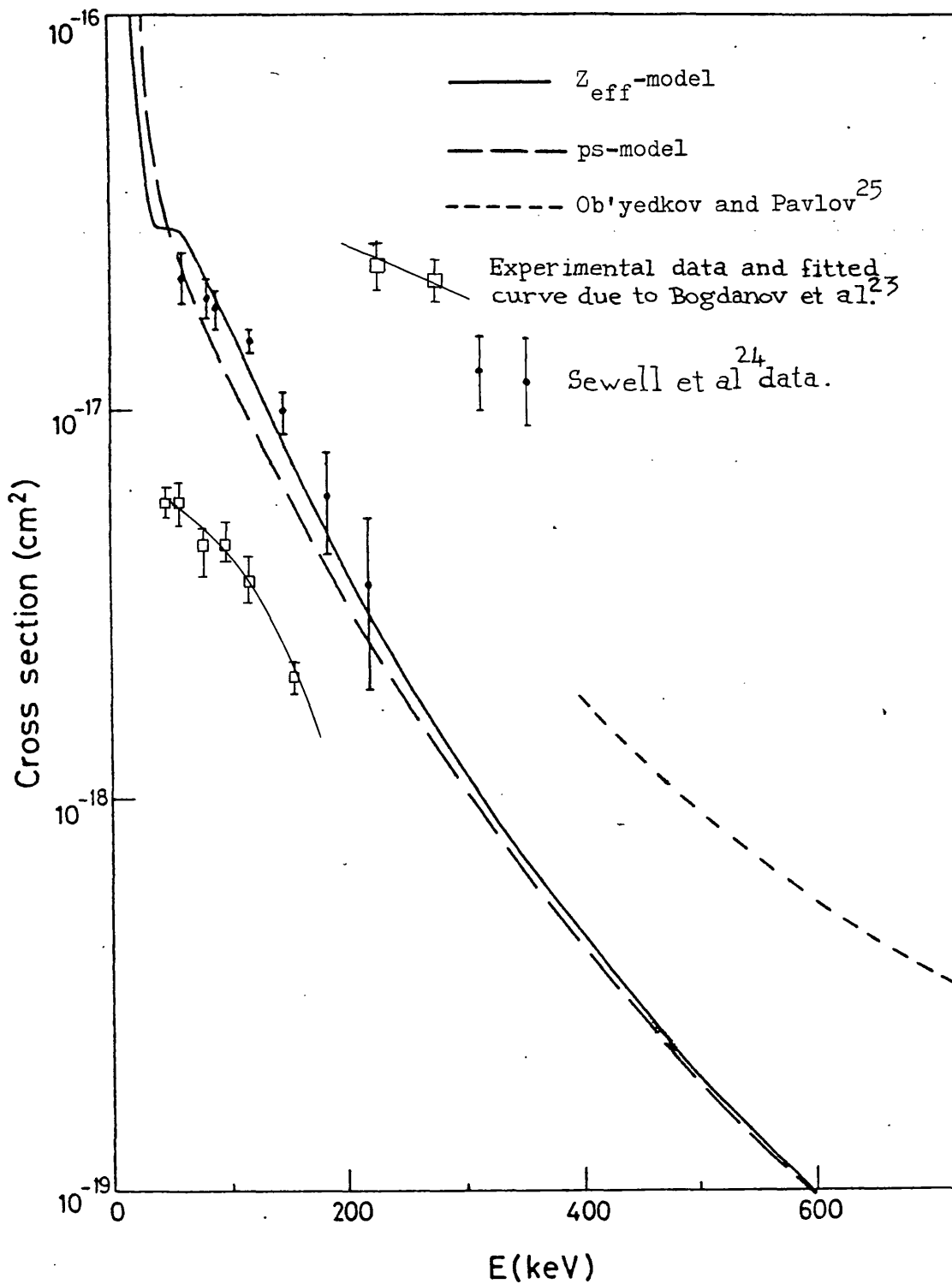


Figure 2.4 The theoretical CDW total cross-sections  $Q$  for protons impinging on  $\text{Li}^+$ , for both the ps and  $Z_{\text{eff}}$ -models, compared with the experimental data of Sewell et al.<sup>24</sup> and the theoretical results of Ob'yedkov and Pavlov<sup>25</sup>.

## References - Part 2

1. C.F. Barnett, 'Proc. 9th Int. Conf. on Physics of Electronic and Atomic Collisions', Ed., J.S. Risley and R.I. Geballe, (Seattle: Univ. Washington Press), 846 (1976)
2. G.F. Bogdanov, A.N. Karkov and Yu. A. Kucharyaev, *Atomnaya Énergiya* (USSR) 19, 1316 (1965)
3. I.M. Cheshire, *Proc. Phys. Soc.* 84, 89 (1964)
4. Dž Belkić and R.K. Janev, *J. Phys. B.* 6, 1020 (1973)
5. A. Salin, *J. Phys. B.* 3, 937 (1970)
6. R.K. Janev and A. Salin, *Fizika.* 4, 165 (1972)
7. J.C. Moore and K.E. Banyard, *J. Phys. B.* 11, 1613 (1978)
8. R.A. Mapleton, *Proc. Phys. Soc.* 85, 1109 (1965)
9. R. McCarroll, *Proc. Roy. Soc. A.* 264, 547 (1961)
10. R.A. Mapleton, *Phys. Rev.* 130, 1829 (1963)  
- , *Phys. Rev.* 145, 25 (1966)  
- , *J. Phys. B. (Proc. Phys. Soc.)* [2] 1, 850 (1968)
11. V.S. Nikolaev, *Sov. Phys. J.E.T.P.* 24, 847 (1967)
12. J.G. Lodge and R.M. May, *Aust. J. Phys.* 21, 793 (1968)
13. J.R. Oppenheimer, *Phys. Rev.* 31, 349 (1928)
14. H.C. Brinkman and H.A. Kramers, *Proc. Acad. Sci. Amsterdam* 33, 973 (1930)
15. E. Clementi and C. Roetti, *Atom. Data Nucl. Data Tables.* 14 (New York, London: Academic Press) (1974)
16. M. Cohen and R.P. McEachran, *Proc. Phys. Soc.* 92 37 (1967)
17. C. Moore, *Atomic Energy Levels*, 1 (Washington: U.S. Govt. Printing Office) (1949)
18. W.L. Wiese, M.W. Smith and B.M. Glennon, *Atomic Transitions Probabilities* (Washington: U.S. Govt. Printing Office) (1966)
19. R.M. Tennent, *Science Data Book* (Publishers: Oliver and Boyd) (1971)
20. R.N. Il'in, V.A. Oparin, E.S. Solov'ev and N.V. Fedorenko, *J.E.T.P. Lett.* 2, 197 (1965)
21. R.N. Il'in, V.A. Oparin, E.S. Solov'ev and N.V. Fedorenko, *Soviet Phys. Tech. Phys.* 11, 921 (1967)

22. C.C.J. Roothaan, L.M. Sachs and A.W.Weiss, Rev. Mod. Phys. 32, 186 (1960)
23. G.F. Bogdanov, A.N. Karkhov, and Yu.A. Kucheryaev, Atomnaya Energiya (USSR) 19, 1316 (1965)
24. E.C. Sewell, G.C. Angel, K.F. Dunn and H.B. Gilbody, J. Phys. B. 13, 2269 (1980)
25. V.D. Ob'yedkov and V.E. Pavlov, Atomnaya Energiya (USSR). 23, 345 (1967)
26. K.E. Banyard and B.J. Szuster, Phys. Rev. A. 16, 129 (1977)

## PART THREE

The Continuum Intermediate States (CIS) method and its application to electron-capture from hydrogen by a simple structured projectile in the form of (a) fast H atoms, and (b) fast Li ions.

## CHAPTER 3.1

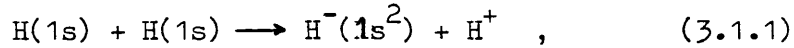
### Introduction

The subject of electron-capture by a structured projectile covers a variety of interactions such as H, He<sup>+</sup>, H<sup>-</sup>, Li<sup>2+</sup>, Be<sup>2+</sup> etc. incident on H or He. These reactions, particularly in the low impact energy region of  $1 \text{ eV} \ll E \ll 1000 \text{ eV}$ , have been investigated using curve-crossing techniques<sup>1</sup>, and methods based on an expansion in terms of molecular eigenfunctions<sup>2</sup>. An example of the latter approach is the "Perturbed Stationary States" or "P.S.S." method which was introduced by Massey and Smith<sup>3</sup>. However, electron-capture involving structured projectiles at higher impact energies such as  $1 \text{ keV} \ll E \ll 200 \text{ keV}$  is also of considerable interest. For example, structured projectiles incident on H are of importance, not only theoretically, but also in connection with the thermo-nuclear fusion research program<sup>4</sup>. The heating of a fusion plasma by injection of H or D atoms will be seriously affected by the presence of a small percentage (1-10%) of highly stripped impurity ions such as O, N, C, Fe, Au etc. These positively charged systems will ionize the H or D atoms either by charge-transfer or ionization, thus causing them to be magnetically deflected out of the plasma to strike the container walls and thereby release more impurities into the plasma. Such reactions were the subject of a theoretical investigation by Olson and Salop<sup>5</sup> using the classical trajectory method to calculate charge-transfer and ionization cross-sections. Electron-capture by heavy charged projectiles is also of great importance in the study of X-ray production which occurs when the electron is captured into an excited state and then undergoes a radiative decay to the ground state. The cross-sections for X-ray production are of interest to the astrophysicist in, for example, cosmic-ray research, where the detection of such X-rays may possibly lead

to a direct measure of the interstellar cosmic-ray intensity. Calculations of X-ray production rates have been made by Watson<sup>6</sup> using the Brinkman-Kramers approximation<sup>7</sup> to evaluate charge-exchange cross-sections. His work on  $F^{q+}$  incident on H, however, has been superseded by that of Belkic and McCarroll<sup>8</sup> who, using the CDW method, obtained much better agreement with experiment.

When the incident structured projectile is a neutral hydrogen atom, charge-exchange reactions may give rise to the formation of the hydrogen negative ion  $H^-$ . The production of  $H^-$  is of importance in astrophysics, since it is found in the atmospheres of stars, and indeed accounts for part of the opacity of our own sun. However, the main and current interest in  $H^-$  lies in the experiments concerned with the building of the first prototype fusion reactor in which neutral hydrogen beams are needed at energies in the range 150-200 keV. The  $H^-$  ions once formed are accelerated to the desired energy and then stripped in a suitable gas target to form the neutral hydrogen atoms. The formation of  $H^-$  in H-H collisions was investigated experimentally by McClure<sup>9</sup> and the corresponding theoretical cross-sections, calculated by Mapleton<sup>10</sup> using a Born approximation<sup>11</sup>, for impact energy  $E > 30$  keV were too large by almost a factor of 10.

The application of the CDW method to charge-exchange between structured systems presents a more difficult problem due to the necessary approximations required with respect to the so called 'passive' electrons which may now reside on both the target and projectile. However, when such collisions involve a one-electron target, the cross-sections may be evaluated by applying the CDW approach to the reverse reaction, and then by dividing by the appropriate factor the desired cross-section is obtained. For example, this procedure was used by Janev and Salin<sup>12,13</sup> and Moore and Banyard<sup>14</sup> when comparing theory with experiment for the reaction



and Moore and Banyard<sup>14</sup> showed that the use of a highly correlated wavefunction for  $H^-$  produced reasonable agreement with experiment down to a projectile energy  $E$  of about 25 keV.

In Part 1 we saw how, for proton projectiles at high impact-energies, the main contribution to the capture cross-section came from regions close to the target nucleus and therefore from small impact parameters. However, when we consider heavy-ion projectiles the probability of capture from large impact parameters increases, with the result that capture into excited-states becomes more important. Shakeshaft<sup>15</sup> has shown that the CDW method is unsatisfactory in predicting a transition amplitude at large impact parameters. The work of Shakeshaft is reviewed in a more recent paper by Belkic<sup>16</sup>, in which he introduces a second-order approximation called the continuum intermediate states (CIS) method. This new method not only predicts a correct transition amplitude at large impact parameters, but is found to be in excellent agreement with experiment for electron-capture by fast  $H^+$  on H atoms. The CIS approach, devised by Belkic<sup>16</sup> for electron-capture by a structureless projectile, is closely related to the CDW method but accounts for distortion effects by inclusion of the continuum intermediate states in only one of the two channels. This feature not only produces considerable simplification from both the analytical and computational viewpoint, but also gives the method greater flexibility for adaptation to the more general case of ion-atom collisions.

Therefore, in Part 3 we present an alternative procedure for determining cross-sections for charge-exchange between simple structured systems (e.g. atoms and ions with one or two electrons). The scheme is based on a modification of the CIS method which, for reasons just outlined, appears to be an appropriate method particularly for heavy-ions

incident on H atoms at large impact energies. In Chapters 3.2 and 3.3 we derive and evaluate the CIS cross-section for capture of an electron 1, say, by a projectile system  $(Z_A, e(2))$  in collision with a target  $(Z_B, e(1))$  and show that, as a result of the approximations, the scheme is most applicable to the case when  $Z_A > Z_B$ . However, as a simple test of the proposed scheme we first apply it to reaction (3.1.1) for which  $Z_A = Z_B$ . Although this reaction may be complicated by the fact that electron correlation may play a non-trivial role, the reaction has the advantage that capture into excited states need not be considered due to the very low probability of finding the  $H^-$  system existing in any other state than its ground state. In fact it is highly questionable whether  $H^-$  can exist at all in an excited state. Indeed the proof that  $H^-$  only exists in its ground state has been the subject of a theoretical investigation by Hill<sup>17</sup>. Also in an experiment designed to measure electron-capture cross-sections in H-H collisions, any  $H^-$  atoms being formed in an excited state, should it exist, would be quickly ionized and the process would be detected as an ionization process, i.e.  $H + H \rightarrow H^+ + H + e$ . Therefore, the electron capture cross-section is calculated for the reaction,  $H(1s) + H(1s) \rightarrow H^-(1s^2) + H^+$ , for impact energies in the range  $10 \text{ keV} < E < 200 \text{ keV}$  and we compare the results with the experimental data of McClure<sup>9</sup>.

For any method, the sensitivity of the calculations with respect to the wavefunction employed is of importance if the general physics of the method is to be understood.

In the case of the Born and CDW cross-section calculations there have been many theoretical investigations with respect to this aim. As emphasised in Part 1 of this thesis the effects of electron correlation on the electron-capture cross-section may be significant when the  $H^-(1s^2)$  system is involved. Thus, in applying the new scheme to reaction

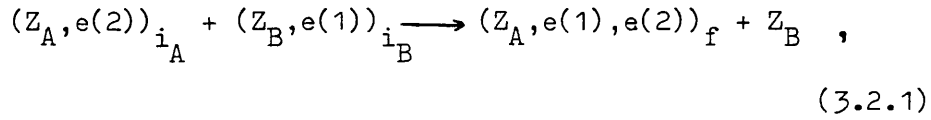
(3.1.1) we use both Hartree-Fock and configuration interaction wavefunctions to describe the  $H^-(1s^2)$  system: this allows us to comment on the influence of electron correlation.

A more appropriate application of the proposed scheme is in the calculation of electron-capture from H atoms by fast Li ions, which has been the subject of a recent experimental investigation by Shah, Goffe and Gilbody<sup>18</sup>. Thus the individual cross-sections for electron capture into the final states  $n\ell = 1s, 2s, 2p, 3s, 3p$  and  $3d$  are examined for  $Li^+$ ,  $Li^{2+}$  and  $Li^{3+}$  incident on H atoms with impact energies in the range  $100 \text{ keV} < E < 10,000 \text{ keV}$ . The individual cross-sections are then used in conjunction with an appropriate  $n^{-3}$  sum rule to evaluate the total cross-sections which are then compared with the experimental data.

CHAPTER 3.2

Derivation of the Continuum Intermediate States (CIS) transition  
amplitude for electron-capture by a simple structured projectile

In this derivation many of the steps involved are similar, if not identical, to those in the derivation of the CDW transition amplitude. Therefore, for the purpose of brevity, we will not repeat steps when it is easier to refer back to Chapter 1.2. Again we will formulate the problem within the impact parameter method and the geometry and labelling of position vectors will be as used in Part 1 for reaction (1.2.1), see Figure 3.1. Let us consider the general reaction:



where  $i$  and  $f$  denote the initial and final states, respectively. The complete Schrodinger equation for the reaction will be

$$\left( \frac{1}{2} \nabla_{\underline{r}_1}^2 + \frac{1}{2} \nabla_{\underline{r}_2}^2 + \frac{Z_A}{s_2} + \frac{Z_A}{s_1} + \frac{Z_B}{x_1} + \frac{Z_B}{x_2} - \frac{1}{s_{12}} - \frac{Z_A Z_B}{R} \right) \Psi(\underline{r}_1, \underline{r}_2, t) = -i \frac{\partial}{\partial t} \Psi(\underline{r}_1, \underline{r}_2, t) \quad , \quad (3.2.2)$$

where again we will choose the reference origin  $O$  to be the mid-point between  $Z_A$  and  $Z_B$ . The correct asymptotic conditions for  $\Psi(\underline{r}_1, \underline{r}_2, t)$  will be

$$\Psi_{i_A}(\underline{r}_1, \underline{r}_2, t) \longrightarrow \Phi_{i_A}(\underline{r}_1, \underline{r}_2, t) \quad \text{and} \quad \Psi_{i_B}(\underline{r}_1, \underline{r}_2, t) \longrightarrow \Phi_{i_B}(\underline{r}_1, \underline{r}_2, t) \quad , \quad (3.2.3)$$

where

$$\Phi_{i_A}(\underline{r}_1, \underline{r}_2, t) = \Omega_{i_A}(\underline{r}_1, \underline{r}_2, t) \exp\left(-i \frac{(Z_A - 1)(Z_B - 1)}{v} \ln(vR - v^2 t)\right) \quad (3.2.4)$$

and

$$\Phi_f(\underline{r}_1, \underline{r}_2, t) = \Omega_f(\underline{r}_1, \underline{r}_2, t) \exp\left(-i \frac{(Z_A - 2)Z_B}{v} \ln(vR + v^2 t)\right) . \quad (3.2.5)$$

The functions  $\Phi_i$  and  $\Phi_f$  are the asymptotic wavefunctions satisfying the asymptotic Schrodinger equation, obtained by setting

$1/s_{12} \rightarrow 1/R$  ,  $Z_A/s_1 \rightarrow Z_A/R$  and  $Z_B/x_2 \rightarrow Z_B/R$  for the initial channel, and  $Z_B/x_1 \rightarrow Z_B/R$  and  $Z_A/s_2 \rightarrow Z_A/R$  for the final channel. The functions  $\Omega_i$  and  $\Omega_f$  are given by

$$\Omega_i(\underline{r}_1, \underline{r}_2, t) = \Psi_{i_A}(\underline{s}_2) \chi_{i_B}(\underline{x}_1) \exp\left(-i \left[ \frac{1}{2} v \cdot \underline{r}_1 - \frac{1}{2} v \cdot \underline{r}_2 + \frac{1}{4} v^2 t + (\epsilon_{i_A} + \epsilon_{i_B}) t \right]\right) \quad (3.2.6)$$

and

$$\Omega_f(\underline{r}_1, \underline{r}_2, t) = \phi_f(\underline{s}_1, \underline{s}_2) \exp\left(-i \left[ -\frac{1}{2} v \cdot \underline{r}_1 - \frac{1}{2} v \cdot \underline{r}_2 + \frac{1}{4} v^2 t + \epsilon_f t \right]\right) , \quad (3.2.7)$$

where  $\Psi_{i_A}$  ,  $\chi_{i_B}$  and  $\phi_f$  are the corresponding bound-state electronic wavefunctions with eigenvalues  $\epsilon_{i_A}$  ,  $\epsilon_{i_B}$  and  $\epsilon_f$  given by the solutions of

$$\left( \frac{1}{2} \nabla_{\underline{r}_2}^2 + \frac{Z_A}{s_2} + \epsilon_{i_A} \right) \Psi_{i_A} = 0 , \quad (3.2.8)$$

$$\left( \frac{1}{2} \nabla_{\underline{r}_1}^2 + \frac{Z_B}{x_1} + \epsilon_{i_B} \right) \chi_{i_B} = 0 \quad (3.2.9)$$

and

$$\left( \frac{1}{2} \nabla_{\underline{r}_1}^2 + \frac{1}{2} \nabla_{\underline{r}_2}^2 + \frac{Z_B}{s_1} + \frac{Z_A}{s_2} - \frac{1}{s_{12}} + \epsilon_f \right) \phi_f = 0 . \quad (3.2.10)$$

It follows that the distorted waves  $\chi_i$  and  $\chi_f$  are defined by the equations

$$\left[ \frac{1}{2} \nabla_{\underline{r}_1}^2 + \frac{1}{2} \nabla_{\underline{r}_2}^2 + \frac{Z_A}{s_2} + \frac{Z_B}{x_1} - \frac{(Z_A - 1)(Z_B - 1)}{R} + \frac{i\delta}{\delta t} + U_i \right] \chi_i(\underline{r}_1, \underline{r}_2, t) = 0 \quad (3.2.11)$$

and

$$\left[ \frac{1}{2} \nabla_{\underline{r}_1}^2 + \frac{1}{2} \nabla_{\underline{r}_2}^2 + \frac{Z_A}{s_1} + \frac{Z_A}{s_2} - \frac{1}{s_{12}} - \frac{(Z_A - 2)Z_B}{R} + \frac{i\delta}{\delta t} + U_f \right] \chi_f(\underline{r}_1, \underline{r}_2, t) = 0 . \quad (3.2.12)$$

Ideally, we would like

$$\begin{array}{ccc} \chi_i \longrightarrow \Phi_i & \text{and} & \chi_f \longrightarrow \Phi_f \\ t \longrightarrow -\infty & & t \longrightarrow +\infty \end{array} \quad (3.2.13)$$

since, with the correct choice of potentials,  $U_i$  and  $U_f$  should vanish in the limit of large internuclear separation.

Adopting the procedure outlined in Chapter 1.2, see equations (1.2.3) to (1.2.25), we can obtain an expression for the 'prior' transition amplitude  $a_{if}$ . Thus, it follows from the equation defining  $\chi_i$ , that  $a_{if}$  is given by

$$a_{if} = i \int_{-\infty}^{+\infty} dt \int \underline{dr}_1 \underline{dr}_2 \Psi_f^* \left( \frac{Z_A}{s_1} - \frac{1}{s_{12}} + \frac{Z_B}{x_2} + \frac{1 - Z_A - Z_B}{R} - U_i \right) \chi_i , \quad (3.2.14)$$

provided that

$$\lim_{t \rightarrow +\infty} \int \underline{dr}_1 \underline{dr}_2 \Psi_f^* \chi_i = 0 . \quad (3.2.15)$$

Alternatively, we may consider the time reversed reaction to obtain  $b_{if}$ , the 'post' transition amplitude

$$b_{if} = i \int_{-\infty}^{+\infty} dt \int \underline{dr}_1 \underline{dr}_2 \left[ \left( \frac{Z_B}{x_1} + \frac{Z_B}{x_2} - \frac{2Z_B}{R} - U_f \right) \chi_f^* \right] \Psi_i , \quad (3.2.16)$$

provided

$$\lim_{t \rightarrow +\infty} \int \underline{dr}_1 \underline{dr}_2 \chi_f^* \Psi_i = 0 . \quad (3.2.17)$$

We will find, as discussed later, that the role played by the passive electron in the evaluation of  $a_{if}$  appears in a different form to that in the determination of  $b_{if}$ , and that, as a result, the choice between

the use of  $a_{if}$  and  $b_{if}$  becomes a matter of expediency.

### The Distorted Wave Functions

As in Chapter 1.2 we represent the solutions of  $\Psi_i$  and  $\Psi_f$  in the form

$$\Psi_i(\underline{r}_1, \underline{r}_2, t) = \Omega_i(\underline{r}_1, \underline{r}_2, t) \mathcal{L}_i(\underline{s}_1, \underline{x}_2, t) \quad (3.2.18)$$

and

$$\Psi_f(\underline{r}_1, \underline{r}_2, t) = \Omega_f(\underline{r}_1, \underline{r}_2, t) \mathcal{L}_f(\underline{x}_1, \underline{x}_2, t) \quad (3.2.19)$$

Substituting  $\Psi_i$  and  $\Psi_f$  into equations (3.2.2) we find that  $\mathcal{L}_i$  and  $\mathcal{L}_f$  are solutions of

$$\begin{aligned} & \left[ \frac{1}{2} \nabla_{\underline{r}_1}^2 + \frac{1}{2} \nabla_{\underline{r}_2}^2 + \frac{Z_A}{s_1} + \frac{Z_B}{x_2} - \frac{1}{s_{12}} - \frac{Z_A Z_B}{R} - \frac{i}{2} \underline{v} \cdot \nabla_{\underline{r}_1} + \frac{i}{2} \underline{v} \cdot \nabla_{\underline{r}_2} + \frac{i\partial}{\partial t} \right] \mathcal{L}_i(\underline{s}_1, \underline{x}_2, t) \\ & = - \sum_{j=1}^2 \left[ \nabla_{\underline{r}_j} \log_e \Psi_{i_A}(\underline{s}_2) \chi_{i_B}(\underline{x}_1) \right] \cdot \left[ \nabla_{\underline{r}_j} \mathcal{L}_i(\underline{s}_1, \underline{x}_2, t) \right] \end{aligned} \quad (3.2.20)$$

and

$$\begin{aligned} & \left[ \frac{1}{2} \nabla_{\underline{r}_1}^2 + \frac{1}{2} \nabla_{\underline{r}_2}^2 + \frac{Z_B}{x_1} + \frac{Z_B}{x_2} - \frac{Z_A Z_B}{R} + \frac{i}{2} \underline{v} \cdot \nabla_{\underline{r}_1} + \frac{i}{2} \underline{v} \cdot \nabla_{\underline{r}_2} + \frac{i\partial}{\partial t} \right] \mathcal{L}_f(\underline{x}_1, \underline{x}_2, t) \\ & = - \sum_{j=1}^2 \left[ \nabla_{\underline{r}_j} \log_e \phi_f(\underline{s}_1, \underline{s}_2) \right] \cdot \left[ \nabla_{\underline{r}_j} \mathcal{L}_f(\underline{x}_1, \underline{x}_2, t) \right], \end{aligned} \quad (3.2.21)$$

respectively. In solving equations (3.2.20, 21) to first-order we neglect the right-hand side and then make the appropriate approximations concerning the passive electron e(2) in order that the first-order solutions,  $\mathcal{L}'_i$  and  $\mathcal{L}'_f$ , will have the correct asymptotic behaviour.

This last condition is satisfied by making the approximation

$$\frac{Z_B}{x_2} = \frac{Z_B}{R} \quad \text{and} \quad \frac{1}{s_{12}} = \frac{1}{s_1} \quad (3.2.22)$$

The equations for  $\mathcal{L}'_i$  and  $\mathcal{L}'_f$  are then given by

$$\left( \frac{1}{2} \nabla_{\underline{r}_1}^2 + \frac{Z_A - 1}{s_1} - \frac{(Z_A - 1)Z_B}{R} - \frac{i}{2} \underline{v} \cdot \nabla_{\underline{r}_1} + \frac{i\partial}{\partial t} \right) \mathcal{L}'_i(\underline{s}_1, t) = 0 \quad (3.2.23)$$

and

$$\left( \frac{1}{2} \nabla_{\underline{r}_1}^2 + \frac{Z_B}{x_1} - \frac{(Z_A - 1)Z_B}{R} + \frac{i}{2} \underline{v} \cdot \nabla_{\underline{r}_1} + \frac{i\partial}{\partial t} \right) \mathcal{L}'_f(\underline{x}_1, t) = 0 \quad (3.2.24)$$

Solving for  $\mathcal{L}'_i$  and  $\mathcal{L}'_f$  we obtain

$$\mathcal{L}'_i(\underline{s}_1, t) = N_A(v) {}_1F_1 \left[ i\nu_1 ; 1 ; i(\underline{v}s_1 + \underline{v} \cdot \underline{s}) \right] \exp \left[ \frac{i(Z_A - 1)Z_B}{v} \ln(\nu R - \sqrt{t}) \right] \quad (3.2.25)$$

and

$$\mathcal{L}'_f(\underline{x}_1, t) = N_B^*(v) {}_1F_1 \left[ -i\nu_2 ; 1 ; -i(\underline{v}x_1 + \underline{v} \cdot \underline{x}_1) \right] \exp \left[ \frac{-i(Z_A - 1)Z_B}{v} \ln(\nu R + \sqrt{t}) \right] \quad (3.2.26)$$

where  $\nu_1 = (Z_A - 1)/v$ ,  $\nu_2 = Z_B/v$ , and  $N_A(v)$  and  $N_B(v)$  are defined in equations (1.2.39a, 40a). Note that by using conditions (1.2.41 - 43b)

$\mathcal{L}'_i$  and  $\mathcal{L}'_f$  and hence  $\Psi_i = \Omega_i \mathcal{L}'_i$  and  $\Psi_f = \Omega_f \mathcal{L}'_f$  can be shown to have the correct asymptotic behaviour given by (3.2.3).

As a result of the approximations (3.2.22), the distortion, by  $Z_B$ , of the passive electron wavefunction centred on  $Z_A$  has been effectively removed. In the cases for which the scheme is proposed, i.e.  $Z_A \gg Z_B$  in which  $e(2)$  will be tightly bound to  $Z_A$  compared with the binding of  $e(1)$  to  $Z_B$ , this is a reasonable approximation to make. In addition, any influence on the formation of  $(Z_A, e(1), e(2))_f$ , in reaction (3.2.1), due to the distortion of  $e(2)$  by  $Z_B$  will arise from the influence of  $e(2)$  on  $e(1)$ , and this will thus involve an electron correlation effect. Thus for  $Z_A \gg 3$ , when electron correlation effects in reaction (3.2.1) should be minimal, the contribution from such a two-step process is expected to be negligible.

However, it is also important to note that in making the approximation  $s_{12} \stackrel{\approx}{=} s_1$  we have effectively pushed the passive electron  $e(2)$  into the projectile nucleus and therefore it will screen the projectile nuclear charge  $Z_A$  by unity. This latter feature contradicts the rationalisation that the maximum contribution to the cross-section will occur when  $e(1)$  experiences the full charge of  $Z_A$ . Fortunately the approximation that  $s_{12} \stackrel{\approx}{=} s_1$  appears only in equation (3.2.20) and, as we shall see later, the formulation of the CIS method is such that only one of the distortion functions,  $\mathcal{L}'_i$  or  $\mathcal{L}'_f$ , need be used, depending on whether we use  $a_{if}$  or  $b_{if}$ .

Up to this point the formulation of  $a_{if}$  and  $b_{if}$  is quite general and the method we finally employ, CDW or CIS, depends ultimately on the choice for  $U_i$  and  $U_f$ . We now turn our attention to solving equations (3.2.11, 12) within the framework of the CIS method as presented by Belkic<sup>16</sup>. Following Belkic<sup>16</sup>, we choose  $U_i$  and  $U_f$  such that the distorted waves  $\chi_i$  and  $\chi_f$  will involve only the unperturbed eigenfunctions  $\Omega_i$  and  $\Omega_f$ , respectively, along with the appropriate phase functions, say  $g_i(t)$  and  $g_f(t)$ . Thus we look for solutions to  $\chi_i$  and  $\chi_f$  in the form

$$\chi_i(\underline{r}_1, \underline{r}_2, t) = \Omega_i(\underline{r}_1, \underline{r}_2, t) g_i(t) \quad (3.2.27)$$

and

$$\chi_f(\underline{r}_1, \underline{r}_2, t) = \Omega_f(\underline{r}_1, \underline{r}_2, t) g_f(t), \quad (3.2.28)$$

where  $g_i(t)$  and  $g_f(t)$  are given by

$$g_i(t) = \exp \left[ \frac{i(Z_A - 1)Z_B}{v} \ln(vR - v^2 t) \right] \quad (3.2.29)$$

and

$$g_f(t) = \exp \left[ \frac{-i(Z_A - 1)Z_B}{v} \ln(vR + v^2 t) \right]. \quad (3.2.30)$$

It follows therefore that the necessary choice for  $U_i$  and  $U_f$  will be

$$U_i = \frac{-(Z_A - 1)}{R} \quad \text{and} \quad U_f = \frac{-Z_B}{R} \quad (3.2.31)$$

Note that  $U_i$  and  $U_f$  are simply the distorting potentials acting on  $e(1)$  at large internuclear separations since, in this limit,  $s_1 \doteq R$ . With this choice of  $U_i$  and  $U_f$  the solutions obtained for  $\chi_i$  and  $\chi_f$  are such that the boundary conditions (3.2.13) are not obeyed since  $U_i$  and  $U_f$  do not vanish in the limit of large internuclear separation, but vary as  $1/R$ . We note also that  $\chi_i$  and  $\chi_f$  are devoid of any continuum intermediate states which arise via the Coulomb functions,

${}_1F_1 \left[ \begin{matrix} \pm i \nu & ; & 1 & ; & \pm i(\nu r + \underline{v} \cdot \underline{r}) \end{matrix} \right]$ , such as those found in the solutions of  $\Psi_i$  and  $\Psi_f$ . By substituting for  $U_i$  and  $U_f$  into equations (3.2.14) and (3.2.16) we finally obtain the CIS 'prior' and 'post' transition amplitudes for reaction (3.2.1),

$$a_{if} = i \int_{-\infty}^{+\infty} dt \int \frac{dr_1}{s_1} \frac{dr_2}{s_{12}} \Psi_f^* \left( \frac{Z_A}{s_1} - \frac{1}{s_{12}} + \frac{Z_B}{x_2} - \frac{Z_B}{R} \right) \chi_i \quad (3.2.32)$$

and

$$b_{if} = i \int_{-\infty}^{+\infty} dt \int \frac{dr_1}{x_1} \frac{dr_2}{x_2} \left[ \left( \frac{Z_B}{x_1} + \frac{Z_B}{x_2} - \frac{Z_B}{R} \right) \chi_f^* \right] \Psi_i \quad (3.2.33)$$

We recall that in solving for  $\Psi_i$  and  $\Psi_f$  the distorting potential  $Z_B/x_2$ , in the equations for  $\Psi_i$  and  $\Psi_f$  (see equations (3.2.20) and (3.2.21)), was set equal to  $Z_B/R$ . This approximation enabled the distortion of the passive electron wavefunction to be removed from the problem and, as argued, is a good approximation for  $Z_A > Z_B$ . A consequence, however, of removing the distortion potential  $Z_B/x_2 - Z_B/R$  from the equations for  $\Psi_i$  and  $\Psi_f$  is that it now appears as a perturbing potential in the matrix elements  $a_{if}$  and  $b_{if}$ . Thus, it would appear reasonable and consistent to make the same approximation in equations (3.2.32) and (3.2.33). Therefore in the scheme presented here

for reaction (3.2.1) we will assume that we can set  $x_2$  equal to R consistently throughout the analysis, and obtain for the prior and post transition amplitudes

$$a_{if} = i \int_{-\infty}^{+\infty} dt \int d\underline{r}_1 d\underline{r}_2 \Psi_f^* \left( \frac{Z_A}{s_1} - \frac{1}{s_{12}} \right) \chi_i, \quad (3.2.34)$$

and

$$b_{if} = i \int_{-\infty}^{+\infty} dt \int d\underline{r}_1 d\underline{r}_2 \left[ \left( \frac{Z_B}{x_1} \right) \chi_f^* \right] \Psi_i, \quad (3.2.35)$$

respectively.

The post transition amplitude  $b_{if}$  involves the solution to  $\Psi_i$  via  $\mathcal{L}'_i$ , in which we had to invoke 'perfect' screening of the projectile nucleus by the passive electron e(2) using the approximation  $1/s_{12} = 1/s_1$ . However, in  $a_{if}$  the relevant potential ( $1/s_{12}$ ) now appears as a perturbing potential within the matrix element and therefore lends itself to the possibility of a more flexible approximation. It also turns out that  $a_{if}$  is the more desirable of the two forms from the point of view of evaluating the cross-section, particularly if complicated wavefunctions are used to describe the excited states of the captured electron.

Finally, we note that for the one-electron reaction

$Z_A + (Z_B, e(1)) \longrightarrow (Z_A, e(1)) + Z_B$  the transition amplitude  $a_{if}$  is easily obtained by removing the  $1/s_{12}$  term and by substituting the appropriate one-electron wavefunctions for  $\chi_i$ ,  $\chi_f^*$ ,  $\Psi_i$  and  $\Psi_f^*$ . Furthermore, for  $Z_A = Z_B = 1$  i.e. protons incident on H, we will obtain the expression given by Belkic<sup>16</sup>.

## CHAPTER 3.3

### Evaluation of the transition amplitude

In this chapter we evaluate the CIS transition amplitude  $a_{if}$  and the cross-section for reaction (3.2.1). We will first consider capture into the ground-state only and treat capture into excited-states separately later. Let us describe the ground-state of the final projectile by the natural expansion of a CI wavefunction, the form of which was described in Chapter 1.3, equation (1.3.2). We can then always reduce the resulting equations to correspond to a simple Hartree-Fock wavefunction as was done in the CDW calculations. For simplicity we will only consider the most usual case of the target and initial projectile being in its ground-state. Thus we have for the bound electronic wavefunctions

$$\Psi_{1s}(\underline{s}_2) = \sqrt{\frac{Z_A^3}{\pi}} e^{-Z_A s_2} \quad , \quad (3.3.1)$$

$$\chi_{1s}(\underline{x}_1) = \sqrt{\frac{Z_B^3}{\pi}} e^{-Z_B x_1} \quad . \quad (3.3.2)$$

and 
$$\phi_{1s}(\underline{s}_1, \underline{s}_2) = D_{\alpha\beta\gamma} \mathcal{Q}_{\alpha\beta}(\underline{s}_1) \mathcal{Q}_{\alpha\gamma}(\underline{s}_2) \quad , \quad (3.3.3)$$

where the form of  $D_{\alpha\beta\gamma}$ ,  $\mathcal{Q}_{\alpha\beta}$  and  $\mathcal{Q}_{\alpha\gamma}$  are defined in Chapter 1.3, equations (1.3.5-8). In order not to repeat trivial steps we will mention only the major features of the analysis and will refer back to Chapter 1.3 when possible.

After substituting the solutions for  $\Psi_f$  and  $\chi_i$  from equations (3.2.19) and (3.2.27) into the expression for  $a_{if}$ , equation (3.2.34), we multiply the phase functions together, substitute for  $\Omega_i$  and  $\Omega_f$  from equations (3.2.6,7) and replace the Coulomb function in  $\Psi_f$  by its integral representation (see Chapter 1.3, equation (1.3.13)) to obtain

for  $a_{if}$  the expression

$$a_{if}(1s) = \frac{N_B(v)(bv)^{\frac{2iZ}{v}}}{2\pi} \int_{-\infty}^{+\infty} dt e^{-i\Delta\epsilon t} \oint \frac{d\mathfrak{z}}{\mathfrak{z}} \left(1 + \frac{1}{\mathfrak{z}}\right)^{-i\nu} \int d\underline{r}_1 \int d\underline{r}_2 e^{-i\underline{v}\cdot\underline{r}_1} \phi_{1s}^*(\underline{s}_1, \underline{s}_2) V_{1,2}^0 \psi_{1s}(\underline{s}_2) \chi_{1s}(\underline{x}_1) e^{-i\mathfrak{z}(\underline{v}\underline{x}_1 + \underline{v}\cdot\underline{x}_1)}, \quad (3.3.4)$$

where  $\Delta\epsilon = \epsilon_A(1s) + \epsilon_B(1s) - \epsilon_F(1s^2)$ ,  $Z = (Z_A - 1)Z_B$ , and  $b$  is the impact parameter.  $V_{1,2}^0$  is the perturbing potential acting on the active electron  $e(1)$  due to the approaching projectile i.e.  $V_{1,2}^0 = Z_A/s_1 - 1/s_{12}$ . At this point we must decide how to handle the electron-electron potential term. If we are to be consistent with the approximation made with respect to  $x_2$  we should set  $V_{1,2}^0 = (Z_A - 1)/s_1$  which invokes perfect screening of the projectile nucleus  $Z_A$  by  $e(2)$ . This approximation would seem reasonable for large  $Z_A$  although it does not allow  $e(1)$  to experience the full charge of  $Z_A$  for which the probability of capture would be a maximum. A more appropriate approximation to  $V_{1,2}^0$  is obtained by replacing the electron-electron potential by the average electrostatic potential acting on  $e(1)$  due to the distribution of charge around  $Z_A$ . Thus  $V_{1,2}^0$  is given by its approximate form  $V_{1,2}^1$

$$V_{1,2}^1 = \frac{Z_A}{s_1} - \frac{1}{s_1} + e^{-2Z_A s_1} \left( Z_A + \frac{1}{s_1} \right), \quad (3.3.5)$$

which has the following useful features

$$V_{1,2}^1 \xrightarrow{s_1 \rightarrow \infty} \frac{Z_A - 1}{s_1} \quad (3.3.6)$$

and 
$$V_{1,2}^1 \xrightarrow{s_1 \rightarrow 0} \frac{Z_A}{s_1} \quad (3.3.7)$$

Substituting for the bound-state electronic wavefunctions (3.3.1-3),

$a_{if}$  may be re-written in the form

$$a_{if}(1s) = \frac{N_B(v)(bv)}{2\pi} \frac{2iZ}{v} D_{\alpha\beta\gamma} \int_{-\infty}^{+\infty} dt e^{-i\Delta\epsilon t} \oint \frac{d\xi}{\xi} \left(1 + \frac{1}{\xi}\right)^{-i\nu_2} I_{\alpha\gamma} R_{\alpha\beta}, \quad (3.3.8)$$

$$\text{where } I_{\alpha\gamma} = \int d\underline{r}_2 \psi_{1s}(\underline{s}_2) \varphi_{\alpha\gamma}(\underline{s}_2) \quad (3.3.9)$$

$$\text{and } R_{\alpha\beta} = \int d\underline{r}_1 \varphi_{\alpha\beta}^*(\underline{s}_1) v_{1,2}^1 \chi_{1s}(\underline{x}_1) e^{-i\underline{v}\cdot\underline{r}_1} e^{-i\underline{\xi}(\underline{v}\underline{x}_1 + \underline{v}\cdot\underline{x}_1)} \quad (3.3.10)$$

Using the Fourier transform method to evaluate the above integrals it is easily shown that

$$a_{if}(1s) = \frac{N_B(v)(bv)}{(2\pi)^7} \frac{2iZ}{v} D_{\alpha\beta\gamma} \int_{-\infty}^{+\infty} dt e^{-i\Delta\epsilon t} \oint \frac{d\xi}{\xi} \left(1 + \frac{1}{\xi}\right)^{-i\nu_2} \\ \times I_{\alpha\gamma} \int d\underline{r}_1 e^{-i\underline{v}\cdot\underline{r}_1} \int d\underline{k} \int d\underline{K} F^*(\underline{k}) G(\underline{K}) \\ \times e^{i\underline{k}\cdot\underline{s}_1} e^{-i\underline{K}\cdot\underline{x}_1}, \quad (3.3.11)$$

where

$$F_{\alpha\beta}^*(\underline{k}) = \int \varphi_{\alpha\beta}(\underline{s}_1) v_{1,2}^1 e^{i\underline{k}\cdot\underline{s}_1} d\underline{s}_1 \quad (3.3.12)$$

and

$$G_{1s}(\underline{K}) = \int \chi_{1s}(\underline{x}_1) e^{-i\underline{\xi}(\underline{v}\underline{x}_1 + \underline{v}\cdot\underline{x}_1)} e^{i\underline{k}\cdot\underline{x}_1} d\underline{x}_1 \quad (3.3.13)$$

Both the  $F^*$  and  $G$  integrals can be solved quite easily by making use of the expression given in Chapter 1.3, equations (1.3.31,32). Carrying out the integrations over  $\underline{r}$  and  $\underline{k}$  (remembering that  $\underline{v}$  is defined in the  $z$ -direction) and finally over time  $t$ , we obtain that  $\underline{k} = \underline{K} + \underline{v}$  and that  $K_z = -v/2 - \Delta\epsilon/v$ . Thus (3.3.11) becomes

$$a_{if}(1s) = \frac{N_B(v)(bv)}{(2\pi)^3 v} \frac{2iZ}{v} D_{\alpha\beta\gamma} \oint \frac{d\xi}{\xi} \left(1 + \frac{1}{\xi}\right)^{-i\nu_2} I_{\alpha\gamma} \\ \int_{-\infty}^{+\infty} dK_x e^{-ibK_x} \int_{-\infty}^{+\infty} dK_y F_{\alpha\beta}^*(K_x, K_y, v/2 - \frac{\Delta\epsilon}{v}) G_{1s}(K_x, K_y, -v/2 - \frac{\Delta\epsilon}{v}). \quad (3.3.14)$$

We recall that in the CDW method the  $F^* G$  function consisted of four  $f^*$  integrals and four  $g$  integrals which results in the final form of  $F^* G$  not being separable with respect to the description of the initial and final states of the 'active' electron - the initial and final states being connected through the final distortion via  $\mathcal{V}_2$ . In the CIS approach we only have one integral for each of the  $F^*$  and  $G$  functions. Consequently  $F^* G$  is separable with respect to the 'active' electron description,  $F^*$  being a function of the final capture state and  $G$  being a function of the initial projectile state. As we shall see, this helps considerably in reducing the amount of calculation necessary if we wish to consider either capture into excited states or capture from different targets.

As in Chapter 1.3 we now transform (3.3.14) into  $\eta$  space, where  $\eta^2 = K_x^2 + K_y^2$ ,  $K_x = \eta \sin \theta$  and  $K_y = \eta \cos \theta$ . Integrating over  $\theta$  and using Cauchy's Theorem to perform the integration over  $\xi$ , the expression for  $a_{if}$  may be written

$$a_{if}(1s) = \frac{N_B(v)(bv)^{\frac{2iZ}{v}}}{v} D_{\alpha\beta\gamma} \int_0^{\infty} \eta J_0(b\eta) I_{\alpha\beta\gamma} F_{\alpha\beta}^*(\eta) G_{1s}(\eta) d\eta. \quad (3.3.15)$$

Substituting (3.3.15) into equation (1.2.28) and noting that

$$\sqrt{\eta\eta'} \int_0^{\infty} J_0(b\eta) J_0(b\eta') b db = \delta(\eta - \eta'), \quad (3.3.16)$$

we obtain for the capture cross section  $\sigma(1s)$  (in units of  $\pi a_0^2$ )

$$\sigma(1s) = \frac{2 |N_B(v)|^2}{v^2} \int_0^{\infty} \eta \{ D_{\alpha\beta\gamma} I_{\alpha\beta\gamma} F_{\alpha\beta}^*(\eta) \}^2 |G_{1s}(\eta)|^2 d\eta. \quad (3.3.17)$$

Following Chapter 1.3, we again obtain a 'passive' overlap integral

$I_{\alpha\beta}$  which, for reasons outlined in the discussion of equations (1.3.38-43), will be non-zero only for those basis orbitals in the natural expansion which have angular symmetry identical to the initial bound state of the projectile. Thus in this particular case only natural orbitals having radial symmetry will contribute to the cross-section.

Let us now examine the solution for  $F_{\alpha\beta}(\eta)$  and  $G_{1s}(\eta)$  separately. The solution to equation (3.3.13) for  $G_{1s}(\underline{K})$  turns out to be

$$G_{1s}(\underline{K}) = 8 \left( \frac{Z_B^3}{\pi} \right)^{\frac{1}{2}} \frac{\pi (Z_B + i \xi v)}{[Z_B^2 + K^2 + 2iZ_B \xi v - 2\underline{k} \cdot \underline{v} \xi]}^2 \quad (3.3.18)$$

After performing the complex integration over  $\xi$  and transforming into  $\eta$  space, we finally obtain for  $G_{1s}(\eta)$  the expression

$$G_{1s}(\eta) = 8\pi \left( \frac{Z_B^3}{\pi} \right)^{\frac{1}{2}} \cdot \frac{2\pi}{C^2(C-D)} \left( \frac{C-D}{C} \right)^{-i\nu_2} \cdot \left\{ -i\nu_2 C + \nu_2 Z_B D - iZ_B(C-D) \right\} \quad (3.3.19)$$

$$\text{where } C = Z_B^2 + \eta^2 + \left( \nu/2 + \frac{\Delta\epsilon}{\nu} \right)^2 \quad (3.3.20)$$

$$\text{and } D = 2\nu \left( \nu/2 + \frac{\Delta\epsilon}{\nu} \right) + i 2Z_B \nu \quad (3.3.21)$$

The solution for  $F_{\alpha\beta}(\eta)$  will depend on the form of the potential  $V_{1,2}^1$ . Let us first write down the solution,  $f_{1s}(\eta)$ , for a potential of the form  $e^{-\xi_\beta s_1} / s_1$ , when  $\psi_{\alpha\beta}(s_1)$  is a simple 1s S.T.O. i.e.  $N_\beta e^{-\xi_\beta s_1}$ : where  $\xi_\beta$  is the exponent and  $N_\beta$  the normalization constant. After integrating over  $s_1$  in equation (3.3.12) and then transforming into  $\eta$  space we arrive at the result

$$f_{1s}(\eta) \Big|_{w=\rho} = \frac{N_\beta 2\pi^{\frac{1}{2}}}{\left( (\xi_\beta + w)^2 + \eta^2 + \left( \frac{\nu}{2} - \frac{\Delta\epsilon}{\nu} \right)^2 \right)} \quad (3.3.22)$$

It follows that if  $\psi_{\alpha\beta}(s_1)$  is an S.T.O. having radial symmetry with a principal quantum number  $n_{\beta}$ , we can write

$$f_{\alpha\beta}(\eta) \Big|_{w=\rho} = (-1)^{n_{\beta}-1} \frac{\partial^{n_{\beta}-1}}{\partial \xi^{n_{\beta}-1}} \left[ f_{1s}(\eta) \Big|_{w=\rho} \right]. \quad (3.3.23)$$

Also by using the partial differential of  $f_{\alpha\beta}(\eta)$  with respect to  $w$  it can be shown that for a potential  $V_{1,2}^1$  in the form

$$V_{1,2}^1 = \frac{(Z_A - 1)}{s_1} + e^{-2Z_A s_1} \left( Z_A + \frac{1}{s_1} \right), \quad (3.3.24)$$

$F_{\alpha\beta}(\eta)$  is given by

$$F_{\alpha\beta}(\eta) = (Z_A - 1) f_{\alpha\beta}(\eta) \Big|_{w=0} - Z_A \frac{\partial}{\partial w} \left[ f_{\alpha\beta}(\eta) \Big|_{w=2Z_A} \right] + f_{\alpha\beta}(\eta) \Big|_{w=2Z_A}. \quad (3.3.25)$$

Due to the separable form of the integrand in (3.3.17), the cross-section for capture into the  $n\ell = 1s, 2s$  and  $2p$  states, for example, can be written as

$$\sigma(n\ell) = \frac{|N_B(v)|^2}{2v^2} \hat{\uparrow} \int_0^{\infty} \eta^{2q+1} \left\{ W_{n\ell}(\eta) \right\}^2 \left| G_{1s}(\eta) \right|^2 d\eta, \quad (3.3.26)$$

where  $q$  depends on the angular symmetry of the capture state, i.e.  $q = 0$  for  $n\ell = 1s, 2s, 2p_z$  and  $q = 1$  for  $n\ell = 2p_x$ , and  $\hat{\uparrow}$  is a multiplication factor equal to 1 if we capture into a singlet state  $n^1S$ , and equal to 3 for capture into a triplet state  $n^3S$ . The CIS integrand is in a particularly convenient form since, for capture into different states, we simply re-calculate  $W_{n\ell}(\eta)$  which is a function of

the 'passive' overlap integral  $I$  and the  $F$  function which depends on the orbital description of the captured state.

Let us now examine the structure of  $W_{nl}(\eta)$  when  $e(1)$  is captured into an excited state, and the spatial wavefunction describing

$[Z_A, e(1), e(2)]_f$  is of the form

$$\phi_f(1,2) = \frac{N_{\pm}}{\sqrt{2}} \left\{ u(1)v(2) \pm v(1)u(2) \right\}, \quad (3.3.27)$$

where  $u$  and  $v$  are separately normalized ground-state and excited-state orbitals, respectively.  $N_{\pm}$  is the total normalization constant given by

$$N_{\pm} = (1 \pm S^2)^{-\frac{1}{2}}, \quad (3.3.28)$$

with  $S$  equal to the overlap integral  $\langle u | v \rangle$ . Usually the orbitals  $u$  and  $v$  are constructed to be orthogonal for which  $S = 0$ . Because of the form of  $\phi_f(1,2)$  and the fact that we label the 'active' electron  $e(1)$ , a probability exists in our analysis for the capture of electron(1) into the ground state of projectile ( $Z_A, e(2)$ ) while, at the same instant, electron (2) is being projected into the excited-state orbital. This is an exchange effect, similar to that observed in Part 2 for electron-capture from Li, and is a direct consequence of having to antisymmetrize the total wavefunction in order to obey the Pauli exclusion principle. The size of the contribution arising from this exchange term will normally be very small if not zero due to the passive overlap integral that occurs between the excited-state orbital  $v(2)$  and the ground-state wavefunction  $\psi_{1s}(2)$  of the initial state projectile. For each orbital in  $\phi_f(1,2)$  we calculate a corresponding  $F(\eta)$  function, say  $F_u(\eta)$  and  $F_v(\eta)$ , representing capture into the orbitals  $u$  and  $v$  respectively;  $W_{nl}(\eta)$  then becomes either  $W_{nl}(\eta)_+$  or  $W_{nl}(\eta)_-$  given by

$$W_{nl}(\eta)_{\pm} = \frac{N_{\pm}}{\sqrt{2}} \left\{ I(\psi_{1s}(2)|v(2))F_u(\eta) \pm I(\psi_{1s}(2)|u(2))F_v(\eta) \right\} .$$

(3.3.29)

It follows from the integration over spins that, for the singlet case we use  $W_{nl}(\eta)_-$  and  $\mathcal{T}$  equal to 1, and for the triplet case we use  $W_{nl}(\eta)_+$  and  $\mathcal{T}$  equal to 3. Consequently, once we have calculated  $W_{nl}(\eta)$  for all the required capture states we will now have the cross-sections for capture from any general one-electron target of charge  $Z_B$ .

## CHAPTER 3.4

### An examination of electron-capture in H-H collisions

As a somewhat severe test of the scheme presented in the previous chapters we now examine the cross-sections for electron-capture in H-H collisions. This is a particularly interesting reaction to consider from the theoretical point of view since in the inward channel the perturbing potential acting on the 'active' electron is due to an approaching neutral atom. Thus we would expect, particularly for capture into a weakly bound state such as  $H^-$ , that electron-capture will occur when the 'active' electron sees the full charge of the H projectile nucleus. Applying the procedure just outlined to reaction (3.1.1) we obtain for the perturbing potential  $V_{1,2}^1$ , in equation (3.3.10), for  $Z_A=1$ ,

$$V_{1,2}^1 = e^{-2s_1} \left( 1 + \frac{1}{s_1} \right) . \quad (3.4.1)$$

$V_{1,2}^1$  now tends to zero for the approaching H atom at large internuclear separations and equals  $1/s_1$  for small  $s_1$ . Thus  $V_{1,2}^1$  is an appropriate potential for the H-H capture process.

The capture cross-sections for reaction (3.1.1) are calculated using the transition amplitude  $a_{if}$  defined in equation (3.2.34). The wavefunction for  $H^-(1s^2)$  was described, firstly, by the HF fitted function of Curl and Coulson<sup>19</sup> and, secondly, by a 'fixed core' representation of the form  $1s1s^1$  in which the exponent of the valence-electron orbital is chosen to be  $(2\epsilon)^{\frac{1}{2}}$ , where  $\epsilon$  is the experimental value of the single-ionisation energy, and the 'fixed core' is a 1s hydrogen orbital. The latter description of  $H^-$  has the advantage of having one electron loosely bound whilst the other electron remains comparatively tightly bound. Such a wavefunction, albeit empirical, could be particularly appropriate at the intermediate energies represented by

experiment since contributions to the capture cross-section from relatively large values of the impact parameter may then be significant. We have also described  $H^-(1s^2)$  by the CI wavefunction of Weiss<sup>20</sup>. This function not only allowed for the high degree of electron correlation in  $H^-$ , and satisfied the energy variation principle, but also enabled us to make numerical comparisons with the CDW results of Moore and Banyard<sup>14</sup>. The energy decrement  $\Delta E$  used in conjunction with the HF and CI wavefunctions was derived in each case from the corresponding theoretical energies whereas, for the 'fixed-core' description of  $H^-$ , we used the experimental value.

In Figure 3.2 the cross-sections  $\sigma(1s)$  are compared with the experimental results of McClure<sup>9</sup>. Also shown are the 'post' and 'prior' theoretical curves of Mapleton<sup>10</sup>, which were used by McClure<sup>9</sup> for comparison with experiment. Mapleton<sup>10</sup> employed a Born approximation to describe reaction (3.1.1) with the ground-state of  $H^-$  being represented by the correlated wavefunction of Chandrasekhar<sup>21</sup>. In Table 3.1 the CIS results, using the HF and CI wavefunctions, are compared, at a few selected energies, with the CDW results of Moore and Banyard<sup>14</sup>. The theoretical cross-sections of Moore and Banyard were obtained by dividing the CDW cross-section for the reverse reaction (i.e.  $H^+ + H^-(1s,1s) \rightarrow H(1s) + H(1s)$ ) by 8. This factor arises from the fact that for protons incident on  $H^-(1s,1s)$  there is an equal probability of capturing either of the 1s shell electrons, and that for the formation of  $H^-(1s,1s)$  in  $H(1s)-H(1s)$  collisions only  $1/4$  of the possible reactions lead to the singlet ( $^1S$ )  $H^-$  atom.

Of the curves presented in Figure 3.2, that derived from the HF wavefunction is perhaps the best. This is somewhat surprising, particularly since for the formation of  $H^-$  we would expect that contributions arising from electron correlation terms to be non-negligible.

This may, as discussed below, arise from the cancellation of opposing effects. The more reasonable split-shell description of  $H^-$  embodied in the empirical 'fixed core' model and the Weiss wavefunction is seen to be reflected in the closeness of curves (b) and (c). Our CIS-based approximation is only capable of responding to a split-shell or radial component of electron correlation and makes no allowance for the effects of angular correlation in  $H^-$ . This arose due to an orthogonality condition in the passive overlap integral and, in this method, is a direct consequence of the form taken for  $V_{1,2}^1$  which, in turn, arises as a result of the approximation applied to the internuclear potential term  $1/s_{12}$ . Since the transition amplitude  $a_{if}$  is evaluated in terms of momentum space, it is possible that the opposing effects of angular and radial correlation - known to exist in momentum space<sup>22</sup> - may produce some cancellations with the result that cross-sections incorporating angular correlation terms may now lie in close proximity to the rather fortuitous HF based curve.

A more correct approach to the electron-electron potential term in  $V_{1,2}^1$  would be to expand  $1/s_{12}$  in terms of its spherical harmonics by use of the expansion

$$\frac{1}{s_{12}} = \sum_{l=0}^{\infty} \frac{4\pi}{(2l+1)} \frac{s_{<}^l}{s_{>}^{l+1}} \sum_{m=-l}^{+l} Y_l^m(\theta_1, \phi_1) Y_l^{m*}(\theta_2, \phi_2) . \quad (3.4.2)$$

The  $Y_l^m$ 's are the normalised spherical harmonics and  $s_{<}$  and  $s_{>}$  are defined as the lesser and greater of the magnitude of position vectors  $\underline{s}_1$  and  $\underline{s}_2$  of electrons (1) and (2) respectively.

Applying the expansion (3.4.2) in the matrix element (3.3.4) while representing the  $H^-$  system by the CI wavefunction expressed in its natural expansion form, results, as a consequence of evaluating the angular integrals, in a series of matrix elements each

one involving a natural orbital within the natural expansion of the CI wavefunction. It is found that the orthogonality condition arising in the integration over the 'passive' electron coordinates acts such that contributions to the cross-section may now result from natural orbitals having the same angular symmetry as the terms in the above expansion. Thus, for terms for which  $l = 0$  only radial correlation terms contribute, for terms for which  $l = 1$  only natural orbitals having p symmetry contribute and for  $l = 2$  only d orbitals contribute - and so on. Consequently by suitable truncation of expansion (3.4.2) at a particular  $l$  value, we are able to observe the effect of progressively introducing the angular correlation terms within the CI wavefunction.

The integration over electron coordinates  $s_1$  and  $s_2$  divides into two parts and contributions to the transition amplitude arise from when the radial coordinate  $s_2$  is  $s_<$ , in the range 0 to  $s_1$  and when  $s_2$  is  $s_>$ , in the range  $s_1$  to  $\infty$ . However, because we have a neutral hydrogen atom projectile and since  $H^-$  is such a weakly bound system we might expect that the contribution to the cross-section for  $s_2 < s_1$  to be very small compared with that which arises when  $s_2 > s_1$ . This follows from the fact that  $s_2 < s_1$  corresponds to the situation in which the passive electron screens the nuclear charge of the projectile. For a hydrogen projectile this would mean an effective charge of almost zero. Thus, in the calculation  $s_2$  may be set to be  $s_>$  for all values of  $s_1$ . This approximation simplifies the calculation a great deal while still allowing angular correlation terms to contribute. Note that we still have a passive overlap integral except that it now contains the potential operator  $1/s_2^{l+1}$ .

Therefore, in order to obtain some idea of the relative influence of the radial and angular correlation within the  $H^-$  wavefunction on the cross-sections for reaction (3.1.1.), the cross-sections were re-calculated

using the expansion (3.4.2) representation for  $1/s_{12}$  instead of the average-static potential used previously. The 35-term CI wavefunction of Weiss<sup>20</sup> was used to describe the  $H^-$  atom, and the cross-section was also calculated using the Hartree Fock wavefunction of Curl and Coulson<sup>19</sup> in order to assess the influence of the radial correlation terms in the CI wavefunction of Weiss. In the calculations  $s_1$  was set to  $s_<$  and  $s_2$  set to  $s_>$  for all  $s_1$  and  $s_2$  as discussed above.

The cross-sections  $\sigma(\mathcal{L}=0)_{CI}$ ,  $\sigma(\mathcal{L}=1)_{CI}$ , and  $\sigma(\mathcal{L}=2)_{CI}$  corresponding to the truncation of expansion (3.4.2) at  $\mathcal{L} = 0, 1$  and  $2$  respectively, when describing the  $H^-$  system with the CI wavefunction, are listed in Table 3.2. For comparison with experiment, we chose an energy range of 20-100 keV. Each cross-section  $\sigma(\mathcal{L}=i)_{CI}$  includes contributions from all the radial correlation terms within the CI wavefunction plus contributions from all angular correlation terms having angular quantum numbers equal to  $i, (i-1), (i-2), \dots, (i-(i-1))$ . Thus for example,  $\sigma(\mathcal{L}=2)$  will include, from the CI wavefunction, all radial correlation terms, and all angular correlation terms which have either p or d symmetry only. Also shown in Table 3.2 is the cross-sections  $\sigma(\mathcal{L}=0)_{HF}$  obtained using the HF wavefunction of Curl and Coulson<sup>19</sup> to describe  $H^-$ , for which only the first radial term ( $\mathcal{L}=0$ ) in expansion (3.4.2) contributes to the  $1/s_{12}$  potential. The percentages,  $\Delta_0, \Delta_1, \Delta_2$ , reported in Table 3.2 show the changes in cross-section as one goes from  $\sigma(\mathcal{L}=0)_{HF}$  to  $\sigma(\mathcal{L}=2)_{CI}$ , and therefore reflects the change in cross-section brought about by progressively including first radial correlation ( $\Delta_0$ ), then angular correlation having p symmetry ( $\Delta_1$ ), and finally angular correlation having d symmetry ( $\Delta_2$ ) into the description of the  $H^-$  system.

As shown in Table 3.2 the percentage changes in cross-section, brought about by introducing electron correlation of successively

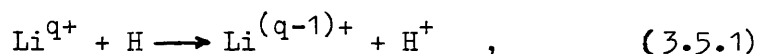
increasing angular symmetry, are seen to alternate in sign. This demonstrates the opposing effects of electron-correlation terms which have different angular symmetry, and which is known to exist in momentum space<sup>22</sup> as discussed earlier.

In Figure 3.3 we compare the cross-sections with the experimental data of McClure<sup>9</sup>. The agreement with experiment when using the CI wavefunction is now reasonably good for  $E > 30$  keV, and is a slight improvement on that obtained when using the average static potential for  $1/s_{12}$ , the results of which were shown in Figure 3.2. We recall that in the average static potential approach only radial correlation could contribute to the cross-section whereas, by using the  $1/s_{12}$  expansion, we have been able to include both radial and angular correlation effects. It is interesting to note that the curve corresponding to the truncation of expansion (3.4.2) at  $\ell = 1$  and  $\ell = 2$  is in close agreement with curve (a) in Figure 3.2, which corresponds to the Hartree-Fock description of  $H^-$  when using the average static potential approach. As stated earlier, the slightly better agreement between curve (a) and experiment compared to curves (b) and (c) in Figure 3.2 was attributed to the omission of the angular correlation effects. Therefore, by using expansion (3.4.2) for  $1/s_{12}$  we have been able to show that this is the case, and is the result, as demonstrated in Table 3.2, of the opposing effects of angular and radial correlation.

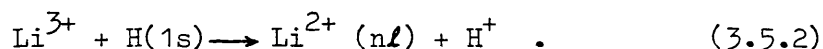
## CHAPTER 3.5

### Electron-capture from H atoms by fast Li ions

We now present and discuss our results obtained by applying the CIS method outlined in Chapters 3.2 and 3.3 to the general electron-capture reaction



for  $q = 1, 2$  and  $3$  and for impact energies  $100 \text{ keV} < E < 10000 \text{ keV}$ . For ease of discussion we will examine the three cases separately in reverse order  $q = 3, 2$  and  $1$ . All the cross-sections are calculated using the 'prior' form of the transition amplitude  $a_{if}$ , and the total cross-sections are compared with the experimental data of Shah, Goffe and Gilbody<sup>18</sup>. Thus, the first reaction we consider is



The electron-capture cross-sections were calculated using both the CIS and CDW methods for  $n\ell = 1s, 2s$  and  $2p$ , and the total cross-sections obtained by means of the formula

$$Q = \sigma(1s) + 1.616(\sigma(2s) + \sigma(2p)) , \quad (3.5.3)$$

which assumes the Oppenheimer<sup>23</sup>  $n^{-3}$  rule for  $n > 2$ . The evaluation of the CIS and CDW total cross-sections, by means of equation (3.5.3), not only allowed us to compare the two methods but provided an initial comparison with experiment. This showed that, for this reaction, equation (3.5.3) underestimates the contributions arising from capture into higher excited states, and that capture into  $n\ell = 3s, 3p$  and  $3d$  has to be considered if a meaningful comparison with experiment is to be made. As a result, the CIS capture cross-sections for  $n\ell = 1s, 2s, 2p, 3s, 3p$  and  $3d$  were calculated and the total cross-sections obtained from

$$Q = \sigma(1s) + \sigma(2s) + \sigma(2p) + 2.081(\sigma(3s) + \sigma(3p) + \sigma(3d)) . \quad (3.5.4)$$

The wavefunctions used for reaction (3.5.2) are obviously 'H-like' eigenfunctions and are therefore, along with the eigenenergies and energy decrement, exact. The results are listed in Table 3.3, and in Figure 3.4 we compare the total cross-sections with the experimental data.

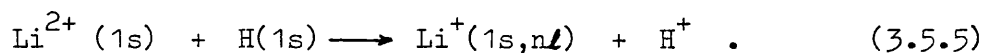
The CIS curve calculated by equation (3.5.4) is an improvement over that calculated with equation (3.5.3), and the CIS curve is in reasonable agreement with experiment for  $E > 400$  keV particularly with respect to the slope and trend at high impact energies. We see from Table 3.3 that for the energy range considered,  $\sigma(n=2) > \sigma(1s)$  for  $E \leq 3000$  keV,  $\sigma(n=3) > \sigma(1s)$  for  $E \leq 2000$  keV and that for  $E \leq 1000$  keV  $\sigma(n=3) > \sigma(n=2)$ . In the light of these trends it would seem unlikely that the CIS curve, calculated using equation (3.5.4), would be improved with respect to the experimental data by calculating capture cross-sections into the  $n=4$  levels, since a lowering of the appropriate curve in Figure 3.4 would imply a larger decrease in cross-section in going from  $\sigma(n=3)$  to  $\sigma(n=4)$  below that predicted by the  $n^{-3}$  rule. We note also that errors due to the use of the  $n^{-3}$  rule usually cause an underestimation of the total cross-section.

Although the CIS and CDW approximations may yield very similar total cross-sections we find that, for this reaction, the relative contributions from capture into excited states may be quite different for the two methods. In order to demonstrate this fact we report in Table 3.4, for both methods, ratios of  $\sigma(n\ell) / \sigma(1s)$  at selected energies for  $n\ell = 2s, 2p, 3s$  and  $3p$ , and in Table 3.5 ratios of  $\sigma(n\ell)_{\text{CIS}} / \sigma(n\ell)_{\text{CDW}}$  are shown at the same energies. From Table 3.5 we see that for  $E \sim 5000$  keV the CIS and CDW ratios for  $\sigma(n\ell) / \sigma(1s)$  become similar to each other for  $n\ell = 2s$  and  $3s$ , while for  $n\ell = 2p$  and  $3p$  the CIS ratios are approximately twice the corresponding CDW ratio.

However, below 3000 keV there appears to be no agreement or recognisable trend between the two methods whatsoever, although the CDW ratios are much larger than those derived from the corresponding CIS results. The reason for this is not due to the larger CDW cross-sections for capture into excited states, but due to the much smaller CDW cross-sections for  $n\ell = 1s$  as compared to the CIS method; note that at 500 keV  $\sigma(1s)_{\text{CIS}} \approx 16 \times \sigma(1s)_{\text{CDW}}$ .

As the impact energy increases we see from Table 3.5 that the CIS and CDW cross-sections are similar in magnitude for capture into the s states while for capture into the p states we have  $\sigma_{\text{CIS}} \approx 2 \times \sigma_{\text{CDW}}$ . This could be a consequence of the CIS method predicting a different transition probability for capture at large impact parameters from that of the CDW method, as reported by Belkic<sup>16</sup> in his original paper on the CIS method. This may become important for capture into excited states having angular quantum number  $\ell \neq 0$  and particularly if projectiles in the form of highly charged nuclei are involved, for which electron-capture at large impact parameters is more likely to occur.

We now turn our attention to a reaction of the type for which the CIS method was modified in the scheme outlined in Chapter 3.2, i.e.



In reaction (3.5.5) we have a structured projectile consisting of a one-electron ion, and therefore the CIS capture cross-sections were calculated using the 'prior' transition amplitude defined in equation (3.2.34), with the perturbing potential  $Z_A/s_1 - 1/s_{12}$  being replaced by  $V_{1,2}^1$  defined in equation (3.3.5). The capture states considered are  $n\ell = 1s, 2s, 2p, 3s, 3p$  and  $3d$ , and the total cross-section is evaluated by means of equation (3.5.4). For capture into the ground state  $n\ell = 1s$  the HF wavefunction of Clementi and Roetti<sup>24</sup> was used to describe the

final ground state  $\text{Li}^+$  ion. For the purpose of obtaining a meaningful comparison with experiment, and also to provide a good test of the scheme proposed in Chapter 3.2, it is imperative to use the best possible wavefunctions to describe the excited states of the final  $\text{Li}^+$  ion. For this reason we decided to use the excited-state wavefunctions of Cohen and McEachran<sup>25,26</sup>. Since the calculations involving the excited-state orbital descriptions proved to be non-trivial and interesting, we first present a description of the Cohen and McEachran<sup>25,26</sup> wavefunctions together with the resulting calculation of  $W_{n\ell}(\eta)_+$  defined in Chapter 3.3, equation (3.3.29).

The excited-state wavefunctions of Cohen and McEachran<sup>25,26</sup> are constructed within the framework of the "fixed-core" approximation. That is the 1s orbital is described by an hydrogenic wavefunction and the appropriate radial equation for the excited-state orbital solved keeping the 1s orbital fixed. A theoretical advantage of the fixed-core method arises from the fact that the various 1s  $n\ell$  total wavefunctions are mutually orthogonal. The wavefunctions, as reported by Cohen and McEachran<sup>25,26</sup>, were found to predict ionization energies in close agreement with experiment and produced expectation values for one-electron operators in good agreement with the (effectively) exact values calculated by Pekeris<sup>27</sup>. The excited-state radial wavefunction is written in the form

$$\phi_f(1,2) = \frac{1}{\sqrt{2}} (u(1)v(2) \pm v(1)u(2)) Y_0^0(\theta, \phi) Y_\ell^m(\theta, \phi), \quad (3.5.6)$$

where  $u$  and  $v$  are separately normalized, mutually orthogonal orbitals.

The 1s orbital  $u$  is represented by the hydrogenic form  $u = 2Z_A^{3/2} \exp(-Z_A r)$ , while the valence orbital  $v$  is expanded in a series of associated Laguerre functions

$$v = N \sum_{j=2l+1}^{\infty} a_j \exp(-\alpha r) r^l L_j^{2l+1}(2\alpha r). \quad (3.5.7)$$

$N$  is a normalization constant,  $a_j$  are the expansion coefficients,  $l$  the angular quantum number of the excited state and  $\alpha = Z_A/n$ . Thus for any excited-state wavefunction we simply have a list of expansion coefficients appropriately truncated to provide an accurate description of the excited state orbital. The associated Laguerre function is defined by the expansion

$$L_{\alpha}^{\beta}(r) = (-1)^{\alpha} \frac{\alpha!}{(\alpha-\beta)!} \left\{ r^{\alpha-\beta} - \frac{\alpha(\alpha-\beta)}{1!} r^{\alpha-\beta-1} + \frac{\alpha(\alpha-1)(\alpha-\beta)(\alpha-\beta-1)}{2!} r^{\alpha-\beta-2} - \dots (-1)^{\alpha+1} \alpha! \right\}. \quad (3.5.8)$$

It follows that we can conveniently express the orbital  $v$  in the form

$$v = N \sum_{j=2l+1}^{\text{MAX}} a_j \exp(-\alpha r) \sum_{i=1}^{j-2l} A_{ij} r^{j-l-i}, \quad (3.5.9)$$

such that the coefficients  $A_{ij}$  are given by

$$A_{ij} = \frac{(-1)^{j+i+1} (j!)^2}{(i-1)! (j-i+1)! (j-2l-i)!}. \quad (3.5.10)$$

In Chapter 3.3 it was shown that, for a wavefunction of the form (3.5.6),  $W_{nl}(\eta)$  can be written

$$W_{nl}(\eta) = \frac{1}{\sqrt{2}} \left\{ I(\psi_{1s}(2) | v(2)) F_u(\eta) \pm I(\psi_{1s}(2) | u(2)) F_v(\eta) \right\}. \quad (3.5.11)$$

The function  $I$  is the passive overlap integral and, since in this case

$\psi_{1s}(2)$  is identical to  $u(2)$ ,  $I(\psi_{1s}(2) | v(2))$  is zero due to the orthogonality of  $u$  and  $v$ . Thus  $W_{nl}(\eta)$  becomes

$$W_{nl}(\eta) = \pm \frac{1}{\sqrt{2}} \left\{ F_V(\eta) \right\}, \quad (3.5.12)$$

where, for a simple orbital of the form  $N_{\beta} s^{n_{\beta}-1} e^{-\xi_{\beta} s}$ ,  $F_V(\eta)$  is given by equations (3.3.22-25). It follows that by substituting the excited-state orbital of the form (3.5.9) for  $\psi_{\mu\beta}$  in equation (3.3.12), and performing the necessary integrations,  $F_V(\eta)$  can be expressed as

$$F_V(\eta) = N \sum_{j=2l+1}^{\infty} a_j \sum_{i=1}^{j-2l} A_{ij} (-1)^n \left[ \frac{\partial^n}{\partial \alpha^n} \cdot \frac{(Z_A - 1)}{A_1^{l+1}} - \frac{\partial^{n+i}}{\partial \lambda^{n+i}} \frac{Z_A}{A_2^{l+1}} + \frac{\partial^n}{\partial \lambda^n} \frac{1}{A_2^{l+1}} \right], \quad (3.5.13)$$

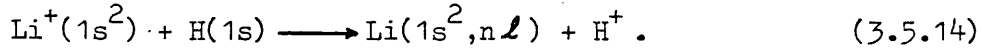
with

$$\begin{aligned} \Omega &= j - 2l - i, \\ \alpha &= Z_A / \eta, \\ \lambda &= \alpha + 2Z_A, \\ A_1 &= \alpha^2 + \eta^2 + \left( \nu/2 - \frac{\Delta E}{\nu} \right)^2, \\ A_2 &= \lambda^2 + \eta^2 + \left( \nu/2 - \frac{\Delta E}{\nu} \right)^2. \end{aligned}$$

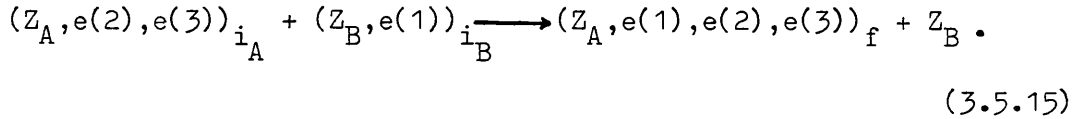
For the excited state wavefunctions of  $\text{Li}^+$  it turns out that  $\Omega$  may have a value as large as 15. To perform fifteen differentiations of a function of the form  $(A_1)^{-\Omega-1}$  would be both tedious and exhausting. The multi-differential calculations needed in  $F_V(\eta)$  were performed by an algebra manipulation computer programme called CAOS<sup>28</sup>, which is a recent, and much improved, addition to the already existing generation of software designed for algebraic manipulation. CAOS<sup>28</sup> calculated and produced all the differential forms required in  $F_V(\eta)$  in less than two seconds of computer time. Thus, the availability of CAOS not only meant a saving in labour but made the Cohen and McEachran wavefunctions viable for cross-section calculations. Therefore a computer programme was

written which could calculate a cross-section for capture into any excited state, and with the orbital being described by a large number of terms in the expansion defining  $v$ . The calculated cross-sections  $\sigma(n\ell)$  and the total cross-sections  $Q_1$  and  $Q_2$  corresponding to two forms of  $V_{1,2}^1$ , i.e.  $V_1 = (Z_A - 1) / s + \exp(-2 Z_A s) \cdot (Z_A + s^{-1})$  and  $V_2 = (Z_A - 1) / s$ , are listed in Tables 3.6 and 3.7, respectively. In Figure 3.5 the CIS curves are compared with experiment. As expected the total cross-sections calculated with  $V_1$ , i.e.  $Q_1$ , are larger than those calculated with  $V_2$ , i.e.  $Q_2$ , at the same impact energy, the difference between the two becoming larger as the impact energy increases. For example at  $E = 500, 1000, 3000$  and  $10000$  keV  $Q_1$  is successively  $1.07, 1.32, 1.84$  and  $3.11 \times Q_2$ . The same trend is seen for the individual capture-states over the total energy range, with the exception of  $\sigma(2s)$  and  $\sigma(3s)$  for which  $Q_1$  is larger than  $Q_2$  only for  $E \gg 400$  keV and  $E \gg 800$  keV, respectively. This is a consequence of  $V_1$  and  $V_2$  differing in form for small electron-nuclear separations, see Figure 3.6, which will become most important at large  $E$  when the capture cross-section is dominated by regions of high momentum. From Figure 3.5 we see that for  $V_{1,2}^1 = V_2$  the CIS curve is slightly lower than the experimental points for  $E > 400$  keV, however, for  $V_{1,2}^1 = V_1$  the agreement with experiment is exceptionally good for  $E > 300$  keV. In Figure 3.7 we show the curve for  $Q_1$  together with the individual cross-section curves for capture into the individual quantum levels  $n = 1, 2$  and  $3$ . For the energy range displayed on the graph we see that  $\sigma(n=2)$ , i.e.  $\sigma(n=2) = \sigma(2s) + \sigma(2p)$ , and  $\sigma(n=3)$ , i.e.  $\sigma(n=3) = \sigma(3s) + \sigma(3p) + \sigma(3d)$ , are greater than  $\sigma(1s)$ , and that the exaggerated total cross-sections at low impact energies is due to the over exaggerated cross-sections for capture into the excited states. For impact energies greater than  $3000$  keV the ordering in cross-sections becomes  $\sigma(1s) > \sigma(n=2) > \sigma(n=3)$ , and for the whole energy range  $\sigma(2p) > \sigma(2s)$  and  $\sigma(3p) > \sigma(3s)$ .

The final reaction we consider in the Li ion series is



For this reaction we have a structured projectile having two bound-electrons in the ground state. Thus the reaction is of the general form



Performing a similar analysis as described in Chapter 3.2 the prior and post transition amplitudes turn out to be

$$a_{if} = i \int_{-\infty}^{+\infty} dt \int \underline{dr}_1 \underline{dr}_2 \underline{dr}_3 \Psi_f^* \left( \frac{Z_A}{s_1} - \frac{1}{s_{12}} - \frac{1}{s_{13}} + \frac{Z_B}{x_2} + \frac{Z_B}{x_3} - \frac{2Z_B}{R} \right) \chi_i \quad (3.5.16)$$

and

$$b_{if} = i \int_{-\infty}^{+\infty} dt \int \underline{dr}_1 \underline{dr}_2 \underline{dr}_3 \left[ \left( \frac{Z_B}{x_1} + \frac{Z_B}{x_2} + \frac{Z_B}{x_3} - \frac{2Z_B}{R} \right) \chi_f^* \right] \Psi_i \quad (3.5.17)$$

respectively, where the necessary choices made for the distorting potentials  $U_i$  and  $U_f$  are

$$U_i = - \frac{(Z_A - 2)}{R} \quad \text{and} \quad U_f = - \frac{Z_B}{R} . \quad (3.5.17)$$

If we now follow the arguments as presented in Chapter 3.2, equation (3.2.32) to equation (3.2.38), and neglect contributions to  $a_{if}$  and  $b_{if}$  arising from potentials of the form  $\left| \frac{Z_B}{x} - \frac{Z_B}{R} \right|$ , we obtain for  $a_{if}$  and  $b_{if}$

$$a_{if} = i \int_{-\infty}^{+\infty} dt \int \underline{dr}_1 \underline{dr}_2 \underline{dr}_3 \Psi_f^* \left( \frac{Z_A}{s_1} - \frac{1}{s_{12}} - \frac{1}{s_{13}} \right) \chi_i \quad (3.5.18)$$

and

$$b_{if} = i \int_{-\infty}^{+\infty} dt \int \underline{dr}_1 \underline{dr}_2 \underline{dr}_3 \left[ \left( \frac{Z_B}{x_1} \right) \chi_f^* \right] \Psi_i . \quad (3.5.19)$$

In solving for  $a_{if}$ , for reaction (3.5.14),  $\Psi_f$  will correspond to the a product of the three-electron wavefunction for  $\text{Li}(1s^2, n\ell)$  and the coulomb wave acting on the active electron due to  $\text{H}^+$ , and  $\chi_i$  will be the product of the two-electron wavefunction for  $\text{Li}^+(1s^2)$  and the hydrogen wavefunction, multiplied by the appropriate phase factor analogous to that occurring in the solution for  $\chi_i$  in Chapter 3.2 equation (3.2.27).

If the  $\text{Li}^+$  ion electrons are described by the HF wavefunction of Clementi and Roetti<sup>24</sup>, which is constructed from a basis set of 1s S.T.O.'s only, then it follows that the two possible approximations to the perturbing potential in  $a_{if}$ , i.e. say  $V_{1,2,3}^0 = \frac{Z_A}{s_1} - \frac{1}{s_{12}} - \frac{1}{s_{13}}$ , that we shall consider are

$$V_1 = \frac{Z_A - 2}{s} + 2 \sum_i c_i e^{-2\xi_i s} \left( \xi_i + \frac{1}{s} \right) \quad (3.5.20)$$

and

$$V_2 = \frac{Z_A - 2}{s}, \quad (3.5.21)$$

where  $\xi_i$  are the S.T.O. orbital exponents and  $c_i$  the usual variational coefficients within the wavefunction. The potential  $V_1$  is of course the average static potential of the  $\text{Li}^+(1s^2)$  ion as seen by the active electron and  $V_2$  is the perfect screening potential.

Since we consider the ground state of the  $\text{Li}^+$  ion to be filled, the capture states considered are  $n\ell = 2s, 2p, 3s, 3p$  and  $3d$ , and the total cross-section is calculated using equation (3.5.4) with  $\sigma(1s) = 0$ . For capture into the 2s level we simply form a neutral Li atom and, for this cross-section, the  $\text{Li}(1s^2, 2s)$  electrons are described by the HF wavefunction of Clementi and Roetti<sup>24</sup>. Since no suitable excited-state wavefunctions could be found for Li it was decided to generate our own

very simple excited-state orbitals within the framework of the 'fixed core' approximation. Thus, the  $1s^2$  shell of the  $\text{Li}(1s^2, n\ell)$  atom is described by the HF orbitals of Clementi and Roetti<sup>24</sup> as for  $\text{Li}(1s^2, 2s)$ , and the  $n\ell$  orbital as described by an STO having an orbital exponent defined by the experimental ionization energy,  $\epsilon_{n\ell}$ , of the particular excited-state. The excited-state eigenfunction is then finally constructed to be orthogonal to all lower eigenfunctions by the Schmidt<sup>29</sup> orthogonalization technique. Thus we obtain for the orthogonal excited-state orbitals

$$\psi_{3s} = \varphi_{3s} - \langle \phi_{1s} | \varphi_{3s} \rangle \phi_{1s} - \langle \phi_{2s} | \varphi_{3s} \rangle \phi_{2s}, \quad (3.5.22)$$

$$\psi_{2p} = \varphi_{2p}, \quad (3.5.23)$$

$$\psi_{3p} = \varphi_{3p} - \langle \varphi_{2p} | \varphi_{3p} \rangle \varphi_{2p}, \quad (3.5.24)$$

and  $\psi_{3d} = \varphi_{3d}, \quad (3.5.25)$

where  $\varphi_{n\ell} = (2\xi_n)^{n+\frac{1}{2}}(2n!)^{-\frac{1}{2}} r^{n-1} \exp(-\xi_{n\ell} r) \cdot Y_{\ell}^m(\theta, \phi) \quad (3.5.26)$

and  $\xi_{n\ell}$  is given by

$$\xi_{n\ell} = \sqrt{2\epsilon_{n\ell}}. \quad (3.5.27)$$

The energy decrements for all the cross-sections were determined using the experimental ionization energies  $\epsilon_{n\ell}$ , obtained from the tables of Charlotte E. Moore<sup>30</sup>.

With these wavefunctions the cross-sections were calculated for both forms of  $V_{1,2}^1$ ,  $V_1$  and  $V_2$ , and the results are listed in Tables 3.8 and 3.9. In Figure 3.8 we compare the total cross-sections  $Q_1$  and  $Q_2$  with the experimental data with which there seems to be good agreement, with the perturbing potential  $V_1$  again providing a better description of  $V_{1,2}^1$ . As in the case of reaction (3.5.5) the two curves

$Q_1$  and  $Q_2$  deviate apart from each other as the impact energy increases, the ratio  $Q_1/Q_2$  increasing from 1.5 to 4 as the energy increases from 1000 keV to 10000 keV.

For the individual capture cross-sections in Tables 3.8 and 3.9 we note an interesting trend that is most clear for  $100 \text{ keV} \leq E \leq 1000 \text{ keV}$ . We see that for capture into  $n\ell = 2s$  and  $3s$  the capture cross-sections, for both forms of  $V_{1,2}^1$  at the same impact energy, differ by more than a factor of two, while for capture into  $n\ell = 2p, 3p$  and  $3d$  the two sets of cross-sections are very similar to each other. At larger energies the difference between the two sets of results for  $n\ell = 2p, 3p$  and  $3d$  increases and the trend is not so noticeable although the differences are still largest for capture into the s-states. A similar trend was observed by Banyard and Szuster<sup>31</sup> when examining the effect of electron-correlation on electron-capture from He by fast protons into the 1s and 2s states as compared to capture into the 2p state. The reason for the trend is simply due to the difference in characteristics between the capture-state wavefunctions which possess angular symmetry compared with capture states which have only radial symmetry. It is the characteristics of the radial wavefunctions at the origin that are of interest since it is this region which contributes most to the cross-section at large impact energies. While the different s-states will have similar characteristics near the origin, the characteristics of the p and d states are quite distinct, the wavefunctions being zero at the origin. Thus it is not surprising that the differences in sensitivity of the cross-sections (for capture into different states) to quantities such as the target description and, as we have seen, approximations made with respect to the perturbing and distorting potentials, will be most enhanced at large impact energies.

Of interest is the extent to which the electron-capture cross-sections for ions of different charge  $q$  in collision with atomic hydrogen scale according to  $q^n$ , where  $n$  is an integer. For the Li-ions considered here Shah, Goffe and Gilbody<sup>18</sup> have stated that the experimental capture cross-sections scale approximately as  $q^3$  at high impact energies, although for the ions  $\text{Li}^{3+}$ ,  $\text{He}^{2+}$  and  $\text{H}^+$  in collision with hydrogen Shah et al<sup>18</sup> found the capture cross-sections to scale approximately as  $q^2$ . In order to see if such a scaling is reflected in the theoretical cross-sections derived here in the CIS approximation, the scaled total cross-sections  $Q(q)/q^3$  for the reaction  $\text{Li}^{q+} + \text{H}(1s) \longrightarrow \text{Li}^{(q-1)+} + \text{H}^+$  are presented in Table 3.10, for  $q = 1, 2$  and  $3$ . The values for  $Q$  are those given in Tables 3.3 to 3.9, and therefore for  $q = 1$  and  $2$  correspond, with respect to the form taken for the perturbing potential in the transition amplitude, to either the average static potential approximation, in the case of  $Q = Q_1$ , or to the perfect screening approximation, in the case of  $Q = Q_2$ . As shown in Table 3.10 the better agreement between  $Q(2)/2^3$  and  $Q(1)/1^3$  with that of  $Q(3)/3^3$  is obtained for the total capture cross-sections  $Q_1$ . The conclusion overall, however, is that the  $q^3$  scaling rule is not seen to hold as clearly as suggested by Shah et al<sup>18</sup> for the experimental cross-sections, although there is fair agreement between  $Q_1(2)/2^3$  and  $Q_1(1)/1^3$  over the energy range  $800 \text{ keV} \leq E \leq 2500 \text{ keV}$ . This is seen more clearly in Table 3.11 where the values for  $(Q(q)/q^3) / (Q(q')/q'^3)$  are shown, when  $Q$  is given by the  $Q_1$  values. Since the agreement with experiment was exceptionally good in the case of the  $\text{Li}^{2+}$  ion in collision with hydrogen, see Figure 3.5, the rather poor results (compared with unity) for  $q' = 3$  can be attributed to the overestimation in the CIS cross-sections for  $\text{Li}^{3+}$  incident on hydrogen compared with experiment, as can be seen in Figure 3.4.

A natural extension of this work, time permitting, would have been to calculate the individual and total electron-capture cross-sections for Li-ions in hydrogen using the continuum distorted wave (CDW) method. As discussed in Chapter 3.2, this would have meant imposing the  $ps^{\dagger}$  approximation when handling the passive electron(s) residing on the  $Li^+$  and  $Li^{2+}$  projectiles in order that the boundary conditions of the problem are preserved, which of course is a natural feature of the exact CDW method as discussed in Part 1. This is achieved indirectly by defining the coulomb wave in the entrance channel in the form of the hyper-geometric function  ${}_1F_1 [i\mathbf{v}; 1; i(vs + \underline{v} \cdot \underline{s})]$ , such that  $\mathbf{v} = q/v$ , where  $v$  is the projectile velocity. Alternatively we could have defined  $\mathbf{v} = q_{\text{eff}}/v$ , where  $q_{\text{eff}}$  is given by  $(-2\mathcal{E}_n)^{\frac{1}{2}}$  and  $\mathcal{E}$  is the binding energy of the active electron in its final quantum state  $n$  of the Li-ion projectile. In this way  $q_{\text{eff}}$  is analogous to  $Z_{\text{eff}}$  defined in Chapter 2.2, equation (2.2.5), and therefore reflects a measure of the effective charge of the incoming projectile as seen by the active electron, as it is gradually ionised into the continuum state of the Li-ion projectile prior to being captured into the quantum state  $n$ .

Fortunately, shortly after the completion of this work, such a calculation was reported by Crothers and Todd<sup>32</sup> who have examined theoretically the  $q^3$  scaling rule<sup>18</sup> for electron-capture by fast multiply-charged ions in hydrogen. Crothers and Todd<sup>32</sup> have performed calculations of electron-capture cross-sections for Li-ions incident on hydrogen using the CDW method over the low end of our energy range, and have compared their results with the experimental data of Shah, Goffe and Gilbody<sup>18</sup>. It is interesting to note that in calculating total cross-sections for  $Li^+$  incident on H within the CDW approximation, Crothers and Todd<sup>32</sup> have used an effective charge for  $Li^+$ , when capturing into the quantum state  $n = 1$ , equal to 1.260 as given by Banyard and Shirtcliffe<sup>33</sup>.

---

<sup>†</sup>ps = perfect screening

This was derived from equation (2.25) in Chapter 2.2. Crothers and Todd did not, however, use an effective charge in the case of  $\text{Li}^{2+}$  incident on H.

Therefore, in Figure 3.9 we compare the CDW total capture cross-sections of Crothers and Todd<sup>32</sup> with our own CIS cross-sections, and with the experimental data of Shah, Goffe and Gilbody<sup>18</sup> for  $\text{Li}^{3+}$ ,  $\text{Li}^{2+}$  and  $\text{Li}^+$  incident on hydrogen. In calculating the total capture cross-section Crothers and Todd have performed a sum over the individual capture cross-sections  $\sigma(nl)$  for  $n = 1$  to 7 and have assumed the Oppenheimer<sup>23</sup>  $n^{-3}$  rule for  $n \gg 8$ , a rather good approximation. For comparison the CDW calculation of Belkic, Gayet and Salin<sup>34</sup> for  $\text{Li}^{3+}$  in H is also shown in Figure 3.9. Belkic et al<sup>34</sup> calculate the total capture cross-section using the Oppenheimer  $n^{-3}$  rule expressed in equation (3.5.4) but did not consider capture into the 3d state of  $\text{Li}^{2+}$ . Note that of the CIS total capture cross-section given in Table 3.3,  $\sigma(3d)$  contributes, via equation (3.5.4), approximately 57% and 40% to the total cross-section for  $E = 500$  keV and 1000 keV, respectively. For the same energies capture into the  $n = 3$  state of  $\text{Li}^{2+}$  contributes 37% and 31% respectively to the total capture cross-section. The importance of capture into the  $n = 3$  states is expected since the third energy level of  $\text{Li}^{2+}$  is in resonance with  $\text{H}(1s)$ , and this will lead to an enhancement of the capture cross-section as a consequence of a zero energy decrement  $\Delta\epsilon$ . This will be particularly noticeable at lower impact energies since  $\Delta\epsilon$  appears in the equations in the form  $(\frac{v}{2} + \frac{\Delta\epsilon}{v})$ , where  $v$  is the projectile velocity (see equations (3.3.14) to (3.3.22) of Chapter 3.3).

From Figure 3.9 it can be seen that the CDW cross-sections of Crothers and Todd<sup>32</sup> are similar to those of the CIS method particularly at high impact energies. For  $\text{Li}^{3+}$  in hydrogen, for which the atomic

wavefunctions used are exact, the CDW method appears to be in slightly better agreement with the experimental points, compared with the CIS method, for impact energy  $E > 800$  keV. Most encouraging, however, is the excellent agreement with experiment obtained for the  $\text{Li}^{2+}$  projectile, for  $E > 300$  keV, when the total cross-sections are derived using our modified CIS approach. The underestimation in total cross-sections for the  $\text{Li}^{2+}$  projectile, due to assuming the  $n^3$  sum rule for capture into states  $n \gg 4$  (see equation (3.5.4)) is not expected to be too serious, since we note that for this reaction  $\sigma(n=2) \approx 2 \times \sigma(n=3)$  over the experimental energy range.

Finally, the rather good agreement for  $\text{Li}^{2+}$  in hydrogen certainly justifies our use of the rather cumbersome but good excited state wave-functions for  $\text{Li}^+(1s, n\ell)$  of Cohen and McEachran<sup>25,26</sup>, for which the prior form of the CIS transition amplitude was ideally suited due to the omission of the coulomb wave in the entrance channel, as discussed in Chapter 3.2 and 3.3. It is this feature of the CIS method that allowed us to modify the perturbing potential in the entrance channel. Such a flexibility, which is not possible in the exact treatment of the CDW method, may prove useful for other more general cases of ion atom collisions.

## CHAPTER 3.6

### Conclusion

Working within the scheme of the continuum intermediate states (CIS) approximation devised by Belkic<sup>16</sup> we have examined a possible procedure for calculating cross-sections for electron-capture from H by one or two electron atom or ion projectiles. Using the proposed method we have investigated electron-capture in H-H and Li<sup>q+</sup>-H collisions and have obtained very satisfactory results for impact energies greater than those for which the CIS method is expected to work. For the Li<sup>3+</sup> projectile the cross-sections were obtained using the CIS method as presented by Belkic<sup>16</sup>. Compared to the CDW method the CIS method was found to be more suitable for adaptation to high energy electron-capture by a structured projectile such as a one or two-electron atom or ion. This arose due to the fact that in the CIS approximation distortion of the active electron is retained in only one of the reaction channels while the perturbing potential corresponding to the other channel is retained in the matrix element, and therefore lends itself more readily available to approximations. In contrast, for the CDW method distortion functions are defined in both the entrance and exit channels and thus for a structured projectile in the entrance channel it is found that only two types of approximation are possible. One is the perfect screening approximation, in which the active electron experiences a charge due to the projectile equal to  $Z_A - N$ , where  $N$  is the number of passive electrons on the projectile and  $Z_A$  the projectile nuclear charge. The other alternative is to define an effective charge as seen by the active electron due to the approaching projectile in a similar way as was done in the case of electron-capture from a many-electron atom seen in Part II. Both these approximations

are not totally satisfactory since they do not allow the active electron to experience the full charge of the projectile nucleus. This may be very important for reactions in which the structured projectile forms, on capturing the electron, a negative ion such as  $H^-$ , and in particular at high impact energies when, as we have seen, the electron is captured into regions of small electron-nuclear separations. In the CIS method, however, the electron-electron potential terms in the matrix element may be treated exactly by using their expansion representation (see equation (3.4.2)), or they may be approximated by some type of average static potential that the active electron experiences due to the passive electron charge cloud residing on the projectile nucleus. In this way the resulting perturbing potential is such that not only may the active electron see the full (unscreened) charge of the projectile nucleus at small electron-nuclear separations, but for large electron-nuclear separations the perturbing potential reduces to that of a perfect screening approximation. Thus in the CIS scheme we were able to simulate the physics of the capture process more accurately.

In an investigation of  $H^-$  production in H-H collisions, using the proposed scheme, we were successful in predicting accurate cross-sections for impact energies  $E > 25$  keV. Due to the importance of electron correlation in  $H^-$  the magnitude of the cross-sections were improved when the expansion representation for  $1/s_{12}$  was used, which allowed both radial and angular correlation to contribute to the cross-section. We noted that any agreement with experiment obtained using the HF wavefunction for  $H^-$  must be fortuitous and results from the fact that the effect on the cross-section upon including angular type correlation terms having a P symmetry is opposite to the effect of adding the radial correlation terms. Thus, there is an "add-subtract" mechanism in operation when we systematically include electron correlation, via the natural expansion

representation of the correlated wavefunction for  $H^-$ , as a consequence of including the higher angular terms within the  $1/s_{12}$  expansion. As a result the final cross-section curve obtained using a fully correlated wavefunction for  $H^-$  may well lie on or near to the curve obtained using the HF wavefunction. Note that in the work of Banyard and Szuster<sup>31</sup> on electron-capture from He by fast protons the inclusion of radial correlation terms within the He wavefunction caused the cross-sections to worsen with respect to experimental data; the inclusion of angular correlation terms may well reverse this trend.

A more appropriate test of the proposed scheme was obtained by applying it to electron-capture from H by fast  $Li^{2+}$  ions, to form  $Li^+$  in both its ground and excited states. A difficulty arising in such reactions involving a one-electron projectile will be in obtaining suitably accurate excited-state wavefunctions used to describe the final two-electron projectile in the exit channel when the electron is captured into an excited state. For the  $Li^{2+}$  projectile excited state capture was of major importance since it contributed  $\sim 90\%$  of the total cross-section over the energy range for which good agreement with experiment was obtained. This justified our using the rather cumbersome but good excited state wavefunctions of Cohen and McEachran<sup>2,5,26</sup>. As stated earlier, for high impact energies the accuracy of the wavefunction in the vicinity of the origin is of importance if a meaningful comparison with experiment is to be made, and thus using a simple hydrogen-like wavefunction to describe the excited state orbital may not be good enough if accurate cross-sections for capture into the excited states are required. Note that in the case of  $Li^+ - H$  collisions although the agreement with experiment was fairly good the gradient of the theoretical curve appeared to be too great and thus the agreement at large impact energies may be doubtful. This was probably due to the rather simple

wavefunctions used to describe the excited states of Li.

In calculating the electron-capture cross-sections for a one or two-electron projectile incident on H, using the proposed CIS scheme, we recall that during the analysis we have omitted contributions to the transition amplitude that come from matrix elements containing the perturbing potentials of the form  $\frac{Z_B}{x_2}$  and  $-\frac{Z_B}{R}$  (see Chapter 3.2, equations (3.2.22-35)). It was argued that the contributions from these terms would be small and that for projectiles having a large nuclear charge the approximation that  $x_2 \approx R$  should be reasonably accurate. In view of the rather good results for  $\text{Li}^{2+}$  and  $\text{Li}^+$  incident on H and in the light of the excellent agreement with experiment for the H-H collision electron-capture cross-sections we may conclude that the approximation is a good one, and that for electron-capture by a one-electron projectile incident on H, when using the prior form of the transition amplitude, we need only consider contributions to the transition amplitude from matrix elements containing the perturbing potential

$$\frac{Z_A}{s_1} - \frac{1}{s_{12}} .$$

In general this approximation should be most accurate

for projectiles having a nuclear charge greater than the nuclear charge of the target, for which the distortion of the projectile's passive electrons, which may contribute to the capture of a target electron via indirect electron-correlation effects, will be relatively small.

Tables and Figures to Part 3

E(keV)	CIS		CDW	
	HF	CI	HF	CI
25	$1.681^{-17}$	$1.173^{-17}$	$2.886^{-17}$	$2.067^{-17}$
50	$3.023^{-18}$	$2.067^{-18}$	$5.093^{-18}$	$3.526^{-18}$
100	$3.268^{-19}$	$2.268^{-19}$	$5.227^{-19}$	$3.600^{-19}$
200	$2.325^{-20}$	$1.650^{-20}$	$3.410^{-20}$	$2.379^{-20}$
400	$1.202^{-21}$	$8.696^{-22}$	$1.527^{-21}$	$1.087^{-21}$
800	$4.845^{-23}$	$3.636^{-23}$	$4.990^{-23}$	$3.618^{-23}$
1000	$1.688^{-23}$	$1.284^{-23}$	$1.570^{-23}$	$1.143^{-23}$

Table 3.1 A comparison of the electron-capture cross-sections  $\sigma(1s)$  measured in  $\text{cms}^2$ , for the reaction  $\text{H}(1s)+\text{H}(1s)\rightarrow\text{H}^-(1s^2)+\text{H}^+$ . The continuum-intermediate states (CIS) results are calculated here for the forward reaction whereas the continuum-distorted wave (CDW) results are those of Moore and Banyard<sup>14</sup> and were derived by them from the calculated results for the reverse reaction. For  $\text{H}^-(1s^2)$ , the Hartree-Fock (HF) function was that of Curl and Coulson<sup>19</sup> and the configuration-interaction (CI) description was taken from Weiss<sup>20</sup>. The superscripts indicate the power of ten by which each entry is to be multiplied.

E(keV)	$\sigma(l=0)_{\text{HF}}$	$\sigma(l=0)_{\text{CI}}$ [ $\Delta_0$ ]	$\sigma(l=1)_{\text{CI}}$ [ $\Delta_1$ ]	$\sigma(l=2)_{\text{CI}}$ [ $\Delta_2$ ]
20	$2.753^{-17}$	$3.163^{-17}$ [+26.0%]	$2.579^{-17}$ [-18.46%]	$2.779^{-17}$ [+7.8%]
40	$6.096^{-18}$	$6.689^{-18}$ [+20.4%]	$5.178^{-18}$ [-22.6%]	$5.648^{-18}$ [+9.1%]
60	$2.085^{-18}$	$2.194^{-18}$ [+14.3%]	$1.440^{-18}$ [-34.4%]	$1.637^{-18}$ [+13.7%]
80	$8.834^{-19}$	$8.971^{-19}$ [+9.1%]	$5.067^{-19}$ [-43.5%]	$6.032^{-19}$ [+19.0%]
100	$4.203^{-19}$	$4.212^{-19}$ [+4.8%]	$2.121^{-19}$ [-49.6%]	$2.649^{-19}$ [+24.9%]
150	$9.964^{-20}$	$9.286^{-20}$ [-7.9%]	$4.019^{-20}$ [-56.7%]	$5.654^{-20}$ [+40.1%]
200	$3.199^{-20}$	$2.867^{-20}$ [-8.0%]	$1.203^{-20}$ [-58.0%]	$1.879^{-20}$ [+66.3%]

Table 3.2 The CIS electron-capture cross-sections in  $\text{cm}^2$ , for the reaction  $\text{H}(1s)+\text{H}(1s)\rightarrow\text{H}^-(1s^2)+\text{H}^+$  when the electron-electron potential in  $V_{1,2}^0$  (see Chapter 3.3 equation (3.3.4)) is represented by truncation of expansion (3.4.2) at  $l = 0, 1$  and 2, and the  $\text{H}^-$  system is described by either the configuration interaction (CI) wavefunction of Weiss<sup>20</sup>, or the Hartree-Fock (HF) wavefunction of Curl and Coulson<sup>19</sup>, for which only the first radial term ( $l=0$ ) in expansion (3.4.2) contributes.

The percentage changes  $\Delta$  are defined as follows:

$$\Delta_0 = \left[ \frac{(\sigma(l=0)_{\text{CI}} - \sigma(l=0)_{\text{HF}})}{\sigma(l=0)_{\text{HF}}} \right] \times 100$$

$$\Delta_1 = \left[ \frac{(\sigma(l=1)_{\text{CI}} - \sigma(l=0)_{\text{CI}})}{\sigma(l=0)_{\text{CI}}} \right] \times 100$$

$$\Delta_2 = \left[ \frac{(\sigma(l=2)_{\text{CI}} - \sigma(l=1)_{\text{CI}})}{\sigma(l=1)_{\text{CI}}} \right] \times 100$$

TABLE 3.3

E keV	$\sigma(1s)$	$\sigma(2s)$	$\sigma(2p)$	$\sigma(3s)$	$\sigma(3p)$	$\sigma(3d)$	Q
100	$1.7775^{-18}$	$6.7034^{-16}$	$3.6572^{-15}$	$4.8400^{-16}$	$2.3508^{-15}$	$5.0785^{-15}$	$2.0797^{-14}$
200	$1.0302^{-17}$	$9.1025^{-17}$	$7.6350^{-16}$	$9.1014^{-17}$	$5.4123^{-16}$	$1.2788^{-15}$	$4.8417^{-15}$
300	$2.2422^{-17}$	$2.9253^{-17}$	$2.7179^{-16}$	$4.2327^{-17}$	$1.6763^{-16}$	$5.0909^{-16}$	$1.8198^{-15}$
400	$2.9829^{-17}$	$1.9122^{-17}$	$1.2520^{-16}$	$2.4281^{-17}$	$6.3881^{-17}$	$2.4126^{-16}$	$8.5969^{-16}$
500	$2.7310^{-17}$	$1.3548^{-17}$	$6.8421^{-17}$	$1.4180^{-17}$	$3.0117^{-17}$	$1.2557^{-16}$	$4.6277^{-16}$
600	$2.0656^{-17}$	$9.2967^{-18}$	$4.2037^{-17}$	$8.2743^{-18}$	$1.7212^{-17}$	$6.9559^{-17}$	$2.6978^{-16}$
800	$1.0715^{-17}$	$4.1787^{-18}$	$1.9508^{-17}$	$2.8847^{-18}$	$8.0300^{-18}$	$2.4356^{-17}$	$1.0780^{-16}$
1000	$5.7997^{-18}$	$1.9330^{-18}$	$1.0450^{-17}$	$1.0839^{-18}$	$4.5401^{-18}$	$9.7117^{-18}$	$5.0097^{-17}$
1500	$1.6329^{-18}$	$4.2337^{-19}$	$2.8707^{-18}$	$1.6502^{-19}$	$1.3361^{-18}$	$1.4376^{-18}$	$1.1043^{-17}$
2000	$6.2137^{-19}$	$1.6305^{-19}$	$9.7335^{-19}$	$5.8031^{-20}$	$4.5478^{-19}$	$3.0994^{-19}$	$3.4699^{-18}$
2500	$2.9184^{-19}$	$8.3451^{-20}$	$3.8057^{-19}$	$3.0061^{-20}$	$1.7515^{-19}$	$8.5902^{-20}$	$1.3617^{-18}$
3000	$1.5791^{-19}$	$4.7859^{-20}$	$1.6601^{-19}$	$1.7443^{-20}$	$7.4945^{-20}$	$2.8512^{-20}$	$6.2337^{-19}$
5000	$2.7130^{-20}$	$7.9409^{-21}$	$1.2463^{-20}$	$2.8319^{-21}$	$5.2702^{-21}$	$1.0400^{-21}$	$6.6558^{-20}$
10000	$1.7249^{-21}$	$3.7923^{-22}$	$2.2912^{-22}$	$1.2595^{-22}$	$8.9635^{-23}$	$7.8936^{-24}$	$2.7983^{-21}$

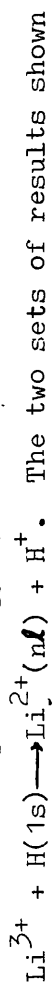
Table 3.3

The CIS individual  $\sigma(nl)$  and total capture cross-sections,  $Q$ , at selected impact energy  $E$ , for the reaction  $\text{Li}^{3+} + \text{H}(1s) \rightarrow \text{Li}^{2+}(nl) + \text{H}^+$  in units of  $\text{cm}^2$ . The total capture cross-section  $Q$  was obtained from the Oppenheimer  $n^{-3}$  rule:  $Q \approx \sigma(1s) + \sigma(2s) + \sigma(2p) + 2.081(\sigma(3s) + \sigma(3p) + \sigma(3d))$ . The superscript denotes the power of ten by which each entry should be multiplied.

$\sigma(n\ell)/\sigma(1s)$	E(keV)	100	300	500	1000	3000	5000
$\sigma(2s)/\sigma(1s)$	CIS	377.1	1.305	0.496	0.333	0.303	0.293
	CDW	84.32	4.519	5.609	1.600	0.471	0.312
$\sigma(3s)/\sigma(1s)$	CIS	272.3	1.888	0.519	0.187	0.110	0.104
	CDW	40.59	2.913	4.715	0.988	0.192	0.113
$\sigma(2p)/\sigma(1s)$	CIS	2057	12.12	2.505	1.802	1.051	0.459
	CDW	115.4	42.69	57.19	6.740	0.569	0.237
$\sigma(3p)/\sigma(1s)$	CIS	1323	7.476	1.103	0.783	0.475	0.194
	CDW	257.1	31.33	34.91	3.518	0.246	0.097

Table 3.4 The ratio  $\sigma(n\ell)/\sigma(1s)$  of individual capture cross-sections,

at selected impact energy E, for the reaction



correspond to the continuum-intermediate states (CIS) method

and continuum distorted wave (CDW) method of calculating the

individual capture cross-sections.

$\sigma^{(nl)}_{\text{CIS}} / \sigma^{(nl)}_{\text{CDW}}$	E(keV)	300	500	1000	3000	5000
$nl = 1s$		2.91	16.0	3.76	1.09	1.14
$= 2s$		0.84	1.414	0.78	0.70	1.07
$= 2p$		0.83	0.70	1.01	2.02	2.21
$= 3s$		1.89	1.76	0.71	0.63	1.05
$= 3p$		0.70	0.51	0.84	2.10	2.30

Table 3.5 Ratio of continuum intermediate states (CIS) individual capture cross-sections  $\sigma^{(nl)}$ , to continuum distorted wave (CDW) individual capture cross-sections at selected impact energy F, for the reaction  $\text{Li}^3+ + \text{H}(1s) \rightarrow \text{Li}^{2+}(nl) + \text{H}^+$ .

TABLE 3.6

E keV	$\sigma$ (1s)	$\sigma$ (2s)	$\sigma$ (2p)	$\sigma$ (3s)	$\sigma$ (3p)	$\sigma$ (3d)	$Q_1$
100	1.6344 <sup>-17</sup>	2.2490 <sup>-16</sup>	1.6108 <sup>-15</sup>	2.9653 <sup>-16</sup>	7.8365 <sup>-16</sup>	1.1094 <sup>-15</sup>	6.4086 <sup>-15</sup>
200	3.2312 <sup>-17</sup>	6.3897 <sup>-17</sup>	4.0707 <sup>-16</sup>	5.6424 <sup>-17</sup>	1.8920 <sup>-16</sup>	1.8469 <sup>-16</sup>	1.3987 <sup>-15</sup>
300	2.3515 <sup>-17</sup>	2.2652 <sup>-17</sup>	1.6132 <sup>-16</sup>	1.5998 <sup>-17</sup>	7.4647 <sup>-17</sup>	4.2506 <sup>-17</sup>	4.8457 <sup>-16</sup>
400	1.3506 <sup>-17</sup>	9.0615 <sup>-18</sup>	7.6996 <sup>-17</sup>	5.4705 <sup>-18</sup>	3.5635 <sup>-17</sup>	1.2461 <sup>-17</sup>	2.1103 <sup>-16</sup>
500	7.9093 <sup>-18</sup>	4.0108 <sup>-18</sup>	4.0912 <sup>-17</sup>	3.1234 <sup>-18</sup>	1.4256 <sup>-17</sup>	4.5157 <sup>-18</sup>	9.6315 <sup>-17</sup>
600	4.8810 <sup>-18</sup>	1.9544 <sup>-18</sup>	2.3392 <sup>-17</sup>	9.1894 <sup>-19</sup>	1.0699 <sup>-17</sup>	1.9677 <sup>-18</sup>	5.8499 <sup>-17</sup>
800	2.1440 <sup>-18</sup>	6.1724 <sup>-19</sup>	8.9200 <sup>-18</sup>	2.3877 <sup>-19</sup>	3.9912 <sup>-18</sup>	5.6205 <sup>-19</sup>	2.1653 <sup>-17</sup>
1000	1.0952 <sup>-18</sup>	2.7473 <sup>-19</sup>	3.9405 <sup>-18</sup>	9.5591 <sup>-20</sup>	1.7233 <sup>-18</sup>	2.2532 <sup>-19</sup>	9.5645 <sup>-18</sup>
1500	3.1534 <sup>-19</sup>	8.2635 <sup>-20</sup>	7.7537 <sup>-19</sup>	2.8057 <sup>-20</sup>	3.2398 <sup>-19</sup>	4.8010 <sup>-20</sup>	2.0059 <sup>-18</sup>
2000	1.2959 <sup>-19</sup>	3.6311 <sup>-20</sup>	2.2395 <sup>-19</sup>	1.2365 <sup>-20</sup>	9.0542 <sup>-20</sup>	1.7875 <sup>-20</sup>	6.4120 <sup>-19</sup>
2500	6.3931 <sup>-20</sup>	1.7951 <sup>-20</sup>	8.2659 <sup>-20</sup>	6.0361 <sup>-21</sup>	3.2512 <sup>-20</sup>	8.8142 <sup>-21</sup>	2.6310 <sup>-19</sup>
3000	3.5096 <sup>-20</sup>	9.5611 <sup>-21</sup>	3.6155 <sup>-20</sup>	3.1613 <sup>-21</sup>	1.3874 <sup>-20</sup>	5.0667 <sup>-21</sup>	1.2681 <sup>-19</sup>
5000	5.5768 <sup>-21</sup>	1.2846 <sup>-21</sup>	3.5101 <sup>-21</sup>	4.0230 <sup>-22</sup>	1.2478 <sup>-21</sup>	1.0898 <sup>-21</sup>	1.6073 <sup>-20</sup>
10000	3.0424 <sup>-22</sup>	5.4929 <sup>-23</sup>	1.4806 <sup>-22</sup>	1.6260 <sup>-23</sup>	4.8408 <sup>-23</sup>	1.1326 <sup>-22</sup>	8.7749 <sup>-22</sup>

Table 3.6

The CIS individual  $\sigma(n\ell)$  and total capture cross-sections  $Q_1$ , at selected impact energy E, for the reaction

$\text{Li}^{2+}(1s) + \text{H}(1s) \rightarrow \text{Li}^+(1s, n\ell) + \text{H}^+$  in units of  $\text{cm}^2$ , when the interacting potential  $V_{1,2}^1$  in Chapter 3.3, equation (3.3.12), is defined as  $(Z_A - 1)/s + \exp(-2Z_A s)(Z_A + 1/s)$ . The total capture cross-section Q was obtained from the Oppenheimer  $n^3$  rule:  $Q \doteq \sigma(1s) + \sigma(2s) + \sigma(2p) + 2.081 (\sigma(3s) + \sigma(3p) + \sigma(3d))$ .

The superscript denotes the power of ten by which each entry should be multiplied.

TABLE 3.7

E keV	$\sigma(1s)$	$\sigma(2s)$	$\sigma(2p)$	$\sigma(3s)$	$\sigma(3p)$	$\sigma(3d)$	$Q_2$
100	$1.2038^{-17}$	$2.2850^{-16}$	$1.4230^{-15}$	$3.1300^{-16}$	$6.6993^{-16}$	$1.0885^{-15}$	$5.9742^{-15}$
200	$2.5488^{-17}$	$6.4554^{-17}$	$3.5738^{-16}$	$5.9444^{-17}$	$1.6055^{-16}$	$1.7927^{-16}$	$1.2783^{-15}$
300	$1.8828^{-17}$	$2.2738^{-17}$	$1.4040^{-16}$	$1.6823^{-17}$	$6.3012^{-17}$	$4.0231^{-17}$	$4.3182^{-16}$
400	$1.0799^{-17}$	$8.9897^{-18}$	$6.6259^{-17}$	$5.7233^{-18}$	$2.9868^{-17}$	$1.1285^{-17}$	$1.8360^{-16}$
500	$6.2861^{-18}$	$3.9020^{-18}$	$3.4732^{-17}$	$2.1949^{-18}$	$1.5653^{-17}$	$3.8305^{-18}$	$9.033^{-17}$
600	$3.8496^{-18}$	$2.8469^{-18}$	$1.4189^{-17}$	$9.2802^{-19}$	$8.7694^{-18}$	$1.5355^{-18}$	$4.3261^{-17}$
800	$1.6637^{-18}$	$5.3754^{-19}$	$7.2008^{-18}$	$2.2067^{-19}$	$3.1734^{-18}$	$3.5988^{-19}$	$1.7214^{-17}$
1000	$8.3756^{-19}$	$2.2050^{-19}$	$3.0578^{-18}$	$7.8893^{-20}$	$1.3223^{-18}$	$1.1570^{-19}$	$7.2725^{-18}$
1500	$2.3560^{-19}$	$6.1625^{-20}$	$5.3732^{-19}$	$2.0818^{-20}$	$2.2435^{-19}$	$1.2953^{-20}$	$1.3717^{-18}$
2000	$9.5770^{-20}$	$2.7149^{-20}$	$1.3667^{-19}$	$9.2387^{-21}$	$5.5896^{-20}$	$2.3605^{-21}$	$4.0005^{-19}$
2500	$4.6905^{-20}$	$1.3484^{-20}$	$4.4069^{-20}$	$4.5447^{-21}$	$1.7756^{-20}$	$5.8050^{-22}$	$1.5207^{-19}$
3000	$2.5568^{-20}$	$7.1805^{-21}$	$1.6783^{-20}$	$2.3830^{-21}$	$6.6716^{-21}$	$1.7630^{-22}$	$6.8741^{-20}$
5000	$3.9301^{-21}$	$9.4120^{-22}$	$9.5313^{-22}$	$2.9614^{-22}$	$3.5949^{-22}$	$5.2673^{-24}$	$7.1998^{-21}$
10000	$1.9761^{-22}$	$3.7029^{-23}$	$1.4544^{-23}$	$1.1009^{-23}$	$4.9894^{-24}$	$3.3710^{-26}$	$2.8255^{-22}$

Table 3.7 .

The CIS individual  $\sigma(nl)$  and total capture cross-sections  $Q_2$ , at selected impact energy  $E$ , for the reaction  $\text{Li}^{2+}(1s) + \text{H}(1s) \rightarrow \text{Li}^+(1s, nl) + \text{H}^+$  in units of  $\text{cm}^2$  when the interacting potential  $V_{1,2}^1$  in Chapter 3.3, equation (3.3.12), is defined as  $(Z_A - 1)/s$ . The total capture cross-section  $Q$  was obtained from the Oppenheimer  $n^{-3}$  rule:  $Q = \sigma(1s) + \sigma(2s) + \sigma(2p) + 2.081 (\sigma(3s) + \sigma(3p) + \sigma(3d))$ . The superscript denotes the power of ten by which each entry should be multiplied.

TABLE 3.8

E keV	$\sigma$ (2s)	$\sigma$ (2p)	$\sigma$ (3s)	$\sigma$ (3p)	$\sigma$ (3d)	$Q_1$
100	$6.3364^{-17}$	$5.3262^{-16}$	$2.7683^{-17}$	$2.8140^{-16}$	$2.2650^{-17}$	$1.2863^{-15}$
200	$1.4923^{-17}$	$1.1796^{-16}$	$7.3251^{-18}$	$7.3881^{-17}$	$6.2812^{-18}$	$3.1494^{-16}$
300	$5.7498^{-18}$	$3.4713^{-17}$	$3.1162^{-18}$	$2.3135^{-17}$	$1.7504^{-18}$	$9.8734^{-17}$
400	$2.9517^{-18}$	$1.2522^{-17}$	$1.6337^{-18}$	$8.6145^{-18}$	$5.6521^{-19}$	$3.7976^{-17}$
500	$1.7582^{-18}$	$5.2159^{-18}$	$9.5825^{-19}$	$3.6575^{-18}$	$2.0863^{-19}$	$1.7014^{-17}$
600	$1.1353^{-18}$	$2.4183^{-18}$	$6.0219^{-19}$	$1.7173^{-18}$	$8.5943^{-20}$	$8.5592^{-18}$
800	$5.4129^{-19}$	$6.5615^{-19}$	$2.7134^{-19}$	$4.7318^{-19}$	$9.6814^{-21}$	$2.7669^{-18}$
1000	$2.8796^{-19}$	$2.2221^{-19}$	$1.3770^{-19}$	$1.6167^{-19}$	$5.2592^{-21}$	$1.1441^{-18}$
1500	$7.9482^{-20}$	$2.7140^{-20}$	$3.5077^{-20}$	$1.9958^{-20}$	$4.3720^{-22}$	$2.2206^{-19}$
2000	$2.8702^{-20}$	$5.6118^{-21}$	$1.2063^{-20}$	$4.1444^{-21}$	$6.6965^{-23}$	$6.8180^{-20}$
2500	$1.2350^{-20}$	$1.5958^{-21}$	$5.0233^{-21}$	$1.1805^{-21}$	$1.4880^{-23}$	$2.6887^{-20}$
3000	$6.0139^{-21}$	$5.6197^{-22}$	$2.3894^{-21}$	$4.1595^{-22}$	$4.2493^{-24}$	$1.2423^{-20}$
5000	$7.0801^{-22}$	$2.8930^{-23}$	$2.6715^{-22}$	$2.1378^{-23}$	$1.1853^{-25}$	$1.3376^{-21}$
10000	$3.0797^{-23}$	$4.9977^{-25}$	$1.1110^{-23}$	$3.6779^{-25}$	$9.1724^{-28}$	$5.5184^{-23}$

Table 3.8

The CIS individual  $\sigma(nl)$  and total capture cross-sections  $Q_1$ , at selected impact energy  $E$ , for the reaction  $\text{Li}^+(1s^2)+\text{H}(1s)\rightarrow\text{Li}(1s^2,nl)+\text{H}^+$  in units of  $\text{cm}^2$ , when the perturbing potential in the transition amplitude, equation (3.5.18), is represented by the average static potential  $V_1$  (see equation (3.5.20)). The total capture cross-section  $Q$  was obtained from the Oppenheimer  $n^{-3}$  rule:

$Q \approx \sigma(1s)+\sigma(2s)+\sigma(2p) + 2.081(\sigma(3s)+\sigma(3p)+\sigma(3d))$ . The superscript denotes the power of ten by which each entry should be multiplied.

TABLE 3.9

E keV	$\sigma$ (2s)	$\sigma$ (2p)	$\sigma$ (3s)	$\sigma$ (3p)	$\sigma$ (3d)	$Q_2$
100	$5.1984^{-17}$	$5.2231^{-16}$	$1.1348^{-17}$	$2.7430^{-16}$	$2.2621^{-17}$	$1.2158^{-15}$
200	$9.9575^{-18}$	$1.1556^{-16}$	$3.1145^{-18}$	$7.2064^{-17}$	$6.2737^{-18}$	$2.9502^{-16}$
300	$2.8816^{-18}$	$3.3883^{-17}$	$1.2190^{-18}$	$2.2494^{-17}$	$1.7478^{-18}$	$8.9749^{-17}$
400	$1.2273^{-18}$	$1.2166^{-17}$	$6.1965^{-19}$	$8.3394^{-18}$	$5.6413^{-19}$	$3.3211^{-17}$
500	$6.7683^{-19}$	$5.0407^{-18}$	$3.6588^{-19}$	$3.5227^{-18}$	$2.0812^{-19}$	$1.4243^{-17}$
600	$4.2971^{-19}$	$2.3235^{-18}$	$2.3428^{-19}$	$1.6447^{-18}$	$8.5672^{-20}$	$6.8416^{-18}$
800	$2.0893^{-19}$	$6.2231^{-19}$	$1.0934^{-19}$	$4.4753^{-19}$	$1.8683^{-20}$	$2.0289^{-18}$
1000	$1.1382^{-19}$	$2.0773^{-19}$	$5.6597^{-20}$	$1.5079^{-19}$	$5.2218^{-21}$	$7.6399^{-19}$
1500	$3.1988^{-20}$	$2.4344^{-20}$	$1.4468^{-20}$	$1.7885^{-20}$	$4.3063^{-22}$	$1.2456^{-19}$
2000	$1.1364^{-20}$	$4.8036^{-21}$	$4.8485^{-21}$	$3.5497^{-21}$	$6.5201^{-23}$	$3.3780^{-20}$
2500	$4.7478^{-21}$	$1.2989^{-21}$	$1.9483^{-21}$	$9.6311^{-22}$	$1.4272^{-23}$	$1.2135^{-20}$
3000	$2.2342^{-21}$	$4.3405^{-22}$	$8.9163^{-22}$	$3.2257^{-22}$	$4.0016^{-24}$	$5.2033^{-21}$
5000	$2.2916^{-22}$	$1.8083^{-23}$	$8.6046^{-23}$	$1.3498^{-23}$	$1.0100^{-25}$	$4.5460^{-22}$
10000	$7.7153^{-24}$	$2.0205^{-25}$	$2.7530^{-24}$	$1.5131^{-25}$	$5.6418^{-28}$	$1.3962^{-23}$

Table 3.9

The CIS individual  $\sigma(n\ell)$  and total capture cross-sections  $Q_2$ , at selected impact energy  $E$ , for the reaction  $\text{Li}^+(1s^2)+\text{H}(1s)\rightarrow\text{Li}(1s^2,n\ell)+\text{H}^+$  in units of  $\text{cm}^2$ , when the perturbing potential in the transition amplitude, equation (3.5.18), is represented by the perfect screening potential  $V_2 = (Z_A - 2)/s$ . The total capture cross-section  $Q$  was obtained from the Oppenheimer  $n^{-3}$  rule:  $Q \approx \sigma(1s) + \sigma(2s) + \sigma(2p) + 2.081(\sigma(3s) + \sigma(3p) + \sigma(3d))$ . The superscript denotes the power of ten by which each entry should be multiplied.

E keV	$Q(3)/3^3$	$Q_1(2)/2^3$	$Q_1(1)/1^3$	$Q_2(2)/2^3$	$Q_2(1)/1^3$
100	$7.703^{+1}$	$8.011^{+1}$	$1.286^{+2}$	$7.468^{+1}$	$1.216^{+2}$
200	$1.793^{+1}$	$1.748^{+1}$	$3.149^{+1}$	$1.598^{+1}$	$2.950^{+1}$
300	$6.740^0$	$6.057^0$	$9.873^0$	$5.398^0$	$8.975^0$
400	$3.184^0$	$2.638^0$	$3.798^0$	$2.295^0$	$3.321^0$
500	$1.714^0$	$1.204^0$	$1.701^0$	$1.129^0$	$1.424^0$
600	$9.992^{-1}$	$7.312^{-1}$	$8.559^{-1}$	$5.408^{-1}$	$6.842^{-1}$
800	$3.993^{-1}$	$2.707^{-1}$	$2.767^{-1}$	$2.152^{-1}$	$2.029^{-1}$
1000	$1.855^{-1}$	$1.196^{-1}$	$1.144^{-1}$	$9.091^{-2}$	$7.640^{-2}$
1500	$4.090^{-2}$	$2.507^{-2}$	$2.221^{-2}$	$1.715^{-2}$	$1.246^{-2}$
2000	$1.285^{-2}$	$8.015^{-3}$	$6.818^{-3}$	$5.001^{-3}$	$3.378^{-3}$
2500	$5.043^{-3}$	$3.289^{-3}$	$2.689^{-3}$	$1.901^{-3}$	$1.214^{-3}$
3000	$2.309^{-3}$	$1.585^{-3}$	$1.242^{-3}$	$8.593^{-4}$	$5.203^{-4}$
5000	$2.465^{-4}$	$2.009^{-4}$	$1.338^{-4}$	$9.000^{-5}$	$4.546^{-5}$
10000	$1.036^{-5}$	$1.097^{-5}$	$5.518^{-6}$	$3.532^{-6}$	$1.396^{-6}$

Table 3.10 Ratios of  $Q(q)/q^3$ , in units of  $10^{-17} \text{ cm}^2$ , where  $Q$  is the total capture cross-section for the reaction  $\text{Li}^{q+} + \text{H}(1s) \rightarrow \text{Li}^{(q-1)+}(nl) + \text{H}^+$  calculated within the CIS approximation. The values of  $Q$ ,  $Q_1$  and  $Q_2$  are those given in Tables 3.3, 3.6, 3.7, 3.8 and 3.9, and were obtained from the Oppenheimer  $n^3$  rule:  $Q \approx \sigma(1s) + \sigma(2s) + \sigma(2p) + 2.081(\sigma(3s) + \sigma(3p) + \sigma(3d))$ . The superscript denotes the power of ten by which each entry should be multiplied.

E keV	$\frac{Q_1(2) 27}{Q(3) 8}$	$\frac{Q_1(1) 27}{Q(3)}$	$\frac{Q_1(2)}{Q_1(1) 8}$
	100	1.04	1.669
200	0.975	1.756	0.056
300	0.899	1.465	0.613
400	0.829	1.193	0.695
500	0.702	0.992	0.708
600	0.732	0.857	0.854
800	0.678	0.693	0.978
1000	0.645	0.617	1.045
1500	0.613	0.543	1.129
2000	0.624	0.531	1.176
2500	0.652	0.533	1.223
3000	0.686	0.538	1.276
5000	0.815	0.542	1.501
10000	1.059	0.532	1.988

Table 3.11 Ratios of  $\{Q(q)/q^3\} / \{Q(q')/q'^3\}$ , where  $Q$  is the total capture cross-section for the reaction  $\text{Li}^{q+} + \text{H}(1s) \longrightarrow \text{Li}^{(q-1)+} + (nl) + \text{H}^+$  calculated within the CIS approximation. For  $q$  (or  $q'$ ) = 1 or 2,  $Q$  is given by the values of  $Q_1$  in Tables 3.6 and 3.8, and were obtained from the Oppenheimer  $n^{-3}$  rule:  $Q \cong \sigma(1s) + \sigma(2s) + \sigma(2p) + 2.081(\sigma(3s) + \sigma(3p) + \sigma(3d))$ . The values for  $Q(q)/q^3$  are given in Table 3.10.

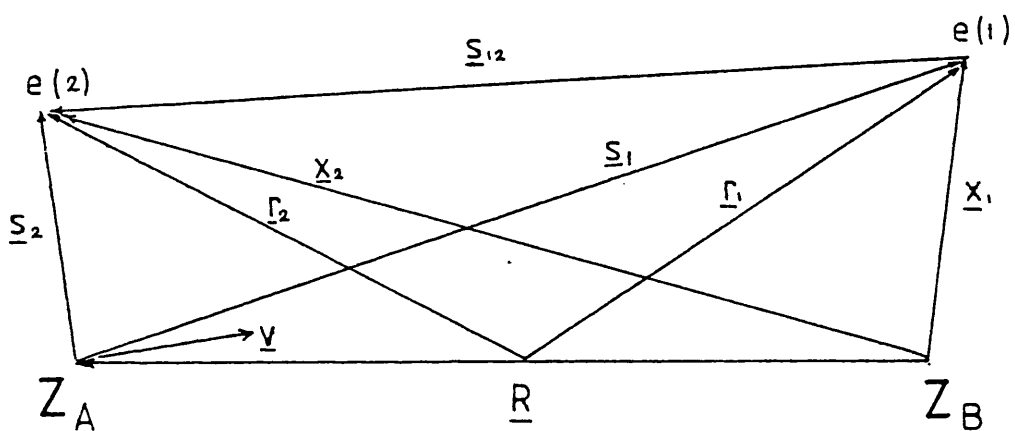


Figure 3.1 Coordinate system for reaction (3.2.1). The arbitrary origin is shown here to be at the mid-point of the internuclear line.

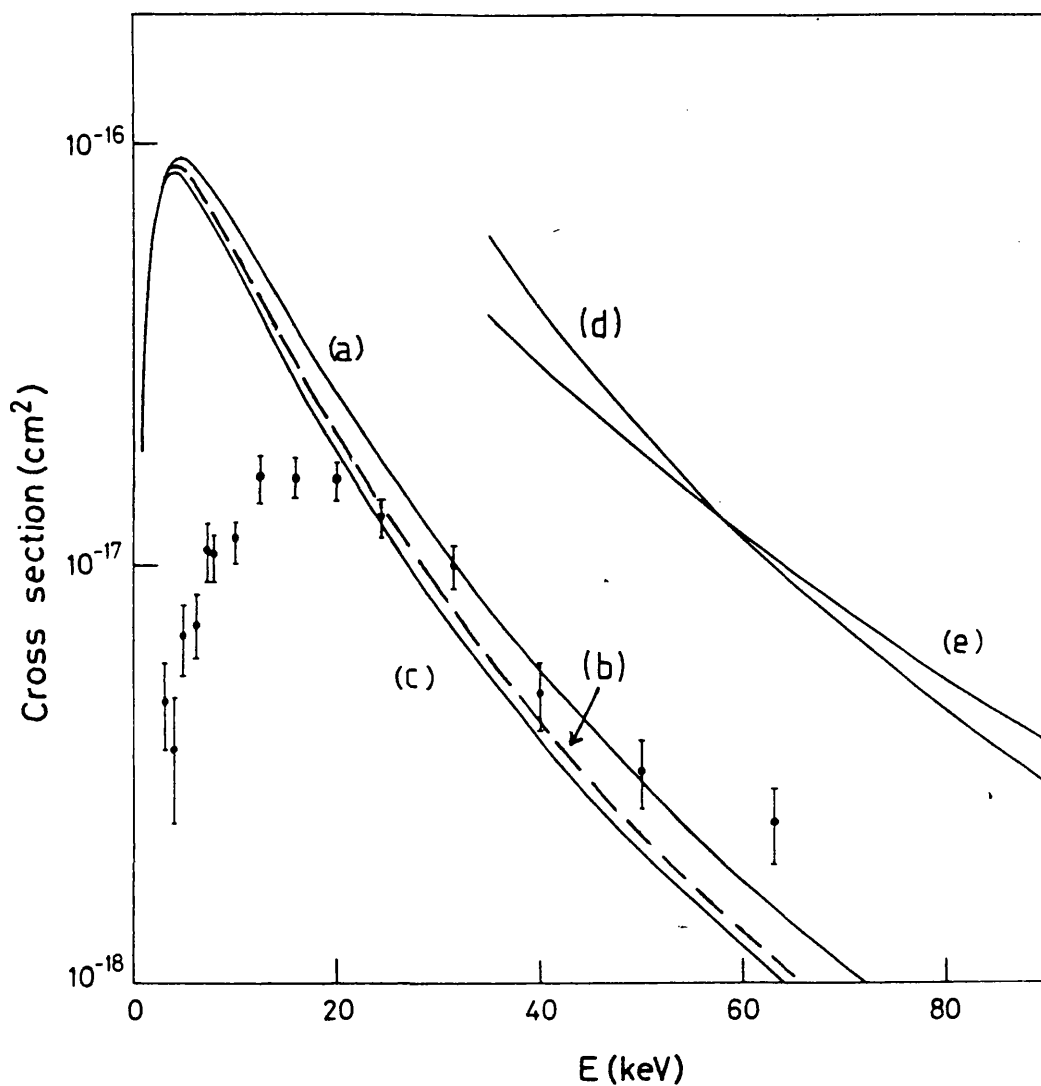


Figure 3.2 Electron-capture cross-sections  $\sigma(1s)$  for  $H(1s) + H(1s) \rightarrow H^-(1s^2) + H^+$ . The CIS results are shown in curves (a), (b) and (c) and are derived, respectively, from the use of the Hartree-Fock (HF) function<sup>19</sup>, the 'fixed core' model and the configuration-interaction (CI) description for  $H^-(1s^2)$ . Curves (d) and (e) are the 'prior' and 'post' results of Kapleton<sup>10</sup> calculated using a Born approximation. The experimental points are those of McClure<sup>9</sup>.

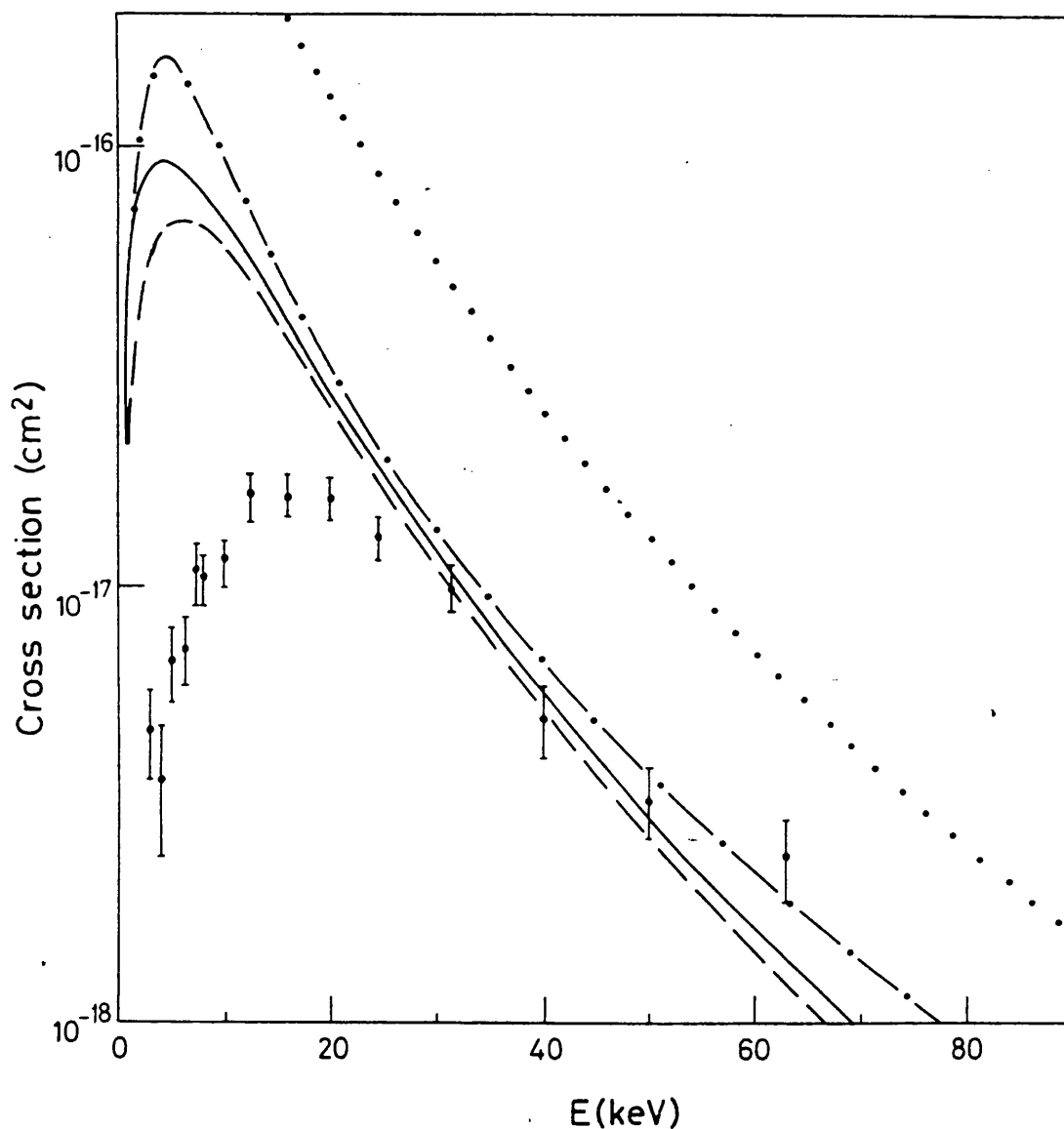


Figure 3.3 The CIS electron-capture cross-sections  $\sigma(1s)$  for  $H(1s)+H(1s) \rightarrow H^-(1s^2)+H^+$  obtained using expansion (3.4.2) for the potential term  $1/s_{12}$  in  $V_{1,2}^0$ , as defined in equation (3.3.4). The curves shown correspond to successive truncations of expansion (3.4.2) at  $l=0$  (— · — ·),  $l=1$  (— — —) and  $l=2$  (————), when describing the  $H^-(1s^2)$  system by the Weiss CI wavefunction<sup>20</sup>. For comparison the curves corresponding to  $1/s_{12}=0$  is also shown. The experimental points are those of McClure<sup>9</sup>.

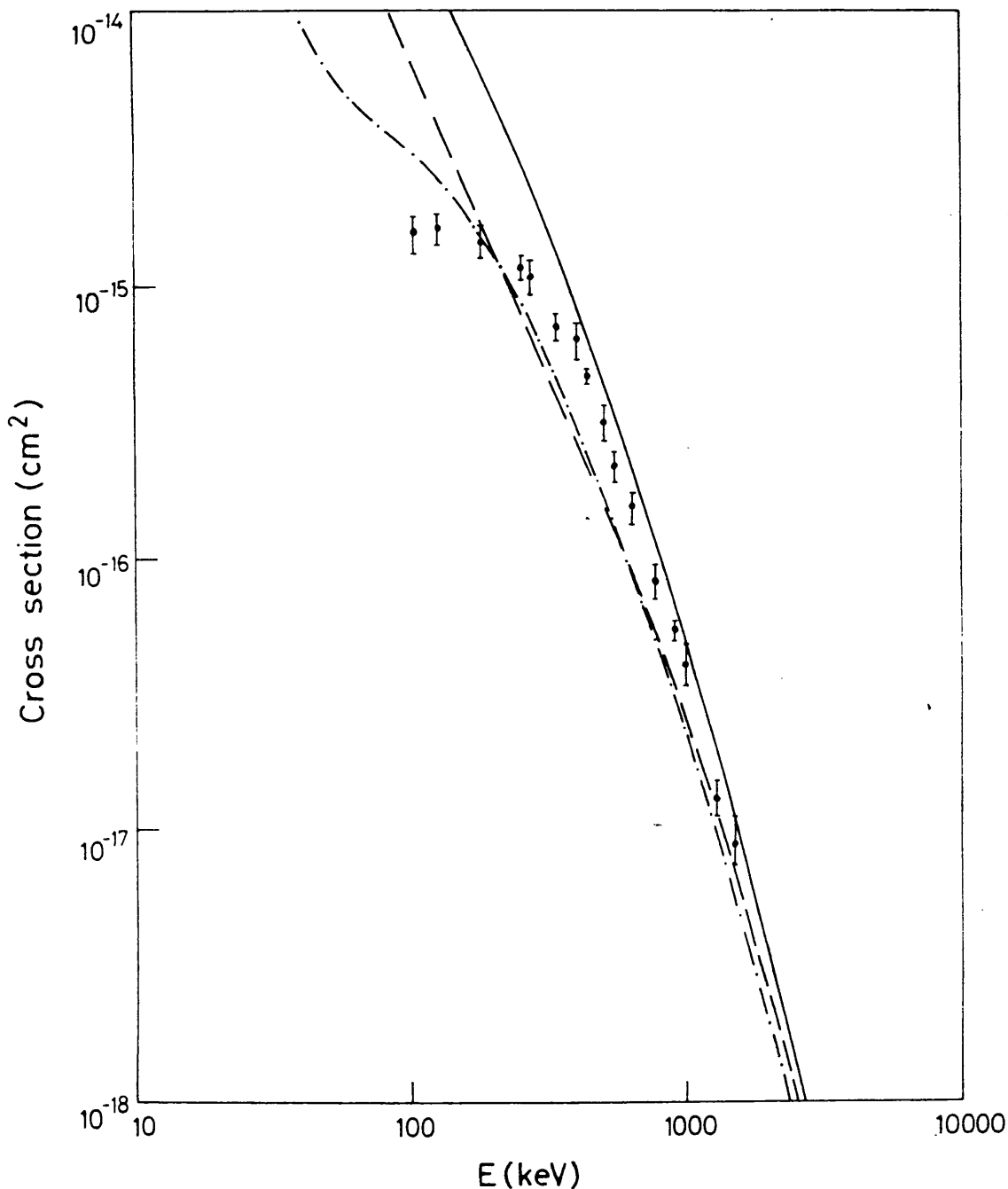


Figure 3.4 The theoretical total electron-capture cross-sections,  $Q$ , for  $\text{Li}^{3+}$  ions incident on hydrogen compared with the experimental data of Shah, Goffe and Gilbody<sup>18</sup>. The broken curves represent the CIS ——— and CDW - - - - cross-sections evaluated using  $Q = \sigma(1s) + 1.616(\sigma(2s) + \sigma(2p))$ , and the full curve is the CIS cross-sections evaluated using  $Q = \sigma(1s) + \sigma(2s) + \sigma(2p) + 2.081(\sigma(3s) + \sigma(3p) + \sigma(3d))$ .

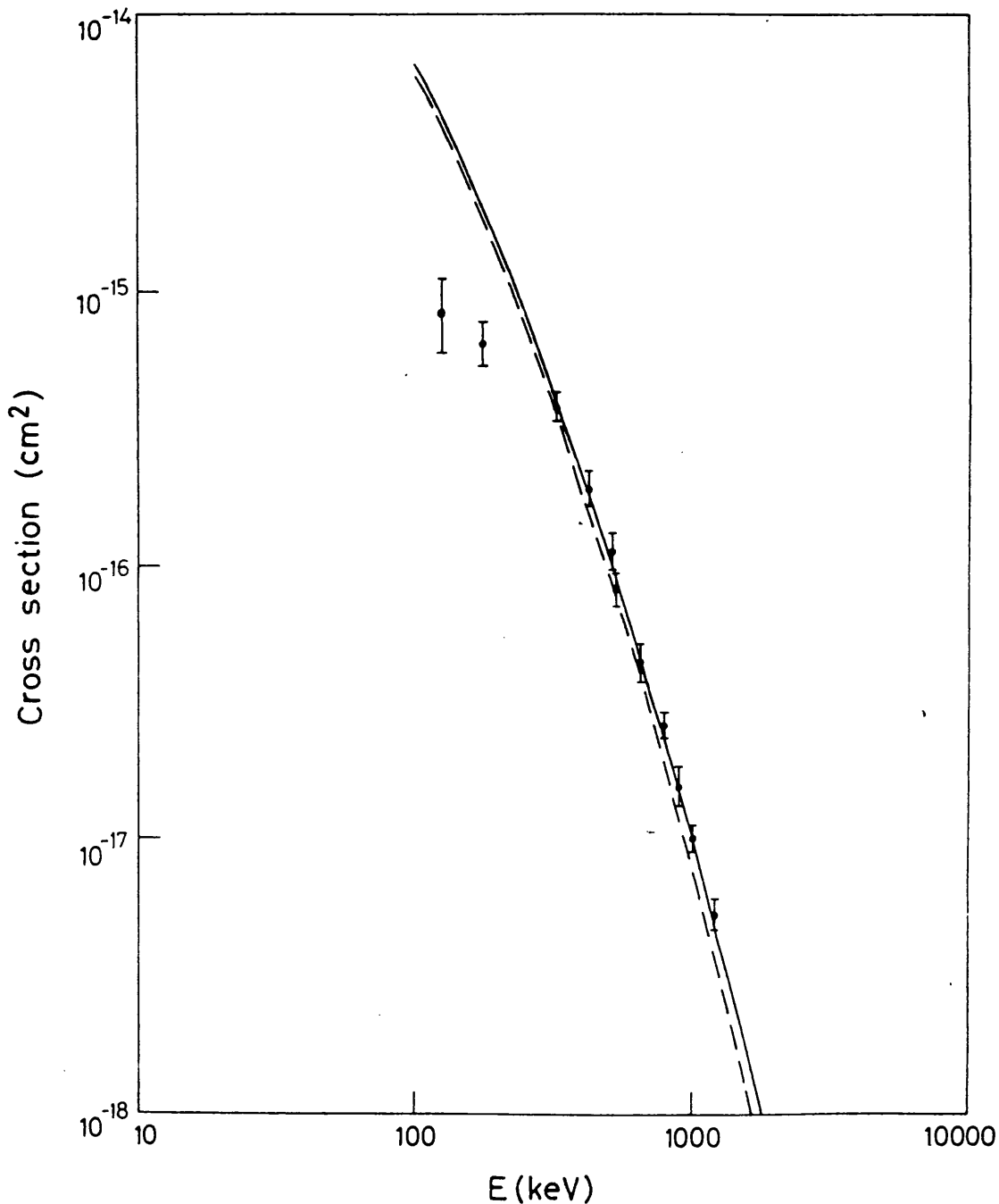
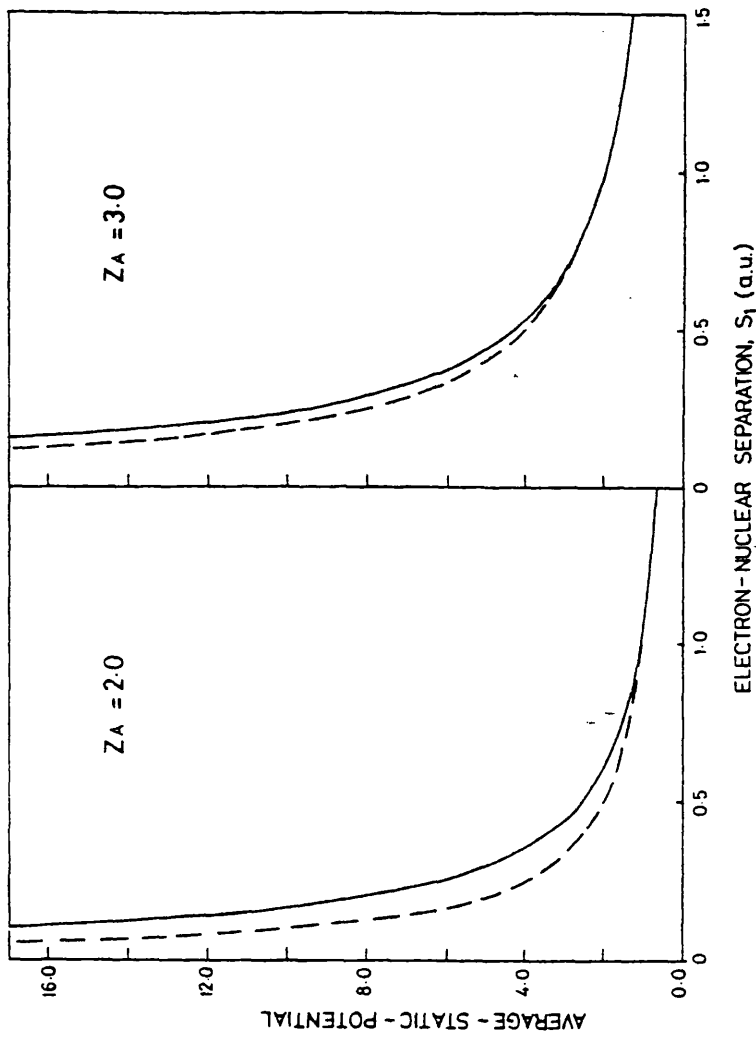


Figure 3.5 The theoretical total electron-capture cross-sections,  $Q$ , for  $\text{Li}^{2+}$  ions incident on hydrogen (see reaction (3.5.5)) compared with the experimental data of Shah, Goffe and Gilbody<sup>18</sup>. The total cross-sections,  $Q_1$  (full line) and  $Q_2$  (broken line), corresponding to the two forms of  $V_{1,2}^1$  i.e.  $V_1 = (Z_A - 1)/s + \exp(-2Z_A s) \cdot (Z_A + s^{-1})$  and  $V_2 = (Z_A - 1)/s$ , as defined in Chapter 3.3, equation (3.3.4), are as listed in Tables 3.6 and 3.7, respectively. The total cross-section  $Q$  is evaluated using  $Q = \sigma(1s) + \sigma(2s) + \sigma(2p) + 2.081(\sigma(3s) + \sigma(3p) + \sigma(3d))$ .



**Figure 3.6** Plots of the average-static-potential  $V_1 = (Z_A - 1)/S + \exp(-2Z_A S) / (Z_A + S^{-1})$  as a function of the electron-nuclear separation,  $S$ , for  $Z_A = 2.0$  and  $Z_A = 3.0$ . Also shown for comparison (broken line) is a plot of the perfect-screening potential  $V_2 = (Z_A - 1)/S$ .

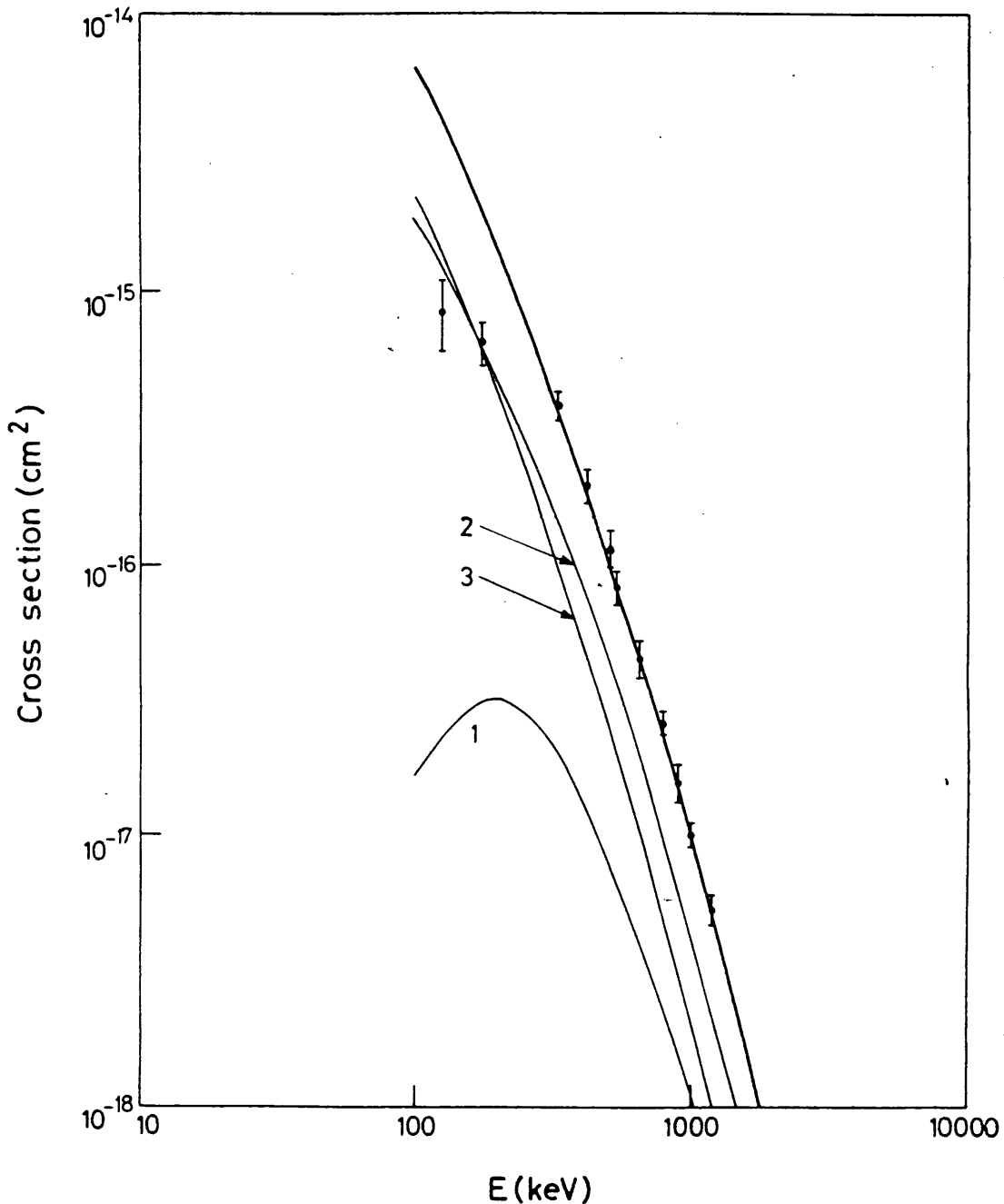


Figure 3.7 The theoretical total electron-capture cross-sections,  $\sigma_1$ , for  $\text{Li}^{2+}$  ions incident on hydrogen (see reaction (3.5.5)) plus the individual cross-section curves  $\sigma(n=1)$ ,  $\sigma(n=2)$  and  $\sigma(n=3)$  for capture into the individual quantum levels  $n=1$ , 2 and 3, when setting  $V_{1,2}^1$  equal to the average-static-potential as defined in Chapter 3.3 equation (3.3.5). The total and individual cross-sections are as listed in Table 3.6 and the experimental points are those of Shah, Goffe and Gilbody<sup>18</sup>.

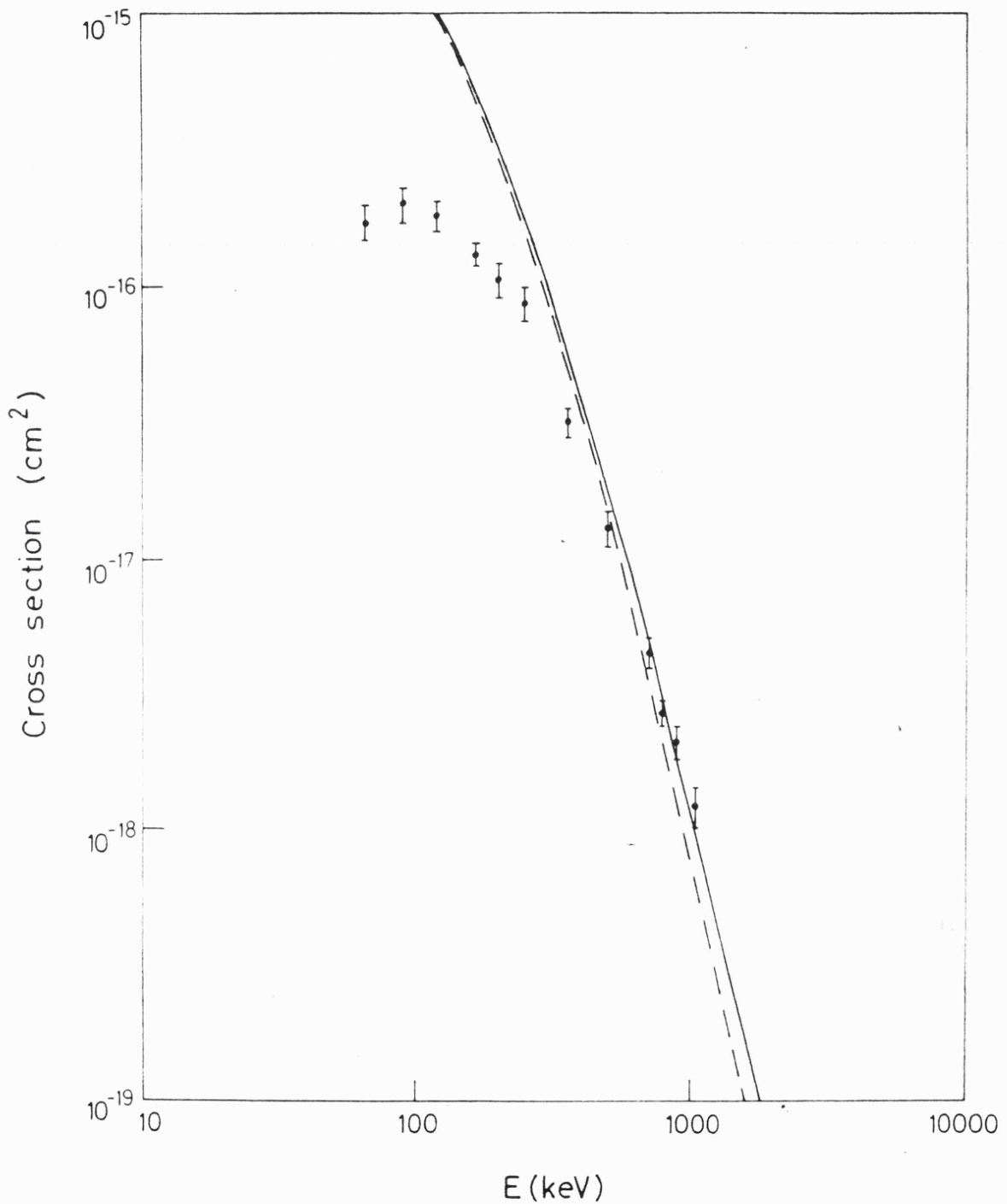


Figure 3.8 The theoretical total electron-capture cross-sections,  $\sigma$ , for  $\text{Li}^+$  ions incident on hydrogen (see reaction (3.5.14) compared with the experimental data of Shah, Goffe and Gilbody<sup>16</sup>. The total cross-sections,  $\sigma_1$  (full line) and  $\sigma_2$  (broken line), corresponding to the two forms of  $V_{1,2,3}^0$ , as defined in equations (3.5.20) and (3.5.21), are as listed in Tables 3.8 and 3.9, respectively.



### References - Part 3

1. J.B. Hasted, 'Physics of Atomic Collisions', (Butterworths Second Edition, 1972), P. 648
2. M.R.C. McDowell and J.P. Coleman, 'Introduction to the Theory of Ion-Atom Collisions', (North-Holland, 1970), P. 419
3. H.S.W. Massey and R.H. Smith, Proc. Roy. Soc. A142, 142 (1933)
4. C.F. Barnett, Proc. 9th Int. Conf. on Physics of Electronic and Atomic Collisions', Ed., J.S. Risley and R.I. Geballe, (Seattle: Univ. Washington Press), 846 (1976)
5. R.E. Olson and A. Salop, Phys. Rev. A. 16, 531 (1977)
6. W.D. Watson, Rev. Mod. Phys. 48, 513 (1976)
7. H.C. Brinkman and H.A. Kramers, Proc. Acad. Sci. Amsterdam 33, 973 (1930)
8. Dž Belkić and R. McCarroll, J. Phys. B. 10, 1933 (1977)
9. G.W. McClure, Phys. Rev. 166, 22 (1968)
10. R.A. Mapleton, Proc. Phys. Soc. 85, 841 (1965)
11. R. McCarroll, Proc. Roy. Soc. A. 264, 547 (1961)
12. R.K. Janev and A. Salin, J. Phys. B. 4, L127 (1971)
13. R.K. Janev and A. Salin, Fizika. 4, 165 (1972)
14. J.C. Moore and K.E. Banyard, J. Phys. B. 11, 1613 (1978)
15. A. Shakeshaft, J. Phys. B. 7, 1734 (1974)
16. Dž Belkić, J. Phys. B. 10, 3491 (1977)
17. R.N.Hill, J. Maths. Phys. 18, 2316 (1977)
18. M.B. Shah, T.V. Goffe and H.B. Gilbody, J. Phys. B. 11, L233 (1978)
19. R.F. Curl and C.A. Coulson, J. Phys. B. 1 325 (1968)
20. A.W. Weiss, Phys. Rev. 122, 1826 (1961)
21. S. Chandrasekhar, Astrophys. J. 100, 176 (1944)
22. K.E. Banyard and C.E. Reed, J. Phys. B. 11, 2957 (1978)
23. J.R. Oppenheimer, Phys. Rev. 31, 349 (1928)
24. E. Clementi and C. Roetti, Atom. Data Nucl. Data Tables 14 (New York, London: Academic Press) (1974)

25. M. Cohen and R.P. McEachran, Proc. Phys. Soc. 92, 37 (1967)
26. M. Cohen and R.P. McEachran, Proc. Phys. Soc. 92, 539 (1967)
27. C.L. Pekeris, Phys. Rev. 115, 1216 (1959)  
       - Phys. Rev. 126, 143 (1962)  
       - Phys. Rev. 126, 1470 (1962)
28. S. Hughes, 'A User's Guide to the Algebra Manipulation Program CAOS', Leicester University (1979)
29. A. Messiah, 'Quantum Mechanics'. (North-Holland Publishing Company) Vol. 1 (1965)
30. C.E. Moore, 'Atomic Energy Levels (As Derived from the Analysis of Optical Spectra)'. Circular 467 of the National Bureau of Standards (United States Department of Commerce) Vol. 1  $^1\text{H}$ - $^{23}\text{V}$ , (1949)
31. K.E. Banyard and B.J. Szuster, Phys. Rev. A. 16, 129 (1977)
32. D.S.F. Crothers and N.R. Todd, J. Phys. B. 13, 2277 (1980)
33. K.E. Banyard and G.W. Shirtcliffe, J. Phys. B. 12, 3247 (1979)
34. Dž Belkić, R. Gayet and A. Salin, Physics Reports (Review Section of Physics Letters). 56, 281 (1979)

APPENDIX A

## APPENDIX A

### The formal quantal derivation of the CDW transition amplitude

The most conventional formulation of the charge-exchange problem is by means of the Lippman-Schwinger development in which the total state wavefunction is expressed in terms of the Greens function operator and the unperturbed eigenfunctions of the system. The validity of such an approach was questioned by Aaron et al<sup>1</sup>, who proved the divergence of the Born series for rearrangement collisions. However, Dettman and Leibfried<sup>2</sup> and Corbett<sup>3</sup> have shown that the divergence of the operator series does not necessarily imply the divergence for both vector series and physical matrix element series. Dodd and Greider<sup>4</sup> have derived a three body theory for rearrangement collisions and provided a possible way of preventing the divergence of the Born operator series in the important case when the mass of one particle is much less or much greater than the other two. Exploiting the work of Dodd and Greider<sup>4</sup>, Gayet<sup>5</sup> has shown that, by a suitable choice of distorting potentials, the calculation of a second order charge-exchange cross-section becomes tractable, and that the expression for the transition amplitude can be shown to be equivalent to that given by the continuum distorted wave method of Cheshire<sup>6</sup> derived within the impact parameter scheme.

Thus, in this appendix we give a description of the wave parameter presentation of the continuum distorted wave method as presented by Gayet<sup>5</sup>. Where appropriate, a comparison is made between the wave parameter presentation and the more transparent impact parameter presentation of the continuum distorted wave method as given in Chapter 1.2.

A1 Formal theory for rearrangement collisions

Let  $\alpha$ ,  $\beta$  and  $\gamma$  be three particles interacting through two body potentials  $V_\alpha$ ,  $V_\beta$ ,  $V_\gamma$  where  $V_i$  is the interaction between the two particles not labelled by  $i$ ; we consider the process

$$\alpha + (\beta + \gamma) \longrightarrow (\alpha + \gamma) + \beta \quad \text{A1.1}$$

with complete hamiltonian

$$H = K + V_\alpha + V_\beta + V_\gamma, \quad \text{A1.2}$$

where  $K$  is the kinetic energy operator for the relative motion of the three particles.

The unperturbed hamiltonian for the entrance channel is

$$H_\alpha = K + V_\alpha = H - v_\alpha, \quad \text{A1.3}$$

where  $v_\alpha$  is the perturbing potential due to the incident projectile.

Conversely for the exit channel we have

$$H_\beta = K + V_\beta = H - v_\beta, \quad \text{A1.4}$$

where  $v_\beta$  is the perturbation due to the remaining target nucleus  $\beta$ .

If  $\Phi_\alpha$  and  $\Phi_\beta$  are the respective eigenfunction of  $H_\alpha$  and  $H_\beta$  with the same eigenvalue  $E$ , then the exact transition amplitude for the process

A1.1 is given by

$$T_{\alpha\beta} = \langle \Phi_\beta | v_\beta | \Psi_\alpha^+ \rangle = \langle \Psi_\beta^- | v_\alpha | \Phi_\alpha \rangle. \quad \text{A1.5}$$

The total wavefunctions  $\Psi_\alpha^+$  and  $\Psi_\beta^-$  are eigenfunctions of the total hamiltonian with eigenvalue  $E$  and can be shown to satisfy

$$\Psi_\alpha^+ = \Omega_\alpha^+ \Phi_\alpha; \quad \Psi_\beta^- = \Omega_\beta^- \Phi_\beta, \quad \text{A1.6}$$

where the Møller operator  $\Omega^\pm$  is defined as

$$\Omega_\alpha^\pm = \lim_{t \rightarrow \mp \infty} e^{iHt} e^{-iH_\alpha t}. \quad \text{A1.7}$$

Using the limiting functions of Gell-Mann and Goldberger<sup>7</sup>,  $\Psi_\alpha^+$  and

$\Psi_\beta^-$  can be shown to satisfy

$$|\Psi_{\alpha}\rangle = (1 + G^+ v_{\alpha}) |\Phi_{\alpha}\rangle \quad A1.8$$

and

$$|\Psi_{\beta}\rangle = (1 + G^- v_{\beta}) |\Phi_{\beta}\rangle \quad A1.9$$

The Greens function  $G^{\pm}$  is given by

$$G^{\pm} = (E - H \pm i\epsilon)^{-1}, \quad (\epsilon > 0) \quad A1.10$$

where the limit  $\epsilon \rightarrow 0$  is to be taken eventually.

Therefore, A1.5 may be written as

$$T_{\alpha\beta} = \langle \Phi_{\beta} | U^+ | \Phi_{\alpha} \rangle \quad A1.11$$

with

$$U^+ = v_{\beta} (1 + G^+ v_{\alpha}), \quad A1.12$$

where  $U^+$  is called the transition operator. This can be shown to satisfy the integral equation

$$U^+ = v_{\beta} + U^+ G_{\alpha}^+ v_{\alpha}, \quad A1.13$$

where

$$G_{\alpha}^+ = (E - H_{\alpha} + i\epsilon)^{-1} \quad A1.14$$

At this point Greider and Dodd<sup>8</sup> introduces the so-called distorting potentials  $W_{\alpha}$  and  $W_{\beta}$  in order to simplify eventually the integrals involving the potentials  $v_{\alpha}$  and  $v_{\beta}$ , but also with the hope that they would be able to prevent the divergence of the operator Born series.

With these potentials are associated the Green functions

$$\mathcal{G}_{\alpha}^+ = (E - H_{\alpha} - W_{\alpha} + i\epsilon)^{-1} \quad A1.15$$

$$\mathcal{G}_{\beta}^- = (E - H_{\beta} - W_{\beta} - i\epsilon)^{-1}, \quad A1.16$$

and the corresponding wave operators

$$\omega_{\alpha}^+ = 1 + \mathcal{G}_{\alpha}^+ W \quad A1.17$$

$$\omega_{\beta}^- = 1 + \mathcal{G}_{\beta}^- W, \quad A1.18$$

from which Greider and Dodd<sup>8</sup> derive the transition operator  $U^+$  which satisfies the integral equation

$$U^+ = \left\{ \omega_{\beta}^{-*} (v_{\beta} - W_{\beta}^*) + U^+ G_{\alpha}^+ (v_{\alpha} - W_{\alpha}) \right\} \omega_{\alpha}^+ , \quad A1.19$$

provided<sup>8</sup> that  $W_{\beta}$  does not lead to the rearrangement state  $\Phi_{\alpha}$ .

Unfortunately Greider and Dodd<sup>8</sup> found that equation A1.19 always contains disconnected diagrams, and as a consequence diverges. Thus to overcome this Dodd and Greider<sup>4</sup> introduce an intermediate channel 'x' corresponding to a perturbing potential  $v_x$  with an associated Greens function

$$\mathcal{G}_x^+ = (E - H + v_x + i\varepsilon)^{-1} , \quad A1.20$$

and showed that  $U^+$  satisfies the integral equation

$$U^+ = \left[ \omega_{\beta}^{-*} (v_{\beta} - W_{\beta}^*) \left\{ 1 + \mathcal{G}_x^+ (v_{\alpha} - W_{\alpha}) \right\} + U^+ G_{\alpha}^+ v_x \mathcal{G}_x^+ (v_{\alpha} - W_{\alpha}) \right] \omega_{\alpha}^+ , \quad A1.21$$

which is useful if the so-called kernel of the integral equation for  $U^+$ , namely

$$K = G_{\alpha}^+ v_x \mathcal{G}_x^+ (v_{\alpha} - W_{\alpha}) \omega_{\alpha}^+ , \quad A1.22$$

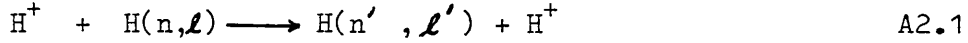
does not diverge as a result of disconnected diagrams, and the equations involving  $\mathcal{G}_x^+$  and  $G_{\alpha}^+$  are manageable. The first condition will be satisfied if, for example,  $v_x$  is a two-body potential which does not appear in  $v_{\alpha} - W_{\alpha}$ , and the second condition is found to be fulfilled in the limit of  $M_{\alpha,\beta} \gg M_{\gamma}$ , due to the equations becoming separable with respect to the electron position coordinates and the internuclear separation vector.

Under these conditions a meaningful first order approximation to  $T_{\alpha\beta}^+$  is given by

$$T_{\alpha\beta}^+ = \left\langle \Phi_{\beta} \left| \omega_{\beta}^{-*} (v_{\beta} - W_{\beta}^*) \left\{ 1 + \mathcal{G}_x^+ (v_{\alpha} - W_{\alpha}) \right\} \omega_{\alpha}^+ \right| \Phi_{\alpha} \right\rangle . \quad A1.23$$

A2 Application to proton-hydrogen charge transfer

Following Gayet<sup>5</sup> we now proceed to derive a solution to  $T_{\alpha\beta}^+$  (A1.23) for the general proton-hydrogen charge transfer reaction



as follows:

Let  $\underline{r}_1$ ,  $\underline{r}_2$  and  $\underline{r}_3$  be the respective position vectors of proton 1, electron 2 and proton 3, for which the electron is initially bound to proton 1, with respect to an arbitrary origin. The scattering problem can now be solved with respect to the more convenient coordinates (see Figure A.1),

$$\begin{aligned} \underline{x} &= \underline{r}_2 - \underline{r}_1 & ; & & \underline{r}_\alpha &= \underline{r}_3 - \frac{M\underline{r}_1 + \underline{r}_2}{M+1} \\ \underline{R} &= \underline{r}_3 - \underline{r}_1 & & & & \\ \underline{s} &= \underline{r}_2 - \underline{r}_3 & ; & & \underline{r}_\beta &= \underline{r}_1 - \frac{M\underline{r}_3 + \underline{r}_2}{M+1} , \end{aligned} \quad A2.2$$

where  $\underline{x}$  and  $\underline{s}$  are the electron position coordinates,  $\underline{R}$  the internuclear separation vector, and  $\underline{r}_\alpha$  and  $\underline{r}_\beta$  are the position vectors of the hydrogen centre of mass with respect to the proton in the incident and exit channel respectively; M is the ratio of the proton mass to the electron mass. Identifying particles 1, 2, and 3 with  $\beta$ ,  $\gamma$  and  $\alpha$  it is readily seen that

$$v_\alpha = -\frac{1}{s} + \frac{1}{R} \quad \text{and} \quad v_\beta = -\frac{1}{x} + \frac{1}{R} , \quad A2.3$$

and the unperturbed solutions for the entrance and exit channels are

$$\Phi_\alpha = \phi_\alpha(\underline{x}) \exp(i\underline{k}_\alpha \cdot \underline{r}) \quad A2.4$$

and 
$$\Phi_\beta = \phi_\beta(\underline{s}) \exp(-i\underline{k}_\beta \cdot \underline{r}) , \quad A2.5$$

where  $\phi_\alpha(\underline{x})$  and  $\phi_\beta(\underline{s})$  are respectively the initial and final bound state solutions. In order to evaluate  $T_{\alpha\beta}^+$  given by expression A1.23 let us first derive a solution for say  $|\zeta^+\rangle$  given by

$$|\xi_\alpha^+\rangle = \{1 + \mathcal{G}_X^+(v_\alpha - W_\alpha)\} \omega_\alpha^+ |\Phi_\alpha\rangle \quad . \quad \text{A2.6}$$

Setting  $|\chi_\alpha^+\rangle = |\omega_\alpha^+ |\Phi_\alpha\rangle$  it is clear from the expression for  $\omega_\alpha^+$  that  $|\chi_\alpha^+\rangle$ , in the limit of  $\epsilon = 0$ , satisfies the equation

$$(E - H_\alpha - W_\alpha) |\chi_\alpha^+\rangle = 0 \quad . \quad \text{A2.7}$$

Gayet<sup>5</sup> now chooses  $W_\alpha$  such that  $\chi_\alpha^+$  is of the form

$$|\chi_\alpha^+\rangle = |\phi_\alpha(\underline{x}) f(\underline{r}_\alpha)\rangle, \quad \text{A2.8}$$

where  $f(\underline{r}_\alpha)$  has the asymptotic form  $\exp(i\mathbf{k}_\alpha \cdot \underline{r}_\alpha)$ .

Since we have that

$$(E - H_\alpha) |\Phi_\alpha\rangle = 0, \quad \text{A2.9}$$

an obvious choice for  $W_\alpha$  is  $W_\alpha = 0$ . Otherwise  $W_\alpha$  must be chosen such that all potentials depending on  $\underline{r}_\alpha$  (or  $\underline{R}$  in the limit  $M \gg 1$ ) decrease more rapidly than  $\underline{r}_\alpha^{-1}$  at infinity.

However, the general solution for  $\xi^+$  is given by

$$|\xi_\alpha^+\rangle = \{1 + \mathcal{G}_X^+(v_\alpha - W_\alpha)\} |\chi_\alpha^+\rangle \quad \text{A2.10}$$

such that in the limit  $\epsilon = 0$  we have

$$(E - H + v_X) |\xi_\alpha^+\rangle = (E - H + v_X + v_\alpha - W_\alpha) |\chi_\alpha^+\rangle \quad . \quad \text{A2.11}$$

Since  $\chi_\alpha^+$  satisfies equation A2.7, equation A2.11 reduces to

$$(E - H + v_X) |\xi_\alpha^+\rangle = v_X |\chi_\alpha^+\rangle \quad . \quad \text{A2.12}$$

The main feature in Gayet's work is the choice made for  $v_X$  such that

$$v_X |\chi_\alpha^+\rangle = 0, \quad \text{A2.13}$$

and that, as a result, the remaining equation for  $\xi_\alpha^+$ , namely

$$(E - K + \frac{1}{x} + \frac{1}{s} - \frac{1}{R} + v_X) |\xi_\alpha^+\rangle = 0, \quad \text{A2.14}$$

becomes solvable. Writing  $\xi_\alpha^+$  in the form

$$|\xi_\alpha^+\rangle = |\phi_\alpha(\underline{x}) h^+\rangle, \quad \text{A2.15}$$

where  $\phi_\alpha(\underline{x})$  satisfies

$$(E_\alpha - K + \frac{1}{x}) | \phi_\alpha(\underline{x}) \rangle = 0, \quad \text{A2.16}$$

then the equation for  $h^+$  becomes

$$(E' - K + \frac{1}{s} - \frac{1}{R}) h^+ + \frac{M+1}{M} \nabla_x \phi_\alpha(\underline{x}) \cdot \nabla_x h^+ + v_x(\phi_\alpha(\underline{x}) h^+) = 0, \quad \text{A2.17}$$

where  $E' = E - E_\alpha$  and  $E_\alpha$  is the energy of the bound state.

Thus,  $E'$  is the kinetic energies of the system. Gayet choses  $v_x$  as an operator such that when applied to an arbitrary function  $y(x, \underline{r}_\alpha)$ , or  $y(s, \underline{r}_\beta)$ , the following relationship holds

$$v_x y = -\frac{M+1}{M} \nabla_x \phi_\alpha(\underline{x}) \cdot \nabla_x \left( \frac{y}{\phi_\alpha(\underline{x})} \right). \quad \text{A2.18}$$

With this form for  $v_x$  equation A2.13 is satisfied and equation A2.17 reduces to

$$(E' - K + \frac{1}{s} - \frac{1}{R}) h^+ = 0. \quad \text{A2.19}$$

For  $M \gg 1$  we have that  $\underline{R} \simeq -\underline{r}_\beta$  and equation A2.19 becomes separable.

The kinetic energy operator  $K$  may be written in two forms

$$K = -\frac{1}{2\mu} \nabla_{\underline{r}_\alpha}^2 - \frac{M+1}{M} \nabla_{\underline{x}}^2 = -\frac{1}{2\mu} \nabla_{\underline{r}_\beta}^2 - \frac{M+1}{M} \nabla_{\underline{s}}^2, \quad \text{A2.20,21}$$

where  $\mu = M(M+1)/(2M+1)$  is the reduced mass of the whole system relative to the centre of mass of the electron and of either proton 1 or 3. The general solution to equation A2.19 is therefore given by the product of two coulomb wavefunctions. Thus we have

$$\begin{aligned} h(\underline{s}, \underline{r}_\beta)^+ &= N_\beta^+ N_s^+ \exp(i\underline{k}_1 \cdot \underline{r}_\beta + i\underline{k}_2 \cdot \underline{s}) \\ &\times F\left(-\frac{i\mu}{k_1}; 1; i\underline{k}_1 \underline{r}_\beta - i\underline{k}_1 \cdot \underline{r}_\beta\right) \\ &\times F\left(+\frac{i}{k_2}; 1; i\underline{k}_2 \underline{s} - i\underline{k}_2 \cdot \underline{s}\right). \end{aligned} \quad \text{A2.22}$$

For  $M \gg 1$  we have that,

$$k_1 = - \frac{M}{M+1} \frac{k_\alpha}{\mu} \xrightarrow{M \rightarrow \infty} - \frac{k_\alpha}{\mu} \quad \text{A2.23}$$

and

$$k_2 = - \frac{M}{(M+1)} \frac{k_\alpha}{\mu} \xrightarrow{M \rightarrow \infty} - \frac{k_\alpha}{\mu} = -v, \quad \text{A2.24}$$

and  $h^+$  may be written as

$$h^+(\underline{s}, \underline{r}_\beta) = \left| \Gamma(1+i\nu) \right|^2 \exp(i \underline{k}_\alpha \cdot \underline{r}_\alpha) F(i\nu; 1; i\nu s + i\nu \underline{s}) \\ \times F(-i\nu; 1; i k_\beta r_\beta + i \underline{k}_\beta \cdot \underline{r}_\beta) \quad (\nu=1/v) \quad \text{A2.25}$$

At this point it is interesting to note that the solution obtained for  $|\xi_\alpha^+\rangle = |\phi_\alpha(\underline{x})h^+\rangle$  is, in the limit of  $M \rightarrow \infty$ , analogous to the solution obtained for our continuum distorted wave functions  $\Omega_i \mathcal{L}'_i$  obtained within the impact parameter formulation presented in Chapter 1.2. The choice made for  $v_x$  corresponds to neglecting the right-hand side of equation (1.2.31) which is done to obtain a first order approximation  $\mathcal{L}'_i$  to the exact solution  $\mathcal{L}_i$ .

The calculation of  $T_{\alpha\beta}^+$  given by expression A1.23 will now be complete upon deriving a solution for  $\omega_\beta^- |\Phi_\beta\rangle$  since we then have

$$T_{\alpha\beta}^+ = \langle \chi_\beta^- | v_\beta - W_\beta | \xi_\alpha^+ \rangle \quad \text{A2.26}$$

where

$$|\chi_\beta^- \rangle = \omega_\beta^- |\Phi_\beta \rangle \quad \text{A2.27}$$

The solution to  $\chi_\beta^-$  will obviously depend on the choice made for  $W_\beta$  and, as in the CDW method of Cheshire<sup>6</sup>, Gayet proceeds to make a choice for  $W_\beta$  such that  $\chi_\beta^-$  represents a continuum distorted wave.

From the definition of  $\omega_\beta^-$  in A1.18 we have that, in the limit of  $\epsilon = 0$ ,  $|\chi_\beta^- \rangle$  satisfies the equation

$$(E - K + \frac{1}{s} - v_\beta + U_\beta) |\chi_\beta^- \rangle = (E - H_\beta) |\Phi_\beta \rangle, \quad \text{A2.28}$$

where

$$U_\beta = v_\beta - W_\beta \quad \text{A2.29}$$

Writing  $|\chi_{\beta}^{-}\rangle$  in the form  $|\phi_{\beta}(\underline{s}) g^{-}\rangle$  and noting that  $\phi_{\beta}$  is an eigenfunction of  $H_{\beta}$  with eigenvalue  $E$  we find that, in the same way as for  $\xi_{\alpha}^{+}$ , equation A2.28 reduces to

$$\begin{aligned} (E'' - K + \frac{1}{x} - \frac{1}{R}) g^{-} + \frac{M+1}{M} \nabla_{\underline{s}} \phi_{\beta}(\underline{s}) \cdot \nabla_{\underline{s}} g^{-} \\ + U_{\beta}(\phi_{\beta}(\underline{s})g^{-}) = 0 \end{aligned} \quad \text{A2.30}$$

Thus, if  $U_{\beta}$  is chosen either as a distorting potential

$$U_{\beta} = -\frac{M+1}{M} \nabla_{\underline{s}} \log_e \phi_{\beta}(\underline{s}) \cdot \nabla_{\underline{s}} \log_e g^{-}, \quad \text{A2.31}$$

or as an operator, analogous to  $v_x$ ,

$$U_{\beta}^{\text{op}} = -\frac{M+1}{M} \nabla_{\underline{s}} \phi(\underline{s}) \cdot \nabla_{\underline{s}} \left( \frac{1}{\phi_{\beta}(\underline{s})} \right), \quad \text{A2.32}$$

then the solution for  $g^{-}$  is determined exactly in the same way as for  $h^{+}$ . Thus, in the limit  $M \gg 1$ , we have

$$\begin{aligned} g^{-}(x, \underline{r}_{\alpha}) = |\Gamma(1+i\nu)|^2 \exp(-ik_{\beta} \cdot \underline{r}_{\beta}) F(-i\nu; 1; -ivx - i\nu \cdot \underline{x}) \\ \times F(i\nu; 1; -ik_{\alpha} \cdot \underline{r}_{\alpha} - ik_{\alpha} \cdot \underline{r}_{\alpha}) \end{aligned} \quad \text{A2.33}$$

Clearly Gayet's solution for  $|\chi_{\beta}^{-}\rangle = |\phi_{\beta}(\underline{s}) g^{-}\rangle$  is comparable to the distorted wave solution  $\chi_f = \Omega_f \mathcal{L}'_f$  given in equation (1.2.45) of Chapter 1.2, and the choice made for  $W_{\beta}$  is analogous to the choice made for the distorting potential  $U_f$  in equation (1.2.47), with  $U_{\beta}^{\text{op}}$  corresponding to the perturbing potential operator  $A_f$  defined in equation (1.2.49) of Chapter 1.2.

Consequently we may now write down the final expression for the transition amplitude, which is analogous to the expression for  $b_{if}$  given in equation (1.2.52). Therefore we have

$$T_{\alpha\beta}^{+} = \langle \chi_{\beta}^{-} | (V_{\beta} - W_{\beta}) | \xi_{\alpha}^{+} \rangle, \quad \text{A2.34}$$

$$= \langle \chi_{\beta}^{-} | U_{\beta} | \xi_{\alpha}^{+} \rangle, \quad \text{A2.35}$$

$$\begin{aligned}
&= - \left| \Gamma(1+i\nu) \right|^4 \int d\underline{s} d\underline{r}_\beta \exp(i\underline{k}_\alpha \cdot \underline{r}_\alpha + i\underline{k}_\beta \cdot \underline{r}_\beta) \phi_\alpha(\underline{x}) \\
&\quad \times F \left[ i\nu; 1; i(\underline{v}\underline{s} + \underline{v} \cdot \underline{s}) \right] F \left[ -i\nu; 1; i(\underline{k}_\beta \underline{r}_\beta + \underline{k}_\beta \cdot \underline{r}_\beta) \right] \\
&\quad \times \nabla_{\underline{s}} \phi_\alpha^*(\underline{s}) \cdot \nabla_{\underline{s}} \left\{ F \left[ i\nu; 1; i(\underline{v}\underline{x} + \underline{v} \cdot \underline{x}) \right] \right. \\
&\quad \quad \left. \times F \left[ -i\nu; 1; i(\underline{k}_\alpha \underline{r}_\alpha + \underline{k}_\alpha \cdot \underline{r}_\alpha) \right] \right\} . \quad \text{A2.36}
\end{aligned}$$

If now we make the impact parameter assumption that  $M \rightarrow \infty$  it follows that

$$\underline{r}_\alpha \rightarrow -\underline{r}_\beta \rightarrow \underline{R} = \underline{b} + \underline{v}t , \quad \text{A2.37}$$

where  $\underline{b}$  is the impact parameter such that  $\underline{b} \cdot \underline{v} = 0$ . McCarroll and Salin<sup>9</sup> have showed that in the limit of  $M \rightarrow \infty$  we can replace the product of the hyper-geometric functions involving  $\underline{r}_\alpha$  and  $\underline{r}_\beta$  by  $e^{\pi\nu} (\mu\nu)^{2i\nu}$ . Introducing also the transverse momentum transfer vector  $\underline{\eta}$  ( $\underline{\eta} \cdot \underline{v} = \underline{\eta} \cdot \underline{b} = 0$ ), and the total momentum transfer defined as

$$\underline{k}_\alpha - \underline{k}_\beta = - \frac{(E_\alpha - E_\beta)}{v^2} \underline{v} - \underline{\eta} , \quad \text{A2.38}$$

it can be shown that  $T_{\alpha\beta}^+$  reduces to

$$\begin{aligned}
T_{\alpha\beta}^+ &= \left| \Gamma(1-i\nu) \right|^2 e^{\pi\nu} (\mu\nu)^{2i\nu} \int d\underline{s} d\underline{R} b^{2i\nu} \exp \left\{ - \left( \frac{1}{2} + \frac{E_\alpha - E_\beta}{v^2} \right) i\nu^2 t - i\underline{\eta} \cdot \underline{b} - i\underline{v} \cdot \underline{s} \right\} \\
&\quad \times \phi_\alpha(\underline{x}) F \left[ i\nu; 1; i(\underline{v}\underline{s} + \underline{v} \cdot \underline{s}) \right] \times \nabla_{\underline{s}} \phi_\beta^*(\underline{s}) \cdot \nabla_{\underline{s}} F \left[ i\nu; 1; i(\underline{v}\underline{x} + \underline{v} \cdot \underline{x}) \right] . \quad \text{A2.39}
\end{aligned}$$

The total cross section is then given by

$$Q_{\alpha\beta} = \int \left| \frac{T_{\alpha\beta}(\underline{\eta})}{2\pi v} \right|^2 d\underline{\eta} . \quad \text{A2.40}$$

The integrand can be shown to be equivalent to that given by Cheshire<sup>6</sup> who, using the impact-parameter formalism, obtained a total cross-section  $Q_{if}$  in the form

$$Q_{if} = \frac{1}{(2\pi)^2} \int |R(\underline{\eta})|^2 d\underline{\eta} . \quad \text{A2.41}$$



$$a_{\alpha\beta}^+ = \frac{1}{(2\pi)^2} \int \frac{T_{\alpha\beta}^+}{v} e^{i\underline{n} \cdot \underline{b}} d\underline{n} . \quad \text{A2.47}$$

Comparing equation A2.44 and A2.45 we see that  $a_{if} = -i a_{\alpha\beta}^+$ , and therefore

$$R(\underline{n}) = -i \frac{T_{\alpha\beta}^+(\underline{n})}{v} . \quad \text{A2.48}$$

Consequently the wave and impact parameter treatments are shown to be equivalent to within an arbitrary phase factor  $e^{i\pi}$  in the transition or scattering amplitudes.

It is important to note that on forming  $|a_{if}|^2$  in equation A2.42 the factor  $(\mu bv)^{2iv}$  disappears and thus may be omitted in the expression for  $Q_{if}$ , or  $Q_{\alpha\beta}$ , indicating that the internuclear potential does not contribute to the capture process when it is treated exactly to first order in  $1/M$  or in the limit as  $M \rightarrow \infty$ . This result was examined in detail by Drisko<sup>11</sup> who showed that the contribution from the proton-proton potential, which plays an important role in the first Born approximation, is exactly cancelled (to order  $1/M$ ) in the high-energy limit by two of the second Born approximation terms.

Summarising, we note that the essential feature of Gayet's work is in the choice for the perturbing potential  $v_x$ , which was chosen to contain the potential operator  $\nabla_{\underline{x}} \phi_{\alpha}(\underline{x}) \cdot \nabla_{\underline{x}}$  which only depends upon  $\underline{x}$  while  $v_{\alpha} - W_{\alpha}$  depends only on  $\underline{s}$  and  $\underline{R}$ . Thus the conditions, originally laid down by Dodd and Greider<sup>4</sup>, concerning the avoidance of disconnected terms in the kernel  $\mathcal{K}$  of the integral equation for the transition operator  $U^+$  written in A1.21 are satisfied. Thus Gayet<sup>5</sup> has shown that the continuum distorted wave approximation leads to a second order method whose transition amplitude is a meaningful first order approximation in a perturbation series.

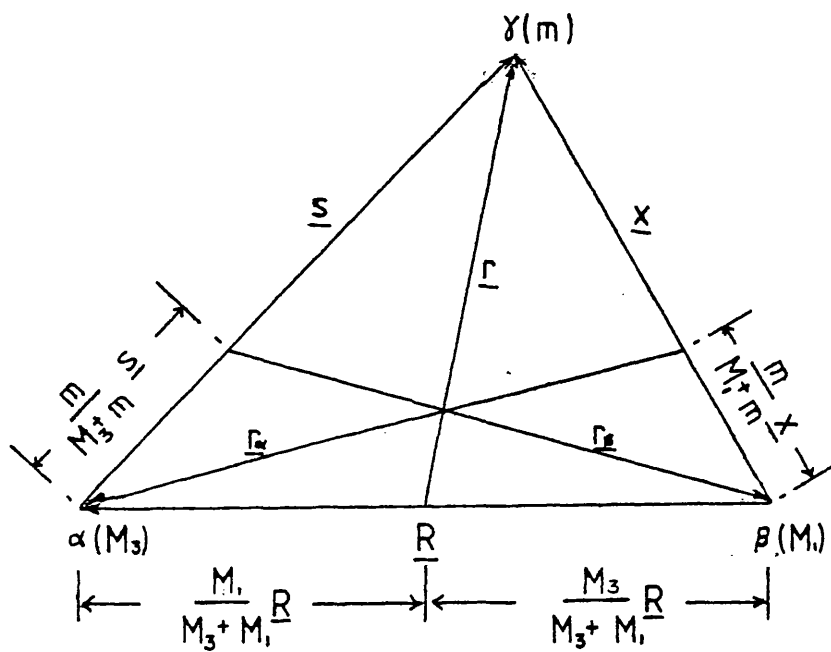


Figure A1 The coordinate system for the reaction  $\alpha + (\beta + \gamma) \rightarrow (\alpha + \gamma) + \beta$ , where  $\alpha$ ,  $\beta$  and  $\gamma$  are particles of mass  $M_3$ ,  $M_1$  and  $m$  respectively.

References - Appendix A

1. R. Aaron, R.D. Amado and B.W. Lee, Phys. Rev. 121, 319 (1961)
2. K. Dettmann and G. Leibfreid, Phys. Rev. 148, 1271 (1966)
3. J.V. Corbett, J. Math. Phys. 9, 891 (1968)
4. L.R. Dodd and K.R. Greider, Phys. Rev. 146, 675 (1966)
5. R. Gayet, J. Phys. B. 5, 483 (1972)
6. I.M. Cheshire, Proc. Phys. Soc. 84, 89 (1964)
7. M. Gell-Mann and M.L. Goldberger, Phys. Rev. 91, 398 (1953).  
Limiting functions are also given on p. 270 of reference 12.
8. K.R. Greider and L.R. Dodd, Phys. Rev. 146, 671 (1966)
9. R. McCarroll and A. Salin, J. Phys. B. 1, 163 (1968)
10. Dž Belkić, R. Gayet and A. Salin, Physics Reports (Review Section of Physics Letters) 56, 281 (1979)
11. R.M. Drisko, Thesis, Carnegie Institute of Technology (1955)
12. M.C.R. McDowell and J.P. Coleman, Introduction to the Theory of Ion Atom Collisions (North-Holland, 1970)

## Electron capture from lithium and its ions by high-energy protons

K E Banyard and G W Shirtcliffe

Department of Physics, University of Leicester, Leicester, England

Received 19 February 1979, in final form 3 April 1979

**Abstract.** The continuum-distorted wave (CDW) method is used to calculate cross sections for electron capture by fast protons from the lithium atom and its related positive ions. With the exception of  $\text{Li}^{2+}(1^2\text{S})$ , each target electronic state is described by a Hartree-Fock wavefunction. The capture states considered are  $(nl) \equiv 1s, 2s$  and  $2p$  and the proton energy range is  $200 \text{ keV} \leq E \leq 10 \text{ MeV}$ , the lower limit being chosen to be roughly appropriate for a CDW description of capture from the lithium ions. For the lithium atom, capture can occur from either the K or L shell and the resulting ion can exist either in its ground state  $1^1\text{S}$  or in one of the excited states  $2^1\text{S}$  or  $2^3\text{S}$ ; cross sections are tabulated for each of these three states for capture into the above hydrogen levels  $(nl)$ . Results for the individual capture states  $(nl)$  are also reported for the  $\text{Li}^+$  target. Total capture cross sections are calculated for each target by means of the Oppenheimer  $n^{-3}$  rule. For  $\text{Li}$  and  $\text{Li}^+$ , total cross sections are also evaluated at  $E < 200 \text{ keV}$  in order that graphical comparisons can be made with the limited experimental data. A procedure for determining the effective screening of the target nucleus by the uncaptured or 'passive' electrons is discussed and the sensitivity of the cross sections with respect to such screening is examined.

### 1. Introduction

When calculating charge-transfer cross sections which involve fast structureless projectiles, the correct high-energy behaviour requires the use of a second-order method. For light target atoms, such as hydrogen or helium, comparison with experiment has shown that one of the most satisfactory second-order procedures is the continuum-distorted wave (CDW) method. This was developed initially by Cheshire (1964) for a proton-hydrogen collision and later modified by Salin (1970) for application to a helium target. In a generalisation of the method for some two-electron systems, Belkić and Janev (1973) comment that the probability of capturing the 'active' electron should be greatest when the 'passive' electron is very close to the target nucleus. The 'passive' electron was then removed from the equations defining the distorted waves by invoking maximum shielding of the nucleus. Thus, in the description of the outward channel, for example, the residual target was represented by the target nucleus with its charge decreased by unity. This 'perfect screening' approximation was also used in a recent examination of electron capture from  $\text{H}^-$  (Moore and Banyard 1978, Banyard and Moore 1978).

Calculations of capture cross sections from large target atoms are still relatively rare and generally restricted to first-order methods. For example, Mapleton (1965) applied the first Born approximation to oxygen and Mapleton (1963, 1965, 1966, 1968), Nikolaev (1967) and Lodge and May (1968) have studied various target atoms using the

Brinkman–Kramers approximation. In the present work our main interest is to apply the CDW method to a many-electron system and, as a simple first example, we evaluate cross sections for the capture of an electron from a Li target atom in its ground state when the resulting ion exists in either a  $1^1S$ ,  $2^1S$  or  $2^3S$  state. For such a system, a ‘passive’ electron will now exist in a different shell from that of the ‘active’ electron. Thus, a modification is suggested to the ‘perfect screening’ procedure used by others for two-electron targets. We also examine the effect of such a modification on the capture cross sections when the target is the related ion  $\text{Li}^+(1^1S)$  and, finally, to complete the ionisation series, results are reported in brief for the one-electron target  $\text{Li}^{2+}(1^2S)$ . In each instance the projectiles are protons within an energy range of  $200 \text{ keV} \leq E \leq 10 \text{ MeV}$ —the lower limit being a rough measure of the minimum  $E$  required for a CDW calculation involving lithium ions. However, in order to achieve a graphical comparison with the limited experimental data, some of the cross sections are evaluated at lower energies. Such reactions are of considerable practical interest in understanding the hot plasmas which occur with the use of lithium arcs in devices such as ‘OGRA’ (Bogdanov *et al* 1965).

## 2. Theory and calculations

For a high-energy projectile of charge  $Z_A$ , energy  $E$  and velocity  $v$ , in collision with a stationary target system, whose nuclear charge is  $Z_B$ , the cross section for electron capture into a state ( $nl$ ) may be expressed as

$$\sigma[nl, F] = 2 \int_0^\infty b |a_{nl,F}(b)|^2 db \quad (1)$$

(in units of  $\pi a_0^2$ ) where  $a_{nl,F}(b)$  is the transition amplitude,  $b$  is the impact parameter and  $F$  signifies the final state of the remaining target electrons;  $a_0$  is the atomic unit of length. Using standard notation (Cheshire 1964, Salin 1970), the prior form of the CDW approximation for  $a_{nl,F}(b)$  for the capture of electron  $j$ , say, from an  $N$ -electron target, where  $N \leq Z_B$ , becomes

$$\begin{aligned} a_{nl,F}(b) = & i \mathcal{N}(\nu_A) \mathcal{N}(\nu_B) (bv)^{2iZ_A[Z_B - (N-1)]/v} \int_{-\infty}^{+\infty} dt e^{-i\Delta\epsilon t} \int d\mathbf{r}_1 \int d\mathbf{r}_2 \dots \int d\mathbf{r}_N e^{-i\mathbf{v}\cdot\mathbf{r}_i} \\ & \times \phi_{nl}^*(s_j) \chi_F^*(\mathbf{x}_1, \mathbf{x}_2, \dots, \mathbf{x}_{j-1}, \mathbf{x}_{j+1}, \dots, \mathbf{x}_N) {}_1F_1[i\nu_B; 1; i(vx_j + \mathbf{v}\cdot\mathbf{x}_j)] \\ & \times \frac{\partial}{\partial x_j} \Psi(\mathbf{x}_1, \mathbf{x}_2, \dots, \mathbf{x}_j, \dots, \mathbf{x}_N) \nabla_{r_j} {}_1F_1[i\nu_A; 1; i(vs_j + \mathbf{v}\cdot\mathbf{s}_j)]. \end{aligned} \quad (2)$$

The position vectors  $s_p$ ,  $x_p$  and  $r_p$  locate electron  $p$ , for example, when measured, in turn, from the projectile A, the target nucleus B, and the mid-point of  $R$ —the internuclear separation  $AB$ —where  $\mathbf{R} = \mathbf{b} + \mathbf{v}t$  and  $t$  is time; spin coordinates in the wavefunctions are to be taken as read. The energy decrement  $\Delta\epsilon$  is the difference between the initial-state energy of the target and the sum of the energies of the charge-exchange products. The initial and final states of the target are described by the normalised antisymmetric wavefunctions  $\Psi(\mathbf{x}_1, \mathbf{x}_2, \dots, \mathbf{x}_j, \dots, \mathbf{x}_N)$  and  $\chi_F(\mathbf{x}_1, \mathbf{x}_2, \dots, \mathbf{x}_{j-1}, \mathbf{x}_{j+1}, \dots, \mathbf{x}_N)$ , respectively, and the capture state of the active electron is represented by  $\phi_{nl}(s_j)$ . Since we have  $N$  indistinguishable electrons, the description of the total system in its final state  $\phi_{nl}\chi_F$  should also be normalised and

antisymmetric: the net effect of such a requirement is to multiply the transition amplitude derived from equation (2) by  $N^{1/2}$ .  $\mathcal{N}(\nu_A)$  and  $\mathcal{N}(\nu_B)$  are the normalisations associated with the confluent hypergeometric functions for the inward and outward distortions, respectively, and

$$\nu_A = Z_A/v \quad \nu_B = [Z_B - (N - 1)]/v. \quad (3)$$

The expression for  $\nu_B$  is a consequence of invoking the 'perfect screening' approximation to represent the interaction between the active and passive electrons, and its magnitude is a function of the net charge on the residual target as seen by the captured electron at infinity. Such a model has the particular advantage of ensuring that the incoming and outgoing waves have the correct asymptotic behaviour as  $t \rightarrow -\infty$  and  $+\infty$ , respectively. However, a relaxation of the asymptotic constraint allows us to adopt a simple but somewhat more realistic way of accounting for the passive electrons in a many-electron system. For capture from the target quantum state  $n'$ , an effective charge for the residual target can be obtained from the experimental ionisation energy by using the hydrogen-like expression

$$\text{Ionisation energy (in atomic units)} = Z_{\text{eff}}^2/2n'^2. \quad (4)$$

In this way the value of  $Z_{\text{eff}}$  reflects the charge seen by the active electron as it is ionised into the continuum prior to capture. Thus, in the expression for  $a_{nl,F}(b)$  we re-define  $\nu_B$  to be  $Z_{\text{eff}}/v$ . For comparison, both models were used to determine the capture cross sections for Li and  $\text{Li}^+$ .

Electron capture from the ground state of Li can occur from either the K or L shell and therefore the reactions considered here are



where  $F$  is  $1^1\text{S}$ ,  $2^1\text{S}$  or  $2^3\text{S}$  and  $(nl) \equiv 1s, 2s$  and  $2p$ . The same  $(nl)$  states were chosen when considering capture from the ground states of  $\text{Li}^+$  and  $\text{Li}^{2+}$ . The Hartree-Fock wavefunctions of Clementi and Roetti (1974) were used to describe the initial states of Li and  $\text{Li}^+$  and the excited-state wavefunctions for  $\text{Li}^+$  were taken from Cohen and McEachran (1967a, b). The ionisation energies were obtained from Moore (1949), Wiese *et al* (1966) and Tennent (1971). For the Li atom target, the  $Z_{\text{eff}}$  values corresponding to  $F \equiv 1^1\text{S}$ ,  $2^1\text{S}$  and  $2^3\text{S}$  in equation (5) are 1.260, 2.208 and 2.177, respectively, and when the target is a  $\text{Li}^+$  ion then  $Z_{\text{eff}} = 2.359$ . The  $\text{Li}^{2+}$  ion was described by using the exact energy and eigenfunction. For reaction (5), we note that integration over spin in the antisymmetrised expression for  $a_{nl,F}(b)$ , when  $F \equiv 1^1\text{S}$ , produces terms in the transition amplitude of an exchange type (in which the label for the active electron is associated with the  $1s$  orbital in Li) as well as the expected terms which arise from the initial occupation of the  $2s$  orbital; and vice versa when  $F \equiv 2^1\text{S}$ . However, in the present method, contributions to the capture cross sections attributable to exchange-type terms account for less than 0.3% of the magnitude of  $\sigma[nl, 1^1\text{S}]$  and  $\sigma[nl, 2^1\text{S}]$  in each instance; no such terms occur when  $F \equiv 2^3\text{S}$ . Therefore, for ease of discussion when considering the Li atom target, we regard  $\sigma[nl, 2^1\text{S}]$  and  $\sigma[nl, 2^3\text{S}]$  as arising from the capture of the appropriate K-shell target electron and  $\sigma[nl, 1^1\text{S}]$  as representing the capture of the L-shell electron.

The  $\sigma[nl, F]$  values for the Li and  $\text{Li}^+$  targets are presented in table 1: the initial entry is based on the  $Z_{\text{eff}}$  approximation and the italics refer to the 'perfect screening'

**Table 1.** Electron-capture cross sections  $\sigma[nl, F]$  for Li and  $\text{Li}^+$  in units of  $\pi a_0^2$  where  $a_0$  is the atomic unit of length. For each  $\sigma[nl, F]$ , the initial entry for a given proton energy  $E$  is derived from the  $Z_{\text{eff}}$  approximation and the 'perfect screening' (PS) value is quoted below it in italics. The superscript denotes the power of ten by which each entry should be multiplied.

$F$ state $E(\text{keV})$	Li atom												$\text{Li}^+$ ion		
	$1^1\text{S}$			$2^1\text{S}$			$2^3\text{S}^a$			$1^2\text{S}$			1s	2s	2p
$H(nl)$	1s	2s	2p												
200	1.868 <sup>-3</sup>	4.606 <sup>-4</sup>	9.147 <sup>-5</sup>	8.166 <sup>-3</sup>	1.048 <sup>-3</sup>	1.467 <sup>-4</sup>	2.167 <sup>-2</sup>	2.789 <sup>-3</sup>	3.983 <sup>-4</sup>	3.550 <sup>-2</sup>	4.474 <sup>-3</sup>	5.893 <sup>-4</sup>	3.550 <sup>-2</sup>	4.474 <sup>-3</sup>	5.893 <sup>-4</sup>
	<i>1.803<sup>-3</sup></i>	<i>3.881<sup>-4</sup></i>	<i>1.185<sup>-4</sup></i>	<i>5.628<sup>-3</sup></i>	<i>7.483<sup>-4</sup></i>	<i>1.013<sup>-4</sup></i>	<i>1.509<sup>-2</sup></i>	<i>2.005<sup>-3</sup></i>	<i>2.629<sup>-3</sup></i>	<i>2.939<sup>-2</sup></i>	<i>3.637<sup>-3</sup></i>	<i>1.016<sup>-3</sup></i>	<i>2.939<sup>-2</sup></i>	<i>3.637<sup>-3</sup></i>	<i>1.016<sup>-3</sup></i>
500	4.357 <sup>-5</sup>	7.374 <sup>-6</sup>	1.519 <sup>-6</sup>	3.878 <sup>-4</sup>	5.212 <sup>-5</sup>	5.751 <sup>-6</sup>	1.019 <sup>-3</sup>	1.369 <sup>-4</sup>	1.564 <sup>-5</sup>	1.794 <sup>-3</sup>	2.401 <sup>-4</sup>	2.292 <sup>-5</sup>	1.794 <sup>-3</sup>	2.401 <sup>-4</sup>	2.292 <sup>-5</sup>
	<i>4.452<sup>-5</sup></i>	<i>7.185<sup>-6</sup></i>	<i>2.064<sup>-6</sup></i>	<i>3.701<sup>-4</sup></i>	<i>4.954<sup>-5</sup></i>	<i>2.794<sup>-6</sup></i>	<i>9.762<sup>-4</sup></i>	<i>1.307<sup>-4</sup></i>	<i>7.300<sup>-5</sup></i>	<i>1.711<sup>-3</sup></i>	<i>2.280<sup>-4</sup></i>	<i>3.611<sup>-5</sup></i>	<i>1.711<sup>-3</sup></i>	<i>2.280<sup>-4</sup></i>	<i>3.611<sup>-5</sup></i>
800	5.312 <sup>-6</sup>	7.983 <sup>-7</sup>	1.641 <sup>-7</sup>	5.778 <sup>-5</sup>	7.711 <sup>-6</sup>	7.604 <sup>-7</sup>	1.517 <sup>-4</sup>	2.024 <sup>-5</sup>	2.072 <sup>-6</sup>	2.685 <sup>-4</sup>	3.580 <sup>-5</sup>	3.002 <sup>-6</sup>	2.685 <sup>-4</sup>	3.580 <sup>-5</sup>	3.002 <sup>-6</sup>
	<i>5.520<sup>-6</sup></i>	<i>8.084<sup>-7</sup></i>	<i>2.233<sup>-7</sup></i>	<i>6.191<sup>-5</sup></i>	<i>8.228<sup>-6</sup></i>	<i>3.473<sup>-6</sup></i>	<i>1.626<sup>-4</sup></i>	<i>2.162<sup>-5</sup></i>	<i>9.088<sup>-6</sup></i>	<i>2.668<sup>-4</sup></i>	<i>3.548<sup>-5</sup></i>	<i>4.773<sup>-6</sup></i>	<i>2.668<sup>-4</sup></i>	<i>3.548<sup>-5</sup></i>	<i>4.773<sup>-6</sup></i>
1000	1.886 <sup>-6</sup>	2.725 <sup>-7</sup>	5.546 <sup>-8</sup>	2.189 <sup>-5</sup>	2.906 <sup>-6</sup>	2.716 <sup>-7</sup>	5.749 <sup>-5</sup>	7.630 <sup>-6</sup>	7.411 <sup>-7</sup>	1.017 <sup>-4</sup>	1.349 <sup>-5</sup>	1.064 <sup>-6</sup>	1.017 <sup>-4</sup>	1.349 <sup>-5</sup>	1.064 <sup>-6</sup>
	<i>1.972<sup>-6</sup></i>	<i>2.794<sup>-7</sup></i>	<i>7.543<sup>-8</sup></i>	<i>2.444<sup>-5</sup></i>	<i>3.231<sup>-6</sup></i>	<i>1.226<sup>-6</sup></i>	<i>6.414<sup>-5</sup></i>	<i>8.479<sup>-6</sup></i>	<i>3.209<sup>-6</sup></i>	<i>1.025<sup>-4</sup></i>	<i>1.357<sup>-5</sup></i>	<i>1.710<sup>-6</sup></i>	<i>1.025<sup>-4</sup></i>	<i>1.357<sup>-5</sup></i>	<i>1.710<sup>-6</sup></i>
2000	6.582 <sup>-8</sup>	8.820 <sup>-9</sup>	1.713 <sup>-9</sup>	8.598 <sup>-7</sup>	1.122 <sup>-7</sup>	9.019 <sup>-9</sup>	2.261 <sup>-6</sup>	2.950 <sup>-7</sup>	2.475 <sup>-8</sup>	3.972 <sup>-6</sup>	5.182 <sup>-7</sup>	3.425 <sup>-8</sup>	3.972 <sup>-6</sup>	5.182 <sup>-7</sup>	3.425 <sup>-8</sup>
	<i>6.960<sup>-8</sup></i>	<i>9.255<sup>-9</sup></i>	<i>2.316<sup>-9</sup></i>	<i>1.042<sup>-6</sup></i>	<i>1.354<sup>-7</sup></i>	<i>4.074<sup>-8</sup></i>	<i>2.731<sup>-6</sup></i>	<i>3.549<sup>-7</sup></i>	<i>1.068<sup>-7</sup></i>	<i>4.118<sup>-6</sup></i>	<i>5.367<sup>-7</sup></i>	<i>5.761<sup>-8</sup></i>	<i>4.118<sup>-6</sup></i>	<i>5.367<sup>-7</sup></i>	<i>5.761<sup>-8</sup></i>
5000	5.790 <sup>-10</sup>	7.452 <sup>-11</sup>	1.409 <sup>-11</sup>	8.038 <sup>-9</sup>	1.032 <sup>-9</sup>	7.397 <sup>-11</sup>	2.117 <sup>-8</sup>	2.718 <sup>-9</sup>	2.044 <sup>-10</sup>	3.684 <sup>-8</sup>	4.732 <sup>-9</sup>	2.703 <sup>-10</sup>	3.684 <sup>-8</sup>	4.732 <sup>-9</sup>	2.703 <sup>-10</sup>
	<i>6.158<sup>-10</sup></i>	<i>7.904<sup>-11</sup></i>	<i>1.896<sup>-11</sup></i>	<i>1.018<sup>-8</sup></i>	<i>1.301<sup>-9</sup></i>	<i>3.461<sup>-10</sup></i>	<i>2.670<sup>-8</sup></i>	<i>3.412<sup>-9</sup></i>	<i>9.078<sup>-10</sup></i>	<i>3.881<sup>-8</sup></i>	<i>4.979<sup>-9</sup></i>	<i>4.836<sup>-10</sup></i>	<i>3.881<sup>-8</sup></i>	<i>4.979<sup>-9</sup></i>	<i>4.836<sup>-10</sup></i>
8000	4.575 <sup>-11</sup>	5.835 <sup>-12</sup>	1.133 <sup>-12</sup>	6.441 <sup>-10</sup>	8.230 <sup>-11</sup>	5.878 <sup>-12</sup>	1.698 <sup>-9</sup>	2.169 <sup>-10</sup>	1.628 <sup>-11</sup>	2.946 <sup>-9</sup>	3.766 <sup>-10</sup>	2.118 <sup>-11</sup>	2.946 <sup>-9</sup>	3.766 <sup>-10</sup>	2.118 <sup>-11</sup>
	<i>4.875<sup>-11</sup></i>	<i>6.204<sup>-12</sup></i>	<i>1.523<sup>-12</sup></i>	<i>8.243<sup>-10</sup></i>	<i>1.048<sup>-10</sup></i>	<i>2.801<sup>-11</sup></i>	<i>2.162<sup>-9</sup></i>	<i>2.749<sup>-10</sup></i>	<i>7.350<sup>-11</sup></i>	<i>3.114<sup>-9</sup></i>	<i>3.975<sup>-10</sup></i>	<i>3.884<sup>-11</sup></i>	<i>3.114<sup>-9</sup></i>	<i>3.975<sup>-10</sup></i>	<i>3.884<sup>-11</sup></i>
10000	1.344 <sup>-11</sup>	1.708 <sup>-12</sup>	3.395 <sup>-13</sup>	1.899 <sup>-10</sup>	2.423 <sup>-11</sup>	1.752 <sup>-12</sup>	5.007 <sup>-10</sup>	6.387 <sup>-11</sup>	4.857 <sup>-12</sup>	8.681 <sup>-10</sup>	1.108 <sup>-10</sup>	6.278 <sup>-12</sup>	8.681 <sup>-10</sup>	1.108 <sup>-10</sup>	6.278 <sup>-12</sup>
	<i>1.433<sup>-11</sup></i>	<i>1.818<sup>-12</sup></i>	<i>4.563<sup>-13</sup></i>	<i>2.440<sup>-10</sup></i>	<i>3.096<sup>-11</sup></i>	<i>8.411<sup>-12</sup></i>	<i>6.401<sup>-10</sup></i>	<i>8.122<sup>-11</sup></i>	<i>2.207<sup>-11</sup></i>	<i>9.184<sup>-10</sup></i>	<i>1.171<sup>-10</sup></i>	<i>1.163<sup>-11</sup></i>	<i>9.184<sup>-10</sup></i>	<i>1.171<sup>-10</sup></i>	<i>1.163<sup>-11</sup></i>

<sup>a</sup> The tabulated results for the  $F \equiv 2^3\text{S}$  state include the multiplicity factor.

(ps) model. For the Li atom, the total cross section  $\Sigma$  for all capture states ( $nl$ ) was obtained from

$$\Sigma = \Sigma(1^1S) + \Sigma(2^1S) + \Sigma(2^3S) \quad (6)$$

where each contribution  $\Sigma(F)$  was determined by using the appropriate form of the Oppenheimer  $n^{-3}$  rule (see, for example, Salin 1970). The  $n^{-3}$  rule was also used to calculate  $\Sigma$  for the  $\text{Li}^+$  and  $\text{Li}^{2+}$  targets and the results for all three systems are given in table 2. As before, the values obtained from the ps model are given in italics. In table 3, the difference between the  $Z_{\text{eff}}$  and the ps values for each cross section is expressed as a percentage change  $\Delta$ , with respect to the ps value, for both Li and  $\text{Li}^+$  at selected  $E$ .

**Table 2.** Total capture cross sections  $\Sigma$  for the Li,  $\text{Li}^+$  and  $\text{Li}^{2+}$  targets; the units are  $\pi a_0^2$ . The initial entry for a given  $E$  is derived from the  $Z_{\text{eff}}$  model and the ps value is quoted below it in italics. For the Li atom,  $\Sigma = \Sigma(1^1S) + \Sigma(2^1S) + \Sigma(2^3S)$ ; see equation (6). The superscript denotes the power of ten by which each entry should be multiplied.

$E(\text{keV})$	Li	$\text{Li}^+$	$\text{Li}^{2+}$
200	3.968 <sup>-2</sup> <i>3.367<sup>-2</sup></i>	4.369 <sup>-2</sup> <i>3.691<sup>-2</sup></i>	1.361 <sup>-2</sup>
500	1.804 <sup>-3</sup> <i>1.860<sup>-3</sup></i>	2.219 <sup>-3</sup> <i>2.138<sup>-3</sup></i>	1.240 <sup>-3</sup>
800	2.661 <sup>-4</sup> <i>3.003<sup>-4</sup></i>	3.312 <sup>-4</sup> <i>3.318<sup>-4</sup></i>	2.156 <sup>-4</sup>
1000	1.005 <sup>-4</sup> <i>1.172<sup>-4</sup></i>	1.252 <sup>-4</sup> <i>1.272<sup>-4</sup></i>	8.506 <sup>-5</sup>
2000	3.916 <sup>-6</sup> <i>4.894<sup>-6</sup></i>	4.864 <sup>-6</sup> <i>5.078<sup>-6</sup></i>	3.441 <sup>-6</sup>
5000	3.644 <sup>-8</sup> <i>4.732<sup>-8</sup></i>	4.493 <sup>-8</sup> <i>4.764<sup>-8</sup></i>	2.998 <sup>-8</sup>
8000	2.918 <sup>-9</sup> <i>3.827<sup>-9</sup></i>	3.589 <sup>-9</sup> <i>3.819<sup>-9</sup></i>	2.306 <sup>-9</sup>
10000	8.604 <sup>-10</sup> <i>1.133<sup>-9</sup></i>	1.057 <sup>-9</sup> <i>1.126<sup>-9</sup></i>	6.686 <sup>-10</sup>

To enable graphical comparisons to be made with the experimental curve for Li (Il'in *et al* 1965), values of  $\Sigma$  were calculated for both models over the energy range 10–180 keV. The curves are shown in figure 1 along with the corresponding theoretical results for  $\Sigma(2^1S) + \Sigma(2^3S)$  and  $\Sigma(1^1S)$ , these two quantities represent total cross sections for electron capture from the K and L shells, respectively. In figure 2, the  $Z_{\text{eff}}$  values for  $\Sigma$  over this energy range are compared with the Li calculations of Il'in *et al* (1967), Nikolaev (1967) and Lodge and May (1968). Il'in *et al* used a Born method in the one-electron approximation and the other workers employed the Brinkman–Kramers approximation along with a correction factor: Nikolaev described the Li atom in terms of hydrogen-like wavefunctions whereas the Lodge and May curve was derived from the Hartree–Fock description given by Roothaan *et al* (1960).

The  $\Sigma$  values for the  $\text{Li}^+$  ion are compared in figure 3 with the experimental curve of Bogdanov *et al* (1965) and the theoretical results of Ob'yedkov and Pavlov (1967). No experimental comparison could be found for the  $\text{Li}^{2+}$  ion.

**Table 3.** The percentage change  $\Delta$  in the capture cross sections  $\sigma[nl, F]$  and  $\Sigma$  for the Li and the  $\text{Li}^+$  targets, at selected  $E$ , when progressing from the rs model to the  $Z_{\text{eff}}$  model. The quantity  $\Delta$  is defined as  $[(\sigma(Z_{\text{eff}}) - \sigma(\text{rs})) / \sigma(\text{rs})] \times 100\%$ .

Target	Li atom										Li <sup>+</sup> ion			
	1 <sup>1</sup> S				2 <sup>1</sup> S				2 <sup>3</sup> S		1 <sup>2</sup> S			
$E(\text{keV})$	1s	2s	2p	1s	2s	2p	1s	2s	2p	$\Sigma$	1s	2s	2p	$\Sigma$
500	-2.1%	+2.6%	-26.4%	+4.8%	+5.2%	+106%	+4.4%	+4.7%	-78.6%	-4.4%	+4.4%	+4.8%	-36.2%	+3.8%
1000	-4.4%	-2.5%	-26.5%	-10.4%	-10.1%	-77.8%	-10.4%	-10.0%	-76.9%	-13.4%	-0.8%	-0.6%	-37.6%	-1.6%
2000	-5.4%	-4.7%	-26.0%	-17.5%	-17.1%	-77.9%	-17.2%	-16.9%	-76.8%	-18.1%	-3.5%	-3.4%	-40.5%	-4.2%
8000	-6.1%	-5.9%	-25.6%	-21.9%	-21.5%	-79.0%	-21.5%	-21.1%	-77.9%	-21.2%	-5.3%	-5.2%	-45.4%	-6.0%

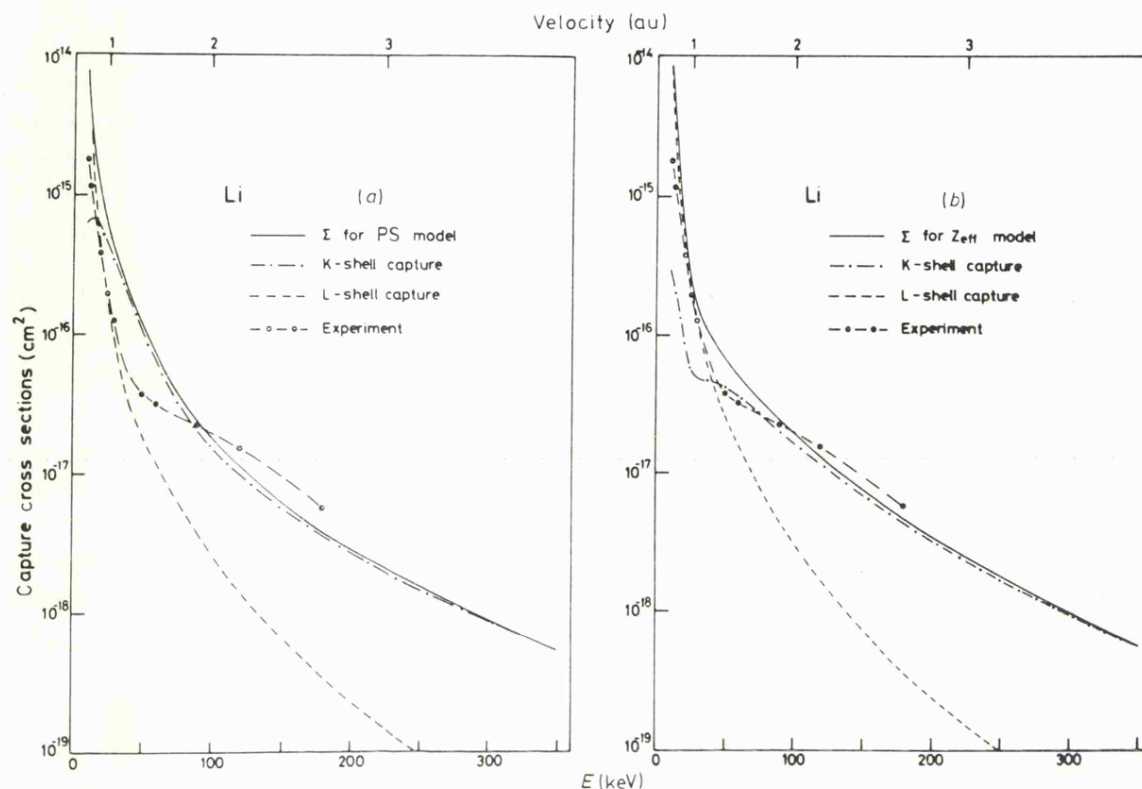


**Figure 1.** A comparison between experiment (Il'in *et al* 1965) and the total capture cross section  $\Sigma$  for Li derived from the CDW calculations using in (a) the PS model and in (b) the  $Z_{\text{eff}}$  model. Also shown in (a) and (b) are the calculated results for electron capture from the K shell (i.e.  $\Sigma(2^1S) + \Sigma(2^3S)$ ) and for capture from the L shell (i.e.  $\Sigma(1^1S)$ ); see equation (6).

### 3. Discussion

The application of the CDW approximation to describe electron capture from a many-electron target atom becomes tractable, at present, only by reducing it to an equivalent one-electron problem. Consequently, when attempting to replace the 'perfect screening' procedure for an  $N$ -electron system by a somewhat more physical model based on the ionisation energy, it was appropriate to use a hydrogen-like formula to determine  $Z_{\text{eff}}$ . In addition, we note that the only direct reference to the passive electrons in the transition amplitude occurs as an overlap integral between their initial and final quantum states. Thus, the influence of inter-electronic interactions within the present form of a CDW calculation arises solely from the correlation effects contained in the target wavefunctions  $\Psi$  and  $\chi_F$ . Although electron correlation is important for a target such as  $\text{H}^-$  (Moore and Banyard 1978), trial calculations in the present energy range suggest that the use of correlated wavefunctions for the Li series should produce a decrease in each cross section, with respect to the Hartree-Fock value, of less than 2%.

Comparison of the values of  $Z_{\text{eff}}$  for electron capture from the K shells of Li and  $\text{Li}^+$  suggests that, for capture from the Li K shell, about 20% of the shielding arises from the 2s electron: this reflects the probability of finding the L-shell electron within the K shell. For Li, a comparison of the results for  $Z_{\text{eff}}$  with the PS model is also of some interest. It is found that the  $Z_{\text{eff}}$  values for K-shell capture correspond to only about 40% of the shielding in the PS model whereas, for L-shell capture, the result for  $Z_{\text{eff}}$  indicates that the K shell provides 87% of perfect screening. The sensitivity of each  $\sigma[nl, F]$  to a

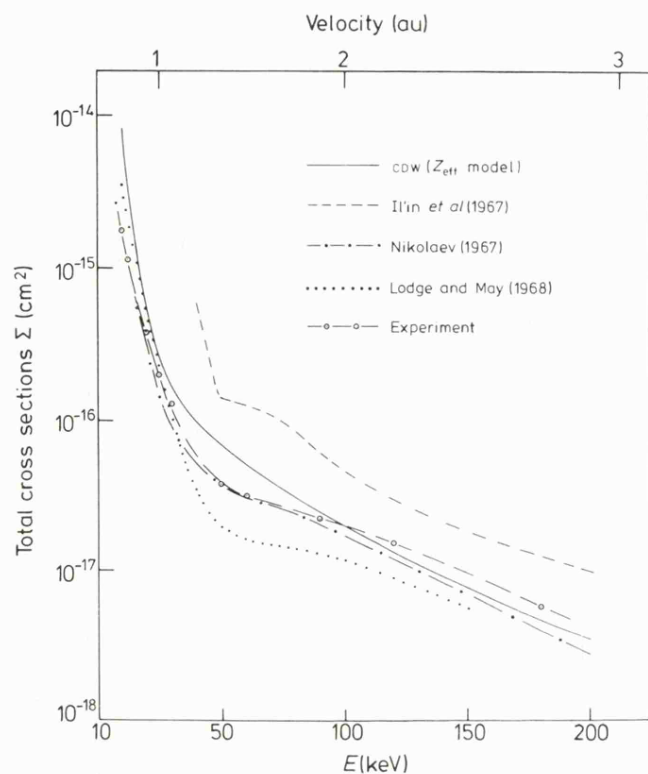


**Figure 2.** A comparison between various theoretical curves for  $\Sigma$  and experiment (Il'in *et al* 1965) for the Li atom. The CDW results were obtained by using the  $Z_{\text{eff}}$  model and the other curves were calculated by Il'in *et al* (1967), Nikolaev (1967) and Lodge and May (1968).

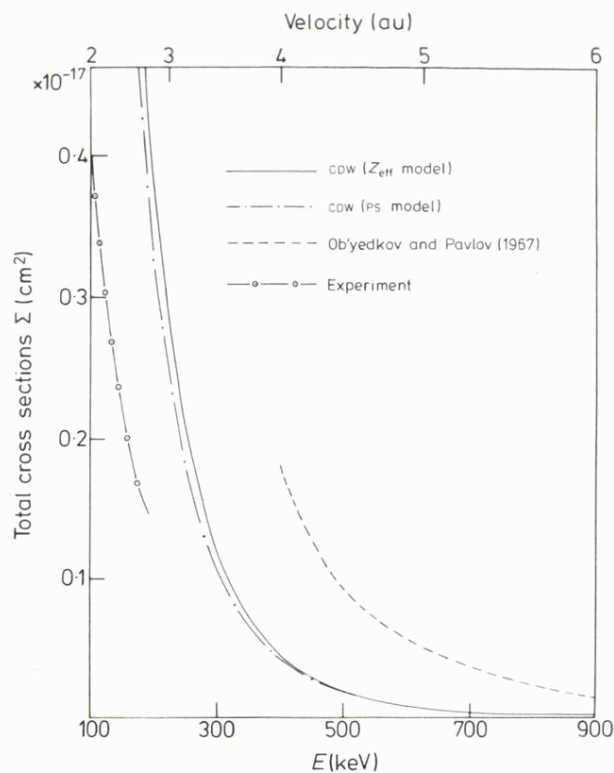


**Figure 3.** A comparison between the theoretical curves for  $\Sigma$  and experiment (Bogdanov *et al* 1965) for the  $\text{Li}^+$  ion. The CDW results were obtained by using, in turn, the PS and  $Z_{\text{eff}}$  models and the other curve was calculated by Ob'yedkov and Pavlov (1967).

change in nuclear shielding can be judged by inspecting the  $Z_{\text{eff}}$  and ps results in table 1; see also the  $\Delta$  values in table 3. At low energies, table 1 shows that when  $(nl) \equiv 1s$  and  $2s$  the  $Z_{\text{eff}}$  cross sections are larger than the ps values whereas, for the  $2p$  capture states, the ordering is reversed—an exception being Li when  $F \equiv 2^1S$ . However, for  $E \geq 1000$  keV, the use of  $Z_{\text{eff}}$  decreases *all*  $\sigma[nl, F]$ . This latter feature is most noticeable for capture from the K shell of the Li atom where, as table 3 shows, the effect becomes larger with increasing  $E$ . At 10 MeV, for example, the  $Z_{\text{eff}}$  calculation yields K-shell cross sections for the  $2p$  capture state which are only about one-fifth of the magnitude of the ps values.

For each  $F$  state table 3 reveals that, as  $E$  increases, a strong similarity occurs between the  $\Delta$  values for  $(nl) \equiv 1s$  and  $2s$ ; this similarity does not extend to the  $2p$  state. A corresponding trend was observed by Banyard and Szuster (1977) in a correlation study of charge exchange in proton-helium collisions. Following their rationalisation, we find that, at high projectile velocities, the major contribution to each  $\sigma[nl, F]$  occurs at small values of the impact parameter. Consequently, the  $\Delta$  values reflect the similarity in the *characteristics* of the  $1s$  and  $2s$  hydrogen orbitals at small electron-proton separations; such characteristics are, in turn, quite distinct from those of a  $2p$  hydrogen orbital.

When  $E \geq 800$  keV, the Li cross sections are ordered as  $\sigma[nl, 2^3S] > \sigma[nl, 2^1S] > \sigma[nl, 1^1S]$  for each choice of  $(nl)$  and, as might be expected, for any given  $F$  state we have  $\sigma[1s, F] > \sigma[2s, F] > \sigma[2p, F]$ . The latter ordering also holds for  $\text{Li}^+$ . Inspection of the total cross sections  $\Sigma$  in table 2 for the ionisation series shows that, for the  $Z_{\text{eff}}$  model,  $\Sigma(\text{Li}^+) > \Sigma(\text{Li}) > \Sigma(\text{Li}^{2+})$  throughout the whole energy range. We also note that, at high energies, the  $Z_{\text{eff}}$  results for  $\Sigma$  are less than the ps values by about 21% for Li and 6% for  $\text{Li}^+$ .

A comparison between the total cross sections *per* K-shell electron for the ion targets reveals that, at low energies,  $\text{Li}^+ > \text{Li}^{2+}$  whereas, when  $E$  is large, the  $\text{Li}^{2+}$  cross sections are significantly greater than the  $\text{Li}^+$  values. Since the transition amplitudes are evaluated in terms of momentum space, the larger momentum possessed by the unshielded active electron in  $\text{Li}^{2+}$  emphasises that, as the projectile velocity increases, the major contribution to each cross section arises increasingly from the high momentum region within the target.

When compared with experiment, the  $Z_{\text{eff}}$  and ps values of  $\Sigma$  for Li reveal some interesting features. Although the results of Il'in *et al* (1965) extend only as far as 180 keV, figure 1 indicates that each CDW curve for  $\Sigma$  is in general accord with experiment—the better agreement being achieved by the  $Z_{\text{eff}}$  approximation. For electron capture from the K shell, the ps results are seen to reach a turning point at about 15 keV, whereas the  $Z_{\text{eff}}$  approximation produces an inflexion at about 40 keV which is similar in shape to that seen in the experimental  $\Sigma$  curve at  $E \sim 60$  keV. However, figure 1(b) shows that the increase in the L-shell capture cross section with decreasing  $E$  masks this inflexion when evaluating the total curve.

For Li, the comparisons in figure 2 between the various theoretical  $\Sigma$  curves and experiment show that, except for the very good Nikolaev curve, the CDW result is superior—especially in the higher energy region. It is to be noted that, unlike the CDW calculation, the Nikolaev curve involved the use of an empirically derived velocity-dependent correcting function.

When the target is a  $\text{Li}^+$  ion, figure 3 shows that although both the CDW curves are a considerable improvement on the theoretical results of Ob'yedkov and Pavlov (1967), when compared with the limited experimental data, the agreement is still poor. Since,

as observed earlier, a  $Z_{\text{eff}}$  cross section exceeds a ps result at low  $E$ , the  $\Sigma$  curve derived from the  $Z_{\text{eff}}$  values is seen to be the poorer cross section. As with the Li atom target, it would be very useful if the comparisons with experiment could be extended to much higher energies.

#### 4. Conclusion

Electron-capture cross sections have been evaluated for fast protons in collision with the Li atom and its related ions. Such reactions are of interest in the hot plasmas which occur in some fusion processes. The calculations were based on the continuum-distorted wave (CDW) approximation and a simple procedure was introduced for assessing the screening of the target nucleus due to the passive electrons.

It was observed that capture into the higher quantum states ( $nl$ ) of hydrogen appeared to be quite sensitive to changes in the screening effects—particularly at high projectile energies  $E$  and especially for capture from the K shell. Although a comparison with experiment of the total cross sections  $\Sigma$  was limited to low  $E$ —where both the CDW method and the  $n^{-3}$  rule tend to become less reliable—the general agreement was, nevertheless, quite satisfactory for the Li target but still poor for  $\text{Li}^+$ . Comparisons with experiments at larger  $E$  would be most informative.

For Li, a systematic increase in the projectile velocity eventually causes capture from the K shell to make a greater contribution to  $\Sigma$  than that from the L shell. This emphasises once again the importance of the high momentum description of the target electrons and hence the need to use accurate wavefunctions in any 'a priori' calculation—even at high projectile velocities.

#### References

- Banyard K E and Moore J C 1978 *J. Phys. B: Atom. Molec. Phys.* **11** 3899  
 Banyard K E and Szuster B J 1977 *Phys. Rev. A* **16** 129  
 Belkić Dž S and Janev R K 1973 *J. Phys. B: Atom. Molec. Phys.* **6** 1020  
 Bogdanov G F, Karkhov A N and Kucheryaev Yu A 1965 *Atomnaya Énergiya (USSR)* **19** 1316  
 Cheshire I M 1964 *Proc. Phys. Soc.* **84** 89  
 Clementi E and Roetti C 1974 *Atom. Data Nucl. Data Tables* vol 14 (New York, London: Academic Press)  
 Cohen M and McEachran R P 1967a *Proc. Phys. Soc.* **92** 37  
 — 1967b *Proc. Phys. Soc.* **92** 539  
 Il'in R N, Oparin V A, Solov'ev E S and Fedorenko N V 1965 *JETP Lett.* **2** 197  
 — 1967 *Sov. Phys.-Tech. Phys.* **11** 921  
 Lodge J G and May R M 1968 *Aust. J. Phys.* **21** 793  
 Mapleton R A 1963 *Phys. Rev.* **130** 1829  
 — 1965 *Proc. Phys. Soc.* **85** 1109  
 — 1966 *Phys. Rev.* **145** 25  
 — 1968 *J. Phys. B: Atom. Molec. Phys.* **1** 850  
 Moore C 1949 *Atomic Energy Levels* NBS Circular No 467, vol 1 (Washington: US Govt Printing Office)  
 Moore J C and Banyard K E 1978 *J. Phys. B: Atom. Molec. Phys.* **11** 1613  
 Nikolaev V S 1967 *Sov. Phys.-JETP* **24** 847  
 Ob'yedkov V D and Pavlov V E 1967 *Atomnaya Énergiya (USSR)* **23** 345  
 Roothaan C C J, Sachs L M and Weiss A W 1960 *Rev. Mod. Phys.* **32** 186  
 Salin A 1970 *J. Phys. B: Atom. Molec. Phys.* **3** 937  
 Tennent R M 1971 *Science Data Book* (Edinburgh: Oliver and Boyd)  
 Wiese W L, Smith M W and Glennon B M 1966 *Atomic Transitions Probabilities* (Washington: US Govt Printing Office)

## Ordering of cross sections for electron capture from He-like targets by fast projectiles

G. W. Shirtcliffe and K. E. Banyard

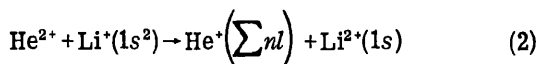
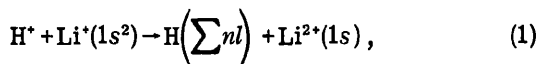
Department of Physics, University of Leicester, Leicester, England

(Received 11 June 1979)

The continuum-distorted-wave (CDW) method is used to determine total electron-capture cross sections  $Q = \sum_{nl} \sigma[nl]$  for proton and  $\alpha$ -particle projectiles incident on  $\text{Li}^+$  in energy ranges of  $100 \leq E \leq 3000$  keV and  $100 \leq E \leq 10000$  keV, respectively. A configuration-interaction (CI) wave function is used to describe the  $\text{Li}^+$  electrons; for comparison, capture cross sections for  $\text{H}^-$  and He are examined. For each system the percentage change in  $Q$ ,  $\Delta(\text{HF} \rightarrow \text{CI})$ , is given for progression from a Hartree-Fock (HF) to a CI description of the target electrons. The main emphasis in this work is devoted to a rationalization of the trends observed in the ordering of  $Q$  for these three targets. This was achieved by an analysis of the CDW expression for an individual capture cross section  $\sigma[nl, n'l']$ , where  $nl$  and  $n'l'$  are the states of the "active" (captured) and "passive" electrons, respectively.

### I. INTRODUCTION

For a helium target the cross sections for electron capture by fast protons are adequately described by the continuum-distorted-wave (CDW) method (see, for example, Salin<sup>1</sup> and Belkić and Gayet<sup>2</sup>). Banyard and Szuster<sup>3</sup> examined the sensitivity of such cross sections with respect to improvements in the He wave function up to and beyond the Hartree-Fock (HF) description; a similar study was made by Moore and Banyard<sup>4</sup> for  $\text{H}^-$ . The CDW method is used here to evaluate the total cross sections  $Q = \sum_{nl} \sigma[nl]$  for the following reactions:



in the energy ranges 100–3000 and 100–10 000 keV, respectively. For each reaction we calculated the cross sections  $\sigma[nl]$  for the capture states  $nl \equiv 1s, 2s$ , and  $2p$ , and  $Q$  was then determined by using the  $n^{-3}$  rule (see, for example, Salin<sup>1</sup>). Besides examining, in brief, the sensitivity of  $Q$  with respect to changes in the  $\text{Li}^+(1s^2)$  wave function, we also analyze the CDW expression for a general capture cross section  $\sigma[nl, n'l']$ , where  $nl$  and  $n'l'$  are the states of the "active" (captured) and "passive" electrons, respectively, in order to rationalize the trends observed when comparing the cross sections for capture from  $\text{H}^-$ , He, and  $\text{Li}^+$ .

### II. RESULTS AND DISCUSSION

The capture cross section  $\sigma[nl]$  for a given projectile energy  $E$  may be written as

$$\sigma[nl] = 2 \int_0^\infty b |a_{nl}(b)|^2 db$$

(in units of  $\pi a_0^2$ , with  $a_0$  as the atomic unit of length), where  $a_{nl}(b)$  is the prior form of the CDW transition amplitude and  $b$  is the impact parameter. In Table I we report the total cross sections  $Q$  for reactions (1) and (2), and for comparison we tabulate the corresponding results for He and  $\text{H}^-$ ; in each case the target electrons are described by the 35-term configuration-interaction (CI) wave function of Weiss.<sup>5</sup> To assess the influence of electron correlation we also quote for each energy  $E$  the percentage change  $\Delta(\text{HF} \rightarrow \text{CI})$  in  $Q$  when going from the HF to the CI description of the target electrons. The HF wave functions for He and  $\text{Li}^+$  were those of Clementi and Roetti,<sup>6</sup> and for  $\text{H}^-$  the fitted functions of Curl and Coulson<sup>7</sup> were used. The  $\Delta(\text{HF} \rightarrow \text{CI})$  values are seen to reflect a rapid decrease in the importance of correlation as we progress from  $\text{H}^-$  to  $\text{Li}^+$ . For a given target it was noted that at a common projectile velocity the proton and  $\alpha$ -particle reactions possessed similar  $\Delta(\text{HF} \rightarrow \text{CI})$  values, the magnitude being almost identical at high velocities.

When  $E > 100$  keV, Table I shows that the ordering in  $Q$  for each projectile is  $Q(\text{Li}^+) > Q(\text{He}) > Q(\text{H}^-)$ . As  $E$  becomes larger the difference between the cross sections for the three systems increases; for example, for protons at 200 keV,  $Q(\text{Li}^+) \approx 9Q(\text{H}^-)$ , whereas at 3000 keV we have  $Q(\text{Li}^+) \approx 150Q(\text{H}^-)$ .

In attempting to account for the above ordering in  $Q$ , we note first that the three systems differ in the size of the distortion acting on the captured, or active, electron in the exit channel. Since in the present form of the CDW method the distortion is a function of the net charge on the residual target (see Belkić and Janev<sup>8</sup>) and thus opposes electron capture, its effect should be to produce an ordering of  $Q$  which is the reverse of that observed. Second, although the energy de-

TABLE I. Total electron-capture cross sections  $Q$ , in units of  $\pi a_0^2$ , for targets  $H^-$ , He, and  $Li^+$  for both proton and  $\alpha$ -particle projectiles. Each system is described by the 35-term configuration-interaction (CI) function of Weiss,<sup>5</sup> and in square brackets we give the percentage change  $[\Delta(HF \rightarrow CI)]$  in going from the Hartree-Fock (HF) to the CI description for the target electrons;  $\Delta(HF \rightarrow CI)$  is defined as  $[(Q_{CI} - Q_{HF})/Q_{HF}] \times 100\%$ .

Protons				$\alpha$ particles			
$E$ (keV)	$H^-$ [ $\Delta(HF \rightarrow CI)$ ]	He <sup>a</sup> [ $\Delta(HF \rightarrow CI)$ ]	Li <sup>+b</sup> [ $\Delta(HF \rightarrow CI)$ ]	$E$ (keV)	$H^-$ [ $\Delta(HF \rightarrow CI)$ ]	He <sup>a</sup> [ $\Delta(HF \rightarrow CI)$ ]	Li <sup>+b</sup> [ $\Delta(HF \rightarrow CI)$ ]
100	6.681 <sup>-2c</sup> [-19.8%]	3.482 <sup>-1</sup> [-4.0%]	1.394 <sup>-1</sup> [-4.5%]	100	1.630 <sup>-1</sup> [-16.4%]	5.196 <sup>-1</sup> [-4.7%]	4.695 <sup>-1</sup> [-5.8%]
200	3.922 <sup>-3</sup> [-17.1%]	3.477 <sup>-2</sup> [-3.8%]	3.683 <sup>-2</sup> [-2.2%]	500	1.700 <sup>-1</sup> [-16.9%]	1.512 <sup>0</sup> [-3.8%]	2.084 <sup>0</sup> [-1.9%]
500	5.585 <sup>-5</sup> [-15.9%]	8.456 <sup>-4</sup> [-4.2%]	2.118 <sup>-3</sup> [-1.3%]	1000	1.268 <sup>-2</sup> [-16.6%]	1.661 <sup>-1</sup> [-4.1%]	3.446 <sup>-1</sup> [-1.4%]
800	5.200 <sup>-6</sup> [-15.9%]	9.912 <sup>-5</sup> [-4.3%]	3.275 <sup>-4</sup> [-1.4%]	2000	6.619 <sup>-4</sup> [-16.4%]	1.203 <sup>-2</sup> [-4.1%]	3.624 <sup>-2</sup> [-1.3%]
1000	1.622 <sup>-6</sup> [-16.0%]	3.418 <sup>-5</sup> [-4.3%]	1.254 <sup>-4</sup> [-1.4%]	4000	2.460 <sup>-5</sup> [-16.0%]	5.947 <sup>-4</sup> [-4.4%]	2.396 <sup>-3</sup> [-1.5%]
2000	3.864 <sup>-8</sup> [-16.2%]	1.064 <sup>-6</sup> [-4.4%]	4.995 <sup>-6</sup> [-1.6%]	6000	3.138 <sup>-6</sup> [-16.1%]	8.794 <sup>-5</sup> [-4.5%]	4.052 <sup>-4</sup> [-1.6%]
3000	4.083 <sup>-9</sup> [-16.3%]	1.270 <sup>-7</sup> [-4.4%]	6.633 <sup>-7</sup> [-1.7%]	10000	2.104 <sup>-7</sup> [-16.3%]	6.932 <sup>-6</sup> [-4.5%]	3.664 <sup>-5</sup> [-1.7%]

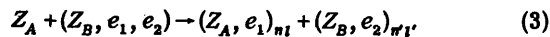
<sup>a</sup>The results for He supersede those reported by Banyard and Szuster (Ref. 3), which contained a small computing error.

<sup>b</sup>Total capture cross section  $Q$  was obtained from the "Oppenheimer  $n^{-3}$  rule":  $Q \approx \sigma[1s] + 1.616(\sigma[2s] + \sigma[2p])$ .

<sup>c</sup>Superscript denotes the power of 10 by which each entry should be multiplied.

crement  $\Delta\epsilon$  (defined as the difference in energy between the initial and final atomic states and determined here from the theoretical values) is different for each of the three systems, the cross sections are found to become insensitive to  $\Delta\epsilon$  in the limit of high projectile velocities. Therefore it would appear that the observed trends in  $Q$  must be dominated by the differences in the target wave functions.

We now proceed by analysis of the individual CDW cross section  $\sigma[nl, n'l']$  to account for the trends in  $Q$  for the more general reaction



when the target electrons are described by an HF wave function

$$\Phi(1, 2) = \sum_p c_p \varphi_p(1) \sum_q c_q \varphi_q(2),$$

where each member of the basis set  $\{\varphi\}$  is normalized and the coefficients  $c_p$  and  $c_q$  are the usual variation constants. The CDW cross section  $\sigma[nl, n'l']$  for a relative impact velocity  $v$  corresponding to an energy  $E$ , when the capture state wave function is  $\Psi_m(1)$ , can be expressed as

$$\sigma[nl, n'l'] = N \left[ I \left( \sum_q c_q \varphi_q(2) | n'l' \right) \right]^2 \int_0^\infty \left| \sum_p c_p f_1(\eta, v, \varphi_p(1), \Delta\epsilon) g_1(\eta, v, \varphi_p(1), \Psi_m(1), \nu_1, \nu_2, \Delta\epsilon) \right|^2 d\eta, \quad (4)$$

where  $N$  is a constant and  $I(\sum_q c_q \varphi_q(2) | n'l')$  is an overlap integral between the initial and final states which describe the passive electron  $e_2$ . The integration over  $\eta$  is a result of performing a Fourier transform of the transition amplitude from position space to a two-dimensional vector space  $\vec{\eta}$  (see Belkić and Janev<sup>6</sup>), and the functions

$\nu_1$  and  $\nu_2$  arise from the distortions due to Coulomb interactions acting in the entrance and exit channels, respectively, and are defined as  $\nu_1 = Z_A/v$  and  $\nu_2 = (Z_B - 1)/v$ . We note that  $f_1$  and  $g_1$  are both functions of  $\varphi_p(1)$ , and hence the strong dependence of the ordering in the cross sections on  $\Phi(1, 2)$  is still not apparent. However, since

the occurrence of the distortion in the exit channel *inhibits* capture, we can, without prejudice, proceed with our analysis by setting  $\nu_2 = 0$  for the general reaction (3). As a consequence of this, the  $\varphi_p(1)$  dependence in  $g_1$  is now removed and the expression for  $\sigma[nl, n'l']$  when  $\nu_2 = 0$  becomes

$$\sigma[nl, n'l']_{\nu_2=0} = NI^2 \int_0^\infty \left[ F_1 \left( \eta, v, \sum_p c_p \varphi_p(1), \Delta\epsilon \right) \right]^2 \times |G_1(\eta, v, \Psi_n, \nu_1, \Delta\epsilon)|^2 d\eta. \quad (5)$$

Except for the presence of the energy decrement  $\Delta\epsilon$ , the functional form of  $G_1$  is independent of the target parameters. At high projectile velocities,  $G_1$  is found to be insensitive to  $\Delta\epsilon$ , and thus for a particular capture state ( $nl$ ) the function  $G_1$  becomes identical for our three examples of a two-electron target ( $Z_B, e_1, e_2$ ). When the basis set  $\{\varphi\}$  is represented, for example, by Slater-type orbitals (STO's), the function  $F_1$  takes the form

$$F_1 = \sum_p c_p (-1)^{s_p} N(s_p, \xi_p) \times \frac{\partial^{(s_p-1)}}{\partial \xi_p^{(s_p-1)}} \left( \frac{\xi_p}{[\xi_p^2 + \eta^2 + (v/2 + \Delta\epsilon/v)^2]^2} \right), \quad (6)$$

where  $s_p$ ,  $\xi_p$ , and  $N(s_p, \xi_p)$  are the principal quantum number, orbital exponent, and normalization constant, respectively, of the basis function  $\varphi_p$ . Analysis of  $F_1^2$  shows that it represents the probability density of finding the active electron  $e_1$  with a  $z$  component of momentum equal to  $|v/2 + \Delta\epsilon/v|$  or, conversely, of finding  $e_1$  with a total momentum  $p \geq |v/2 + \Delta\epsilon/v|$ , and therefore  $F_1^2$  can be interpreted as a two-dimensional momentum density. We note that the  $z$  component of momentum is not unique, and its definition is simply a consequence of choosing our coordinate

system such that  $\vec{\eta} \cdot \vec{v} = 0$ , with  $\vec{v} \equiv (0, 0, v_z)$ .

Let us now particularize reaction (3) by choosing  $Z_A$  to be a proton and by setting  $nl = n'l' = 1s$  for the targets  $H^-$ , He, and  $Li^+$ . In Fig. 1 for each system we plot  $F_1^2$  and  $G_1^2$  as a function of  $\eta$  for  $\sigma[1s, 1s]_{\nu_2=0}$  at  $E = 500, 1000,$  and  $2000$  keV. For subsequent discussion and ease of comparison Table II contains  $\sigma[1s, 1s]$  and  $\sigma[1s, 1s]_{\nu_2=0}$  at a few selected  $E$ ;  $R$  (as defined later) is a ratio of the cross sections for different targets when  $\nu_2 = 0$ . Throughout Fig. 1 and Table II each target was described by the HF wave function; for  $H^-$  we note that  $\sigma[1s, 1s] = [1s, 1s]_{\nu_2=0}$ . As anticipated, Fig. 1 shows that the  $G_1^2$  functions for each target are very similar, particularly at large  $E$  values. Therefore the ordering of the cross sections in Table II is a direct consequence of the differences in the electron densities in momentum space as represented by  $F_1^2$ . When the projectile velocity is increased, the active electron is captured from regions of increasingly higher momentum within the target atom; thus the cross sections reflect the characteristics of the target wave functions near the origin. Indeed, in the limit as  $v \rightarrow \infty$  the function  $F_1$  may be expressed as

$$F_1 \xrightarrow{(v \rightarrow \infty)} \sum_p c_p \left. \frac{\partial \varphi_p(1)}{\partial x_1} \right|_{x_1=0} \frac{1}{(\eta^2 + \frac{1}{4}v^2)^2}, \quad (7)$$

and hence

$$\sigma[nl, n'l']_{\nu_2=0} \xrightarrow{(v \rightarrow \infty)} NI^2 \left( \sum_p c_p \left. \frac{\partial \varphi_p(1)}{\partial x_1} \right|_{x_1=0} \right)^2 \times \int_0^\infty |G_2(\eta, v, \Psi_n, \nu_1)|^2 d\eta, \quad (8)$$

where  $\vec{x}_1$  is the position vector of the active electron with respect to the target nucleus. The  $\eta$  and  $v$  dependence in Eq. (8) occurs only in the new function  $G_2$ , and in the limit we note that this

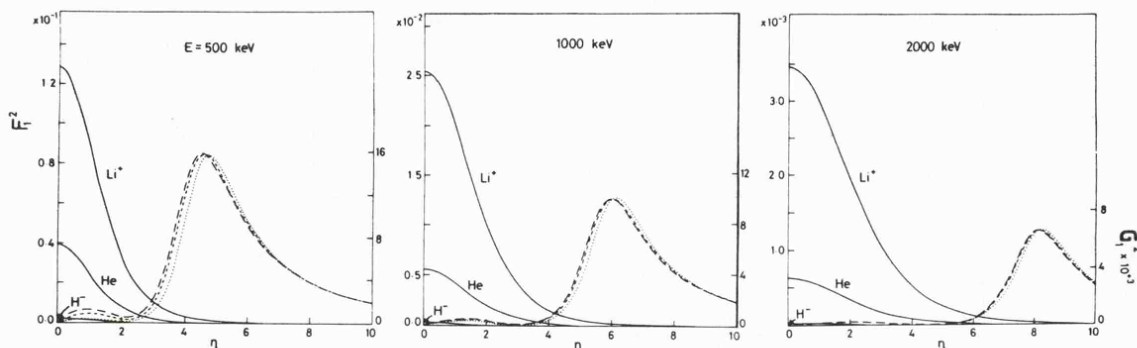


FIG. 1. Plots at three selected impact energies  $E$  of  $F_1^2$  and  $G_1^2$  against  $\eta$  for each of the targets  $H^-$ , He, and  $Li^+$  corresponding to  $\sigma[1s, 1s]_{\nu_2=0}$  in Eq. (5). The projectiles are protons and the target electrons are described by the Hartree-Fock wave functions stated in text. Curves for  $G_1^2$  are long-dashed  $H^-$ , short-dashed He, and dotted  $Li^+$ .

TABLE II. Cross sections  $\sigma[1s, 1s]$  and  $\sigma[1s, 1s]_{\nu_2=0}$  in units of  $\pi a_0^2$ , at selected  $E$  for electron capture by protons from the targets  $H^-$ , He, and  $Li^+$ . Since the distortion in the exit channel due to the Coulomb interaction is zero for  $H^-$  (i.e.,  $\nu_2=0$ ), we note that  $\sigma[1s, 1s] = \sigma[1s, 1s]_{\nu_2=0}$ . We also tabulate values of  $R = (\sigma_a[1s, 1s]/\sigma_b[1s, 1s])_{\nu_2=0}$  for (i)  $a \equiv He$  and  $b \equiv H^-$  and (ii)  $a \equiv Li^+$  and  $b \equiv He$ . In each instance the target electrons are described by Hartree-Fock wave functions.

$E$ (keV)	$H^-$	He	$Li^+$	He ( $\nu_2=0$ )	$R_{(i)}$	$Li^+$ ( $\nu_2=0$ )	$R_{(ii)}$
500	$4.760^{-5}{}^a$	$6.880^{-4}$	$1.718^{-3}$	$8.239^{-4}$	17.3	$1.986^{-3}$	2.4
1000	$1.427^{-6}$	$2.833^{-5}$	$1.025^{-4}$	$3.621^{-5}$	25.4	$1.382^{-4}$	3.8
3000	$3.665^{-9}$	$1.068^{-7}$	$5.484^{-7}$	$1.420^{-7}$	38.7	$8.465^{-7}$	6.0
5000	$2.077^{-10}$	$6.766^{-9}$	$3.880^{-8}$	$9.063^{-9}$	43.6	$6.137^{-8}$	6.8
10000	$4.042^{-12}$	$1.434^{-10}$	$9.181^{-10}$	$1.944^{-10}$	48.1	$1.483^{-9}$	7.6

<sup>a</sup>Superscript denotes the power of 10 by which each entry should be multiplied.

function is also independent of  $\Delta\epsilon$ . Therefore, if we examine the ratio  $R[nl, n'l']$  of the cross sections for two targets  $a$  and  $b$  when the distortion in the exit channel is removed, we obtain

$$R[nl, n'l'] = \frac{\sigma_a[nl, n'l']}{\sigma_b[nl, n'l']} \Big|_{\nu_2=0} \xrightarrow{(\omega \rightarrow \infty)} \frac{I_a^2 S_a^2}{I_b^2 S_b^2}, \quad (9)$$

where  $S$  is the slope or gradient of the HF wave function for the active electron at the origin ( $x_1=0$ ) and, as before,  $I$  is the passive overlap integral. In Table II we present the ratios  $R[1s, 1s]$

for (i)  $a \equiv He$  and  $b \equiv H^-$  and (ii)  $a \equiv Li^+$  and  $b \equiv He$ . As  $E$  increases, these ratios are seen to approach the values of 52.8 for (i) and 8.86 for (ii) predicted by Eq. (9), which again illustrates how the ordering of the cross sections is dictated by the relative behavior of the target wave functions. In passing, we note that when  $H^-$ , He, and  $Li^+$  are described by HF wave functions the passive overlap integral for  $n'l' = 1s$  is 0.922, 0.984, and 0.993, respectively; thus, the limiting ratios in this instance are governed essentially by the relative

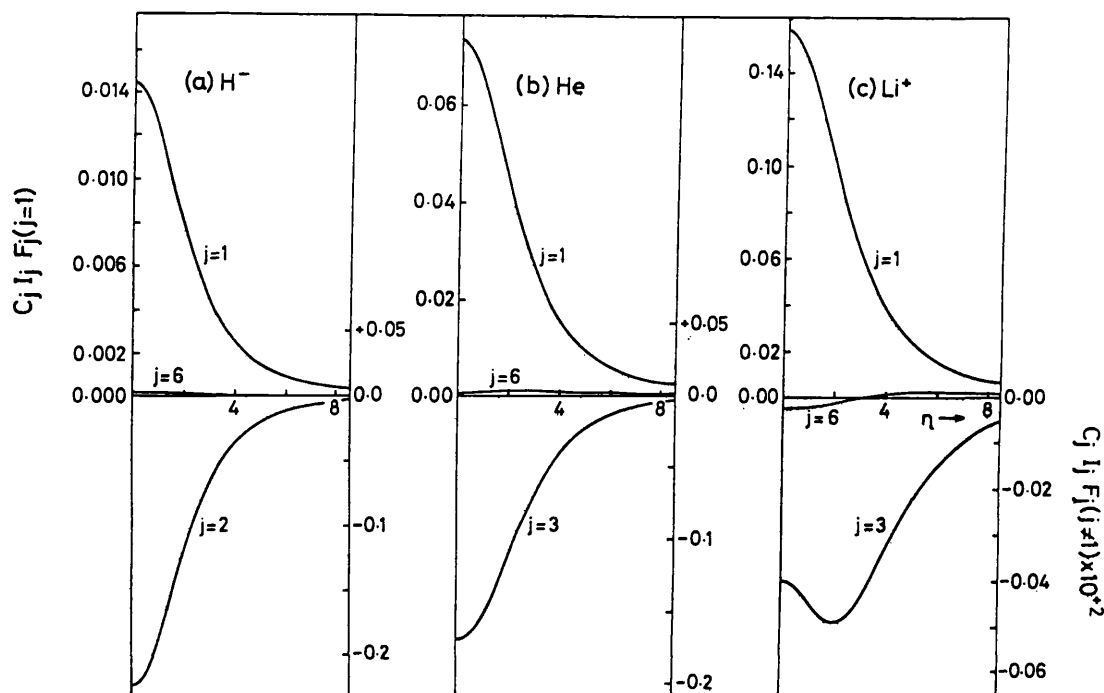


FIG. 2. Plots of  $C_j I_j F_j$  vs  $\eta$ , defined in Eq. (10), corresponding to  $j$ th natural configuration within natural expansion formulation of  $\sigma[1s, 1s]_{\nu_2=0}$  for a proton impact energy of 1000 keV. (a)  $H^-$  for  $j=1, 2$ , and 6, (b) He for  $j=1, 3$ , and 6, and (c)  $Li^+$  for  $j=1, 3$ , and 6. Each target was described by the natural expansion of 35-term CI wave function of Weiss,<sup>5</sup> and the  $j$  values quoted represent natural configurations constructed from orbitals of radial symmetry.

values of  $S$ .

If  $\Phi(1, 2)$  is a correlated wave function, it is of interest to examine the form of the function, say  $\mathcal{F}^2$ , which replaces  $I^2F_1^2$  in Eq. (5). For a discussion of electron correlation, a particularly convenient form for any CI wave function is to express it as a natural expansion (see, for example, Löwdin<sup>9</sup>). Thus  $\mathcal{F}^2$  can then be written as

$$\mathcal{F}^2 = \left[ \sum_j C_j I_j \left( \sum_i b_{i,j} \varphi_i(2) | n'l' \right) \times F_j \left( \eta, \nu, \sum_k b_{k,j} \varphi_k(1), \Delta\epsilon \right) \right]^2, \quad (10)$$

where for the Weiss<sup>5</sup> function the basis set  $\{\varphi\}$ , which is used to describe  $\Phi(1, 2)$ , consists of normalized STO's. The coefficients  $b_{i,j}$  and  $b_{k,j}$ , together with  $\{\varphi\}$ , define the natural orbitals which are given by the summations over  $i$  and  $k$ ; the summation of all the natural configurations  $j$ , each weighted by the coefficient  $C_j$ , represents the total CI wave function. When  $j > 1$ , each natural configuration in the summation corresponds to the addition of a correlation term composed of  $\varphi$ 's with either radial or angular symmetry; when  $j = 1$  only, we recover the  $I^2F_1^2$  term in Eq. (5). Thus, by using the natural expansion and by setting  $\nu_2 = 0$ , the nature of the influence of the correlation terms on the CDW cross section becomes transparent and we see that the *relative* importance of each natural orbital is determined solely by its occupation coefficient  $C_j$  and its passive overlap integral  $I_j$ . As a consequence, when improving the target wave function up to a CI description, any change in the cross section at large  $\nu$  will be independent of the projectile charge

$Z_A$  but may be strongly influenced by the final state of the *passive* electron. When  $n'l' = 1s$ ,  $I_j$  is nonzero only for those natural orbitals of radial symmetry; therefore, only radial correlation terms in  $\Phi(1, 2)$  contribute to the cross sections in the present CDW calculations. In Fig. 2 we show, for  $\sigma[1s, 1s]_{\nu_2=0}$ ,  $C_j I_j F_j$  vs  $\eta$  for  $j = 1, 3$ , and 6 for He and  $\text{Li}^+$  and  $j = 1, 2$ , and 6 for  $\text{H}^-$  at  $E = 1000$  keV. The curves not only indicate the dominance of the  $j = 1$  term but also show that as we go from  $\text{H}^-$  to  $\text{Li}^+$  the higher natural orbitals become rapidly less important; it is noted that at  $\eta = 0$  for  $\text{H}^-$ ,  $C_2 I_2 F_2 \approx \frac{1}{7} C_1 I_1 F_1$ , while for  $\text{Li}^+$  at  $\eta = 0$ ,  $C_3 I_3 F_3 \approx \frac{1}{300} C_1 I_1 F_1$ .

### III. SUMMARY

The rationalization of the trends in the present CDW cross sections became tractable by setting  $\nu_2 = 0$ . Hence we have shown that, as the projectile velocity increases, the active electron is captured from regions of increasingly higher momentum within the target atom and that in this region it is the characteristics of the wave function which govern the trends in  $Q$  when comparing different targets. The nature of the distortion acting on the captured electron in the exit channel (i.e., when  $\nu_2 \neq 0$ ) is such that it reduces the size of each cross section, and this effect will increase as  $Z_B$  increases. Thus, when considering two-electron targets of large nuclear charge, it would be interesting to see if the final distortion could ever dominate the wave function in its influence on  $Q$  and so produce trends which are the reverse of those examined here.

<sup>1</sup>A. Salin, J. Phys. B **3**, 937 (1970).

<sup>2</sup>Dz. S. Belkić and R. Gayet, J. Phys. B **10**, 1923 (1977).

<sup>3</sup>K. E. Banyard and B. J. Szuster, Phys. Rev. A **16**, 129 (1977). See also J. Phys. B **10**, L503 (1977).

<sup>4</sup>J. C. Moore and K. E. Banyard, J. Phys. B **11**, 1613 (1977).

<sup>5</sup>A. W. Weiss, Phys. Rev. **122**, 1826 (1961).

<sup>6</sup>E. Clementi and C. Roetti, At. Data Nucl. Data Tables

**14**, 177 (1974).

<sup>7</sup>R. F. Curl and C. A. Coulson, Proc. Phys. Soc. London **85**, 647 (1964). See also J. Phys. B **1**, 325 (1968).

<sup>8</sup>Dz. S. Belkić and R. K. Janev, J. Phys. B **6**, 1020 (1973).

<sup>9</sup>P.-O. Löwdin, Phys. Rev. **97**, 1474 (1975). See also P.-O. Löwdin and H. Shull, Phys. Rev. **101**, 1730 (1956).

## Charge exchange between simple structured projectiles in high-energy collisions

K. E. Banyard and G. W. Shirtcliffe

*Department of Physics, University of Leicester, Leicester, England*

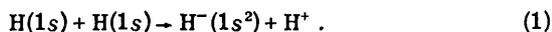
(Received 20 November 1979)

The continuum-intermediate-states approximation has been adapted for application to charge-exchange collisions between high-energy structured projectiles. A critical test of the scheme is provided by the reaction  $H(1s) + H(1s) \rightarrow H^-(1s^2) + H^+$ ; the overall agreement with the limited experimental data is encouraging.

### I. INTRODUCTION

Electron capture from small atomic targets by fast structureless projectiles such as protons and  $\alpha$  particles can be described quite successfully by modifying the continuum-distorted-wave (CDW) method developed by Cheshire.<sup>1</sup> However, its application to charge exchange between structured systems is more difficult. Therefore, in a desire to examine such high-energy collisions between simple atoms, or ions, we suggest an adaptation of the method of continuum intermediate states (CIS). The CIS approach, devised by Belkić<sup>2</sup> for electron capture by a structureless projectile, is closely related to the CDW method but accounts for distortion effects in only one of the two channels. This feature not only produces considerable simplification from both the analytical and computational viewpoint, but also provides flexibility for generalization to electron capture by structured projectiles. In addition, the CIS method has the particular advantage of being more reliable than the CDW approximation for describing capture at large impact parameters (Shakeshaft,<sup>3</sup> Belkić<sup>2</sup>).

The reliability of the approximations involved in the proposed scheme is tested here by examining the reaction



For this example, a comparison can be made with capture cross sections derived from the results of a CDW calculation for the reverse reaction; see Janev and Salin<sup>4,5</sup> and Moore and Banyard.<sup>6</sup> The former workers described the  $H^-$  target by a  $1s1s'$  wave function, whereas, in an electron correlation study, the latter workers used the wave function of Weiss.<sup>7</sup> The only experimental results available for reaction (1) are those of McClure<sup>8</sup> and, unfortunately, these are restricted to impact energies  $E \leq 63$  keV.

### II. METHOD

The cross section  $\sigma(nl)$  for the capture of electron 1, say, by a fast structured projectile system

$(Z_A, e_2)$  of energy  $E$  in collision with a target  $(Z_B, e_1)$  considered to be at rest, is written as

$$\sigma(nl) = 2 \int_0^\infty b |a_{if}(b)|^2 db \quad (2)$$

(in units of  $\pi a_0^2$ ), where  $b$  is the impact parameter and  $(nl)$  is the capture state. Atomic units are used throughout unless stated otherwise. It follows from the definition of the prior form of the transition amplitude (see, for example, Cheshire<sup>1</sup> that, for this reaction,  $a_{if}$  can be expressed as

$$a_{if} = i \int_{-\infty}^{+\infty} dt \int d\vec{r}_1 d\vec{r}_2 \Psi_f^{-*} \left( \frac{Z_A}{s_1} - \frac{1}{s_{12}} + \frac{Z_B}{x_2} + \frac{(1 - Z_A - Z_B)}{R} - U_i \right) \chi_i, \quad (3)$$

where  $\chi_i$  is the initial distorted wave satisfying

$$\left( \frac{1}{2} \nabla_1^2 + \frac{1}{2} \nabla_2^2 + \frac{Z_B}{x_1} + \frac{Z_A}{s_2} - \frac{(Z_A - 1)(Z_B - 1)}{R} + i \frac{\partial}{\partial t} + U_i \right) \chi_i = 0. \quad (4)$$

The position vectors  $\vec{s}_j$ ,  $\vec{x}_j$ , and  $\vec{r}_j$  locate electron  $j$  relative to  $Z_A$ ,  $Z_B$ , and the midpoint of  $R$ , respectively, where  $R$  is the internuclear separation. The final-state complete wave function  $\Psi_f^-$  is determined in the same manner as in the CDW method and therefore it incorporates the ground-state electronic wave function of the  $(Z_A, e_1, e_2)$  system and the distortion effects due to inclusion of continuum intermediate states which arise from the interaction of the active electron 1 with  $Z_B$  in the outward channel. In the CIS approximation, we choose the arbitrary distorting potential  $U_i$  such that  $\chi_i$  involves only the eigenfunctions for  $(Z_A, e_2)$  and  $(Z_B, e_1)$  along with an appropriate phase function of the form defined by Belkić.<sup>2</sup> This requirement is satisfied by  $U_i = -(Z_A - 1)R^{-1}$  and, as a consequence, Eq. (3) becomes

$$a_{if} = i \int_{-\infty}^{+\infty} \left[ \left\langle \Psi_f^- \left| \left( \frac{Z_A}{s_1} - \frac{1}{s_{12}} \right) \right| \chi_i \right\rangle + \left\langle \Psi_f^- \left| Z_B \left( \frac{1}{x_2} - \frac{1}{R} \right) \right| \chi_i \right\rangle \right] dt. \quad (5)$$

When the passive electron 2 remains tightly bound to  $Z_A$  throughout the whole interaction, then it is not unreasonable to suppose that the second matrix element provides a negligible contribution to  $a_{if}$ . Thus, in the calculation of  $\sigma(nl)$ , we consider only the first term in Eq. (5). The reliability of this approximation should increase when  $Z_A \gg Z_B$ ; such a relationship between the nuclear charges should also emphasize the importance of capture at large impact parameters and thus support our use of the CIS approach. Consequently, a very severe test of the present scheme is provided by applying it to the forward direction of reaction (1).

For this initial calculation, the interelectronic interaction was approximated by the average electrostatic potential due to the passive electron being described by a  $1s$  hydrogen atom orbital. Thus, in Eq. (5),

$$\left( \frac{Z_A}{s_1} - \frac{1}{s_{12}} \right) \rightarrow e^{-2s_1} \left( 1 + \frac{1}{s_1} \right), \quad (6)$$

when  $Z_A = 1$ .  $H^-(1s^2)$  was described, firstly, by the Hartree-Fock (HF) fitted function of Curl and Coulson<sup>9</sup> and, secondly, by a "fixed-core" representation of the form  $1s1s'$  in which the exponent of the valence-electron orbital is chosen to be  $(2\epsilon)^{1/2}$ , where  $\epsilon$  is the experimental value of the single-ionization energy, and the fixed core is a  $1s$  hydrogen orbital. The latter description of  $H^-$  has the advantage of having one electron loosely bound whilst the other electron remains comparatively tightly bound. Such a wave function, albeit empirical, could be particularly appropriate at the intermediate energies represented by experiment<sup>8</sup> since contributions to  $\sigma(1s)$  from relatively large values of the impact parameter may then be significant. Finally, we used the configuration-interaction (CI) wave function of Weiss.<sup>7</sup> This function not only allowed for the high degree of electron correlation in  $H^-$ , and satisfied the energy variation principle, but it also enabled us to make numerical comparisons with the CDW results<sup>6</sup> at large  $E$  values. The energy decrement  $\Delta\epsilon$  used in conjunction with the HF and CI wave functions was derived in each case from the corresponding theoretical energies, whereas, for the fixed-core description of  $H^-$ , we used the experimental value.

### III. RESULTS AND DISCUSSION

Although the CIS method, like the CDW approach, is essentially a high-energy approximation, the

comparison of our theoretical capture cross sections with experiment is limited to the data of McClure<sup>8</sup> (see Fig. 1). Also shown in Fig. 1 are the "post" and "prior" theoretical curves of Mapleton<sup>10</sup> used by McClure<sup>8</sup> for comparison with experiment. Mapleton<sup>10</sup> employed a Born approximation to describe reaction (1) with the ground state of  $H^-$  being represented by the correlated wave function of Chandrasekhar.<sup>11</sup> In Table I we compare the CIS-based results, using the HF and CI wave functions, with the CDW cross sections<sup>6</sup> for projectile energies  $E$  up to 1 MeV. The difference between the HF and CI values measures the influence of electron correlation within the current formulations of the CIS and CDW methods.

Figure 1 shows that the three CIS-based curves represent a considerable improvement on the Mapleton cross sections when compared with experiment, although at low energies the peak values are still too large. It is to be noted that, as observed for the CDW results,<sup>4-6</sup> each theoretical curve appears to fall off too rapidly as  $E$  increases in value. Additional experimental cross sections at higher energies would provide a most useful check with theory.

Of the curves presented in Fig. 1, that derived from the HF wave function is perhaps the best—this is somewhat surprising and may, as discussed

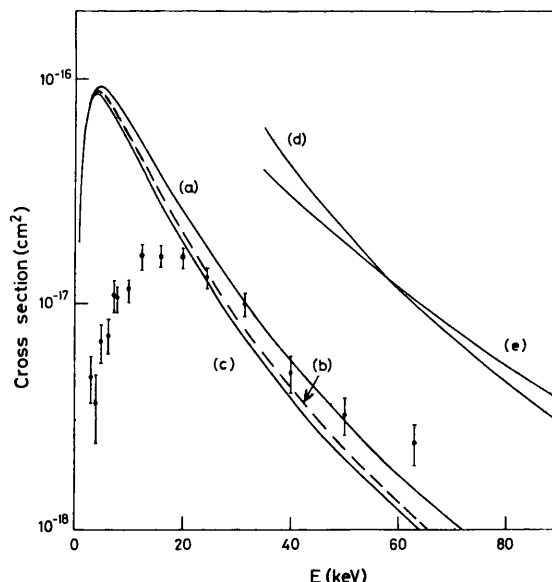


FIG. 1. Electron-capture cross sections  $\sigma(1s)$  for  $H(1s) + H(1s) \rightarrow H^-(1s^2) + H^+$ . The CIS results are shown in curves (a), (b), and (c) and are derived, respectively, from the use of the Hartree-Fock (HF) function, the "fixed-core" model, and the configuration-interaction (CI) description for  $H^-(1s^2)$ . Curves (d) and (e) are the "prior" and "post" results of Mapleton (Ref. 10) calculated using a Born approximation. The experimental points are those of McClure (Ref. 8).

TABLE I. A comparison of the electron-capture cross sections  $\sigma(1s)$ , measured in  $\text{cm}^2$ , for the reaction  $\text{H}(1s) + \text{H}(1s) \rightarrow \text{H}^-(1s^2) + \text{H}^+$ . The continuum-intermediate-states (CIS) results are calculated here for the forward reaction, whereas the continuum-distorted-wave (CDW) results are those of Moore and Banyard (Ref. 6) and were derived by them from the calculated results for the reverse reaction. For  $\text{H}^-(1s^2)$ , the Hartree-Fock (HF) function was that of Curl and Coulson (Ref. 9) and the configuration-interaction (CI) description was taken from Weiss (Ref. 7).

$E$ (keV)	CIS		CDW	
	HF	CI	HF	CI
25	$1.681 \times 10^{-17}$	$1.173 \times 10^{-17}$	$2.886 \times 10^{-17}$	$2.067 \times 10^{-17}$
50	$3.023 \times 10^{-18}$	$2.067 \times 10^{-18}$	$5.093 \times 10^{-18}$	$3.526 \times 10^{-18}$
100	$3.268 \times 10^{-19}$	$2.268 \times 10^{-19}$	$5.227 \times 10^{-19}$	$3.600 \times 10^{-19}$
200	$2.325 \times 10^{-20}$	$1.650 \times 10^{-20}$	$3.410 \times 10^{-20}$	$2.379 \times 10^{-20}$
400	$1.202 \times 10^{-21}$	$8.696 \times 10^{-22}$	$1.527 \times 10^{-21}$	$1.087 \times 10^{-21}$
800	$4.845 \times 10^{-23}$	$3.636 \times 10^{-23}$	$4.990 \times 10^{-23}$	$3.618 \times 10^{-23}$
1000	$1.688 \times 10^{-23}$	$1.284 \times 10^{-23}$	$1.570 \times 10^{-23}$	$1.143 \times 10^{-23}$

below, arise from a cancellation of opposing effects. The more reasonable split-shell description of  $\text{H}^-$  embodied in the empirical fixed-core model and the Weiss wave function is seen to be reflected in the closeness of curves (b) and (c); both curves lie slightly below the experimental points when  $E > 25$  keV. Our CIS-based approximation is only capable of responding to a split-shell or radial component of electron correlation and makes no allowance for the effects of angular correlation in  $\text{H}^-$ . Since the transition amplitude  $a_{if}$  is evaluated in terms of momentum space, it is possible that the opposing effects of angular and radial correlation—known to exist in momentum space<sup>12</sup>—may produce some cancellations. Thus, if the present method could be modified to allow for angular correlation, curve (c) might be raised. This is now under investigation.

For both descriptions of  $\text{H}^-$ , Table I indicates that for  $E < 800$  keV, the CIS values are smaller

than the corresponding cross sections derived from a CDW calculation for the reverse reaction. The relative merit of the two schemes is difficult to judge since, ideally, the comparisons with experiment should be made in the higher-energy region of Table I.

#### IV. SUMMARY

In view of the severity of the test of the present method, represented by its application to reaction (1), the comparison between theory and experiment was, overall, quite encouraging. The general procedure outlined above is now being examined in more detail and the method is also being applied to electron capture by fast Li ions impinging on H atoms. Such reactions have been the subject of a recent experimental investigation by Shah, Goffe, and Gilbody.<sup>13</sup> The preliminary comparisons are pleasing.

<sup>1</sup>I. M. Cheshire, Proc. Phys. Soc. London **84**, 89 (1964).

<sup>2</sup>Dz. Belkić, J. Phys. B **10**, 3491 (1977).

<sup>3</sup>R. Shakeshaft, J. Phys. B, **7**, 1734 (1974).

<sup>4</sup>R. K. Janev and A. Salin, J. Phys. B **4**, L127 (1971).

<sup>5</sup>R. K. Janev and A. Salin, Fizika **4**, 165 (1972).

<sup>6</sup>J. C. Moore and K. E. Banyard, J. Phys. B **11**, 1613 (1978).

<sup>7</sup>A. W. Weiss, Phys. Rev. **122**, 1826 (1961).

<sup>8</sup>G. W. McClure, Phys. Rev. **166**, 22 (1968).

<sup>9</sup>R. F. Curl and C. A. Coulson, Proc. Phys. Soc. London **85**,

647 (1964); see also R. F. Curl and C. A. Coulson, J. Phys. B **1**, 325 (1978).

<sup>10</sup>R. A. Mapleton, Proc. Phys. Soc. London **85**, 841 (1965).

<sup>11</sup>S. Chandrasekhar, Astrophys. J. **100**, 176 (1944).

<sup>12</sup>K. E. Banyard and C. E. Reed, J. Phys. B **11**, 2957 (1978).

<sup>13</sup>M. B. Shah, T. V. Goffe, and H. B. Gilbody, J. Phys. B **11**, L233 (1978).